Late Quaternary changes in the Westerly Winds over the Southern Ocean

Submitted by Alexander Whittle, to the University of Exeter

as a thesis for the degree of

Doctor of Philosophy in Physical Geography

In February 2021

I certify that all material in this thesis which is not my own work has been identified and that any material that has previously been submitted and approved for the award of a degree by this or any other University has been acknowledged.

(Signature) .....

Abstract

The latitudinal position and intensity of the Southern Hemisphere westerly winds (SHW) has important and far-reaching implications for global climate and the physical environment in the southern high latitudes. Despite this, our ability to project how they will change in the future is reduced by limited understanding of their behaviour over centennial to millennial timescales. Peatland archives on the sub-Antarctic Islands are uniquely located inside the core wind-belt (50-55˚S), and hence ideally situated to reconstruct changes in westerly wind behaviour. However, suitable proxies to develop reconstructions of wind-strength throughout the region are lacking. Westerly winds are shown to enrich the sub-Antarctic Islands with salt-spray in concentrations that are proportional to wind-strength. This research has tested the potential for peat-dwelling testate amoebae to act as a bioindicator for variations in salt-spray deposition through time. Measurements of communities in variably salt-enriched environments - spanning a gradient from predominantly freshwater to salt-marsh - revealed a strong relationship between the productivity of testate amoeba communities and salinity, which allows past salt-concentrations to be inferred from sub-fossil assemblages. Presented here are two reconstructions of SHW intensity over the South Atlantic, based primarily on changes in the productivity of testate amoeba communities. The first provides a high-resolution record of the changes in wind-intensity over recent decades, extending beyond the observational record to 1920 CE, and demonstrating that present-day wind conditions are unprecedented over the last century. The second record, collected from the same site, provides a c. 8000-year reconstruction of wind-intensity over the South Atlantic, based on changes in testate amoeba productivity as part of a multi-proxy analysis that includes three independent proxies to track the deposition of salt-spray aerosols and minerogenic particles into the peat record on Bird Island (sub-Antarctica). Three significant phases of intensified winds during this period (0.45-1.15, 2.8-3.65 and 4.45-8 k yr BP) indicate long-term correspondence between temperature and wind-strength at 54˚S. These observations suggest that with climatic warming in the 21st Century, the westerly wind belt will continue to intensify and displace southwards, leading to increased wind-stress over the Southern Ocean. Implications of this shift are expected to include; reduced precipitation supply to the Southern Hemisphere continents, reduced Antarctic ice-sheet stability and increased contributions to global sea-level, and weakening of the Southern Ocean carbon sink, allowing accumulation of more CO_2 in the atmosphere.

Contents

List of Figures

Figure numbers prefixed with 'S' refer to those included in Supplementary Information.

List of Tables

Table numbers prefixed with 'S' refer to those included in Supplementary Information.

List of Appendices

Acknowledgements

My thanks go to Dr Angela Gallego-Sala for her continual encouragement, thoughtfulness, advice and enthusiasm that will remain a constant source of inspiration in helping guide my path beyond my PhD.

To all of my supervisors, I am grateful for the generosity they have shown in giving me their time. Specifically, I would like to thank Professor Dominic Hodgson for opening-up so many opportunities for my research with the British Antarctic Survey, and facilitating the incredible opportunity to conduct fieldwork in the sub-Antarctic. To Professor Dan Charman for overseeing the project, and providing me with a clear sense of direction. I wish to thank Dr Steve Roberts for his support throughout the project, especially in sharing his expertise of core-scanning applications and in creating opportunities for me to gain hands on experience. I am also grateful to Dr Matt Amesbury for sharing his knowledge of Southern Hemisphere testate amoebae, and providing insights to improve many aspects of my research.

The fieldwork would not have been possible without the support of the Collaborative Antarctic Science Scheme, and the Natural Environmental Research Council studentship that funded this project. I would also like to thank the staff of the Bird Island research station, with whom we lived for two months, for their assistance in conducting fieldwork in challenging conditions, and the Captain and crew of the *RRS Ernest Shackleton* for accommodating the logistical requirements of this project.

I also extend my gratitude to Angela Elliot, Dr Joanna Zaragoza-Castells, Dr Steve Haley and Mandy Lee, who made my laboratory work in Exeter possible, and to Dr Tom Roland for keeping me entertained with interesting discussions on all manner of subjects while I was analysing testate amoebae.

I wish to thank Dr Rob Barnett for his limitless enthusiasm, his willingness to spend time discussing testate amoebae in saline environments, and for continually championing my work. My thanks also go to Dr Alan Warren for inspiring my interest in taxonomy, supporting my work on the Ogden and Penard collections of testate amoebae at the Natural History Museum, and for the many fascinating conversations on protistology.

Members of the International Society for Testate Amoeba Research, made me feel incredibly welcome among their ranks at my first meeting in Belfast (2018), and I am grateful to have benefitted from the support of the community throughout my PhD.

I am grateful to Alice Doolan, who helped in preparing some of the testate amoebae samples analysed in the short-core record from Bird Island, and Rachel Nash who generously gave time to isolate mineral grains from the long-core record for analysis.

I would also like to thank the friends whom I have been fortunate to meet during my PhD; Rob Yarlett, Dom Walker, Anna Jackman, Camille Le Guen, Nicole Sanderson, Katie Journeaux, Nicola Ellis, Holly East, and Jamie Johnson.

I would like to extend my thanks to Dr Paul Halloran and Professor Edward Mitchell for dedicating their time to read and examine my thesis.

Finally, I would like to thank my family: my parents for their continued support and for instilling in me the curiosity and confidence to pursue my studies to this level, and to Gen for her patience and support of my endeavours.

Chapter 1

Introduction

In this chapter the importance of the Southern Hemisphere Westerly winds as a crucial component of the Earth system is introduced, along with the need for more direct and longer-term (palaeo) records of wind-behaviour over the Southern Ocean. The aims and key research questions of this thesis, which seeks to address this knowledge gap, are introduced in Section 1.5. The general background for the methodological approach is introduced in Sections 1.6-1.7.

1.1. The Southern Hemisphere Westerly Winds

The ocean carbon sink is the product of surplus uptake of atmospheric CO_2 at the surface of the world oceans via the biological pump and diffusion, relative to degassing (loss) of carbon from deep-waters driven to the surface by upwelling (Anderson et al. 2009; Sigman et al. 2010). It is a critical, large magnitude component of the global carbon cycle and an important determinant of the future Earth system (Friedlingstein et al. 2006; Gruber et al. 2009). In total the ocean sink has sequestered ~50% of emissions from fossil fuel burning, and ~30% of all anthropogenic emissions, including cement production and land-use change (Gruber et al. 2009). The Southern Ocean alone represents ca. 40% of the total sink (Orr et al., 2001), moderating the climatic effects of enhanced greenhouse warming since the industrial revolution (Le Quéré et al. 2007).

The Southern Annular Mode (SAM) is defined as the mean sea level pressure difference between 40°S and 65°S. It is the principle mode of atmospheric circulation variability over the Southern Ocean and oscillates between high and low-index polarities (Marshall, 2003). During periods when SAM trends toward a high-index state, the circumpolar vortex strengthens and the belt of surface airflow, termed the Southern Hemisphere Westerly Winds (SHW), intensifies and migrates poleward (Marshall, 2003). Conversely, the SHW migrate northward toward the equator, dissipate, and decrease in intensity during phases of more-negative SAM index.

With the exception of the Andes in southern South America, the SHW are virtually unhindered by topographic barriers to circumpolar rotation. They are therefore a strongly zonal and symmetric component of the climate system (Fletcher and Moreno, 2012), and the strongest time-averaged winds found globally (Hodgson and Sime, 2010). Currently the core wind-belt extends from ~30°-60°S (Lamy et al. 2010; Knudson et al. 2011; Fletcher and Moreno, 2012) and reaches maximum intensity in the sub-Antarctic latitudes between 50°-55°S (Lamy et al. 2010; Fig. 1.1).

The latitudinal position and intensity of the wind belt is known to undergo shifts at a variety of timescales. Seasonally, during summer, the belt contracts poleward and strengthens (accompanied by more-positive values of the SAM index), whereas during winter it expands northward and weakens (Hodgson and Sime, 2010; Lamy et al. 2010; Varma et al. 2012). Over inter-annual to decadal timescales, atmospheric-ocean phenomena (e.g. SAM and El Niño) adjust the pressure systems and are thought to perturb the direction of westerly airflow (Knudson et al. 2011). Meanwhile, on much larger glacial-interglacial time-scales, global climate changes are thought to be responsible for governing variability in the strength and position of the wind-belt (Toggweiler et al. 2006).

The observational record indicates that in response to the combined effects of stratospheric ozone depletion and anthropogenic emissions of greenhouse gases, the SHW belt has strengthened (~6%; 2001-2010 relative to 1981-1990) and migrated further towards Antarctica (~3.5-2°S for winter and summer respectively) throughout the past 50 years (Thompson and Solomon, 2002; Toggweiler, 2009; Thompson et al. 2011; Mayewski et al. 2013; Watson et al. 2014; Mayewski et al. 2015). Projections indicate that with further warming this trend will persist through the 21st century (Toggweiler and Russell, 2008; Stager et al., 2012; Bracegirdle, 2013; Mayewski et al. 2015).

This is concerning because the SHW are crucial for Southern Ocean circulation through their association with the Antarctic Circumpolar Current (ACC) (Chavaillaz et al. 2013) and the upwelling section of the meridional overturning circulation. The SHW continually ‘pump’ dense interior water to the surface by pushing surface waters away from the Antarctic coastline, driving Ekman transport (Russell et al. 2006; Toggweiler and Russell, 2008). Changes in wind behaviour can therefore influence ocean circulation in a way that increases

degassing of stored carbon from deep within the ocean, and through this mechanism can ultimately contribute to determining the strength (and persistence) of the Southern Ocean sink (Sigman et al. 2010).

It is proposed that a similar trend to the one recently observed, occurred during previous periods of deglaciation, with variability in the position and intensity of the wind-belt contributing significantly to glacial-interglacial variability in atmospheric CO_2 concentrations (Toggweiler et al. 2006; Anderson et al. 2009; Sigman et al. 2010). During the last deglaciation, a large quantity of oceanic CO_2 entered the atmosphere, increasing the atmospheric concentration by ~50% (Hodgson and Sime, 2010). The possible effect of changing wind patterns on the global carbon cycle at this time have been discussed controversially (Toggweiler et al. 2006; Menveil et al. 2008; Anderson et al. 2009; Moreno et al. 2010). Toggweiler et al. (2006) used a general circulation model to suggest that the injection of oceanic CO_2 to the atmosphere could have been driven by a poleward migration of the SHW by 7-10°S of their glacial position. They indicate that this would align the winds more squarely to the ACC, increasing driving stress and promoting stronger upwelling of deep-water, ultimately allowing CO_2 to degas and accumulate in the atmosphere (Toggweiler and Russell, 2008). Conversely, during the preceding glacial period, atmospheric CO_2 concentrations were suppressed by reduced wind-driven upwelling that allowed the ocean to become more stratified and carbon to accumulate at depth. This theory is supported, at least in the direction of change of the wind-belt during the last deglaciation, by some initial empirical data (e.g. Moreno et al. 2010; Whittaker et al. 2011) but there is also active debate (Menveil et al. 2008).

Drawing evidence from several glacial to inter-glacial cycles, Anderson et al. (2009) showed that periods of inferred Southern Ocean upwelling coincided with increasing atmospheric CO_2 concentrations and temperature (as recorded in Antarctic ice-cores). However, it is important to acknowledge that this data demonstrates that changes occurred concurrently and does not indicate a causal link between wind behaviour and global climate. Whether these proposed linkages also operate over shorter timescales remains an open question. A major problem in further assessment of this debate is the lack of suitable paleo-data to investigate past wind conditions, and hence the SHW remain a significant knowledge gap in our current understanding of past climate and our ability to

accurately predict future climatic change (Stager et al., 2012; Saunders et al. 2018; Perren et al. 2020).

Beyond the carbon cycle, variability in the strength and latitudinal position of the SHW belt has also been linked to widespread environmental change throughout the southern high latitudes, including:

1. Climatic warming on the Antarctic Peninsula (Vaughan et al. 2003). Since the 1950s the Antarctic Peninsula has warmed by ~0.56°C per decade (Turner et al. 2009). Although there has been a recently observed shift to overall cooling since the late 1990s (Steig, 2016), the warming on the east coast has been related to the poleward migration of the westerlies in recent decades, which bring warmer air-masses further south (Steig, 2016).

2. Increased basal melting of ice-shelves surrounding the West Antarctic ice-sheet and Antarctic Peninsula (Marshall et al. 2006; Pritchard et al. 2012; Holland et al. 2019). For each 1°C rise in ocean temperature basal melt rates can increase by ~10 m $year^{-1}$ (Rignot and Jacobs, 2002). Greater westerly wind influence drives incursions of comparatively warm Circumpolar Deep Water against the grounding lines of the Antarctic ice-sheets (Spence et al. 2014a). The reverse bed-slopes of the West Antarctic ice-sheet make it inherently vulnerable to runaway retreat, and could lead to rapid collapse (Mayewski et al. 2015). Modelling suggests that stronger westerly winds over the Amundsen Sea were responsible for rapid basal melt of surrounding ice-shelves, consequential reduction in latitudinal stress and an acceleration in the flow of associated glaciers (Bracegirdle, 2013). Such changes in mass loss have important and far-reaching implications for global sea-level.

3. Changing sea-ice extent (Purich et al. 2016). Changes in wind conditions may also alter sea ice thickness and extent (Bintanja et al. 2013), and affect the rate of deep water formation (Spence et al. 2014b). Changes in sea-ice extent also influence the area available for exchange of CO_2 between the atmosphere and the open ocean.

4. Rate of Agulhas leakage (Biastoch et al. 2009). Changes in SHW behaviour affect the transport of warm, salty waters from the Indian Ocean into the Atlantic Ocean, which plays a crucial role in global ocean circulation (Gordon, 1986).

5. Precipitation supply to continents surrounding the Southern Ocean. The SHW dominate climate and precipitation patterns between 30-70°S (Moy et al. 2008; Fletcher and Moreno, 2011; Varma et al. 2012). As a result of the changing wind-behaviour over recent decades, storm-tracks that would normally carry moisture to the continental regions surrounding the Southern Ocean, have been diverted further poleward (Abram et al. 2014). Precipitation in New Zealand has consequently reduced (Ummenhofer and England, 2007; Ummenhofer et al. 2009), and droughts and wildfires have occurred in south-western Australia (Cai et al., 2011), South Africa (Reason and Rouault, 2005), and southern South America (Garreaud, 2018).

1.2. Reconstructing Southern Hemisphere westerly wind behaviour

Reconstructing past changes in SHW behaviour to provide information on the range of natural variability and linkages to changes in the physical environment beyond the instrumental time-period, is a major priority for palaeoclimate science. However, there are a number of specific challenges to developing detailed reconstructions, for example; the sparseness of land in the latitudes over which they blow, obtaining a suitable proxy that preserves a record of changes in airflow millennia in the past, and disentangling signals of changes in intensity from latitudinal shifts of the core-belt. The following section critically evaluates key examples of the current palaeoenvironmental archives and proxies that have been used for SHW conditions from within or close to the core-wind belt.

Precipitation supply. To date, most palaeoclimatic reconstructions of the SHW derive from southern South America the only continental landmass to intersect the core westerly wind belt. Here, wind-speed is strongly correlated with precipitation, which can be reconstructed using standard palaeo-climate tools (e.g. changes in sub-fossil pollen assemblages (Moreno et al. 2018), lake level (Roberts et al. 2021), sediment geochemistry (Lamy et al. 2001)). Migrations of the wind-belt through time have also been inferred by sampling archives spaced along a latitudinal transect (Moy et al. 2008; Lamy et al. 2010).

Correlation between wind conditions, precipitation and climate arises due to the barrier presented to circumpolar airflow by the Andes Cordillera. On the western side of the Andes, where intense rainfall is driven by orographic uplift, instrumental records indicate a strong positive correlation (R=0.4-0.8) between

rainfall and wind-speed (Kilian and Lamy, 2012). This produces a strong west-east rainfall gradient, with high precipitation (>4 m year^{-1}) hyper-humid conditions on the western side, and a rain shadow in the east (Kilian and Lamy, 2012). Here, a negative moisture balance prevails since yearly precipitation drops to <40 cm and moisture depleted winds drive high rates of evaporation (Villa-Martínez and Moreno, 2007).

Vegetation assemblages reflect the gradient in precipitation. Broadly, magellanic moorland dominates in the western Fjords, whereas Patagonian steppe vegetation covers the semi-desert region to the east, although a more complex sequence of localised ecotones is superimposed onto this gradient (Villa-Martínez and Moreno, 2007). Therefore, the geographic position of each of these ecotones and their specific community composition constitutes a highly sensitive system for detecting hydrological changes through time. Moreno et al. (2009) infer changes in SHW behaviour by calculating a normalised palaeo-vegetation ratio to detect fluctuations in the physiognomy of past plant communities; from '*Nothofagus*' dominated forest (associated with wetter conditions) to Poaceae dominated steppe (associated with more arid conditions). The same method has also been applied for subsequent work by Moreno et al. (2010) where two similar normalized vegetation ratios were calculated to infer changes in past precipitation levels. Further examples include, Musotto et al. (2016) and Tonello et al. (2009), who both use biological proxies to interpret changing ecological conditions linked to precipitation from peatlands in Argentina.

However, the use of changing vegetation patterns to first reconstruct precipitation and then infer past westerly wind conditions is prone to a number of significant uncertainties. Primarily, vegetation reflects a bioclimatic record, which includes signals from secondary variables such as the number of growing degree days, temperature, and seasonal availability of plant-available moisture (Kohfeld et al. 2013). It is therefore uncertain whether reconstructed changes reflect temperature or precipitation signals more strongly (Saunders et al. 2015). Temperature does not display the same high degree of correlation with wind conditions and therefore poses a complication to the interpretation of these records. Consequently, the assumption that the relationship between modern plants and climate remains constant through time, is also problematic.

Zimmermann et al. (2015) reconstruct fluctuations in lake level at Laguna Potrok Aike, using the proportion of planktonic diatoms within the sediment to investigate changes in precipitation delivery. Laguna Potrok Aike is located in the rain-shadow to the east of the Andes, and therefore its hydrology is related to precipitation bearing easterly airflow of Atlantic origin during periods of decreased westerlies. Therefore, the interpretation works by anti-correlation (i.e. increased lake levels imply weaker westerly winds). A summary of lake-level fluctuations in southern Patagonia and their relationship to westerly wind conditions is presented in a recent review by Roberts et al. (2021).

The high axial range of the South Island of New Zealand also intersects the northern boundary of the westerly wind belt, which produces a similar rainfall gradient; 6-14 m year^{-1} on the west coast, and a rain shadow in the east. Knudson et al. (2011) use sediments from fjords on the west coast as a record of past precipitation conditions. Fjords are semi-enclosed systems, with one or more marine sills and steep sides. Consequently, their circulation consists of a low-density brackish surface water outcrop over high-density saline water beneath. Precipitation induced run-off into the fjords determines the ratio between the contributions of terrestrial versus marine organic matter that accumulates in their sediment record. Knudson et al. (2011) differentiate these contributions by measuring the C:N and δ^{13}C of the sediment. Samples with a high C:N ratio and depleted δ^{13}C are interpreted as higher in terrestrial organic matter, and vice versa. Therefore, periods in the record that are enriched with higher terrestrial organic matter imply a wetter climate with stronger winds. The authors suggest that this technique provides a more direct link to precipitation, less influenced by temperature than other proxies, however the study also serves as an example of the highly convoluted proxies that are used in wind reconstruction.

Precipitation changes reconstructed from the growth rate and stable isotope ratio (δ^{18}O and δ^{13}C) of speleothems have also been used to study changes in westerly wind behaviour, from both southern South America (Schimpf et al. 2011) and New Zealand (Whittaker et al. 2011). A major benefit of the use of speleothems is that they contain a long record (e.g. ~80 k year (Whittaker et al. 2011)), yet can provide high resolution data because of their continual growth that can be constrained by Uranium series dating. However, similarly to the bioclimatic signal recorded by plants, speleothems reflect cave ‘drip-rate’ and not

precipitation directly. Therefore, geological alterations of water filtration pathways above, and changes in cave ventilation, can complicate the interpretation of the record they provide. Furthermore, in order to understand the isotopic signal, caves need to be well monitored, meaning that substantial resources are needed, making reconstructions of this type rare.

Mass balance (i.e. the ratio between accumulation of ice and its eventual ablation) determines the extent of glaciers and ice-sheets. Therefore, reconstructions of changes in their extent by dating moraine features has also been used to study westerly wind changes. The majority of such investigations have focussed on the South Island of New Zealand because glaciers in the Southern Alps are considered to be highly sensitive to changes in SHW strength and position (Knudson et al. 2011). Putnam et al (2010), use ^{10}Be dating to analyse a moraine complex formed by glacial advance which coincided with the Antarctic cold reversal. In this context, the authors suggest that glacial expansion provides evidence of an equatorward shift in the westerlies, since periods when the SHW move southwards are associated with decreasing frequency of moist airflow over the Southern Alps and glacial retreat.

Glaciological evidence of SHW changes has also been reported in southern South America. Precipitation rates currently peak within the core of the westerly wind belt (close to 50°S) and decline with distance to the north or south (Hulton et al. 2002). Simplistic glacier modelling has shown that the known extent of the Patagonian ice-sheet during the Last Glacial Maximum can be replicated only if the lower temperatures were accompanied by a migration in the zone of peak precipitation relative to its current position. This implies that precipitation would have been lower at 50°S and increased further to the north (42°S, Hulton et al. 2002), suggesting that during this period westerlies shifted approximately 10°N of their current position. Indeed this shift during glacial periods, and a more southerly (~52°S) position during inter-glacial periods, is now generally accepted (Van Daele et al. 2016). A general limitation in the use of glaciers for westerly wind reconstruction is that advance and retreat occurs over long periods of time, and hence the temporal resolution of their record (in terms of dated moraines) is low. The record is also subject to overprinting, when periods of re-advance occur after retreat. The potential usage of glaciological evidence for reconstructing changes over centennial or decadal scales is therefore severely limited.

An uncertainty common to all precipitation based proxies for westerly winds is the assumption that modern correlations between wind and precipitation hold over long timescales. However, a significant body of evidence suggests that this is not the case. For example, Van Daele et al. (2016) highlighted that during the Last Glacial Maximum the growth of the Patagonian ice-sheet, which covered the crest of the Andes (Hulton et al. 2002) until 20 k year BP caused an increased orographic effect irrespective of wind conditions, and hence there was a stronger precipitation deficit in the rain shadow than is observed today.

Atmospheric transport. Deposition of mineral particles (e.g. dust and tephra) transported in the atmosphere from a known source region and deposited into a remote down-wind archive, is another approach used to reconstruct the SHW. Ombrotrophic peatlands are ideal archives for this purpose since they receive inputs of water solely from the atmosphere, and hence are not subject to inputs of mineorgenic material carried by surface run-off.

Björk et al (2012) measure rates of sand influx into a peat bog in Tierra del Fuego. Using a microscope, they counted particles in the size fractions 125-350, 350-700, and >700 μm, and infer that deposition of larger particles occurs during periods of stronger winds. Furthermore, they reconstructed the provenance of the particles, which was interpreted as a crude measure of relative wind direction in the past. Similarly, Vanneste et al. (2015) measured the variable rate of mineral dust accumulation by quantifying the concentrations of rare earth elements in bulk peat samples from an ombrotrophic peatland archive in Tierra del Fuego. However, it has been suggested that wind strength is not the sole factor in determining size distribution of deposited particles. Stochastic variability, such as distance from the source area, the distribution of available particle sizes at the source, and the proportion of dry to wet deposition of dust are all suggested as complicating secondary variables (Kohfeld et al. 2013). In addition, Kohfeld et al. (2013) also point out that dust deposition reflects a suite of additional factors, for example; atmospheric residence times, aridity and areal extent of the source region, and the wind trajectory. Taken together, they suggest that such records should be interpreted cautiously and as part of the wider palaeo-climate picture (Kohfeld et al. 2013).

In addition to mineral particles, organic particles transported in the atmosphere, can also be used. Strother et al. (2014) quantify the influx rate of non-native South

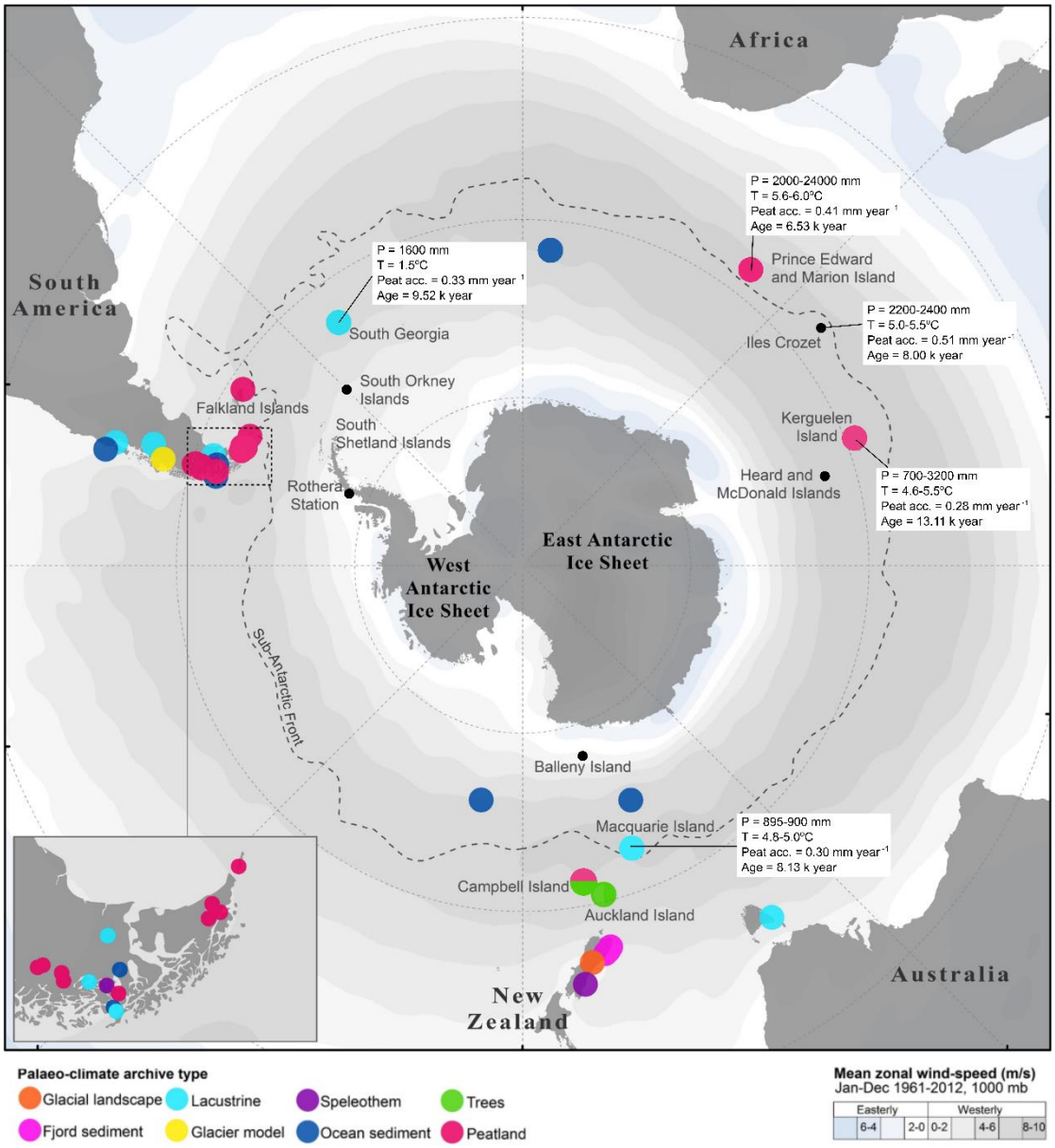

Figure 1.1 | Distribution of westerly wind reconstructions based on different proxies and archives from close to the core westerly wind belt. Westerly wind belt (grey-shading) shown using 20th century re-analysis data of 1,000 mb zonal wind (composite mean) from 1982-2012 (Kalnay, 1996; NOAA, 2016). Positive values (grey) indicate airflow in the westerly direction and negative (blue) indicates easterly. The position of the sub-Antarctic front is shown by the dotted line. Boxes provide key bioclimatic data for the sub-Antarctic Islands; yearly precipitation in mm (P), and yearly mean temperature in ˚C (T). Temperatures on South Georgia (the location used in this thesis) and Heard Island are significantly lower than the other islands due to their more poleward latitude. Accumulation rate (Peat.acc) of peatlands was deduced from published basal dates, and is presented in mm $year^{-1}$. The average age of peat deposits on each island is also shown.

American pollen grains into the sediment of a lake on Annenkov Island (South Georgia). However, concentrations of non-native pollen were low due to isolation of the site making the record is potentially unreliable (Strother et al. 2014). For the method to yield a reliable reconstruction, a suitable source region should be sufficiently isolated so that deposition rates are not constant, but not isolated to the extent that only very small (and hard to detect) concentrations arrive. The vegetation history of the source region must also be accurately known to ensure that the rates of pollen emission to the atmosphere were constant through time (Turney et al. 2016a).

Turney et al. (2016a) apply the same technique using a peatland archive on the Falkland Islands (more proximal to the source in southern South America). They support their pollen data with counts of small (<50 μm) charcoal, suggesting that the similar size of the grains also implies a South American (i.e. not local) origin. Unfortunately, many of the peatlands on the Falkland Islands have been subjected to anthropogenic drainage and continuous erosion by the westerly winds. Consequently, 'old-pollen' can become remobilised and re-deposited at the surface, complicating the record. Additional examples of this method include; Markgraf et al. (2003), Moreno et al., (2009) and Mayr et al. (2007) who study wind transported pollen deposited in archives in southern South America.

Wind exposure. Tree-line reconstruction is a recently developed SHW proxy that is reliant on the sensitivity of ligneous plants to temperature and exposure to westerly airflow. So far the method has been applied exclusively to the evergreen angiosperm *Dracophyllum* on Auckland and Campbell islands by Turney et al. (2016b). The proxy interpretation follows that *Dracophyllum* cannot colonise areas of low temperatures and exposure (i.e. the conditions currently found on west facing slopes). Therefore, Turney et al. (2016b) suggest that dated fragments of subfossil *Dracophyllum* recovered from eroding peat deposits above the present day tree-line altitude must indicate periods of less intense westerly winds over the islands.

Although a useful addition to the available data, the potential usage of this proxy is very limited. The majority of islands in the sub-Antarctic are devoid of trees, and so more records from other locations to confirm the interpretations cannot be developed. Crucially, the chronological framework means that short (decadal) timescale changes cannot be resolved from longer-term signals because minor

tree-line fluctuations within the general trend are indistinguishable. The method also produces a discontinuous record of tree-line with temporal gaps where no sub-fossils were sampled. The interpretation of such gaps is difficult and may indicate either error in sampling (i.e. insufficient number of samples) or the deleterious effect of intense winds on *Dracophyllum* colonisation during the time-period. Poor preservation of sub-fossil wood in certain locations also cannot be ruled out.

Circulation in the Southern Ocean. Climate reconstructions from deep-ocean cores inside the westerly wind belt are rare, however it is important to acknowledge the contribution that they have made in informing our knowledge of past SHW behaviour. Anderson et al. (2009) measured the concentration of biogenic silica produced by marine diatoms deposited in the ocean sediment as a proxy for upwelling. Biogenic silica is produced in the euphotic layer of the ocean, and the highest present day productivity occurs in the region of strongest wind-driven deep water upwelling, where vital nutrients are delivered to the surface. Therefore, periods of high productivity deposit more silica into the sediment when the organisms die. Because upwelling in the Southern Ocean is principally controlled by the SHW, changes in the concentrations of silica therefore reflect changes in wind behaviour. Using this proxy, Anderson et al. (2009) show that two separate periods of increased upwelling occurred concurrently with increasing de-glacial CO_2 levels.

1.3. How reliable are existing records of the Southern Hemisphere westerly winds?

Reconstructions of the SHW, currently face a number of limitations that affect their reliability. As demonstrated in Section 1.2, the primary limitation is that most of the current proxies are based on a convoluted series of assumptions to provide a wind reconstruction from a secondary variable (e.g. vegetation (pollen) as a proxy for precipitation, and then precipitation as a proxy for wind behaviour, based on present day correlation between wind-strength and precipitation). Our current understanding of past SHW conditions is significantly reliant on these palaeo-hydrology based studies, which are concentrated in southern South America and New Zealand. However, such levels of separation between the reconstructed variable and wind behaviour decrease the reliability of the resultant

reconstruction, and the modern day correlations between variables do not necessarily remain constant through time.

More reliable records can come from proxies that are directly related to wind changes because less assumptions are required. However, these direct wind records remain elusive and underdeveloped since, unlike for precipitation, suitable proxies are not readily available in the conventional palaeoenvironmental toolkit.

Furthermore, the lack of records for large parts of the Southern Ocean (even where terrestrial archives are present) is problematic as it prevents accurate extrapolation of wind changes across the region, particularly because many reconstructions originate from either southern South America or outside the core westerly wind belt (50-55°S) where changes are harder to detect. The number of records from within the mid-Southern Ocean, at equivalent or more poleward latitudes than southern South America decreases rapidly, and this limits our ability to isolate the signals of latitudinal shifts, expansion and contraction, and weakening or strengthening of the wind belt (Kohfeld et al. 2013) or to fully assess the hemispheric symmetry of such changes (Fletcher and Moreno, 2012).

Although the number of SHW reconstructions have proliferated in recent years, these new records have been derived from a wide variety of methods, many of which are applicable only to specific geographic regions. Determining whether these records are complimentary is therefore a complex task, and a major source of uncertainty. Indeed, it is a likely reason why palaeodata and palaeodata-model inter-comparisons frequently return contradictory results (Kohfeld et al. 2013).

1.4. Deposition of salt-spray into sub-Antarctic terrestrial ecosystems as a novel basis for Southern Hemisphere westerly wind reconstruction

Avoiding continental landmasses with complex orographic effects, and instead applying multi-proxy (and independent) methods to track wind intensity from archives in the sub-Antarctic, circumvents the issues faced by many existing reconstructions. The latter is particularly important for the use of newly developed proxies by providing a test of whether different proxies record congruent patterns, and validating that they are responding to the external forcing of the SHW, as opposed to local or internal dynamics at the study site (Saunders et al. 2018).

The sub-Antarctic refers to a section of the Antarctic biome between the polar and sub-tropical front in the Southern Ocean (Van der Putten et al. 2012). The region has a limited area of landmass, with six major island groups comprising a combined land area of ~26,000 km^2 (Hodgson et al. 2014). Because of their position in the mid-Southern Ocean and the core of the westerly wind-belt, terrestrial ecosystems on these sub-Antarctic islands receive high concentrations of oceanic salts from spray that is driven inland by the prevailing westerly winds (Fig. 1.2). This causes an observable west-east gradient in conductivity (a direct proxy for salinity), which has been recorded in freshwater pools and lakes throughout the region (e.g. Macquarie Island (Buckney and Tyler, 1974; Saunders et al. 2009; Saunders et al. 2018), Campbell Island (Saunders et al. 2015), and Marion Island (Van Nieuwenhuyze, 2015; Perren et al. 2020)). In such cases, measurements of ions within these freshwater bodies indicates oceanic equivalent ratios (i.e. Cl>SO_4>Mg>Ca>K), which confirms the predominant oceanic source of salt inputs (Saunders et al. 2015).

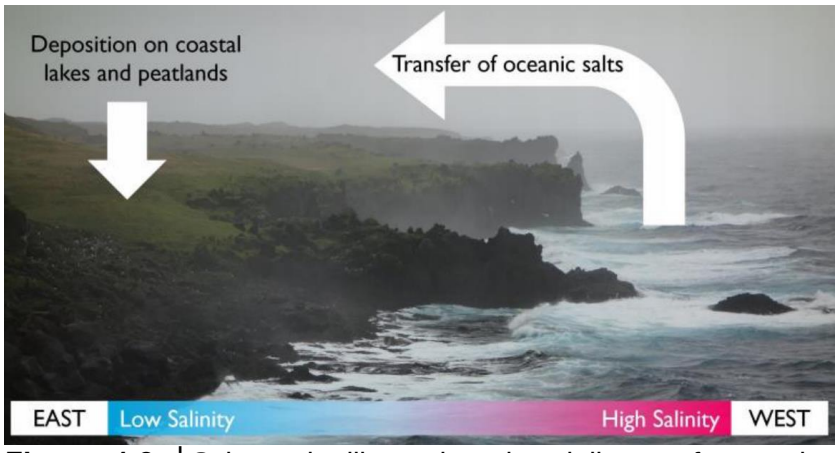

Figure 1.2 | Schematic illustrating the delivery of oceanic salt-spray aerosols to terrestrial environments on the sub-Antarctic Islands. Photograph source: Dominic Hodgson.

Recent research efforts have sought to exploit this conductivity gradient as a proxy for SHW behaviour. Saunders et al. (2009, 2015), demonstrate that the diatom flora of water-bodies on Campbell and Macquarie Island are independently and significantly influenced by conductivity (salinity). This has formed the basis for the development of a diatom-conductivity transfer function which can be used to reconstruct changes in sea-spray inputs (and therefore SHW intensity) from assemblages of sub-fossil diatoms preserved in lake sediments (Van Nieuwenhuyze, 2015; Saunders et al. 2018; Perren et al. 2020);

where the interpretation follows that periods of more (or less) sea spray reflects stronger (or weaker) winds (Saunders et al. 2018).

1.5. Research aims and questions

Peat-forming ecosystems are distributed throughout the sub-Antarctic region and could serve as useful archives to apply a similar salt-spray aerosol based proxy for SHW at sites where lacustrine sediments are either unavailable or where the preservation of diatoms is poor. Peatlands may also provide a more sensitive system for reconstructing lower-magnitude wind-changes (compared to lakes) due to lower levels of dilution of salt-spray inputs.

Indeed, a small body of research has demonstrated the influence of oceanic salt deposition on freshwater peatland ecosystem functioning in other regions of the world (e.g. Kleinebecker et al. 2008; Henman and Poulter, 2008; Whittle and Gallego-Sala, 2016). However, these changes are either not easy to reconstruct directly from the peat record itself, and/or are unsuitable for the creation of a high-precision reconstruction of past salinity conditions. A possible solution (and main proposition of this thesis) is the use of testate amoebae (peat-dwelling shelled microbial eukaryotes) as a biological marker to track past salinity conditions. The research therefore set out to address **two main aims**:

1. To establish whether communities of sub-Antarctic peat-dwelling testate amoebae can act as a proxy for changing SHW conditions.
2. To develop new Holocene records of SHW dynamics from within the core-belt region, over the Southern Ocean.

These aims were further divided into **four key research questions**:

1. How do testate amoeba communities respond to changing salinity conditions?
2. Do contemporary salinity conditions at the surface of peatlands in the sub-Antarctic reflect westerly wind intensity?
3. How has the latitudinal position and intensity of the SHW-belt varied during the Holocene?
4. What do the results tell us about how the behaviour of SHW will change in future and what likely environmental impacts can be anticipated?

The following sections (1.6 and 1.7) provide an introduction to the use of peat-forming ecosystems in the sub-Antarctic and the testate amoebae they contain for palaeoclimate analysis. Section 1.8 subsequently outlines the structure of this thesis, linking the main aims and research questions to the chapters that address them.

1.6. Sub-Antarctic peatlands as a palaeo-climate archive

Peatlands are biotic landscapes formed by the accumulation of a carbon rich soil (peat) composed of partially decayed plants that once grew at the surface (Clymo et al. 1998). They are characteristically waterlogged ecosystems, low in nutrients, and often acidic, with plant and microbial communities specifically adapted to these conditions. Anoxia of the soil matrix and acidic conditions strongly reduces the rate of decomposition processes allowing organic material to accumulate over time. Peatland accumulation also records palaeo-climate conditions because markers representative of biotic and abiotic conditions at the time of formation, such as testate amoebae, are incorporated into the stratigraphy as vertical growth layers are added.

Palaeo-climate reconstructions from peatlands can be separated into two categories based on the temporal resolution of information that they provide. At a coarse resolution, peatland initiation dates and their spatial distribution give a useful constraint for the timing of events such as deglaciation (Hodgson et al. 2014), sea-level change (Magnan et al. 2014), and broad climatic shifts towards conditions suitable for peat expansion (Gallego-Sala et al. 2016). At a finer resolution the properties of the peat itself represent a record that contains information of autogenic changes. The stratigraphy can also be viewed as a depository for allochtonous material (e.g. dust, pollen) that is indicative of wider environmental changes during the period of peat development (Charman, 2002).

The global distribution of peatlands is strongly governed by climate suitability because persistent accumulation requires a positive moisture balance, yet they occur globally from tropical to polar latitudes (Yu et al. 2010). Deposits in the Southern Hemisphere are mostly located in Patagonia (Leon et al. 2021), Tasmania and New Zealand (Yu et al. 2010; Rydin and Jeglum, 2013). Suitable climatic space (i.e. cool temperature, high precipitation) is also available in the sub-Antarctic. Further south, the Antarctic Peninsula also supports limited areas

of peat forming ecosystems, referred to as moss banks (e.g. Royles et al. 2013; Amesbury et al. 2017).

The low-diversity of plant species found on the sub-Antarctic Islands make the peatlands floristically distinctive at the global scale (Van der Putten et al. 2012). For example, *Sphagnum* species which are a key builder of most high-latitude peatlands (van Breemen, 1995), are either absent or of minor importance to peat formation. Furthermore, most sub-Antarctic peatlands have not developed into raised bogs, they do not possess a surface micro-topography of mounds and hollows (e.g. Yeloff et al. 2011), and are comprised of vegetation that also colonises other non-peat forming habitats. All sub-Antarctic peatlands may therefore be categorised as oligotrophic to eutrophic fens, since they receive water from beyond their limit (Van der Putten et al. 2012; Charman 2002), and enrichment by oceanic spray is also a constant feature (Bergstrom and Selkirk, 2000).

As with all peatlands, those present in the sub-Antarctic are stratified deposits (i.e. they possess layers accumulated from annual productivity at the surface) (e.g. Van der Putten et al. 2008; McGlone et al. 2010; Yeloff et al. 2011). Timing of initiation is an important pre-requisite for palaeo-environmental studies as it determines the time-period covered by the record. Basal dates of peat deposits have recently been compiled to constrain the timing of deglaciation in the sub-Antarctic (Hodgson et al. 2014). However, these data provide only a coarse indication of the time-span of potential records due to the lag between land becoming ice-free and peat initiation, and the unknown rate of peatland expansion to current extent. Local-scale factors, specific to individual islands, (e.g. sea-level change, ice-cover, the influence of wild-life, and volcanism) may have also influenced the rate of peat formation. Additionally, there are a number of reports of peatlands developed on nunatacks (glacial refugia) that could therefore feasibly pre-date glaciation (Van der Putten et al. 2010). These factors mean that it is difficult to accurately predict where fieldwork efforts should be directed in order to obtain the longest available peat records.

The relationship between the age of a peat deposit and its depth (i.e. the resolution) is also a crucial consideration in finding archives suitable for palaeo-environmental research. For this review, further studies publishing basal dates of peatlands were added to the list generated by Hodgson et al. (2014), and average

accretion (resolution) was calculated (i.e. age divided by depth) (Fig 1.1). The average rate of accretion in the sub-Antarctic was 0.38 mm year^{-1}, with substantially slower rates recorded on South Georgia and Heard Island which are located further South. The implication of these relatively slow average accumulation rates is that sub-Antarctic peatlands are unlikely to yield decadal resolution records (at least in older sections of the sequences). Further, if rates are slow due to high levels of decomposition, their ability to preserve certain proxies may be limited. Nevertheless, sub-Antarctic peatlands offer unique and potentially highly valuable terrestrial archives that warrant further research.

1.7. Testate amoebae as a bio-indicator of environmental change

The term testate amoebae encapsulates a polyphyletic group of predominantly freshwater, unicellular, shell-forming microorganisms (Fig. 1.3) from at least three eukaryotic lineages (Kosakyan et al. 2016). The group have long been of interest in palaeoecology because; (1) taxa have unique ecological optima, they produce decay resistant external shells (tests) and can be identified to a low taxonomic level (Charman, 2001; Mitchell et al. 2008), and (2) communities are diverse, globally distributed and respond quickly to a range of perturbations to their environment.

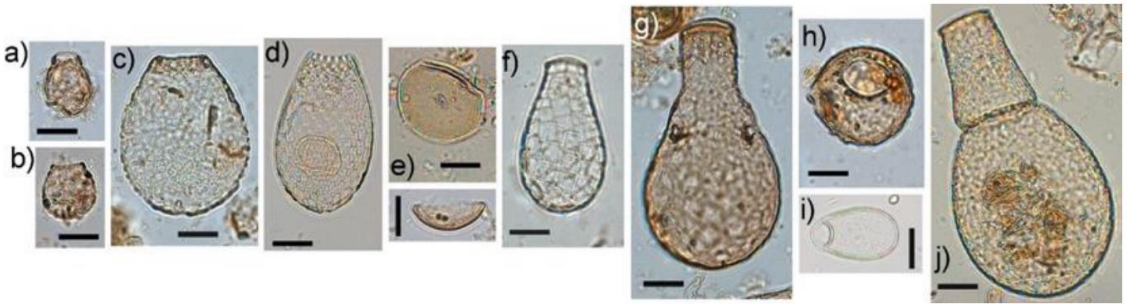

Figure 1.3 | Testate amoebae taxa typical of a coastal peatland on Marion Island (Chapter 3). a) *Pseudodifflugia* spp.1 and *P.* spp.2 (b), c) *Argynnia dentistoma,* d) *Euglypha compressa,* e) *Microchlamys patella,* f) *Quadrulella symmetrica,* g) *Certesella certesi,* h) *Phryganella acropodia,* i) *Corythion dubium,* and j) *Apodera vas.* Scale bars = 25 µm. Photograph source: Alex Whittle.

Testate amoebae do not form colonies like other protists; individuals consist of a single eukaryotic cell enclosed by the test, which is thought to provide protection against desiccation, predators or possibly pathogens (Hansell, 2011). Every taxa possess at least one aperture (opening) in the test structure which allows part of the cytoplasm that surrounds the cell nuclei, to protrude. Termed the

pseudopodium, this facilitates feeding, attachment to substrates, and movement (via gliding through the water film in soil or damp vegetation (Hansell, 2011)). Testate amoebae are predominantly heterotrophic mainly feeding on small bacteria, micrometazoa (e.g. rotifers, nematodes), other testate amoebae, fungi and algae through the mechanism of phagocytosis (Yeates and Foissner, 1995; Gilbert et al. 2000; Fournier et al. 2015; Dumack et al. 2018) and complex feeding behaviours, such as apparent pack-hunting, have been observed (Geisen et al. 2015). A smaller number of species also use endosymbionts (green algae) capable of photosynthesis (mixotrophic amoebae) (Marcisz et al. 2016; van Bellen et al. 2017) which can provide food when prey is unavailable (Jassey et al. 2013).

Cell size typically ranges across an order of magnitude (20-200 µm), allowing observation with a light microscope. Tests composition can be proteinaceous, siliceous and calcareous, while structurally, tests can be sub-divided into two main categories: idiosomic tests are formed of material secreted by the parent during cell division, whereas xenosomic tests are made of agglutinated materials, such as mineral grains, diatom frustules and pollen. These are collected from prey-organisms and the environment, and fixed together using a secreted organic cement.

Almost all freshwater habitats worldwide support communities of testate amoebae, from; lakes, water courses, peatlands, non-ombrotrophic wetlands, to supra-glacial meltwater (Santibanez et al. 2011). The highest abundance and diversity is found in warm regions that experience high rainfall and have high soil organic matter content (e.g. tropical and temperate rainforests (Krashevska et al. 2007); in such environments concentrations range from hundreds to tens-of-thousands per cubic-centimetre of substrate-material. Nevertheless, colder climate environments, and even extreme latitudes, also support a significant testate amoeba fauna (e.g. Patterson and Kumar, 2002; Royles et al. 2013; Scott and Asioli, 2014; Swindles et al, 2015a,b). Despite being predominantly non-marine organisms, communities have previously been reported in brackish environments, including: marginal marine soils such as higher salt marshes (Roe et al. 2002; Barnett et al. 2017), lakes exposed to coastal inundation (Nicholls and MacIsaac, 2004), beaches (Golemansky, 1998; Golemansky and Todorov, 1999), and mangroves (Duleba and Debenay, 2003).

Testate amoebae are useful and well established palaeoenvironmental bioindicators (Mitchell et al. 2008). The specific optima and tolerance for colonisation of each taxon means that the community composition (relative abundance and diversity of taxa present) serves as a unique signature of the dominant environmental conditions at the specific sampling location. Assuming suitable conditions, testate amoebae can reproduce 10-27 times per year (Charman, 2001), so populations quickly respond to short-term environmental changes (Mitchell et al. 2008; Krashevska et al. 2013). A further advantage is that they are bonded to their depositional substrate, and are often damaged if the sediment is reorganised. Assemblages therefore provide a direct link to the environmental conditions at the time of sediment formation.

Previous research has established a secure ecological background for the development of testate amoeba-based transfer-functions for use in reconstructing bog-surface wetness (i.e. depth to water-table) in peatlands around the world (e.g. Charman, 1997; Charman et al. 2007; Swindles et al. 2014; van Bellen et al. 2015; Amesbury et al. 2016). In addition, they have also been used to reconstruct other autogenic variables including: pH, nutrient status and temperature. Further proposed uses include: environmental monitoring for habitat restoration (e.g. Creevy et al. 2018), the retrieval of cryptotephra used as a dating method in peatlands (Delaine et al. 2016), and even snow-layer identification for the accumulation on glaciers (Zapata and Fernandez, 2008). Recently, because testate amoebae form a significant proportion of the microbial biomass in peatlands, changes in their biomass (a community level metric) have been used as an indicator of total microbial activity on the Antarctic Peninsula (Royles et al. 2013; Royles et al. 2016; Amesbury et al. 2017). Testate amoebae have also been used alongside foraminifera and diatoms as an accurate biomarker of past sea-level changes (e.g. Gehrels et al. 2001; Roe et al. 2002; Charman et al. 2002; Charman et al. 2010; Barnett et al. 2016; Barnett et al. 2017). Surface assemblages on salt-marshes are therefore known to exhibit zonation along transects of elevation relative to sea-level (Barnett et al. 2017).

Specifically to palaeoecology, preferential preservation is a source of uncertainty in environmental reconstructions using testate amoebae, however there is very little empirical work on the subject. The problem arises because tests of different species may be more (or less) resilient to decay, and therefore preferential

preservation can severely alter the original assemblage and lead to an erroneous environmental interpretation (Charman, 1997). Swindles and Roe (2007) examined the dissolution characteristics of tests in acidic environments analogous to long term preservation in a *Sphagnum* peatland. Using concentrated mineral acid (HCl), they found a large range of susceptibility depending on the species. Species from the genus Euglypha, composed of thin siliceous plates, were particularly prone to dissolution, whereas some morphologically similar taxa (e.g. *Assulina muscorum*) remained relatively unaffected. To overcome this limitation a commonly adopted approach is to remove species that are known to be fragile from the original calibration (training-set) that is used to relate the response of (present-day) assemblages to known abiotic conditions; although this could be at the expense of potential environmental information, especially when the surface diversity is low. In addition to dissolution, in cold-climate ecosystems, it is possible that freeze-thaw cycles may cause the degradation of tests (Balik, 1994). However, despite their use as proxies for bog surface wetness in permafrost peatlands (e.g. Swindles et al, 2015a,b), to date, no empirical observations of this effect have been made.

Identification of testate amoeba species in palaeoecology is based on test morphological characters (morphospecies). Commonly used characteristics are size, morphology, composition, and colour (Charman et al. 2000), because these remain visible in sub-fossil specimens from the sediment record. Most palaeoecology studies aim for a species level identification because the more taxa that are included, the greater the resolution of environmental information that is inferable from the record.

However, there are a number of problems associated with achieving high taxonomic resolution. Charman et al. (1999) point out that divisions between many taxa which display gradational morphological variability become essentially arbitrary, and that subsequently many of the taxa described as new species are likely nothing more than an atypical morphological extreme individual produced by intra-specific variation (Charman, 2001; Bobrov and Mazei, 2004). Indeed, a high degree of intra-specific variability is common, for example individuals of the taxa *Apodera vas*, which have been observed to range from 111 to 234 µm in length (Zapata and Fernandez, 2008). A wider problem is that convention has allowed new species to be described without genetic data, from observation of

only a small number of individuals (Reczuga et al. 2015), and in some cases (due to methodological limitations, such as when a species is rare) without high-magnification Scanning Electron Microscope images (Reczuga et al. 2015). In addition to these considerations, a recent review by Kosakyan et al. (2016) highlighted the inaccessibility of original species descriptions (many of which are more than 100 years old), confusing nomenclature, lack of or inaccessibility of type-specimens, and the small size of the organisms, amongst the principal challenges for accurate species-level identification of testate amoebae.

The environmental reconstruction goal of many studies using testate amoebae leads some authors to overlook the ecological basis of the proxy and the wider scientific value of taxonomic study. For example, although there are an increasing number of studies focussing on palaeoenvironmental uses of testate amoebae, some demonstrate sub-optimal taxonomic practice. Arguably this may be necessary due to time and logistic limitations. Such practices, include the use of open-taxonomy schemes (where taxa are attributed a unique analyst specific code rather than an accepted species name) and not creating an archival record of either 'type' specimens or micrographs of observed taxa, which are crucial in checking taxonomic standardisation between analysts and to allow future reassessment, if required. At the same time, the number of true taxonomic studies is falling, due to decreasing expertise and availability of funding (Kosakyan et al. 2016). With this trend in mind, this thesis also set out to contribute to the advancement of taxonomic study by synthesising existing records of diversity from the Southern Ocean region (Chapter 2; see Section 1.8).

Of particular relevance to this project, since features of sub-fossil tests become harder to detect with time, is an ongoing discussion into the suitable balance between 'splitting' of groups of morphologically similar taxa, versus 'grouping' them together into a single taxon. 'Splitting' increases the resolution of a taxonomy, and retains the maximum amount of environmental data (Charman, 2001). The risks, however, are: (1) that taxonomic inconsistencies will arise, especially in large collaborative datasets (e.g. Amesbury et al. 2016), which can affect the resultant palaeoenvironmental interpretation, and (2) that from a biogeographical viewpoint an erroneous high rate of endemism may be concluded (Mitchell et al. 2008). An example of the later is the questionable

division and assumption of endemism for the taxa *Argynnia antarctica* on Marion Island in the sub-Antarctic (Heger et al. 2009).

The shortcomings outlined here are particularly acute in palaeoecological research using testate amoebae in the sub-Antarctic, where equivalent studies of taxonomy and identification guides that exist for the Northern Hemisphere are not currently available. Establishment of a precise taxonomy becomes a fundamental prerequisite in palaeoecology if comparisons are to be made between different regions, i.e. the tolerance of a species to salinity in two sub-Antarctic islands cannot be compared if an unknowing comparison between two different taxa is actually being made.

An increasingly adopted method, functional trait based analysis, is complementary to taxonomic identification (Fournier et al. 2016) and offers a potential solution to the issues of taxonomic uncertainty. In this method, which is explored in Chapter 3, assemblages are defined by measurable traits, rather than taxonomic names. Because a functional trait is a factor that plays a role in determining the fitness of an organism to colonise a certain environment (Violle et al. 2007; Green et al. 2008), a more mechanistic understanding of the links between assemblages and environmental conditions can be established in comparison to using taxonomy alone (Fournier et al. 2015; van Bellen et al. 2017).

1.8. Overview of this thesis

Chapters 2-6 are structured in the form of research papers, and therefore each include more specific literature reviews, methods, results and discussions, conclusions. For clarity they include individual reference lists and supplementary information at the end of each chapter. Chapters 2-4 primarily address the first aim of the thesis; to establish whether communities of sub-Antarctic peat-dwelling testate amoebae can act as a proxy for changing SHW conditions.

Chapter 2: Testate amoebae of the Southern Ocean region and their use in palaeoenvironmental studies: where do we go from here? This chapter provides a contextualisation of the research within existing literature on testate amoebae specifically within the Southern Ocean region. An extensive review of available literature from the region was conducted to summarise the history of prior research efforts, to provide estimates of the compound diversity and

distribution of species for the first time, and guide the trajectory of research in the future. Since very little palaeoenvironmental research using testate amoebae has been conducted in the region prior to this study, particular focus is given to their potential applications. The challenges posed to these applications are also discussed, along with proposed solutions that could allow unique and robust palaeoenvironmental reconstructions to be obtained.

Chapter 3: Salt-enrichment impact on biomass production in a natural population of peatland dwelling Arcellinida and Euglyphida. Addressing the first key question of the thesis, this chapter examines how variable salt concentrations deposited by the SHW affect a natural population of testate amoebae on the surface of a freshwater peatland on sub-Antarctic Marion Island. Here we consider the response in terms of overall community productivity, shifts in the relative abundance of individual taxa, and changes in prevalence of particular functional traits. This study was published in the journal *Microbial Ecology* in 2019. A video summary can be found in Appendix 1.

Chapter 4: Low-salinity transitions drive abrupt microbial response to sea-level change. Building on Chapter 3, this chapter examines whether the observed responses of testate amoebae to differing salinity conditions on Marion Island are consistent with similar (but longer) salinity gradients in the Northern Hemisphere (Canada). This allows assessment of whether trends observed on Marion Island (Chapter 3) can be considered localised or widely geographical applicable. In so doing the chapter considers the bioindicator potential of testate amoebae for salinization related to coastal change more generally, especially the inundation of freshwater ecosystems by sea-level change. This study has been formatted as a manuscript to the journal *Ecology Letters* in January 2021 and is in review.

Chapter 5: Recent intensification of the Southern Hemisphere westerly winds as detected in the response of terrestrial testate amoebae in the sub-Antarctic

Expanding on Chapters 2-4, this chapter addresses the second key research question. Using field observations collected on Bird Island (South Georgia) combined with regression-modelling, the link between contemporary surface-water conductivity and SHW behaviour is examined. Having established this relationship, the chapter concludes the first aim of the thesis by applying the

method developed in Chapters 3-4 to provide a decadal-scale reconstruction of SHW intensity, using the productivity of testate amoebae (as part of a multi-proxy analysis) from a short monolith core collected on the islands west coast. This reconstruction is subsequently compared against regional observational and high-resolution palaeo-records.

Chapter 6: Long-term correspondence between Westerly wind intensity and temperature during the Holocene. Chapter 6 presents a c. 8,000-year reconstruction of wind-strength over Bird Island. The reconstruction is primarily based on the testate amoeba-based proxy for salinity developed throughout the thesis. This record is combined as part of a multi-proxy analysis, which includes an independent measure of wind-blown salt- and mineral-aerosol deposition measured using micro-X-ray fluorescence geochemical core scanning. Addressing research questions 3-4, the record of wind-intensity over Bird Island is examined in the context of selected regional records to track changes in the latitudinal position of the wind-belt through time. The chapter finally evaluates the relationship between the intensity and position of the SHW-belt and temperature in the extratropics in order to project how wind-behaviour will change in a warming climate. The likely implications of these changes on the physical environment are discussed.

Chapter 7: Draws together the conclusions of the thesis as a whole, in relation to the aims and research questions.

1.9. References

Abram, N. J., Mulvaney, R., Vimeux, F., Phipps, S. J., Turner, J. and England, M. H. (2014) Evolution of the Southern Annular Mode During the past millennium, *Nature Climate Change*, 4:564-569.

Amesbury, M. J., Swindles, G. T., Bobrov, A., Charman, D. J., Holden, J., Lamentowicz, M., Mallon, G., Mazei, Y., Mitchell, E. A. D., Payne, R. J., Roland, T. P., Turner, T. E. and Warner, B. G. (2016) Development of a New Pan-European Testate Amoeba Transfer Function for Reconstructing Peatland Palaeohydrology, *Quaternary Science Reviews*, 152: 132–51.

Amesbury, M. J., Roland, T. P., Royles, J. Hodgson, D. A., Convey, P., Griffiths, H. and Charman, D. J. (2017). Widespread Biological Response to Rapid Warming on the Antarctic Peninsula, *Current Biology*, 27: 1–7.

Anderson, R. F., Ali, S., Bradtmiller, L. I., Nielsen S. H. H., Fleischer, M. Q., Anderson, B. E. and Burckle, L. H. (2009), Wind-Driven Upwelling in the Southern Ocean and the Deglacial Rise in Atmospheric CO_2, *Science*, 323: 1443–48.

Balik, V. (1994) On the soil testate amoebae fauna (Protozoa: Rhizopoda) of the Spitsbergen Islands (Svalbard), Archiv Für Protisten Kunde, 144: 365-372.

Barnett, R. L., Garneau, M. and Bernatchez, P. (2016) Salt-Marsh sea-Level indicators and transfer function development for the Magdalen Islands in the Gulf of St. Lawrence, Canada, *Marine Micropaleontology*, 122: 13–26.

Barnett, R. L., Newton, T. L., Charman, D. J. and Gehrels, W. R. (2017) Salt-marsh testate amoebae as precise and widespread indicators of sea-level change, *Earth-Science Reviews*, 164: 193–207.

Bergstrom, D. M. and Selkirk, P. M. (2000) Terrestrial Vegetation and Environments on Heard Island, *Papers and Proceedings of the Royal Society of Tasmania*, 133(2): 33– 46.

Biastoch, A., Böning, C. W., Schwarzkopf, F. U. and Lutjeharms, J. R. E. (2009) Increase in Agulhas leakage due to poleward shift in the southern hemisphere westerlies, *Nature,* 462: 495–498.

Bintanja, R., van Oldenborgh, G. J., Drijfhout, S. S., Wouters, B. and Katsman, C. A. (2013) Important role for ocean warming and increased ice-shelf melt in Antarctic sea-ice expansion, *Nature Geoscience*, 6: 376–79.

Björck, S., Rundgren, M., Ljung, K., Unkel, I. and Wallin, Å. (2012) Multi-proxy analyses of a peat bog on Isla de Los Estados , easternmost Tierra Del Fuego: a unique record of the variable Southern Hemisphere Westerlies since the last deglaciation, *Quaternary Science Reviews*, 42: 1–14.

Bobrov, A. and Mazei, Y. (2004) Morphological Variability of Testate Amoebae (Rhizopoda: Testacealobosea: Testaceafilosea) in Natural Populations, *Acta Protozoologica*, 43: 133–146.

Bracegirdle, T. J. (2013) Climatology and recent increase of westerly winds over the Amundsen Sea derived from six reanalyses, *International Journal of Climatology*, 33 (4): 843–51.

Buckney, R. T. and Tyler, P. A. (1974) Reconnaissance limnology of Sub-Antarctic islands. II. Additional features of the chemistry of Macquarie Island lakes and tarns, *Marine and Freshwater Research*, 25: 89–95.

Cai, W., Van Rensch, P., Borlace, S. and Cowan, T. (2011) Does the Southern Annular Mode contribute to the persistence of the multidecade-long drought over southwest Western Australia?, *Geophysical Research Letters,* 38: L14712, doi:10.1029/2011GL047943.

Charman, D.J. (2002) Peatlands and Environmental Change, Wiley, Chichester.

Charman, D.J., Hendon, D. and Packman, S. (1999) Multiproxy surface wetness records from replicate cores on an ombrotrophic mire: implications for Holocene palaeoclimate records, *Journal of Quaternary Science*, 14(5): 451–463.

Charman, D. J., Hendon, D. and Woodland, W. A. (2000), The identification of testate amoebae (Protozoa: Rhizopoda) in peats, Quaternary Research Association, London.

Charman, D. J., Roe, H. M. and Gehrels, W. R. (2002) Modern distribution of saltmarsh testate amoebae: regional variability of zonation and response to environmental variables, *Journal of Quaternary Science*, 17: 387–409.

Charman, D. J., Blundell, A. and ACCROTELM Members. (2007) A new European testate amoebae transfer function for palaeohydrological reconstruction on ombrotrophic peatlands, *Journal of Quaternary Science*, 22 (3): 209–21.

Charman, D. J., Gehrels, W. R., Manning, C. and Sharma, C. (2010) Reconstruction of recent sea-level change using testate amoebae, *Quaternary Research*, 73: 208–219.

Charman, D. J. (1997) Modelling hydrological relationships of testate amoebae (Protozoa: Rhizopoda) on New Zealand peatlands, *Journal of the Royal Society of New Zealand*, 27(4): 465–483.

Charman, D. J. (2001) Biostratigraphic and palaeoenvironmental applications of testate amoebae, *Quaternary Science Reviews*, 20: 1753–64.

Chavaillaz, Y., Codron, F. and Kageyama, M. (2013) Southern westerlies in LGM and future (RCP4.5) climates, *Climate of the Past*, 9 (2): 517–24.

Clymo, R. S., Turunen, J. and Tolonen, K. (1998) Carbon Accumulation in Peatland, *Oikos*, 81 (2): 368–88.

Creevy, A. L., Anderson, R., Rowson, J.G. and Payne, R.J. (2081) Testate amoebae as functionally significant bioindicators in forest-to-bog restoration, *Ecological Indicators,* 84: 274-282.

Delaine, M., Fernández, L. D., Armynot du Châtelet, E., Recourt, P., Potdevin, J-L., Mitchell, E. A. D. and Bernard, N. (2016) Cinderella's helping pigeons of the microbial world: The potential of testate amoebae for identifying cryptotephra, *European Journal of Protistology*, 55: 152-164.

Duleba, N. and Debenay, J.P. (2003) Hydrodynamic circulation in the estuaries of Estacao Ecologica Jurtia-Itatins, Brazil, inferred from foraminifera and thecamoebian assemblages, *Journal of Foraminiferal Research*, 33: 62-93.

Dumack, K., Kahlich, C., Lahr, D. J. G. and Bonkowski, M. (2018) Reinvestigation of *Phryganella paradoxa* (Arcellinida, Amoebozoa) Penard 1902, *Journal of Eukaryotic Microbiology,* 0: 1-12.

Fletcher, M-S, and Moreno, P. I. (2011) Zonally symmetric changes in the strength and position of the Southern Westerlies drove atmospheric CO2 variations over the past 14 k.y., *Geology*, 39 (5): 419-22.

Fletcher, M-S. and Moreno, P. I. (2012) Have the Southern Westerlies Changed in a zonally symmetric manner over the last 14,000 years? A hemisphere-wide take on a controversial problem, *Quaternary International*, 253: 32–46.

Fournier, B., Lara, E., Jassey, V. E. J. and Mitchell, E. A. D. (2015) Functional traits as a new approach for interpreting testate amoeba palaeo-records in peatlands and assessing the causes and consequences of past changes in species composition, *The Holocene*, 25(9): 1375–1383.

Fournier, B., Coffey, E. E. D., van der Knaap, W. O., Fernández, L. D., Bobrov, A. and Mitchell, E. A. D. (2016) A legacy of human-induced ecosystem changes: spatial processes drive the taxonomic and functional diversities of testate amoebae in *Sphagnum* peatlands of the Galapagos, *Journal of Biogeography*, 43: 533–543.

Friedlingstein, P., Cox, P., Betts, R., Bopp, L., von Bloh, W., Brovkin, V., Cadule, P., Doney, S., Eby, M., Fung, I., Bala, G., John, J., Jones, C., Joos, F., Kato, T., Kawamiya, M., Knorr, W., Lindsay, K., Matthews, H. D., Raddatz, T., Rayner, P., Reick, C., Roeckner, E., Schnitzler, K, -G., Schnur, R., Strassmann, K., Weaver, A. J., Yoshikawa, C. and Zeng, N. (2006) Climate-carbon cycle feedback analysis: Results from the C^4MIP Model Intercomparison, *Journal of Climate*, 19: 3337-3353.

Gallego-Sala, A. V., Charman, D. J., Harrison, S. P., Li, G. and Prentice, I. C. (2016) Climate-driven expansion of blanket bogs in Britain during the Holocene, *Climate of the Past*, 12 (1): 129–36.

Garreaud, R. D. (2018) Record-breaking climate anomalies lead to severe drought and environmental disruption in western Patagonia in 2016, *Climate Research,* 74: 217-229.

Gehrels, R. W., Roe, H. M. and Charman, D. J. (2001) Foraminifera, testate amoebae and diatoms as sea-level indicators in UK saltmarshes: a quantitative multiproxy approach, *Journal of Quaternary Science*, 16 (3): 201–20.

Geisen, S., Rosengarten, J., Koller, R., Mulder, C., Urich, T. and Bonkowski, M. (2015) Pack hunting by a common soil amoeba on nematodes, *Environmental Microbiology,* 17(11): 4538-4546.

Gilbert, D., Amblard, C., Bourdier, G., Francez, A-J. and Mitchell, E. A. D. (2000) Le regime alimentaire des Thécamoebiens (Protista, Sarcodina), *L'Année Biologique,* 39(2): 57-68.

Golemansky, V. G, and Todorov, M. T. (1999) First report of the interstitial testate amoebae (Protozoa: Testacea) in the marine supralittoral of the Livingston Island (the Antarctic), *Bulgarian Antarctic Research Life Sciences*, 2: 43-47.

Golemansky, V. G. (1998) Interstitial testate amoebae (rhizopoda: Arcellinida and Gromida) from the Finnish Coast of the Baltic Sea and summary checklist of the interstitial testate amoebae in the Baltic Sea, *Acta Protozoologica*, 37: 133–137.

Gordon, A. L. (1986) Interocean exchange of thermocline water, *Journal of Geophysical Research,* 91: 5037–5046.

Green, J.L., Bohannan, B. J. M. and Whitaker, R. J. (2008) Microbial biogeography: from taxonomy to traits, *Science*, 320: 1039–1043.

Gruber, N., Gloor, M., Mikaloff-Fletcher, S. E., Doney, S. C., Dutkiewicz, S., Follows, M. J., Gerber, M., Jacobson, A. R., Joos, F., Lindsay, K., Menemenlis, D., Mouchet, A., Müller, S. A., Sarmiento, J. L. and Takahashi, T. (2009) Oceanic sources, sinks, and transport of atmospheric CO_2, *Global Biogeochemical Cycles*, 23: GB1005.

Hansell, M. (2011) Houses made by protists, *Current Biology*, 21(13): R485–R487.

Heger, T. J., Mitchell, E. A. D., Ledeganck, P., Vincke, S., van de Vijver, B. and Beyens, L. (2009) The curse of taxonomic uncertainty in biogeographical studies of free-living terrestrial protists: a case study of testate amoebae from Amsterdam Island, *Journal of Biogeography*, 36 (8): 1551–60.

Henman, J. and Poulter, B. (2008) Inundation of freshwater peatlands by sea level rise: Uncertainty and potential carbon cycle feedbacks, *Journal of Geophysical Research*, 113.

Hodgson, D. A. and Sime, L. C. (2010) Southern westerlies and CO_2, *Nature Geoscience*, 3: 666–67.

Hodgson, D. A., Graham, A. G. C., Roberts, S. J., Bentley, M. J., Cofaigh, C. O., Verleyen, E., Wyverman, W., Jomelli, V., Favier, V., Brunstein, D., Verfaillie, D., Colhoun, E. A., Saunders, K. M., Selkirk, P. M., Mackintosh, A., Hedding, D. W., Nel, W., Hall, K., McGlone, M. S., Van der Putten, N., Dickens, W. A. and Smith, J. A. (2014) Terrestrial and submarine evidence for the extent and timing of the Last Glacial Maximum and the onset of deglaciation on the maritime-Antarctic and sub-Antarctic Islands, *Quaternary Science Reviews*, 100: 137–58.

Holland, P. R., Bracegirdle, T. J., Dutrieux, P., Jenkins, A. and Steig, E. J. (2019) West Antarctic ice loss influenced by internal climate variability and anthropogenic forcing, *Nature Geoscience,* 12: 718-724.

Hulton, N. R. J., Purves, R. S., McCulloch, R. D., Sugden, D. E. and Bentley, M. J. (2002) The Last Glacial Maximum and deglaciation in southern South America, *Quaternary Science Reviews*, 21: 233–41.

Jassey, V. E J., Chiapusio, G., Binet, P., Buttler, A., Laggoun-Défarge, F., Delarue, F., Bernard, N., Mitchell, E. A. D., Toussaint, M-L., Francez, A-J. and Gilbert, D. (2013) Above- and belowground linkages in Sphagnum peatland: climate warming affects plant-microbial interactions, *Global Change Biology*, 19 (3): 811–23.

Kalnay, E., Kanamitsu, M., Kistler, R., Collins, W., Deaven, D., Gandin, L., Iredell, M., Saha, S., White, G., Woollen, J., Zhu, Y., Chelliah, M., Ebisuzaki, Higgins, W., Janowiak, J., Mo, K. C., Ropelewski, C., Wang, J., Leetmaa, A., Reynolds, R., Jenne, R. and Joseph, D. (1996) The NCEP/NCAR 40-Year Reanalysis Project, *Bulletin of the American Meteorological Society*, 77: 437-471.

Kilian, R. and Lamy, F. (2012) A review of Glacial and Holocene paleoclimate records from southernmost Patagonia (49-55°S), *Quaternary Science Reviews*, 53: 1–23.

Kleinebecker, T., Hölzel, N. and Vogel, A. (2008) South Patagonian ombrotrophic bog vegetation reflects biogeochemical gradients at the landscape level, *Journal of Vegetation Science*, 19 (2): 151–60.

Knudson, K. P., Hendy, I. L. and Neil, H. L. (2011) Re-examining Southern Hemisphere westerly wind behavior: insights from a late Holocene precipitation reconstruction using New Zealand fjord sediments, *Quaternary Science Reviews*, 30: 3124–38.

Kohfeld, K. E., Graham, R. M., de Boer, A. M., Sime, L. C., Wolff, E. W., Le Quéré, C. and Bopp, L. (2013) Southern Hemisphere westerly wind changes during the Last Glacial Maximum: paleo-data synthesis, *Quaternary Science Reviews*, 68: 76–95.

Kosakyan, A., Gomaa, F., Lara, E. and Lahr, D. J. G. (2016) Current and future perspectives on the systematics, taxonomy and nomenclature of testate amoebae, *European Journal of Protistology*, 55: 105–117.

Krashevska, V., Bonkowski, M., Maraun, M. and Scheu, S. (2007) Testate amoebae (protista) of an elevational gradient in the tropical mountain rain forest of Ecuador, *Pedobiologia*, 51: 319–331.

Krashevska, V., Sandmann, D., Maraun, M. and Scheu, S. (2013) Moderate changes in nutrient input alter tropical microbial and protist communities and belowground linkages, *The International Society for Microbial Ecology Journal*, 8: 1126–1134.

Lamy, F., Hebbeln, D., Röhl, U., Wefer, G. (2001) Holocene rainfall variability in southern Chile: a marine record of latitudinal shifts of the Southern Westerlies, *Earth and Planetary Science Letters,* 185: 369-382.

Lamy, F., Kilian, R., Arz, H. W., Francois, J-P., Kaiser, J., Prange, M. and Steinke, T. (2010) Holocene changes in the position and intensity of the southern westerly wind belt, *Nature Geoscience*, 3: 695–99.

Le Quéré, C., Rödenbeck, C., Buitenhuis, E. T., Conway, T. J., Langenfelds, R., Gomez, A., Labuschagne, C., Ramonet, M., Nakazawa, T., Metzl, N., Gillett, N. and Heimann, M. (2007) Saturation of the Southern Ocean CO_2 sink due to recent climate change, *Science,* 316: 1735-1737.

Leon, C. A., Gabriel, M., Rodriguez, C., Iturraspe, R., Savoretti, A., Pancotto, V., Benitez-Mora, A., Valdes, A., Diaz, M. F., Oberpaur, C., Domínguez, E., Fernandez, L. D., Mackenzie, R., Roland, T. P., Mauquoy, D. and Silva, C. (2021) Peatlands of Southern South America: a review, *Mires and Peat*, 27(3).

Magnan, G., Garneau, M. and Payette, S. (2014) Holocene development of maritime ombrotrophic peatlands of the St. Lawrence North Shore in eastern Canada, *Quaternary Research*, 82: 96–106.

Marcisz, K., Colombaroli, D., Jassey, V. E. J., Tinner, W., Kolaczek, P., Galka, M., Karpinska-Kolaczek, M., Slowinski, M. and Lamentowicz, M. (2016) A novel testate amoebae trait-based approach to infer environmental disturbance in *Sphagnum* peatlands, *Scientific Reports*, 1–11.

Markgraf, V., Bradbury, J. P., Schwalb, A., Burns, S. J., Stern, C., Ariztegui, D., Gilli, A., Anselmetti, F. S., Stine, S. and Maidana, N. (2003) Holocene palaeoclimates of southern Patagonia: limnological and environmental history of Lago Cardiel, Argentina, *The Holocene*, 13 (3): 597-607.

Marshall, G. J., Orr, A., van Lipzig, N. P. M and King, J. C. (2006) The impact of a changing Southern Hemisphere Annular Mode on Antarctic Peninsula summer temperatures, *Journal of Climate,* 19(20): 5388-5404.

Marshall, G. J. (2003) Trends in the Southern Annular Mode from Observations and Reanalyses, *Journal of Climate*, 16: 4134–43.

Mayewski, P. A., Maasch, K. A., Dixon, D., Sneed, S. B., Oglesby, R., Korotkikh, E., Potocki, M., Grigholm, B., Kreutz, K., Kurbatov, A. V., Spaulding, N., Stager, J. C., Taylor, K. C., Steig, E. J., White, J., Bertler, N. A. N., Goodwin, I. D., Simoes, J. C., Jana, R., Kraus, S. and Fastook, J. (2013) West Antarctica's Sensitivity to Natural and Human Forced Climate Change Over the Holocene, *Journal of Quaternary Science*, 28 (1): 40–48

Mayewski, P. A., Bracegirdle, T., Goodwin, I., Schneider, D., Bertler, N. A. N., Birkel, S., Carleton, A., England, M. H., Kang, J-H., Khan, A., Russell, J., Turner, J. and Velicogna, I. (2015) Potential for Southern Hemisphere climate surprises, *Journal of Quaternary Science*, 30 (5): 391–95.

Mayr, C., Wille, M., Haberzettl, T., Fey, M., Janssen, S., Lücke, A., Ohlendorf, C., Oliva, G., Schäbitz, F., Schleser, G. H. and Zolitschka, B. (2007) Holocene variability of the Southern Hemisphere westerlies in Argentinean Patagonia (52˚S), *Quaternary Science Reviews,* 26: 579-584.

McGlone, M. S., Turney, C. S. M., Wilmshurst, J. M., Renwick, J. and Pahnke, K. (2010) Divergent trends in land and ocean temperature in the Southern Ocean over the past 18,000 years, *Nature Geoscience*, 3 (9): 622–26.

Menveil, L., Timmerman, A., Mouchet, A. and Timm, O. (2008) Climate and marine carbon cycle response to changes in the strength of the Southern Hemispheric westerlies, *Palaeoceanography*, 23: PA4201.

Mitchell, E.A.D., Charman, D.J. and Warner, B.G., (2008) Testate amoebae analysis in ecological and palaeoecological studies of wetlands: past, present and future, *Biodiversity and Conservation*, 17: 2115–2137.

Moreno, P. I., Francois, J. P. Villa-Martinez, R. P. and Moy, C. M. (2009) Millennial-scale variability in Southern Hemisphere westerly wind activity over the last 5000 years in SW Patagonia, *Quaternary Science Reviews*, 28: 25–38.

Moreno, P. I., Francois, J. P., Moy, C. M. and Villa-Martínez, R. (2010) Covariability of the Southern Westerlies and atmospheric CO2 during the Holocene, *Geology*, 38 (8): 727–30.

Moreno, P. I., Vilanova, I., Villa-Martínez, R., Dunbar, R. B., Mucciarone, D. A., Kaplan, M. R., Garreaud, R. D., Rojas, M., Moy, C. M., De Pol-Holz, R., Lambert, F. (2018) Onset and Evolution of Southern Annular Mode-Like Changes at Centennial Timescale, *Scientific Reports,* 8: 3458.

Moreno, P. I., Francois, J. P. Villa-Martinez, R. P. and Moy, C. M. (2009) Millennial-scale variability in Southern Hemisphere westerly wind activity over the last 5000 years in SW Patagonia, *Quaternary Science Reviews*, 28: 25–38.

Moy, C. M., Dunbar, R. B., Moreno, P. I., Francois, J-P., Villa-Martínez, R., Mucciarone, D. M., Guilderson, T. P. and Garreaud, R. D. (2008) Isotopic evidence for hydrologic change related to the westerlies in SW Patagonia, Chile, during the last millennium, *Quaternary Science Reviews*, 27: 1335–49.

Musotto, L. L., Borromei., A. N., Bianchinotti, M. V. and Coronato, A. (2016) Late Quaternary palaeoenvironmental reconstruction of central Tierra Del Fuego (Argentina) based on pollen and fungi, *Quaternary International*, 442: 13-25.

Nicholls, K.H., MacIsaac, H.J. (2004) Euryhaline, sand dwelling testate rhizopods in the Great Lakes, *Journal of Great Lakes Research*, 30(1): 123–132.

NOAA (2016) NCEP reanalysis data provided by the NOAA/OAR/ESRL PSD, Boulder, Colorado, USA, from their website, http://www.esrl.noaa.gov/psd, accessed 24-06- 16.

Orr, J. C., Maier-Reimer, E., Mikolajewicz, U., Monfay, P., Sarmiento, J. L., Toggweiler, J. R., Taylor, N. K., Palmer, J., Gruber, N., Sabine, C. L., Le Quéré., C., Key, R. M. and Boutin, J. (2001) Estimates of anthropogenic carbon uptake from four three dimensional global ocean models, *Global Biogeochemical Cycles*, 15 (1): 43-60.

Patterson, R.T. and Kumar, A. (2002) A review of current testate rhizopod (thecamoebian) research in Canada, *Palaeogeography Palaeoclimatology Palaeoecology*, 180: 225– 51.

Perren, B. B., Hodgson, D. A., Roberts, S. J., Sime, L., Van Nieuwenhuyze, W., Verleyen, E. and Vyverman, W. (2020) Southward migration of the Southern Hemisphere westerly winds corresponds with warming climate over centennial timescales, *Communications Earth and Environment,* 1(58): 1-8.

Pritchard, H. D., Ligtenberg, S. R. M., Fricker, H. A., Vaughan, D. G., van den Broeke, M. R. and Padman, L. (2012) Antarctic ice-sheet loss driven by basal melting of ice shelves, *Nature,* 484: 502-505.

Purich, A., Cai, W. J., England, M. H. and Cowan, T. (2016) Evidence for link between modelled trends in Antarctic sea ice and underestimated westerly wind changes, *Nature Communications,* 7: 10409.

Putnam, A. E., Denton, G. H., Schaefer, J. M., Barrell, D. J. A., Andersen, B. G., Finkel, R. C., Schwartz, R., Doughty, A. M., Kaplan, M. R. and Schlüchter, C. (2010) Glacier advance in southern middle-latitudes during the Antarctic Cold Reversal, *Nature Geoscience*, 3: 700–704

Reason, C. J. C. and Rouault, M. (2005) Links between the Antarctic Oscillation and winter rainfall over western South Africa, *Geophysical Research Letters,* 32: L07705.

Reczuga, M, K., Swindles, G. T. Grewling, L. and Lamentowicz, M. (2015) Arcella peruviana sp. nov . (Amoebozoa : Arcellinida , Arcellidae), a new species

from a tropical peatland in Amazonia, *European Journal of Protistology*, 51 (5): 437–49.

Rignot, E. and Jacobs, S. S. (2002) Rapid Bottom Melting Widespread near Antarctic Ice Sheet Grounding Lines, *Science*, 296: 2020–23

Roberts, S. J., McCulloch, R., Van Nieuwenhuyze, W., Sterken, M., Heirman, K., Van Wichelen, J., Diaz, C., Van de Vyver, E., Emmings, J., Whittle, A., Hodgson, D. A., Vverman, W. and Verleyen, E. (2021) Late Glacial and Holocene history of the Última Esperanza region of Southern Patagonia, *Quaternary Science Reviews* (in review).

Roe, H. M., Charman, D. J. and Gehrels, W. R. (2002) Fossil testate amoebae in coastal deposits in the UK: implications for studies of sea-level change, *Journal of Quaternary Science*, 17 (5-6): 411–29

Royles, J., Amesbury, M. J., Convey, P., Griffiths, H., Hodgson, D. A., Leng, M. J. and Charman, D. J. (2013) Plants and soil microbes respond to recent warming on the Antarctic Peninsula, *Current Biology*, 23 (17) : 1702–6.

Royles, J., Amesbury., M. J., Roland, T. P., Jones, G. D., Convey, P., Griffiths, H., Hodgson, D. A. and Charman, D. J. (2016) Moss stable isotopes (carbon-13 , oxygen-18) and testate amoebae reflect environmental inputs and microclimate along a latitudinal gradient on the Antarctic Peninsula, *Oecologia*, 181 (3): 931–45.

Russell, J. L., Dixon, K. W., Gnanadesikan, A., Stouffer, R. J. and Toggweiler, J. R. (2006) The Southern Hemisphere Westerlies in a Warming World : Propping Open the Door, *Journal of Climate*, 19: 6382–90.

Rydin, H. and Jeglum, J. K. (2013) The Biology of Peatlands 2nd edn., Oxford University Press, Oxford, UK.

Santibanez, A. P. A., Kohshima, S., Scheihing, A. R. A., Silva, R. R., Jaramillo, M. J. I., Labarca, P. P. J. and Casassa,R. G. (2011) First Record of Testate Amoebae on Glaciers and Description of a New Species Puytoracia Jenswendti nov. sp. (Rhizaria, Euglyphida), *Acta Protozoologica*, 50: 1–14.

Saunders, K. M., Hodgson, D. A. and McMinn, A. (2009) Quantitative relationships between benthic diatom assemblages and water chemistry in Macquarie Island lakes and their potential for reconstructing past environmental changes, *Antarctic Science*, 21 (1): 35– 49.

Saunders, K. M., Hodgson, D. A., McMurtrie, S. and Grosjean, M. (2015) A diatom conductivity transfer function for reconstructing past changes in the Southern Hemisphere westerly winds over the Southern Ocean, *Journal of Quaternary Science*, 30 (5): 464–77.

Saunders, K. M., Roberts, S. J., Perren, B., Butz, C., Sime, L., Davies, S., Van Nieuwenhuyze, W., Grosjean, M. and Hodgson, D. A. (2018) Holocene

dynamics of the Southern Hemisphere westerly winds and possible links to CO_2 outgassing, *Nature Geoscience,* 11: 650-655.

Schimpf, D., Kilian, R., Kronz, A., Simon, K., Spötl, C., Wörner, G., Deininger, M. and Mangini, A. (2011) The Significance of chemical, isotopic, and detrital components in three coeval stalagmites from the superhumid southernmost Andes (53°S) as highresolution palaeo-climate proxies, *Quaternary Science Reviews*, 30: 443–59.

Scott, D.B. and Asioli, A. (2014) A Testate Rhizopod Assemblage in an Extreme Environment: The Antarctic Permanently Ice-covered Lake Hoare (Taylor Valley*), Journal of Foraminiferal Research*, 4: 177–186.

Sigman, D. M., Hain, M. P. and Haug, G. H. (2010) The polar ocean and deglacial cycles in atmospheric CO2 concentration, *Nature*, 466: 47-55.

Spence, P., Griffies, S. M., England, M. H., McC. Hogg, A., Saenko, O. A. and Jourdain, N. C. (2014a) Rapid subsurface warming and circulation changes of Antarctic coastal waters by poleward shifting winds, *Geophysical Research Letters*, 41: 4601–10.

Spence, P., van Sebille, E., Saenko, O. A., and England, M. H. (2014b) Using Eulerian and Lagrangian Approaches to Investigate Wind-Driven Changes in the Southern Ocean Abyssal Circulation, *Journal of Physical Oceanography*, 44 (2): 662–75.

Stager, J. C., Mayewski, P. A., White, J., Chase, B. M., Neumann, F. H., Meadows, M. E., King, C. D. and Dixon, D. A. (2012) Precipitation variability in the winter rainfall zone of South Africa during the last 1400 yr linked to the austral westerlies, *Climate of the Past*, 8: 877–87.

Steig, E. J. (2016) Cooling in the Antarctic, *Nature*, 535: 358–59.

Strother, S., Salzmann, U., Roberts, S. J., Hodgson, D. A., Woodward, J., Van Nieuwenhuyze, W., Verleyen, E., Vyverman, W. and Moreton, S. G. (2014) Changes in Holocene climate and the intensity of Southern Hemisphere Westerly Winds based on a high-resolution palynological record from sub-Antarctic South Georgia, *The Holocene*, 25 (2): 1–17.

Swindles, G. T. and Roe, H. M. (2007) Examining the dissolution characteristics of testate amoebae (Protozoa: Rhizopoda) in low pH conditions: Implications for peatland palaeoclimate studies, *Palaeogeography Palaeoclimatolog, Palaeoecology*, 252: 486–96.

Swindles, G. T., Amesbury, M. J., Turner, T. E., Carrivick, J. L., Woulds, C., Raby, C., Mullan, D., Roland, T. P., Galloway, J. M., Parry, L., Kokfelt, U., Garneau, M., Charman, D. J. and Holden, J. (2015a) Evaluating the use of testate amoebae for palaeohydrological reconstruction in permafrost peatlands, *Palaeogeography Palaeoclimatology Palaeoecology*, 424: 111–22.

Swindles, G. T., Morris, P. J., Mullan, D., Watson, E. J., Turner, E., Roland, T. P., Amesbury, M. J., Kokfelt, U., Schoning, K., Pratte, S., Gallego-Sala, A., Charman, D. J., Sanderson, N., Garneau, M., Carrivick, J., Woulds, C., Holden, J., Parry, L., Galloway, J. M. (2015b) The long-term fate of permafrost peatlands under rapid climate warming, *Scientific Reports*, 1–6.

Swindles, G. T., Reczuga, M., Lamentowicz, M., Raby, C. L., Turner, T. E., Charman, D. J., Gallego-Sala, A., Valderrama, E., Williams, C., Draper, F., Honorio Coronado, E. N., Roucoux, K. H., Baker, T. and Mullan, D. J. (2014) Ecology of Testate Amoebae in an Amazonian Peatland and Development of a Transfer Function for Palaeohydrological Reconstruction, *Microbial Ecology*, 68: 284–98.

Thompson, D. W. J. and Solomon, S. (2002) Interpretation of recent Southern Hemisphere climate change, *Science*, 296: 895-899.

Thompson, D. W. J., Solomon, S., Kushner, P. J., England, M. H., Grise, K. M. and Karoly, D. J. (2011) Signatures of the Antarctic ozone hole in Southern Hemisphere surface climate change, *Nature Geoscience*, 4: 741–49.

Toggweiler, J. R. and Russell, J. (2008) Ocean circulation in a warming climate, *Nature*, 451 (7176): 286–88.

Toggweiler, J. R., Russell, J. L. and Carson, S. R. (2006) Midlatitude westerlies, atmospheric CO_2, and climate change during the ice ages, *Paleoceanography*, 21: 1–15.

Toggweiler, J. R. (2009) Shifting Westerlies, *Science*, 323 (5920): 1434–35.

Tonello, M. S., Mancini, M. V. and Seppä, H. (2009) Quantitative reconstruction of Holocene precipitation changes in southern Patagonia, *Quaternary Research*, 72 (3): 410–20.

Turner, J., Bindschadler, R., Convey, P., di Prisco, G., Fahrbach, E., Gutt, J., Hodgson, D., Mayewski, P., and Summerhayes, C. (2009). Antarctic Climate Change and the Environment, Scientific Committee on Antarctic Research, Cambridge, UK.

Turney, C. S. M., Jones, R. T., Fogwill, C., Hatton, J., Williams, A. N., Hogg, A., Thomas, Z. A., Palmer, J., Mooney, S. and Reimer, R. W. (2016a) A 250-year periodicity in Southern Hemisphere westerly winds over the last 2600 years, *Climate of the Past*, 12: 189–200.

Turney, C. S. M., McGlone, M., Palmer, J., Fogwill, C., Hogg, A., Thomas, Z. A., Lipson, M., Wilmshurst, J. M., Fenwick, P., Jones, R. T., Hines, B. E. N. and Clark, G. F. (2016b) Intensification of Southern Hemisphere westerly winds 2000-1000 years ago: evidence from the subantarctic Campbell and Auckland Islands (52-50°S), *Journal of Quaternary Science*, 31(1): 12–19.

Ummenhofer, C. C. and England, M. H. (2007) Interannual extremes in New Zealand precipitation linked to modes of Southern Hemisphere climate variability, *Journal of Climate,* 20: 5418-5440.

Ummenhofer, C. C., Gupta, A. and England, M. H. (2009) Causes of late twentieth-century trends in New Zealand precipitation, *Journal of Climate,* 22: 3-19.

van Bellen, S., Mauquoy, D., Hughes, P. DM., Roland, T. P., Daley, T. J., Loader, N. J., Street-Perrott, F. A., Rice, E. M., Pancotto, V. A. and Payne, R. J. (2015) Late Holocene climate dynamics recorded in the peat bogs of Tierra del Fuego, South America, *The Holocene*, 1–13.

van Bellen, S., Mauquoy, D., Payne, R. J., Roland, T. P., Hughes, P. D. M., Daley, T. J., Loader, N. J., Alayne Street-Perrott, F., Rice, E. M. and Pancotto, V. A. (2017) An alternative approach to transfer functions? Testing the performance of a functional trait-based model for testate amoebae, *Palaeogeography Palaeoclimatology Palaeoecology,* 468: 173-183.

Van Breemen, N. (1995) How Sphagnum Bogs down Other Plants, *Trends in Ecology and Evolution*, 10 (7): 270–75.

Van Daele, M., Bertrand, S., Meyer, I., Moernaut, J., Vandoorne, W., Siani, G., Tanghe, N., Ghazoui, Z., Pino, M., Urrutia, R. and De Batist, M. (2016) Late Quaternary evolution of Lago Castor (Chile, 45.6°S): Timing of the deglaciation in northern Patagonia and evolution of the southern westerlies during the last 17 kyr, *Quaternary Science Reviews*, 133: 130–46.

Van der Putten, N., Hébrard, J. P., Verbruggen, C., Van de Vijver, B., Disnar, J-R., Spassov, S., de Beaulieu, J-L., De Dapper, M., Keravis, D., Hus, J., Thouveny, N. and Frenot, Y. (2008) An integrated palaeoenvironmental investigation of a 6200 year old peat sequence from Ile de la Possession, Iles Crozet, sub-Antarctica, *Palaeogeography Palaeoclimatology Palaeoecology*, 270: 179–95.

Van der Putten, N., Verbruggen, C., Ochyra, R., Verleyen, E. and Frenot, Y. (2010) Subantarctic flowering plants: pre-glacial survivors or post-glacial immigrants?, *Journal of Biogeography*, 37 (3): 582–92.

Van der Putten, N., Mauquoy, D., Verbruggen, C. and Björck, S. (2012) Subantarctic peatlands and their potential as palaeoenvironmental and palaeoclimatic archives, *Quaternary International*, 268: 65–76.

Van Nieuwenhuyze, W. (2015) Reconstruction of Holocene paleoenvironmental changes in the sub-Antarctic region, PhD thesis, University of Ghent. http://hdl.handle.net/1854/LU-7032839.

Vanneste, H., De Vleeschouwer, F., Martínez-Cortizas, A., von Scheffer, C., Piotrowska, N., Coronato, A. and Le Roux, G. (2015) Late-glacial elevated dust deposition linked to westerly wind shifts in southern South America, *Scientific Reports*, 1–10.

Varma, V., Prange, M., Merkel, U., Kleinen, T., Lohmann, G., Pfeiffer, M., Renssen, H., Wagner, A., Wagner, S. and Schulz, M. (2012) Holocene evolution of the Southern Hemisphere westerly winds in transient simulations with global climate models, *Climate of the Past*, 8: 391–402.

Vaughan, D. G., Marshall, G. J., Connolley, W. M., Parkinson, C., Mulvaney, R., Hodgson, D. A., King, J. C., Pudsey, C. J. and Turner, J. (2003) Recent rapid regional climate warming on the Antarctic Peninsula, *Climatic Change,* 60(3): 243-274.

Villa-Martínez, R. and Moreno, P. I. (2007) Pollen evidence for variations in the southern margin of the westerly winds in SW Patagonia over the last 12,600 years, *Quaternary Research*, 68: 400–409.

Violle, C., Navas, M.L., Vile, D., Kazakou, E., Fortunel, C., Hummel, I. and Garnier, E. (2007) Let the concept of trait be functional!, *Oikos*, 116(5): 882-892.

Watson, A. J., Meredith, M. P. and Marshall, J. (2014) The Southern Ocean, carbon and climate, *Philosophical Transactions of the Royal Society A*, 372: 1-4.

Whittaker, T. E., Hendy, C. H. and Hellstrom, J. C. (2011) Abrupt millennial-scale changes in intensity of Southern Hemisphere westerly winds during marine isotope stages 2 – 4, *Geology*, 39: 455–59.

Whittle, A. and Gallego-Sala, A. V. (2016) Vulnerability of the peatland carbon sink to sealevel rise, *Scientific Reports*, 1-11.

Yeates, G. W. and Foissner, W. (1995) Testate amoebae as predators of nematodes, *Biology and Fertility of Soils,* 20: 1-7.

Yeloff, D., Mauquoy, D., Barber, K., Way, S., van Geel, B. and Turney, C. S. M. (2007) Volcanic Ash Deposition and Long-Term Vegetation Change on Subantarctic Marion Island, *Arctic Antarctic and Alpine Research*, 39 (3): 500–511.

Yu, Z., Loisel, J., Brosseau, D. P., Beilman, D. W. and Hunt, S. J. (2010) Global peatland dynamics since the Last Glacial Maximum, *Geophysical Research Letters*, 37: 1–5.

Zapata, J. and Fernández, L.D. (2008) Morphology and Morphometry of Apodera vas (Certes, 1889) (Protozoa: Testacea) from Two Peatlands in Southern Chile, *Acta Protozoologica*, 47: 389–395.

Zimmermann, C., Jouve, G., Pienitz, R., Francus, P and Maidana, N. I. (2015) Late Glacial and Early Holocene cyclic changes in paleowind conditions and lake levels inferred from diatom assemblage shifts in Laguna Potrok Aike Sediments (southern Patagonia, Argentina), *Palaeogeography Palaeoclimatology Palaeoecology*, 427: 20–31.

Chapter 2

Testate amoebae of the Southern Ocean region and their use in palaeoenvironmental studies: where do we go from here?

2.1. Introduction

Testate amoebae are unicellular eukaryotes, comprised of at least three unrelated taxonomic groups that include the orders of Arcellinida, Euglyphida, and Stramenopila (Kosakyan et al., 2016). All organisms within this polyphyletic assemblage are unified by the presence of a shell (test), which encapsulates the cell and can be comprised of proteinaceous, calcareous or siliceous materials. Tests are characterised by at least one aperture (opening) which allows part of the cytoplasm that surrounds the cell nuclei, to protrude. Termed the pseudopodium, this facilitates feeding, attachment to substrates, and movement (Hansell, 2011). Tests are either self-secreted (termed idiosomic), or comprised of agglutinations of particles collected from either prey organisms (e.g. diatoms) or the surrounding environment (termed xenosomic). Although all unicellular, size ranges greatly between different taxa spanning an order of magnitude from ~15 to over 250 µm in length. Distinctive morphologies and test architectures permit identification to a low taxonomic level. Crucially tests are also resistant to decay, which allows identification of both living and dead specimens that can be collected from sub-fossil sediment.

Testate amoebae play a key role within microbial food-webs (e.g. Gilbert et al. 1998; Mitchell et al. 2003; Mitchell 2004; Jassey et al. 2013a; Ju et al. 2014; Geisen et al. 2018): they are predominantly heterotrophic, and use a range of food sources including bacteria, fungi, organic material, micro-metazoa (e.g. rotifers and nematodes) and other protists (Yeates and Foissner, 1995; Gilbert et al, 2000; Geisen et al, 2015; Dumack et al, 2018). Certain (mixotrophic) species also contain endosymbionts (green algae) that are capable of photosynthesis and provide energy to the cell during periods when other prey are unavailable (Jassey et al. 2013b; Marcisz et al. 2016; van Bellen et al. 2017).

To date, approximately two-thousand species of testate amoeba have been described (Mitchell et al, 2008). They are found ubiquitously in almost all freshwater environments on Earth including mosses, soils, lakes, running water

and even the surface of glaciers (Santibaneza et al. 2011). The highest abundance and diversity of species is found in warm regions that experience high rainfall and that have high soil organic matter content (e.g. tropical and temperate rainforests (Krashevska et al. 2017)). Nevertheless, colder climate environments, and even the extreme polar latitudes, also support a significant testate amoeba fauna (e.g. Patterson and Kumar, 2002; Royles et al. 2013; Scott and Asioli, 2014; Swindles et al, 2015a,b). The distribution of active communities also extends into moderately saline (brackish) environments including: marginal marine soils such as higher salt marshes (Roe et al. 2002; Barnett et al. 2017), lakes exposed to coastal inundation (Nicholls and MacIsaac, 2004), beaches (Golemansky, 1998; Golemansky and Todorov, 1999), and mangroves (Duleba and Debenay, 2003).

Communities are known to respond strongly to a range of abiotic stimuli, both in terms of shifting patterns in the relative abundance of individual species (e.g. Charman et al. 1997; Gehrels et al. 2001; Payne et al. 2006; Amesbury et al. 2016) and at the community level, in terms of overall productivity and biomass (e.g. Royles et al. 2013; Amesbury et al. 2017; Whittle et al. 2019; Chapter 4-6). Exploiting these responses to abiotic stimuli, recent research has increasingly focussed on extracting palaeoenvironmental information from fossil assemblages preserved in sediment records. In such studies, testate amoebae have now been used as bioindicators of various environmental variables including: pH (e.g. Mitchell et al. 2013), temperature (e.g. Royles et al. 2013; Amesbury et al. 2017; Charman et al. 2018), salinity (e.g. Whittle et al. 2019; Chapter 4-6), and sea-level change (e.g. Charman et al, 1998 ; Gehrels et al. 2001; Barnett et al. 2017). Despite the applicability to address these palaeoenvironmental questions, testate amoebae are most established as a proxy for the reconstruction of hydrological parameters, particularly water-table depth in ombrotrophic peatlands. These moisture related parameters have long been identified as a primary ecological variable governing the structure of testate amoeba communities (e.g. Jung, 1936), and this relationship has been rigorously and widely tested with quantitative ecological techniques (Amesbury et al, 2016). Application of a transfer function is central to most contemporary palaeoenvironmental research using testate amoebae. These statistical tools apply known environmental optima and tolerance of living specimens of different species (collected from surface samples spaced along an environmental gradient, e.g. from high to low water-

table level) to infer a semi-quantitative estimate of past environmental conditions from sub-fossil specimens found in a sediment core (Imbrie and Kipp, 1971; Warner and Charman, 1994; Woodland et al. 1998). Such techniques have become an established part of the palaeoenvironmental toolkit, and have been applied widely throughout the world, from the high northern latitudes (e.g. Li et al, 2015; Swindles et al. 2015a,b; Zhang et al., 2018), temperate regions (Amesbury et al. 2016, 2018), the tropics (e.g. Swindles et al. 2014) and southern extratropics (Charman, 1997; van Bellen et a. 2015).

Studies of both the taxonomy and biomonitoring applications of testate amoebae within the Northern Hemisphere strongly outweigh those from the South. Within the Southern Hemisphere, islands in the Southern Ocean and the continental Antarctic can be considered frontiers, remaining amongst the most understudied places by both taxonomists and palaeo-ecologists. Environmental conditions in this region can be some of the harshest of anywhere on Earth, with challenges to colonisation posed by low mean annual temperatures, limited free water availability, extreme seasonality, geographical isolation, and low levels of resource supply in comparison with lower latitudes (Lawley et al. 2004; Bokhorst et al. 2007). Yet not all environments are prohibitively hostile for communities of testate amoebae and there exist potential palaeoenvironmental archives in which they are likely to be found (e.g. Royles et al. 2012; Van der Putten, 2012a; Loisel et al. 2017; Supplementary Fig. 2.1).

For the first time, this review covers the known diversity and distribution of testate amoebae throughout the Southern Ocean region. In presenting the state of current research, we aim to; 1) provide a framework to help identify the pressing research questions needed to advance the study of testate amoeba taxonomy and distribution in this region, and 2) to explore the possible opportunities and challenges to their future application in regional palaeoenvironmental studies.

First we introduce the geographical setting (Section 2.2) and methods used in the compilation of records (Section 2.3). Sections 2.4.1-2.4.3 then explore the current known diversity of the Southern Ocean region, through a focus on the history of research, diversity of each geographical region, and an analysis of the trends in diversity that are apparent within those regions. Sections 2.4.4 and 2.4.5 subsequently focus on the use of testate amoebae in palaeoenvironmental

research, exploring both the challenges currently presented and the future direction of such research.

2.2. Geographical setting

The Southern Ocean region comprises areas to the south of the subtropical front (Rintoul, 2011) and is divided here into four major components; (1) the sub-Antarctic (South Georgia, Marion Island, Iles Crozet, Iles Kerguelen, Heard Island, Macquarie Islands (following Van der Putten et al. 2012a)); (2) other islands in the Southern Ocean between 40-55˚S, and the maritime Antarctic which we further divide into (3) islands and archipelagos of the scotia-arc (South Shetland, South Orkney, South Sandwich Islands, Bouvet Island) and (4) the Antarctic peninsula (Fig. 2.1).

Islands in the Southern Ocean between 40-55˚S exhibit comparatively benign temperate oceanic climates, with mean monthly temperatures that do not drop below 0˚C, even during winter (e.g. Broughton and McAdam, 2005). Precipitation mostly falls as rain and vegetation and soils are generally abundant and well developed.

Most of the sub-Antarctic Islands lie further south (50-60˚S) clustered mainly within 10-15 degrees of the polar front, an oceanic and climate boundary at the meeting point between warmer waters of the lower latitudes and the Antarctic Circumpolar Current (ACC) (Fig. 2.1). These small islands are grouped by the ocean basins in which they occur; 1) Atlantic (South Georgia), 2) Indian (Marion Island, Iles Crozet, Iles Kerguelen and Heard Island), and 3) Pacific (Macquarie Island). Lying further south beyond the extent of the winter ice-pack the climate of the sub-Antarctic is oceanic and cool. Mean annual temperatures remain above 0˚C, and precipitation predominantly falls as rain (Pendlebury and Barnes-Keoghan, 2007). In contrast to areas further south, water availability is not a limiting factor. Average precipitation generally exceeds 1000 mm and leads to the presence of pools and streams (van de Vijver and Beyens, 1999). The islands are located within the core of the Southern Hemisphere Westerly winds, which peak in strength between 50 and 55˚S (Lamy et al. 2010) and constitute an important feature of the environment (Hodgson et al. 2014). Although extensive in coverage, sub-Antarctic vegetation consists of a low number of phanerogams and is devoid of tree species making it incomparable with equivalent latitudes in

the north (Van der Putten et al., 2012b). Soils are often well developed and cloak a large amount of the landscape, no permafrost is present.

The maritime Antarctic comprises archipelagos of the Scotia arc (South Orkney, South Shetland and South Sandwich Islands) and the west coast of the Antarctic Peninsula, a narrow landmass projecting ~1250 km north of the main continent (Fig. 2.1). The climate is harsher than the sub-Antarctic and highly seasonal, with considerable marine influence in summer when sea-ice reaches its minimum extent. Mean air temperatures are generally negative for most of the year (Convey, 2003) and liquid water is limited. Sufficient moisture to support the growth of plants becomes available following the spring snow melt and summer precipitation (Royles et al., 2012), although inland waterbodies are sparse (Heywood, 1977). The flora is dominated by cryptograms with only two species of higher plants (Convey et al. 2011). Soils are comparatively sparse within the landscape and less developed than in the sub-Antarctic. They are typically moist, low in organic matter, and lacking physical stability, with freeze-thaw action leading to overturning and the development of patterned ground (Lawley et al. 2004). Landscapes become progressively less verdant with distance south. The Antarctic Peninsula consists of terrain similar to the southern cordillera of the Andes, and is near totally ice covered. Limited ice-free patches, mainly close to the coast, are sparsely colonised by mosses (see overview of Antarctic Peninsula vegetation provided in Smith (1996)).

Although falling partly within the geographical scope of this review, the continental mainland of South America, including Tierra del Fuego, is omitted and readers are referred to Fernández et al. (2015) for a comprehensive checklist of testate amoebae in Chile. Testate amoebae of the continental Antarctic, also omitted from this review, are included in a recent checklist of heterotrophic protists compiled by Thompson et al. (2019).

2.3. Methods

Database compilation. We conducted extensive searches for records of testate amoebae within Web of Science, Google Scholar, Biodiversity Heritage Library and the archives of the British Antarctic Survey (Cambridge). Citations within the resultant records were used to identify relatively inaccessible and historical works

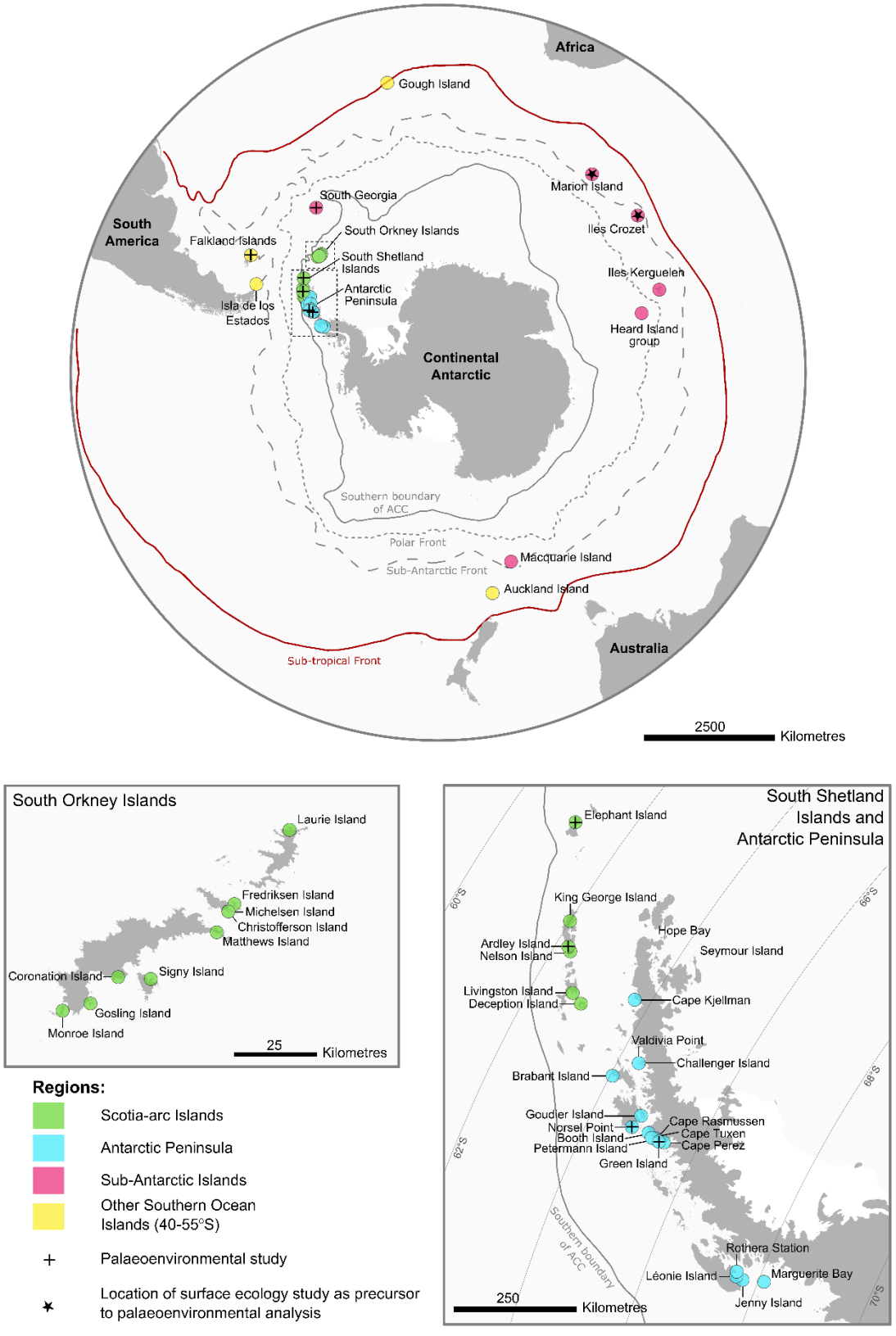

Figure 2.1 | Distribution of existing records of testate amoeba diversity within the Southern Ocean region.

not listed in online catalogues. No age limit was set for inclusion of historical works.

Definition of testate amoeba morphospecies (herein referred to as species) relies principally on variation in test (shell) morphology, size and construction style, and occasionally aspects of the cell that can only be observed in live specimens. Subjective decisions by analysts are needed to determine the level of intraspecific variation that is acceptable before a taxon is either (1) grouped with an existing taxon, or (2) designated a new species or sub-specific taxon. Consequently, the status of many varieties ('v.', 'var.') and forms ('f.') is often questionable because they are designated without detailed descriptions, lack support from sufficient morphological data, and/or are based on features with limited taxonomic significance. To ensure standardisation between studies, which are likely to have been conducted at varying taxonomic resolutions, we adopt a conservative approach where only 'full species' are included in the database. Identified varieties or forms (subspecific and infrasubspecific taxa) are grouped with their closest full species designation. Our approach also takes into account the potential occurrence of adaptive polymorphism (Schonborn, 1992) and morphological plasticity (Wanner, 1995; 1999, Bobrov and Mazei, 2004), the potential for which remains largely understudied in the Southern Ocean region (Roland et al, 2017).

All records were processed to update taxonomic nomenclature and possible synonymies were removed prior to incorporation into the database. Only studies where taxa were identified at genus level (or lower) were included. Identifications made only to genus level (e.g. *Difflugia* spp.) were assembled in a secondary list of 'taxa'. Taxonomy was based on Mazei and Tsyganov (2006), Todorov and Bankov (2019), and Mazei and Warren (2012, 2014, 2015).

Despite these taxonomic decisions to homogenise existing data, identification errors within original sources are expected and considered an important caveat to the use of the species list presented here. Misidentifications are likely to have arisen as a combined result of: the age range of studies, continual progress in microscopy, taxonomic developments, varying identification references applied between studies and differing levels of taxonomic expertise between analysts. However, assessing the accuracy of identifications is rendered impossible by the general absence of deposited slides, photographs or original sample material.

Therefore, beside updating taxonomic nomenclature we maintained all identifications made by original authors, despite known examples of taxonomic confusion. For example, identifications of *Difflugia globulosa* and *Phryganella acropodia* are known to have been used interchangeably. The primary separation of these species requires observations of living cells, yet whether live and/or sub-fossil specimens were examined is not known consistently for all studies (see Vincke et al. (2004a)). In such cases we therefore maintained both species and follow the designation made by the original authors of the study. Misidentifications of *Nebela collaris* are also expected, since confusion with specimens of *Nebela (Argynnia) dentistoma* within drawings published by Leidy (1879), a frequently used taxonomic resource, was identified by Penard (1902). Both species are relatively common among some faunas. Further, we synonymised *Tracheleuglypha acolla* and *Tracheleuglypha dentata*, following Ogden and Couteaûx (1988). Although more recent work suggest they may indeed be considered individual species (Todorov and Bankov, 2019), a number of studies included in this review were conducted close to the time of the Ogden and Couteaûx, (1988) publication, and it is not known which taxonomic guidelines had been followed by analysts.

Metadata including location, environment and habitat type, and sampling date were collected (Appendix 2). Studies were excluded where descriptions of sampling location or environment type had insufficient detail. The number of samples analysed in each study was recorded, and where this information was not stated we assume the number of samples to be equal to the number of sites in the study. Sample types were classified primarily by environment (aquatic, terrestrial or marine) and secondarily by habitat type (e.g. moss, organic sediment, streams; see Fig. 2.3).

Diversity analyses. The completed dataset was used to calculate the total known diversity of testate amoebae recorded to date within the Southern Ocean region, including both species and infraspecific taxa. Lists of compound diversity specific to each of the major regions and islands were derived from the dataset.

To account for variation in sampling effort (number of samples) between regions, sample-based rarefaction analysis was used to estimate the curve for diversity expected as a function of the number of samples observed. For comparison between regions, extrapolation of these curves to asymptote values (assuming

infinite sampling effort) was used to estimate true diversity, following Chao et al. (2014). Extrapolation curves were calculated up to double the reference sample size. Rarefaction (interpolation) and extrapolation curves, with 95% confidence intervals (bootstrapping, 100 replications) were constructed along with estimations of asymptote values, using 'R' (R core Team, 2017) and the package 'iNEXT' (Hsieh et al. 2020).

To assess variation in the latitudinal range of species we divided the Southern Ocean region into 5˚ bands from 40˚S to 65˚S. Known diversity, including aquatic and terrestrial environments, was then synthesised for all sites occurring in each band, and the number of bands that each species occupied was determined. The average distribution (in number of latitudinal bands) was then calculated for reported assemblages at each site, giving equal weighting to each species.

2.4. Results and Discussion

2.4.1. Known diversity of testate amoebae in the Southern Ocean region

A total of ~1,252 samples from 37 studies, 44 individual locations and dating from 1904 to present were identified (see Box 2.1). Table 2.1 lists all studies that were included in the compilation. The full database, which can be interrogated to provide species lists for both individual regions and islands, is available in Appendix 2.

Spatially, the distribution of existing samples in the Southern Ocean region are weighted heavily towards the sub-Antarctic islands, which account for 70% of the total inventory (Table 2.2). In all regions, the number of samples from terrestrial environments outweighs those from aquatic ecosystems, such as lakes and streams (Fig. 2.3). Within these terrestrial environments, collections have been made in a wide range of habitats, however the majority of attention has focussed on mosses and organic sediments, which together account for 75% of samples (Fig. 2.3). The most diverse range of habitats have been sampled in the sub-Antarctic, reflecting both the intensity of sampling and the presence of more complex environments compared to the maritime region. Although similarly complex landscapes with an abundance of suitable habitats for testate amoeba colonisation are present on other islands 40-55˚S, many of these are not represented by existing studies (Fig. 2.3).

Box 2.1: History of testate amoebae research in the Southern Ocean Region

Possibly the earliest published records of testate amoebae faunas in the southern high latitudes were derived from samples collected during an expedition to Cape Horn between 1882-1883 by Certes (1891). By the early 20th century more systematic studies had commenced on the remote islands within the Southern Ocean. The first included reports on the presence of several cosmopolitan taxa inhabiting moss cushions collected on Ile St Paul, Amsterdam Island, the Crozet archipelago, Heard Island, and Gaussberg (continental Antarctic), by the German South Polar Expedition in 1901-03 (Richters, 1904; Richters, 1907). Simultaneously, material was collected by the Swedish South-polar Expedition, on Isla de los Estados (Cape Horn), the Falkland Islands, South Georgia and the Antarctic Peninsula (Richters 1908). Further collections from sites on the Antarctic Peninsula were made several years later in 1908-1910 by the Deuxieme Expedition Antarctique Francaise and detailed observations of the faunas were reported by Penard (1913) (Fig. 2.2). Although outside the area covered in this study, early collections were also made on the Antarctic Continent (in the surroundings of Cape Royds, Ross Island), during Ernest Shackleton's British Antarctic (Nimrod) Expedition of 1907-1909 (Murray, 1910).

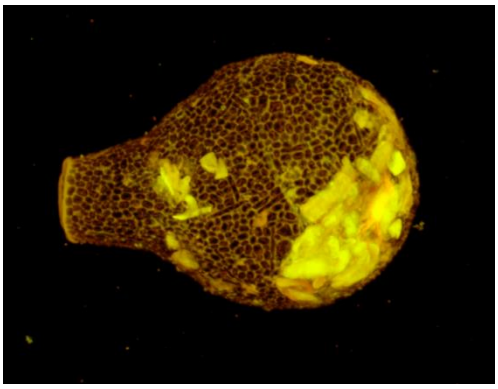

Figure 2.2 | Specimen of the testate amoeba species *Padaungiella lageniformis*. Collected during the Deuxieme Expedition Antarctique Francaise on Goudier Island (Antarctic Peninsula) in 1908, and imaged using a modern laser confocal microscope. Specimen held in the Penard Collection of glass testate amoebae slides at the Natural History Museum, London. Photograph source: Alex Whittle, Alex Ball and Richard Turney.

Cycles of research interest have occurred since these exploratory studies, however the extreme remoteness of the region has continually hindered access. Research efforts at sites not served by research stations have typically attempted to document the diversity found within a small number of samples collected during time-limited field campaigns. Most studies have stopped short of robust ecological investigation due to the absence of sufficient micro-environmental data and thorough sampling of available habitats. It was not until the 1970s that some of the first in-depth investigations of diversity and ecology were conducted (Smith, 1974, 1996; Bonnet, 1981; Beyens et al, 1995). Much of the research attention during this period focused toward quantifying the distribution of species, and ultimately the unique insights into microorganism biogeography that could be obtained in the region (see Wilkinson, 1994; Smith and Wilkinson, 2007; see also Wilkinson et al. 2011). Attempts were made throughout this period to map spatial distributions of taxa (Smith, 1978; Wilkinson, 1994), and explanations that invoked limiting dispersal and climatic conditions were made (Smith, 1996). However, insufficient sampling combined with nomenclatural confusion has hindered the continued use of this data as a suitable 'baseline list' for diversity.

In the mid-2000s further studies conducted extensive sampling in the sub-Antarctic and greatly increased the known diversity. Following these works, possible applications of testate amoebae as bioindicators were tentatively suggested for the first time (Vincke et al., 2004b; Vincke, et al., 2004c). Driven by widening acknowledgement of the importance of environmental changes in the Southern Ocean region for future global climate, and the role of palaeoecology studies in contextualising these changes, interest in the testate amoebae faunas has been reinvigorated in the past decade. Palaeoclimate information from previously unexplored archives has recently been unlocked by methodological advances in testate amoebae analysis (Royles et al., 2013; Whittle et al., 2019; Chapter 4-6).

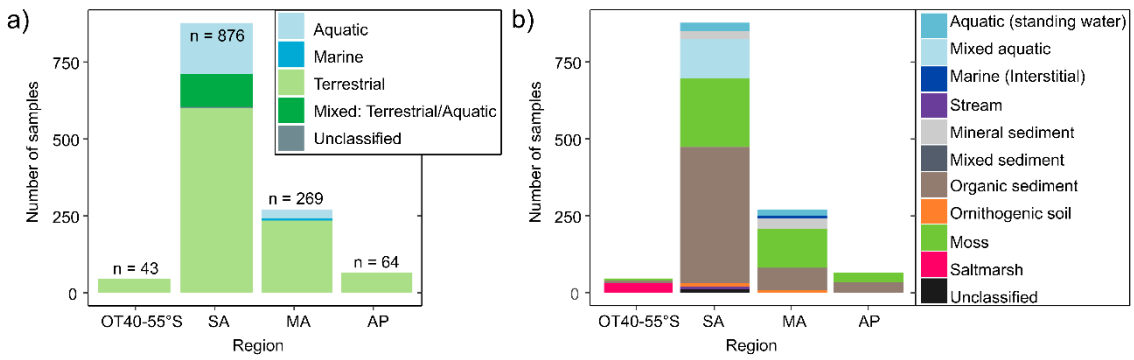

Figure 2.3 | Distribution of sampling efforts between environments (a) and habitats (b) of the Southern Ocean region. OT40-55˚S; Other Islands 40-55˚S, AP; Antarctic Peninsula, MA; Maritime Antarctic (Scotia-arc Islands), SA; Sub-Antarctic Islands.

Total known diversity consisted of 153 full species belonging to 52 genera. The terrestrial fauna contained the highest diversity of species (126), compared to 90 species found in aquatic environments. The majority of these species (72) occurred in both ecosystems. Diversity peaked in the Indian and Atlantic sectors of the sub-Antarctic and broadly declines southwards through the scotia-arc islands and Antarctic Peninsula (Fig. 2.4). Diversity within the major sub-divisions of the Southern Ocean region is summarised in Table 2.2.

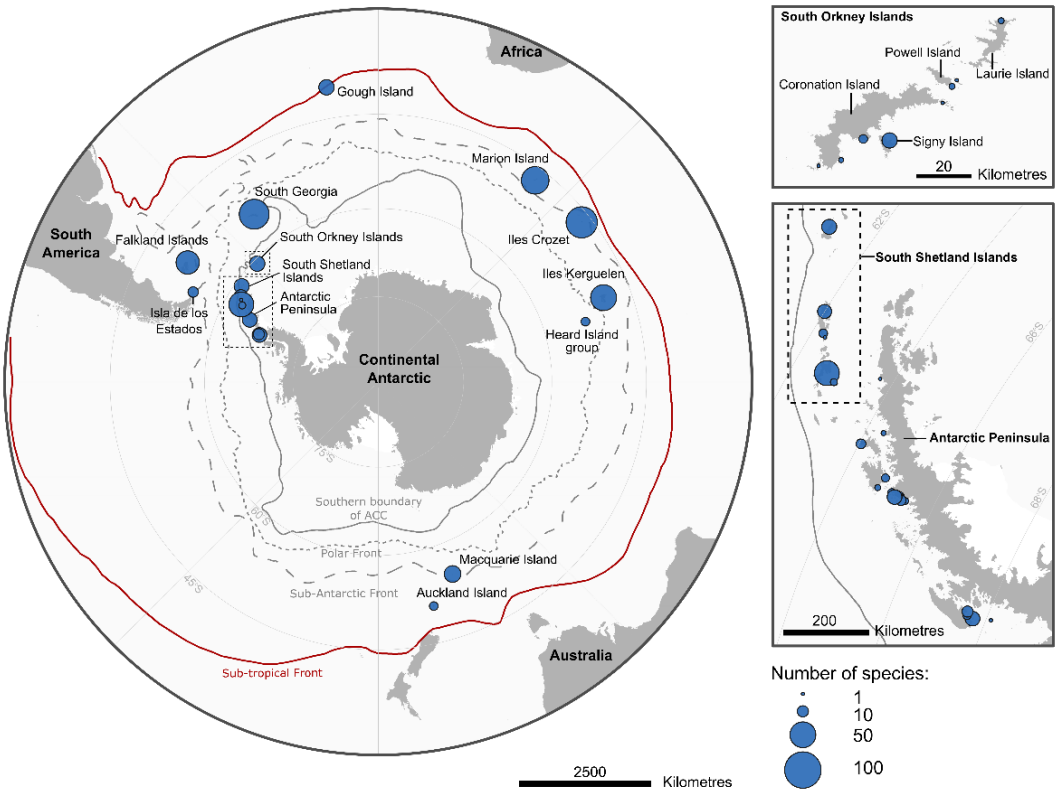

Figure 2.4 | Compound diversity of testate amoebae in the Southern Ocean region.

Table 2.1 | List of studies included in the compilation of the dataset.

Region	Location	Latitude	Longitude	Reference
Other Southern Ocean Islands (40-55˚S)	Auckland Island	-50.73	166.07	Penard (1911)
	Falkland Islands	-51.69	-57.85	Richters (1908) Smith (1970) Newton (2017)
	Gough Island	-40.31	-9.93	Murray (1908) Penard (1912) Sandon and Cutler (1924)
	Isla de los Estados	-54.75	-64.02	Richters (1908)
Sub-Antarctica (South Atlantic)	South Georgia	-54.26	-36.44	Richters (1908) Sandon and Cutler (1924) Smith (1982) Smith and Headland (1983) Beyens et al. (1995) Vincke et al. (2006a)
Sub-Antarctica (South Indian)	Heard Island	-53.12	73.73	Richters (1904) • Richters (1907)
	Ile de la Possession	-46.42	51.84	Richters (1904) • Richters (1907) Smith (1975) Vincke et al. (2004a,b,c) Vincke et al. (2006b) Vincke et al. (2007)
	Kerguelen Island	-49.22	69.43	Richters (1904) • Richters (1907) Bonnet (1981)
	Marion Island	-46.88	37.85	Grospietsch (1971) Whittle et al. (2019)
Sub-Antarctica (South Pacific)	Macquarie Island	-54.71	158.84	Penard (1911)
South Orkneys (Maritime Antarctic)	Christoffersen Island	-60.72	-45.03	Smith (1974)
	Coronation Island	-60.64	-45.71	Smith (1974)
	Fredriksen Island	-60.72	-44.98	Smith (1974)
	Gosling Island	-60.63	-45.91	Smith (1974)
	Laurie Island	-60.68	-44.48	Smith (1974)
	Matthews Island	-60.74	-45.16	Smith (1974)
	Michelsen Island	-60.72	-45.03	Smith (1974)
	Monroe Island	-60.59	-46.05	Smith (1974)
	Saddle Island			Smith (1974) Heal (1965)
	Signy Island	-60.70	-45.59	Smith (1973) Hawthorn and Ellis-Evans (1984)
South Shetlands (Maritime Antarctic)	Ardley Island	-62.21	-58.93	Royles et al. (2016)
	Deception Island	-62.92	-60.60	Penard (1913) Smith (1985)
	Elephant Island	-61.10	-54.88	Sandon and Cutler (1924) Smith (1972) Royles et al. (2016)
	King George Island	-62.00	-58.07	Penard (1913) Mieczan and Adamczuk (2015) Golemansky and Todorov (1999) Golemansky and Todorov (2004)
	Livingston Island	-62.70	-60.40	See also: Todorov and Golemansky (1996) Todorov and Golemansky (1999)
	Nelson Island*	-62.28	-59.05	Richters (1908)
Antarctic Peninsula (Maritime Antarctic)	Brabant Island	-64.03	-62.54	Smith (1987)
	Booth Island	-65.08	-64.01	Penard (1913)
	Cape Kjellmann	-63.72	-59.39	Richters (1908)
	Cape Perez	-65.40	-64.09	Penard (1913)
	Cape Rasmussen	-65.24	-64.08	Penard (1913)
	Cape Tuxen	-65.27	-64.12	Penard (1913)
	Challenger Island	-64.35	-61.57	Richters (1908)
	Goudier Island	-64.82	-63.49	Penard (1913)
	Green Island	-65.32	-64.151	Peanrd (1913) Royles et al. (2016)
	Jenny Island	-67.72	-68.38	Penard (1913)
	Léonie Island	-67.59	-68.34	Penard (1913)
	Marguerite Bay	-68.10	-68.08	Penard (1913)
	Moss Islands **			Richters (1908)
	Norsel Point	-64.76	-64.08	Royles et al. (2016)
	Paulet Island **			Richters (1908)

	Peterman Island	-65.17	-64.14	Penard (1913)
	Rothera Station	-67.56	-68.12	Smith (1986)
	Valdivia Point **			Richters (1908)
*	It is most likely from records of the expedition log that this sample was collected during a short visit ashore on Nelson Island.			
**	Samples examined but no testate amoebae observed.			
•	Provisional records with samples subjected to re-examination by a later study			

Table 2.2 | Regional diversity totals. Sampling effort refers to the number of samples observed.

Region	Number of locations	Sampling effort	Diversity (species)	Diversity (taxa)
Other Southern Ocean Islands (40-55˚S)	4	43	49	99
Sub-Antarctica (total)	6	876	127	220
Atlantic ocean region	1	301	67	82
Indian ocean region	4	573	106	132
Pacific ocean region	1	2	21	21
Scotia arc islands	34	333	69	83
South Orkney Islands	10	129	19	24
South Shetland Islands	6	140	58	64
Antarctic Peninsula	18	64	32	36

Other Southern Ocean Islands (40-55˚S)

The diversity of testate amoebae on islands outside of the sub-Antarctic (Van der Putten et al. 2012a) but lying in the Southern Ocean between 40 and 55˚S remains only vaguely known. We identified 43 samples of terrestrial environments collected from four locations; the Falkland Islands, Gough Island, Auckland Island and Isla de los Estados. Regional diversity comprises of 49 species (28 genera), with a further 10 taxa (17.0%) not identified to species level. Within this assemblage the majority of genera (19) are represented by only one species. Meanwhile, *Euglypha* and *Difflugia* are the most diverse genera with 6 species each.

The majority of samples in this region (77%) were collected from the Falkland Islands. In one of the first studies of testate amoebae on the Southern Ocean islands, Richters (1908) examined two samples of mosses from Port Stanley and Port Louis. A further three samples from peatlands were collected in 1969 and analysed by Smith (1970). Data was subsequently published as part of a wider

synthesis (Smith, 1978). One further study published close to this time by Vucetich (1975) could not be obtained for this review and consequently it is expected that the provisional total (41 species from 24 genera and 6 unidentified taxa), may underestimate the true known diversity of the islands. Recently, Newton (2017) examined samples from the surface of a salt-marsh as part of a reconstruction of past changes in sea-level, making this habitat the most heavily sampled in the region (see Fig. 2.3b).

Results of only two sampling expeditions have been published from Gough Island, and none have been conducted in recent decades. Known diversity consists of 18 species (12 genera) from 7 samples of mosses and organic sediment. Four taxa were not identified to species level. The first of these samples, a small fragment of moss collected in 1904, was examined by Murray (1908) and subsequently passed to Swiss protistologist Eugene Penard who designated one taxon (*Parmulina brucei*) as a new species (Penard, 1912). Having also been observed in the Columbian Andes the species was not considered endemic to the island. A further five samples of organic rich soil close to a sealers camp were obtained in 1922, and reported by Sandon and Cutler (1924). It is possible that non-native testate amoeba taxa brought to the island by humans, were included since it was remarked that 'common vegetables' had been cultivated by sealers, close to the sampling area.

Auckland Island and Isla de los Estados have each been sampled once, both more than 100 years ago. Reported diversity is very low with just 6 species (6 genera) and 8 species (7 genera) known respectively. No records were found for other islands occurring within this latitudinal band.

Sub-Antarctic Islands

Records of 17 studies from six distinct locations were identified in the sub-Antarctic region (Fig. 2.1). These studies comprise of 876 samples from which a total of 127 species and 39 genera have been observed. A compiled list of the currently reported diversity of the sub-Antarctic region, with details of the taxonomic updates applied, is provided in Supplementary Table 2.1. Across all sampled environments *Difflugia* and *Centropyxis* were the most diverse of these genera with 22 species (17.3% of the assemblage) and 17 species (13.4%) respectively. The genus *Euglypha* also represents a diverse component of the

assemblage (13 species, 10.2%). Known diversity from terrestrial environments is comparatively higher than aquatic ecosystems with 104 and 89 species respectively, however aquatic samples are significantly less numerous (163 compared to 602). Taxa identified only to genus level represent a major fraction of the assemblage (42.5%).

As part of statistical protocol, certain studies in the sub-Antarctic such as Vincke et al. (2004b) excluded samples containing a small number of individuals from analysis. In such cases it is not possible to determine whether this process led to the loss of possible rare species from the published fauna and consequently the underestimation of total diversity.

Communities of testate amoebae on île de la Possession are the most well studied in the sub-Antarctic, considering both the number of samples collected and range of environments they originate from. The fauna is also the most diverse with 73 species and 26 taxa observed from analysis of 467 samples. Despite sampling bias weighted toward terrestrial environments, aquatic and terrestrial faunas are similarly diverse (56 species, 91 samples and 60 species, 267 samples respectively). Moss dwelling species were observed by Richters (1907) and later by Vincke et al. (2004c) who developed a transfer function relating composition of assemblages to moisture-content. Communities inhabiting soils have been sampled throughout the island, including the soil surface (Smith, 1975; Vincke et al., 2004a), soils influenced by proximity to wandering albatross nests (Vincke et al., 2007), and vertical zonation within near surface layers (Vincke et al., 2006b). In a study dedicated solely to freshwater-bodies (Vincke et al., 2004b) observed a clear west to east gradient in community composition related to pH and conductivity, which is governed strongly by deposition of wind-blown salt-spray; a transfer function was developed for the former variable (see Section 2.4.5).

Within the fauna of île de la Possession, particularly in more recent studies, a high percentage of taxa remain unidentified beyond genus level (50.3%). This taxonomic uncertainty is attributed by the authors to limited regional morphological studies, possible insular endemism and environmentally induced plasticity within single genotypes. The current total diversity of ‘full species’ might therefore substantially underestimate true diversity. Whether numerous identifications to genus level (numbered sequentially as ‘Genus’ spp. 1, spp.2

etc.) are consistent between papers of different ages is an important caveat to the high diversity of taxa reported in studies conducted by Vincke. Since this is unclear from the literature, we treated these records as unique taxa, however this could indicate substantially over exaggerated diversity of taxa if indeed these designations were maintained consistently between different publications. After thorough searches of the literature one known record (Vanhoffen, 1908), also absent from an earlier list compiled by (Smith, 1978), could not be obtained. This early study contained a small number of samples and after thorough modern sampling it is not expected that additional taxa would be contributed to the current known diversity of the island.

Communities on other islands in the Indian Ocean province of the sub-Antarctic are also comparatively well known. Marion Island has only two published studies reporting an intriguing fauna comprised of 57 species from 40 samples. Grospietsch (1971) first examined twelve samples comprised of organic sediments, mosses and an aquatic sample from a stream. Peat environments were found to be the most diverse, notably supporting populations of species with Southern Hemisphere limited distributions (*Certesella certesi, C. martiali* and *Apodera vas*). Coastal environments influenced by salt-spray deposition were characterised by the absence of these large species, and instead were dominated by *Corythion dubium, Euglypha laevis,* and *Centropyxis* taxa.

Grospietsch (1971) described several new varieties and forms in addition to designating *Nebela (Argynnia) antarctica* as a new endemic species. However, this designation was based on morphological data taken from a limited number of specimens (n=38) and subsequent measurements of test size variation among *Argynnia* specimens on Amsterdam Island have questioned its validity (Heger et al. 2009). Within the Amsterdam Island population, test size variability was continuous, bridging the purported gap between *Argynnia dentistoma* and *A.antarctica* and conforming with the original description of the former taxa (Penard, 1890).

In the second study of testate amoebae on Marion Island, Whittle et al. (2019) investigated communities within a transect of variable coastal salt-spray deposition and demonstrated the suitability of changes in community biomass for bio-indication of salinity changes. One species (*Quadrulella symmetrica)* was

reported for the first time in the Southern Ocean region. No records of testate amoeba research on nearby Prince Edward Island were identified.

On Kerguelen Island, 50 species have been observed from 65 samples. In the most recent study, which represents the majority of sampling efforts, Bonnet (1981) reported a fauna consisting of mostly cosmopolitan species within samples taken from mosses, lichens, and organic deposits associated with common vegetation. An early report by Vanhoffen (1912) which is known to report 6 species, but not included in a review by Smith (1978), could not be located for inclusion in this compilation. Richters (1907) provided the initial and only other existing account of the fauna on Kerguelen Island, and also the only known study on Heard Island where just 6 species are so far known.

Only one record is available within the Pacific Ocean region of the sub-Antarctic (Fig. 2.4). This provisional record from Macquarie Island suggests a diverse fauna with 21 species yielded from just two samples (Penard, 1911).

South Georgia is the sole landmass within the Atlantic province of the sub-Antarctic. Sampling of both terrestrial (234 samples) and aquatic (67 samples) environments have revealed a total diversity of 67 species, with many present in both ecosystems (49 and 52 species respectively). Preliminary accounts were made from moss (Richters, 1908) and soil samples (Sandon and Cutler, 1924) although more thorough observations were not made until the 1980s. Smith (1982) compared the diversity of terrestrial dwelling communities with those of Kerguelen and Marion Island and suggested that the lower relative diversity on South Georgia related to its colder and drier climate. Active populations in four soil types were monitored by Smith and Headland (1983) through a 15 month period to examine the seasonal cycle in productivity. Aquatic environments from small pools to lakes >100 m long were surveyed by Beyens et al. (1995) and one taxon (*Microcorycia husvikensis*) which is thought to be endemic to South Georgia, was described as a new species (Beyens and Chardez, 1997; Badewitz, 2004).

Maritime Antarctic (Islands of the Scotia-arc and the western Antarctic Peninsula)

Islands of the Scotia-arc archipelago within the maritime Antarctic are relatively well sampled with 269 samples collected from both aquatic (28) and terrestrial

(234) environments. Known diversity consists of 62 species from 28 genera, and an additional 11 taxa not identified to species level. Highest diversity is found within the genera *Euglypha* (14.5% of the assemblage), *Difflugia* (11.3%) and *Centropyxis* (11.3%).

Within the South Orkney Islands 19 species have been reported from 129 samples. Taxa not identified to species level account for 20.8% of the assemblage. Peat soils associated with carpets of *Drepanocladus uncinatus* moss represent the only sampled environments on eight of these islands (Smith, 1974), whereas communities inhabiting soils beneath common vegetation (Heal, 1965), the benthos of freshwater lakes (Hawthorn and Ellis-Evans, 1984) and terrestrial mosses (Smith, 1973) have all been examined on Signy Island. Faunas collected on Signy Island are dominated by *Corythion dubium* and *Phryganella acropodia*, the later recorded in particularly high numbers in moss peats, grass soils and in association with *Prasiola* algae (Smith, 1973; 1978).

Records made by Smith from the South Orkney Islands are subject to some uncertainty uncovered in the compilation of this dataset. An unpublished record was identified within the British Antarctic Survey archives from 1969 purporting to show up to 49 taxa found within 91 samples collected from a variety of habitats on Signy Island (Smith, 1969). A full list of samples is given within this record, indicating location and sampling date. Subsequent reference is made to these within the published results of Smith (1978), where they are integrated with results from a further study concerning other islands in the South Orkney group, but excluding Signy (Smith, 1974). It is notable that this report by the same author suggests a much lower overall diversity of species throughout the whole South Orkneys (~11 species). A review published in 1996, without specific data sources, suggests a total diversity of ~26 species occurring in the South Orkney Islands (Smith, 1996). It is therefore not possible to isolate the diversity found by Smith on Signy Island alone, and therefore we omit these results from the data compilation. It is assumed that the large discrepancy in diversity between the first and subsequent reports is because the unpublished list from 1969 represented a provisional taxonomy, which was then revised at a later date.

Six reports of testate amoeba colonisation have been made from 140 samples taken in the South Shetland Islands and reveal a total of 58 species. Diversity is substantially elevated compared to other locations primarily because the fauna

of Livingston Island has been sampled extensively (79 samples) and collections have been made in habitats not investigated elsewhere, such as the marine littoral zone (Golemansky and Todorov, 1999, 2004; Todorov and Golemansky, 1999).

Corythion dubium and *Microcorycia radiata,* which was reported for the first time in the Antarctic, dominated the faunas of moss-banks on Ardley and Elephant Island (Royles et al. 2016). Earlier sampling of other terrestrial environments on these islands was also conducted by Sandon and Cutler (1924) and Smith (1972). On Deception Island, successional changes in the colonization of tephra from pyroclastic volcanic eruptions of varying age were studied by Smith (1985). With the exception of *Corythion dubium,* which appeared in deposits just 12 years old, testate amoebae were found only in tephra colonised by bryophytes and over 150 years old. No testate amoebae were identified after observations of earlier samples collected on the island (Penard, 1913). Terrestrial taxa on King George island have been studied by Penard (1913) and more recently by Mieczan and Adamczuk (2015).

The Antarctic Peninsula remains substantially less studied than the islands of the Scotia-arc archipelago. Here communities are generally dominated by a small number of globally ubiquitous taxa, especially *Corythion dubium* (Royles et al., 2016) and overall diversity comprises of 32 species from 15 genera. Compared with other regions, taxa not identified to species level represent a relatively small component of the total assemblage (11.1%). Similarly to locations further north, *Difflugia* and *Euglypha* are the most diverse genera (6 species, 18.8% of assemblage), although notably 3 species of the genus *Diplochlamys* are also known (Penard, 1913). Seven genera are represented by a single species.

Distribution of the 64 existing samples is highly dispersed throughout the Antarctic Peninsula, but generally clustered around established research stations. Many areas have been sampled only once during early exploration and not revisited in recent decades; the only observations from 11 sites are derived from reports in excess of 100 years old (Richters, 1908; Penard, 1913). More thorough sampling has been completed at Rothera Station (Smith, 1986), Brabant Island (Smith, 1987), and the fauna of moss banks at Norsel Point (Anvers Island), Green Island and Alexander Island have recently been studied in detail (Royles et al. 2013, 2016; Amesbury et al. 2017; Roland et al. 2017).

2.4.2. Completeness of sampling

To assess the completeness of species diversity, regional rarefaction curves were generated for each major environment type (Fig. 2.5). When all sampled environments were combined, a shallow point on the curve was reached for all regions, although the fauna of the Antarctic Peninsula remains significantly less complete than other regions (Table 2.3). This implies that existing observations are sufficient to capture the majority of species present. However, these curves represent only the faunas within the range of investigated habitats, which are shown to vary greatly between regions (Fig. 2.3).

True diversity at the regional scale can only be estimated with confidence if sampling sufficiently reflects the range of habitats available for testate amoeba colonisation. Because the overall complexity of ecosystems decreases with distance southwards we suggest that sampling on the Antarctic Peninsula, Scotia-arc and Sub-Antarctic Islands reflects available habitats, albeit in uneven proportions and with known exceptions (such as the absence of consistent sampling in the marine interstitial zone which is present in all regions but so far sampled only in the Scotia-arc Islands). However, within the region of other islands (40-55˚S), salt-marsh samples which dominate existing efforts, poorly represent the range of available habitats. Therefore, diversity in these locations is expected to be significantly underestimated. Capturing the heterogeneity of habitat types occurring on these islands is therefore a necessary priority for future sampling efforts.

Rarefaction curves based on current samples are also sensitive to the uneven distribution of sampling effort between individual habitats and environments. In regions where they have been studied, aquatic environments have been subjected to less sampling effort (Fig. 2.3). In the sub-Antarctic, rarefied species accumulation rates and extrapolated trajectories are similar to those from terrestrial environments, indicating that faunas derived from equal sampling effort are likely to be similarly diverse and suggest that aquatic sampling remains comparatively incomplete (Table 2.3). Conversely, on the Scotia-arc islands, aquatic species accumulation rates are much slower and nearing saturation, suggesting a species poor fauna compared to terrestrial environments, where the majority of species have already been captured. Unfortunately, further analysis

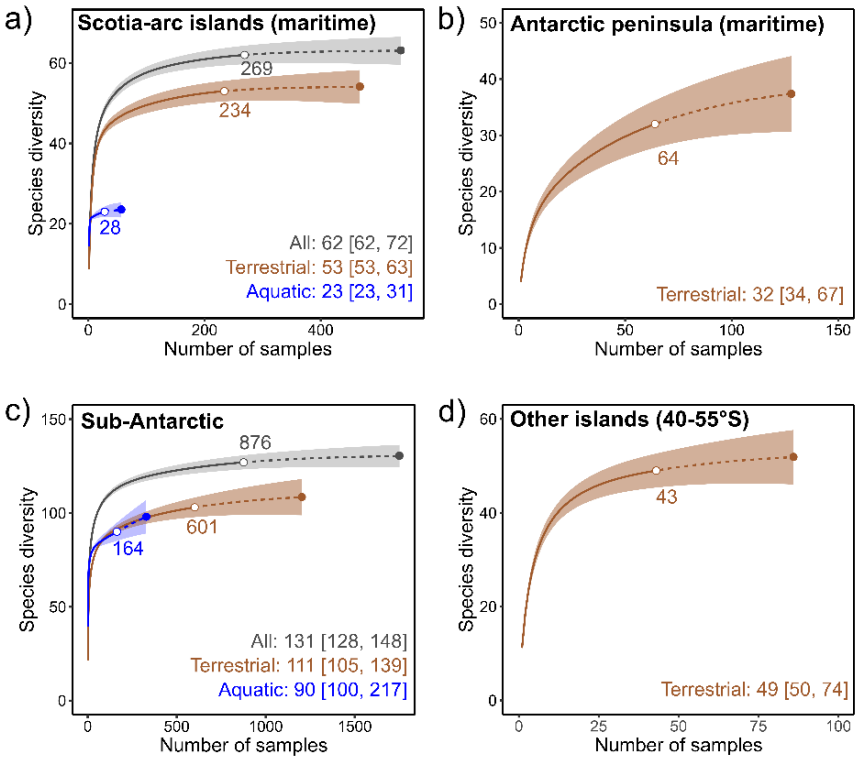

Figure 2.5 | Sample-based rarefaction (solid line) and extrapolation curves (dashed line) of regions and major environment types (terrestrial – brown, aquatic – blue, and total – grey) in the Southern Ocean region. a) Soctia-arc Islands, b) Antarctic peninsula, c) sub-Antarctic Islands, and d) other island in the southern ocean (40-55˚S). Extrapolations made to two times the total existing sampling effort for each environment. Rarefaction estimated as mean of 100 bootstrapping runs, to estimate 95% confidence intervals (shaded areas). Values in brackets indicate upper and lower estimates of asymptotic diversity.

Table 2.3 | Observed and predicted total diversity, by region.

Region	Environment type	Observed diversity (number of species)	Estimated total diversity (number of species)	Completeness (%)
Sub-Antarctic	All	127	131	97
	Terrestrial	103	111	93
	Aquatic	90	126	71
Southern Ocean Islands (40-55˚S)	Terrestrial	49	53	92
Scotia-arc islands	All	62	63	98
	Terrestrial	53	54	98
	Aquatic	23	24	96
Antarctic Peninsula	Terrestrial	32	40	80

of sampling completeness at scales more ecologically relevant to testate amoebae, is limited by the small number of samples for certain habitats (Fig. 2.3). However, while it is not possible to examine individual rarefaction curves, it is likely that highly sampled habitats such as mosses and organic sediments, are close to reaching completeness. Relatively under-sampled viable habitats, including standing water and the marine interstitial zone, are where undiscovered species are likely to be found. Priority should now focus on increasing the number of samples analysed from those habitats.

Beside habitats already sampled and represented in rarefaction analysis, it is expected that further diversity remains to be recorded from those absent from existing inventories. Previously unsampled environments, such as areas around hot volcanic springs or fumaroles which may have provided refugia during periods of glacial expansion (Convey and Lewis-Smith, 2006), are expected to yield further diversity and possibly currently undescribed taxa. Taxa not identified to species level are numerous through all regions on the Southern Ocean, but were not included in rarefaction analysis. Addition of these taxa, pending more thorough taxonomic analysis, is therefore likely to be a substantial source of additional diversity to all regions. Additionally, regional diversity totals are likely to increase once locations that are not well represented by current sampling efforts are included. Our analysis allows these regions to be identified, however we specifically suggest that targets for further sampling include Macquarie Island in the sub-Antarctic, and Bouvet Island in the Maritime Antarctic islands.

2.4.3. Regional trends in diversity

General ecological principles suggest that more extreme (stressful) environments are expected to be less biodiverse. Moving poleward through the Southern Ocean region, environmental stresses become progressively more severe, and corresponding declines in the diversity of many groups have been recorded, including arthropods, other protozoa, bacteria and lichens (e.g. Lawley et al. 2004, Rinnan et al, 2009).

Previous studies suggest that the diversity of testate amoebae broadly complies with this trend (Smith, 1982, 1996; Smith and Wilkinson, 1987). However, these assessments were limited by the relative paucity of data and consequential lack of accurate diversity totals. Substantially more records are now available. After

compiling and synthesising these records we applied sample-based rarefaction curves to calculate estimations of total species richness, in order to reduce the impact of variable sampling effort (between locations) on the observed diversity (Section 2.4.2). In contrast to previous assessments which used all available data (grouping both aquatic and terrestrial environments), we filtered the data so that only those from terrestrial environments are included. This is an important consideration when drawing direct comparisons of diversity between locations because aquatic environments are not present throughout the entire region, and variability in the severity of impacts of different climatic conditions on aquatic and terrestrial communities of testate amoebae is expected. We compared these estimates of total diversity with observational climate data collected from stations in the nearest proximity to the sampling sites.

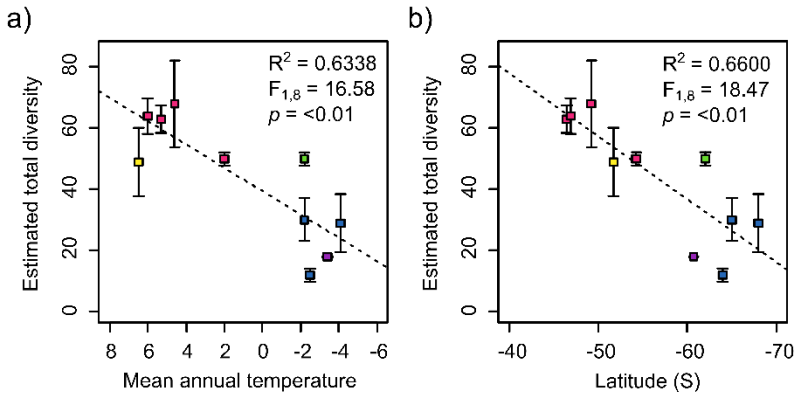

Figure 2.6 | Relationship of predicted species richness of testate amoeba in terrestrial environments to a) mean annual temperature and b) latitude, in the sub-Antarctic, Scotia-arc Islands, Antarctic Peninsula and other islands lying between 40-55˚S. Other Southern Ocean Islands (yellow), sub-Antarctic (red), South Shetlands Islands (green), South Orkney Islands (purple) and the Antarctic Peninsula (blue).

Significant relationships were found between diversity, mean annual temperature (R^2=0.63, p=<0.01) and latitude (R^2=0.66, p=<0.01) supporting the earlier assessments and suggesting that climatic conditions have an important impact on the diversity of testate amoeba communities throughout the region (Fig. 2.6). The South Shetland Islands in the Scotia-arc region represent a notable deviation from the overall trend with a diversity total that is significantly higher than would be expected for both the latitude and mean temperature of the islands (green data point, Fig. 2.6). This is particularly interesting since an earlier assessment indicated that the fauna of the islands was relatively depauperate for its latitude (Smith, 1982). The reason for this remains unclear, however the possibility of

authors subscribing to a more ‘splitting’ focussed taxonomic approach compared to those working in other regions, cannot be ruled out. If indeed this pattern of higher than expected diversity in the South Shetland Islands in the Scotia-arc region is proven to hold after further sampling throughout the region, it suggests that perhaps the relationship between diversity, latitude and climate is more complex and less linear than current data implies.

Unlike overall diversity, the proportion of species that are distributed over a wide latitudinal range increases with distance South; that is to say, species inhabiting more poleward sites are likely to occur over a greater latitudinal range, and can therefore be considered more generalist (Fig. 2.7a). Consequently, assemblages further south are shown to have considerably fewer species which are unique to the specific latitudinal band that they occur within, indicating that more southerly assemblages are predominantly species-poor subsets of those further to the north (Fig. 2.7b).

This pattern provides evidence in of support Rapoport’s rule, a macroecological principle that describes the tendency of species latitudinal ranges to increase with increasing latitude (Stevens et al. 1989). The occurrence of such a pattern in the range sizes of this important group of microbial eukaryotes in the Southern high-latitudes (spanning ~2,800 km from ~45-70˚S) is significant. Firstly, while many previous studies have observed trends consistent with this rule, a disproportionate number originate from the temperate North and frequently use short latitudinal transects, leading critics to argue that it is a localised phenomenon. Indeed, to date Rapoport’s rule is particularly understudied in the high latitudes of the southern hemisphere, leading to the suggestion that its applicability might be limited to the northern hemisphere, because of less land cover and narrower temperature ranges in the south (Gaston and Chown, 1999; Lundmark, 2006; Veter et al. 2013). Secondly, although support is available from studies of many groups of organisms (arthropods, reptiles, mammals, birds, plants and pathogens), very few have focused on the soil microbiome, which may display significant physiological and ecological differences (e.g. in providing more stable environmental conditions throughout the year). Although studies are rare, a recent study of soil fungi found a high mean latitudinal range size in Antarctic communities, and concluded in support of the rule (Cox et al. 2016).

A range of possible hypotheses have been proposed to explain the pattern, including; climatic variability (Stevens, 1989; France, 1992), climatic extremes (Pither, 2003), interspecific competition (Pianka, 1989), biogeographic boundaries and differing glacial (Blackburn and Gaston, 1996; Smith et al. 1994) and extinction histories (Araújo et al., 2008; Jansson, 2003). In the absence of sufficient data to assess the possible effects of interspecific competition, our data support a role of climate, although limitations in meridional dispersal across the Southern Hemisphere westerly wind belt cannot be ruled out. Further research would be beneficial in testing the observed relationship against more specific climatic variables (for example; seasonality, number of growing degree days, moisture availability).

Following this, if an insignificant role of dispersal limitation is assumed, the close relationship between climate and the distribution and diversity of testate amoebae suggests that there is potential for changing global climatic conditions to alter these patterns. Our results suggest that under increasing global temperatures more species are likely to colonise into the sub-Antarctic resulting in an increase in the species richness found there. Simultaneously, the range of species currently limited in distribution to the sub-Antarctic are likely to extend further south onto the Scotia-arc Islands and Antarctic Peninsula.

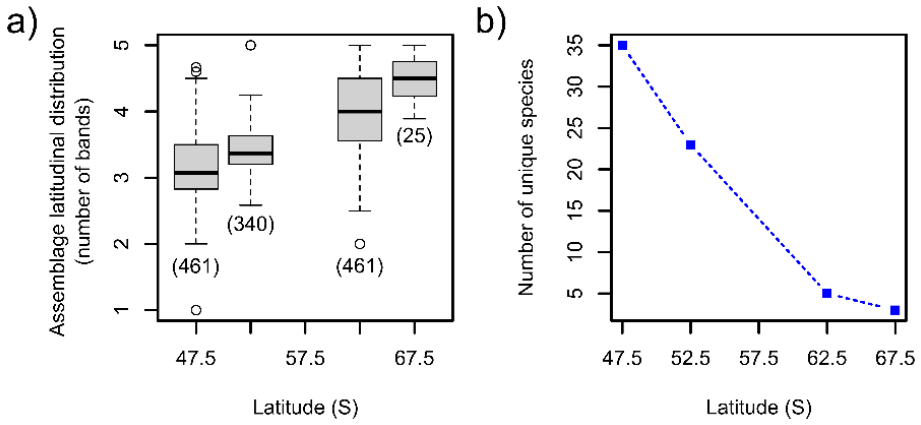

Figure 2.7 | a) Latitudinal range of taxa (measured in the number of 5˚ latitudinal bands averaged by assemblage). Bracketed values show the number of samples included in each band, b) number of unique species for each latitudinal band.

2.4.4. Testate amoebae based palaeoclimate analysis in the Southern Ocean region

Changes in the climate of the Southern Hemisphere high-latitudes have far-reaching implications for global climate, ocean circulation and sea-level change, yet many knowledge gaps remain. Palaeoclimatic reconstructions offer opportunities to gain a longer-term understanding of environmental evolution by providing records that far pre-date the instrumental record. These records can also be used to place recent changes within a longer-term context, and to provide the constraints required by models that provide a more mechanistic understanding of the environmental processes under investigation.

Although sparse, owing to the limited land-area, ecosystems that are known to record archives of environmental change are widely distributed throughout the Southern Ocean region, and offer substantial potential to help address major regional palaeoclimate questions (Chapter 1). However, suitable proxies to extract records are often lacking, primarily because 'standard' palaeoenvironmental methods from the Northern Hemisphere are generally not readily applicable (e.g. Van der Putten, 2012b).

Our data demonstrates the availability of widespread and well developed communities of testate amoebae, yet their potential as bioindicators of past environmental conditions in this region remains largely understudied. In Table 2.4 we summarise the challenges to the successful application of testate amoeba based proxies in the Southern Ocean region, and offer solutions for how these might be overcome in future studies.

2.4.5. Future directions

In this section we briefly outline possible directions and existing applications of testate amoeba based palaeoclimate research in the Southern Ocean region, focussing on the palaeoenivonmental parameters that they can help to reconstruct.

Water chemistry (conductivity and pH): The use of sub-Antarctic testate amoebae as bioindicators of conductivity has recently been demonstrated (Whittle et al. 2019; Chapter 4-6). One specific application of conductivity reconstructions is within a novel proxy that has been applied to advance

understanding of past changes in the Southern Hemisphere Westerly Winds (SHW) that blow over the Southern Ocean (see Saunders et al. 2015, 2018).

Changes in the pattern of these winds influence: the capacity of the Southern Ocean as a carbon and heat sink, ice-shelf stability on the Antarctic Peninsula and west-Antarctic ice-sheet, sea-ice extent, temperature on the Antarctic Peninsula, and the distribution of rainfall provided to surrounding mid-latitude continents. Despite the importance of the SHW, our understanding of how they have changed over longer timescales is limited because most existing reconstructions infer changes using archives from outside the core wind belt in southern South America, and typically rely on indirect proxies that are several steps removed from wind-conditions.

The approach relies on the response of testate amoebae (or other organisms such as diatoms, e.g. Saunders et al. 2018) to changes in the magnitude of wind-driven salt-spray aerosol deposition. On the sub-Antarctic Islands, which are located inside the core westerly wind belt, salt-spray aerosols are carried inland where they are deposited into otherwise freshwater environments in concentrations that are proportional to wind-strength. Observations have demonstrated a strong response of peatland-dwelling testate amoeba community productivity to salinization, with productivity decreasing significantly under higher salinity conditions (Whittle et al. 2019; Chapter 4). The use of community-level metrics (such as productivity) is advantageous in being less reliant on taxonomy than traditional transfer function based approaches and for allowing information to be extracted from low diversity assemblages (see Table 2.4). This technique has been applied as part of a multi-proxy analysis to reconstruct westerly wind changes on Bird Island (South Georgia) over both decadal (Chapter 5) and millennial (Chapter 6) timescales.

Testate amoeba communities inhabiting sub-Antarctic lakes may also offer further potential for the reconstruction of SHW. Vincke (2004b) developed a transfer function for pH in freshwater habitats on Ile de la Possession (Iles Crozet). Since salt-spray aerosols have been shown to significantly alter both the conductivity and pH of sub-Antarctic lakes, we suggest that further development of testate amoeba training-sets and records from lake sediments for this purpose have the potential to substantially advance our understanding of changes in wind patterns.

A major advantage of using testate amoebae in lakes and peatlands over other currently available proxies for SHW is that they are applicable throughout the sub-Antarctic so long as suitable archives are available (Chapter 1). By allowing data to be obtained from a number of islands, wind-records provided by testate amoebae would allow examination of the key questions of how the latitudinal position of the wind-belt has moved in the past and the extent to which these changes were symmetrical between the main ocean sectors (Chapter 1).

Moisture balance: In recent decades, observational records show that the climate of the sub-Antarctic has warmed rapidly and the level of precipitation has decreased, partly in response to changes in SHW behaviour. Although modern ecological data is sparse, there are indications that sub-Antarctic moss dwelling testate amoebae could be used for hydrological reconstructions to provide longer term context to these changes, using a traditional transfer function based approach. Vincke et al. (2004c) developed a transfer function for F-values (moisture content) of mosses on Ile de la Possession (Iles Crozet), however this was not applied to subfossil assemblages in a sediment core and it is not known whether peatland-dwelling taxa respond in the same way. More in depth studies of surface ecology will be needed to establish a robust link between species and moisture related metrics. Most areas of sub-Antarctic peatland are not considered ombrotrophic, which would normally be a pre-requisite criteria for hydrological reconstructions, however research has proven the use of testate amoeba for palaeohydrology in minerogenic wetlands (Payne, 2011). This suggests that these archives could be useable for this purpose. There is also substantial potential for this technique to be applied on other Southern Ocean islands, for example the Falklands where there are extensive *Sphagnum* moss dominated peatlands. An important caveat to this, is that the diversity of testate amoebae would need to be sufficient for developing a statistically robust transfer function, which likely limits the regional applicability of this approach to the more northerly sub-Antarctic islands with warmer climates (Chapter 1) (and other islands further north).

Sea-level: Zonation of testate amoebae with elevation in salt-marsh environments is a well-established technique to accurately predict past changes in mean sea-level (Charman et al. 1998; Barnett et al. 2017) and has recently been applied on the Falkland islands (Newton, 2017). Further application of this

technique is strongly constrained by the availability of suitable archives, which will require further exploration of the wider Southern Ocean region.

Temperature: Temperatures on the Antarctic Peninsula have risen by up to 0.56˚C per decade since the 1950s, making it one of the rapidly warming regions on Earth (Turner et al. 2009). Combined with these warming temperatures, precipitation and wind speed have also increased significantly. These recent climatic changes have been associated with observed changes in the physical environment, however while these changes are not disputed, records are largely limited to the instrumental period (mid-1960s onwards).

Testate amoebae in moss banks on the Antarctic Peninsula represent rare records of terrestrial biological changes extending beyond this period, and have been the subject of the most intensive palaeoecological research in the Southern Ocean region (see Fig. 2.1). However, the insufficiently low diversity of testate amoebae that inhabit these moss banks has prevented the application of a transfer-function based approach to develop reconstructions. Instead, Royles et al. (2013; 2016) and Amesbury et al. (2017) obtained records by reconstructing changes in biomass of the entire community, as part of a multi-proxy analysis. These records show an uptick in biomass of testate amoebae in moss banks throughout the Antarctic Peninsula that is consistent in timing with the onset of recent warming.

In addition to productivity, it has been suggested that changes in the distribution of testate amoebae could be used to broadly track further warming within the Southern Ocean region, with the expectation that species currently limited to more Northern areas will progressively expand their distributions southwards. The current study could therefore provide a crucial role as a baseline for diversity observed to date. However, as discussed in Section 2.4.2, the diversity of species currently known at many locations remains incomplete. As a result, this will continue to prevent the confident attribution of reports of species in areas not previously reported, to changing climate.

2.5. Concluding remarks

Environmental conditions in the Southern Ocean region can be among the harshest on Earth. Despite this, our synthesis of ~1252 samples from 37 studies

and 44 locations, revealed a regional testate amoeba fauna consisting of 153 species.

Estimates of total diversity calculated using rarefaction curves, provide further evidence for the existence of a broad-scale decline (or depauperisation) in terrestrial diversity with distance poleward through the region. Assemblages in more poleward areas are comprised of species distributed over a greater latitudinal range, suggesting that very few species are unique to the high latitudes. This indicates that communities are a subset of assemblages further north. Therefore, with future climatic warming, it is expected that species will migrate southwards into areas where they have not previously been recorded. However, although this study provides the most up to date baseline which could help in monitoring these migrations in the future, the gaps in sampling and incompleteness of species lists in many areas provide a strong caveat for the use of current species lists in this way. For such conclusions to be made, it is clear that further studies will be needed to establish true baseline diversity levels. Perhaps more feasibly, it is possible that in future, distributions of taxa reconstructed from the fossil record may be able to shed light on previous migrations of species over longer time-scales.

For the first time, the database provides a framework to guide future research efforts; both in filling gaps in our knowledge of the diversity and distribution of species, and in exploring the opportunities and challenges associated with the potential use of testate amoebae in palaeoenvironmental studies.

Our data indicates that the distribution of existing sampling in the region is heavily weighted to the sub-Antarctic Islands, and to a lesser degree the Scotia-arc Islands in the Maritime Antarctic. The number of samples obtained from the Antarctic Peninsula, and especially the other islands between 40-55˚S, remains sparse.

Environments that (to our knowledge) have not been sampled to date, such as hot volcanic springs or fumeroles on the South Sandwich Islands, represent a tantalising opportunity for future study, with the possibility of yielding further diversity or previously undescribed taxa. Notably the potential fauna of Bouvet Island, often referred to as the most isolated island in the world, has not been

studied but represents a fascinating example in the study of testate amoeba biogeography.

Throughout the region, terrestrial sampling strongly outweighs the number of aquatic samples. However, in addition to the fauna inhabiting terrestrial archives (e.g. peat records), the potential for aquatic species to yield palaeoenvironmental records has been suggested; although various factors crucial to this application, including the preservation of tests in lacustrine sediments, remain unknown. Gaining a better understanding of the taphonomy and ecological controls on these assemblages should therefore be a priority for future research, especially in the sub-Antarctic where open-water lakes are common.

Sub-Antarctic Macquarie Island, is particularly noteworthy for its lack of sampling, but potentially high diversity and abundance of terrestrial archives. We therefore suggest that it may provide an ideal test-site for the development of testate amoeba based palaeoecology in the sub-Antarctic. Considering the region as a whole, we suggest that with further development of methodological approaches to address the challenges currently posed, testate amoeba could be used as credible and widespread indicators of; water chemistry (salinity and pH), moisture balance, sea-level and temperature, within palaeoenvironmental studies.

Table 2.4 | Challenges associated with the use of testate amoebae for palaeoenvironmental investigations in the Southern Ocean region.

Challenge	Description	Potential impacts on reconstruction	Possible solution
Taxonomy	Unidentified taxa represent a large proportion of the diversity from assemblages in many of the current records. Taxonomic uncertainty hinders the comparison of ecological trends and accurate quantification of the distribution of taxa within the region. Uncertainty in the consistency of designations also hinders attempts to compare the optima-tolerance of individual species between regions. Lack of specific identification references covering the region slows the rate of enumeration of populations during sample analysis.	• Allows inconsistent and overly-excessive 'grouping' or 'splitting' of taxonomic units, causing either potentially valuable ecological information to be discarded or uncertainty to be introduced in the resultant reconstruction, respectively. • Inefficient laboratory analysis reduces the number of samples that can be processed. • Possible misinterpretations when comparing with studies conducted by other authors.	Prioritisation of increased taxonomic focus (including molecular and morphological studies) in the region to develop alongside palaeoenvironmental applications. Routine publishing of photographs of identified and unidentified taxa to allow subsequent re-analysis pending taxonomic advancement. Increased use of methods for reconstructions that are less reliant on taxonomy, such as community-level metrics (e.g. biomass, concentration) or functional trait based analysis
Preservation of tests	Freeze-thaw conditions are suggested to reduce the number of preserved tests entering the sedimentary record in identifiable condition, which is especially pertinent in permafrost regions with frequent cycles (Balik, 1994; Vincke et al. 2004a). The substrate conditions of palaeoclimate archives (both terrestrial and aquatic) in the Southern Ocean regions are poorly studied (relative to the Northern Hemisphere) and may be unsuitable for long-term preservation of tests in certain areas. Assessment of differential preservation of testate amoebae in lake sediments has previously been carried out in Europe (see Ruzicka, 1982), however the suitability of preservation conditions in lakes throughout the sub-Antarctic have not been investigated to date.	• Hinder or completely prevent analysis using testate amoebae from palaeoenvironmental records. • Possibly lead to inaccurate environmental interpretations in instances of preferential preservation of certain species. • Lead to inaccurate quantification of changes in population sizes or biomass through time, if certain taxa are preferentially lost or if preservation conditions varied between different periods of the stratigraphy.	Routine recording of the ratio between well-preserved and poorly-preserved tests during identification to establish whether a down-core trend in preservation is identifiable, and allow standardisation if necessary. Removal of species found in surface assemblages but not within cores. Prioritising lab-based experimental studies to better constrain this factor.
Disturbance	Although anthropogenic disturbance in the Southern Ocean region is much less than in other areas of the world, the impact of research bases, bird nesting sites and the presence of seal colonies is a major consideration.	Lead to inaccurate or inconsistent environmental interpretations.	Careful site selection to avoid areas of known disturbance. Further quantification of the known effects of these disturbances on assemblages. Use of geochemical analysis alongside testate amoeba data to identify the signal of past disturbance within cores.
Low diversity assemblages	Traditional approach of using transfer functions that underpins most testate amoeba based palaeo-climate reconstructions is reliant on sufficient diversity. Limited diversity assemblages, particularly of those in locations further South, is likely to prevent the application of transfer functions.	Prevent reconstruction using conventional methodologies, especially in more Southerly regions.	Use of community-level metrics (e.g. biomass, concentration) that are not dependent on diversity.
Small population sizes	Testate amoeba populations, especially those in more southerly parts of the Southern Ocean region are often very low in concentration.	Significantly impacts on the efficiency of analysis. Within individual studies this can potentially mean that a lower number of surface calibration samples can be analysed and/or a lower resolution is achievable within sediment cores.	Lower count totals than would be normally expected in Northern peatland ecosystems (Payne and Mitchell, 2009). Apply pre-determined rules to follow during analysis, for example counting the entirety of one slide and not a certain number of tests, to ensure consistency of data.

Low number of live individuals	Populations consisting of a low proportion of live individuals have been reported on the Antarctic Peninsula (e.g. Roland et al. 2017), and in the sub-Antarctic (Vincke, 2004a). This has meant that it has not been possible to obtain live specimens for culturing which hinders laboratory based studies, and taxonomic investigations.	Introduces uncertainty in surface ecology studies used as a basis for reconstructions. A high dead to living ratio means that it is difficult to know whether observed assemblage relates to the environmental conditions recorded at the time of sampling, or whether the assemblage is still recovering from a major environmental perturbation. Prevents molecular analysis if no/very few live specimens can be obtained.	Routine counting of the living to dead cell ratio in surface studies, meaning that ecological analysis can be based on only cells living at the time of sampling.
Lack of modern analogues	Robust transfer function development, or other palaeoenvironmental interpretations based on population biomass/productivity, depend on the availability of good quality modern 'training' data-sets and the assumption that species-environment relationships remain stable through time. Normally this assumption is tested by assessing the similarity of species responses over broad geographical areas (e.g. Amesbury et al. 2018), however owing to the limited land-area and significant differences between environments (including plant biogeographic provinces) in the Southern Ocean region, direct comparison is often not possible. This is further compounded by the insufficient number of ecological studies currently available to researchers.	• Potential for erroneous interpretations of sections of cores where environmental conditions were different to any found in the modern environment (i.e. included in the modern/surface 'training-set'). • Increases uncertainty in the assumption that species-environment responses have remained constant through time.	Extensive surface calibration studies conducted at the locations where reconstructions are to be made, in order to more-fully characterise modern species-environment responses. This could be supplemented with the use of similar environmental gradients in other regions, if broad-scale responses to environmental conditions are to be tested (e.g. Chapter 3-4) Combine these studies with controlled laboratory based tests of species responses where extensive sampling is not possible. Collection of detailed ecological data relevant to testate amoebae and thorough descriptions of samples when future sampling is undertaken to provide a larger database of ecological information for subsequent studies.
Seasonality	Reflections of seasonality in the activity of testate amoebae, both in terms of population size (productivity) and relative prevalence of individual species (composition), are an important consideration for the correct interpretation of fossil assemblages (see Supplementary note 2.1).	If the majority of activity only occurs during parts of the year, the interpreted climate signal can be biased by these periods. This is particularly problematic for studies in the maritime Antarctic where seasonality has already been shown to be significant control on testate amoeba activity (e.g. Smith, 1978).	Suitably acknowledge the bias in the record when interpreting the reconstruction. Remove species that are known to undergo large-magnitude seasonal fluctuations if this runs counter to the aims of the analysis.

2.6. References

Amesbury, M.J., Booth, R.K., Roland, T.P., Bunbury, J., Clifford, M.J., Charman, D.J., Elliot, S., Finkelstein, S., Garneau, M., Hughes, P.D. and Lamarre, A. (2018) Towards a Holarctic synthesis of peatland testate amoeba ecology: Development of a new continental-scale palaeohydrological transfer function for North America and comparison to European data, *Quaternary Science Reviews*, 201: 483-500.

Amesbury, M.J., Roland, T.P., Royles, J., Hodgson, D.A., Convey, P., Griffiths, H. and Charman, D.J. (2017) Widespread biological response to rapid warming on the Antarctic Peninsula, *Current Biology*, 27(11): 1616-1622.

Amesbury, M.J., Swindles, G.T., Bobrov, A., Charman, D.J., Holden, J., Lamentowicz, M., Mallon, G., Mazei, Y., Mitchell, E.A., Payne, R.J. and Roland, T.P. (2016) Development of a new pan-European testate amoeba transfer function for reconstructing peatland palaeohydrology, *Quaternary Science Reviews*, 152: 132-151.

Araújo, M. B., Nogúes-Bravo, D., Diniz-Filho, J. A. F., Haywood, A. M., Valdes, P. J. and Rahbek, C. (2008). Quaternary climate changes explain diversity among reptiles and amphibians. *Ecography*, 31: 8-15.

Badewitz, H.J. (2004) The genus Microcorycia Cockerell, 1911 (Testacealobosia, Rhizopoda, Protozoa). A critical monograph of the genus including a first description of a new species: Microcorycia scutella n. sp., *Lauterbornia*, 50: 111-146.

Balik, V. (1994) On the soil testate amoebae fauna (Protozoa: Rhizopoda) of the Spitsbergen Islands (Svalbard), *Archiv Für Protisten Kunde,* 144: 365-372.

Barnett, R.L., Newton, T.L., Charman, D.J. and Gehrels, W.R. (2017) Salt-marsh testate amoebae as precise and widespread indicators of sea-level change, *Earth-Science Reviews*, 164: 193-207.

Beyens, L. and Chardez, D. (1997) New testate amoebae taxa from the Polar Regions, *Acta Protozoologica,* 36: 137-142.

Beyens, L., Chardez, D. De Baere, and C. Verbruggen. (1995) The Aquatic Testate Amoebae Fauna of the Strømness Bay Area, South Georgia, *Antarctic Science,* 7(1): 3–8.

Blackburn, T. M. and Gaston, K. J. (1996) Spatial patterns in the geographic range sizes of bird species in the New World, *Philosophical Transactions of the Royal Society of London. Series B, Biological Sciences*, 351: 897-912.

Bobrov, A.A. and Mazei, Y. (2004) Morphological variability of testate amoebae (Rhizopoda: Testacealobosea: Testaceafilosea) in natural populations, *Acta Protozoologica*, 43:133–146.

Bokhorst, S., Huiskes, A., Convey, P. and Aerts, R. (2007) External nutrient inputs into terrestrial ecosystems of the Falkland Islands and the Maritime Antarctic region, *Polar Biology*, 30(10): 1315-1321.

Bonnet, L. (1981) Thecamoeniens (Rhizopoda Testacea), *Bull. Com. Nat. Fran. Res. Antarct.* 48: 23–32.

Broughton, D.A. and McAdam, J.H. (2005) A checklist of the native vascular flora of the Falkland Islands (Islas Malvinas): New information on the species present, their ecology, status and distribution. *The Journal of the Torrey Botanical Society*, 132(1): 115-148.

Certes, A. (1891) Protozaires. In: *Mission Scientifique Du Cap Horn,* 1882-1883, 165–78.

Chao, A., Gotelli, N.J., Hsieh, T.C., Sande, E.L., Ma, K.H., Colwell, R.K. and Ellison, A.M. (2014) Rarefaction and extrapolation with Hill numbers: a framework for sampling and estimation in species diversity studies, *Ecological Monographs*, 84: 45–67.

Charman, D. J. (1997) Modelling hydrological relationships of testate amoebae (Protozoa: Rhizopoda) on New Zealand peatlands, *Journal of the Royal Society of New Zealand*, 27(4): 465-483.

Charman, D.J., Amesbury, M.J., Roland, T.P., Royles, J., Hodgson, D.A., Convey, P. and Griffiths, H. (2018) Spatially coherent late Holocene Antarctic Peninsula surface air temperature variability, *Geology*, 46(12): 1071-1074.

Charman, D.J., Roe, H.M. and Gehrels, W.R. (1998) The use of testate amoebae in studies of sea-level change: a case study from the Taf Estuary, south Wales, UK, *The Holocene*, 8(2): 209-218.

Convey, P. (2003) Maritime Antarctic climate change: signals from terrestrial biology. Antarctic research series, In: Antarctic Peninsula Climate Variability: Historical and Paleoenvironmental Perspectives, (eds.) Domack, E., Levente, A., Burnet, A., Bindschadler, R., Convey, P. and Kirby, M.

Convey, P., W. Hopkins, D., J. Roberts, S. and N. Tyler, A. (2011) Global southern limit of flowering plants and moss peat accumulation, *Polar Research*, 30(1).

Convey, P. and Lewis-Smith, R. I. (2006) Geothermal bryophyte habitats in the South Sandwich Islands, maritime Antarctic, *Journal of Vegetation Science,* 17: 529-538.

Cox, F., Newsham, K. K., Bol, R., Dungait, J. A. J. and Robinson, C. H. (2016) Not poles apart: Antarctic soil fungal communities show similarities to those of the distant Arctic, *Ecology Letters*, 19: 528-536.

Duleba, W. and Debenay, J.P. (2003) Hydrodynamic circulation in the estuaries of Estação Ecológica Juréia-Itatins, Brazil, inferred from foraminifera and thecamoebian assemblages, *The Journal of Foraminiferal Research*, 33(1): 62-93.

Dumack, K., Kahlich, C., Lahr, D.J. and Bonkowski, M. (2018) Reinvestigation of Phryganella paradoxa (Arcellinida, Amoebozoa) Penard 1902, *Journal of Eukaryotic Microbiology*, 66(2): 232-243.

Fernández, L.D., Lara, E. and Mitchell, E.A. (2015) Checklist, diversity and distribution of testate amoebae in Chile, *European Journal of Protistology*, 51(5): 409-424.

France, R. (1992) The North American latitudinal gradient in species richness and geographical range of freshwater crayfish and amphipods, *The American Naturalist*, 139: 342-354.

Gaston, K. J. and Chown, S. L. (1999) Why Rapoport's rule does not generalise, *Oikos*, 84: 309-312.

Gehrels, W.R., Roe, H.M. and Charman, D.J. (2001) Foraminifera, testate amoebae and diatoms as sea-level indicators in UK saltmarshes: a quantitative multiproxy approach. *Journal of Quaternary Science,* 16(3): 201-220.

Geisen, S., Mitchell, E. A., Adl, S., Bonkowski, M., Dunthorn, M., Ekelund, F., Fernández, L. D., Jousset, A., Krashevska, V., Singer, D. and Spiegel, F. W. (2018) Soil protists: a fertile frontier in soil biology research, *FEMS Microbiology Reviews*, 42(3): 293-323.

Geisen, S., Rosengarten, J., Koller, R., Mulder, C., Urich, T. and Bonkowski, M. (2015) Pack hunting by a common soil amoeba on nematodes, *Environmental microbiology*, 17(11): 4538-4546.

Gilbert, D., Amblard, C., Bourdier, G. and Francez, A-J. (1998) The microbial loop at the surface of a peatland: Structure, function, and impact of nutrient input, *Microbial Ecology,* 35:83–93.

Gilbert, D., Amblard, C., Bourdier, G., Francez, A-J. and Mitchell, E. A. D. (2000) Le regime alimentaire des Thécamoebiens (Protista, Sarcodina), *L'Année Biologique,* 39(2): 57-68.

Golemansky, V. and Todorov, M. (2004) Additional data and summarized check-list on the Rhizopods (Rhizopoda: Amoebida & Testacea) from Livingston Island, South Shetlands, the Antarctic, *Bulgarian Antarctic Research Life Sciences*, 4: 83–93.

Golemansky, V. G. (1998) Interstitial testate Amoebae (Rhizopoda: Arcellinida and Gromida) from the Finnish coast of the Baltic Sea and summary check list of the interstitial testate Amoebae in the Baltic Sea, *Acta Protozoologica*, 37(3): 133-137.

Golemansky, V. G. and Todorov, M. T. (1999) First report of the interstitial testate amoebae (Protozoa: Testacea) in the marine supralittoral of the Livingston Island (the Antarctic), *Bulgarian Antarctic Research Life Sciences,* 2: 43-47.

Grospietsch, T. (1971) 'Beitrag zur ökologie der Testaceen Rhizopoden von Marion Island', in Van Zinderen-Bakker, E. M., Winterbottom, J. M., and Dyer, R. A. (eds) *Marion and Prince Edward Island, Report on the South African Biological and Geological Expedition 1965-1966*. Cape Town: Balkema, pp. 411–423.

Hansell, M. (2011) Houses made by protists, *Current Biology,* 21(13): PR485-487.

Hawthorn, G. R. and Ellis-Evans, J. C. (1984) Benthic protozoa from maritime Antarctic freshwater lakes and pools, *British Antarctic Survey Bulletin*, 62: 67–81.

Heal, O. W. (1965) Observations on Testate Amoebae (Protozoa: Rhizopoda) from Signy Island, South Orkney Islands, *British Antarctic Survey Bulletin,* 6: 43–47.

Heger, T.J., Mitchell, E.A., Ledeganck, P., Vincke, S., Van de Vijver, B. and Beyens, L. (2009) The curse of taxonomic uncertainty in biogeographical studies of free-living terrestrial protists: a case study of testate amoebae from Amsterdam Island, *Journal of Biogeography*, 36(8): 1551-1560.

Heywood, R.B. (1977) Antarctic freshwater ecosystems: a review and synthesis. In: Adaptations within Antarctic ecosystems (ed. by G. A. Llano), Smithsonian Institute, Washington D.C.

Hodgson, D. A., Graham, A. G. C., Roberts, S. J., Bentley, M. J., Cofaigh, C. O., Verleyen, E., Wyverman, W., Jomelli, V., Favier, V., Brunstein, D., Verfaillie, D., Colhoun, E. A., Saunders, K. M., Selkirk, P. M., Mackintosh, A., Hedding, D. W., Nel, W., Hall, K., McGlone, M. S., Van der Putten, N., Dickens, W. A. and Smith, J. A. (2014) Terrestrial and submarine evidence for the extent and timing of the Last Glacial Maximum and the onset of deglaciation on the maritime-Antarctic and sub-Antarctic Islands, *Quaternary Science Reviews*, 100: 137–58.

Hsieh, T.C., Ma, K.H. and Chao, A. (2020) iNEXT: Interpolation and Extrapolation for Species Diversity. R package version 2.0.20, http://chao.stat.nthu.edu.tw/wordpress/software_download/.

Imbrie, J. and Kipp, N.G. (1971) A new micropaleotological method for quantitative paleocli- matology: application to a Late Pleistocene Caribbean core. In: Turekian, K.K. (Ed.), The Late Cenozoic Glacial Ages. Yale University Press, New Haven.

Jansson, R. (2003). Global patterns in endemism explained by past climatic change. *Proceedings of the Royal Society of London. Series B: Biological Sciences*, 270(1515): 583-590.

Jassey, V. E., Chiapusio, G., Binet, P., Buttler, A., Laggoun-Défarge, F., Delarue, F., Bernard, N., Mitchell, E. A., Toussaint, M. L., Francez, A. J. and Gilbert, D. (2013a) Above-and belowground linkages in Sphagnum peatland: Climate warming affects plant-microbial interactions, *Global Change Biology*, 19(3): 811-823.

Jassey, V. E., Meyer, C., Dupuy, C., Bernard, N., Mitchell, E. A. D., Toussaint, M. L., Metian, M., Chatelain, A. P. and Gilbert, D. (2013b) To what extent do food preferences explain the trophic position of heterotrophic and mixotrophic microbial consumers in a Sphagnum peatland?, *Microbial ecology,* 66(3): 571-580.

Ju, L., Yang, J., Liu, L. and Wilkinson, D. M. (2014) Diversity and distribution of freshwater testate amoebae (Protozoa) along latitudinal and trophic gradients in China. *Microbial ecology*, 68(4): 657-670.

Jung, W. (1936) Thekamöben ursprünglischer lebender deutscher Hochmoore. *Abhandlung Landesmuseum der Provinz Westfalen,* 7:1–87

Kosakyan, A., Gomaa, F., Lara, E. and Lahr, D. J. G. (2016) Current and future perspectives on the systematics, taxonomy and nomenclature of testate amoebae, *European Journal of Protistology,* 55: 105-117.

Krashevska, V., Sandmann, D., Marian, F., Maraun, M. and Scheu, S. (2017) Leaf litter chemistry drives the structure and composition of soil testate amoeba communities in a tropical montane rainforest of the Ecuadorian Andes, *Microbial ecology,* 74(3): 681-690.

Lamy, F., Kilian, R., Arz, H. W., Francois, J-P., Kaiser, J., Prange, M. and Steinke, T. (2010) Holocene changes in the position and intensity of the southern westerly wind belt, *Nature Geoscience*, 3: 695–99.

Lawley, B., Ripley, S., Bridge, P. and Convey, P. (2004) Molecular analysis of geographic patterns of eukaryotic diversity in Antarctic soils, *Applied and Environmental Microbiology*, 70(10): 5963-5972.

Leidy, J. (1879) Fresh-water rhizopods of North America. Report of the United States Geological Survey of the Territories, 12: 1–324.

Li, H., Wang, S., Zhao, H. and Wang, M. (2015) A testate amoebae transfer function from Sphagnum-dominated peatlands in the Lesser Khingan Mountains, NE China, *Journal of Paleolimnology*, 54(2): 189-203.

Loisel, J., Yu, Z., Beilman, D.W., Kaiser, K. and Parnikoza, I. (2017) Peatland ecosystem processes in the maritime Antarctic during warm climates, *Scientific reports*, 7(1): 1-9.

Lundmark, C. (2006) Global patterns in bird diversity, *Bioscience*, 56: 784.

Marcisz, K., Colombaroli, D., Jassey, V.E., Tinner, W., Kołaczek, P., Gałka, M., Karpińska-Kołaczek, M., Słowiński, M. and Lamentowicz, M. (2016) A novel testate amoebae trait-based approach to infer environmental disturbance in *Sphagnum* peatlands, *Scientific reports,* 6(1): 1-11.

Mazei, Y. and Tsyganov, A. (2006) Freshwater Testate Amoebae. KMK, Moscow (In Russian).

Mazei, Y. and Warren, A. (2012) A survey of the testate amoeba genus Difflugia Leclerc, 1815 based on specimens in the E. Penard and C.G. Ogden collections of the Natural History Museum, London. Part 1: Species with shells that are pointed aborally and/or have aboral protuberances, *Protistology,* 7(3): 121-171.

Mazei, Y. and Warren, A. (2014) A survey of the testate amoeba genus Difflugia Leclerc, 1815 based on specimens in the E. Penard and C.G. Ogden collections of the Natural History Museum, London. Part 2: Species with shells that are pyriform or elongate, *Protistology,* 8(4): 133-171.

Mazei, Y. and Warren, A. (2015) A survey of the testate amoeba genus Difflugia Leclerc, 1815 based on specimens in the E. Penard and C.G. Ogden collections of the Natural History Museum, London. Part 3: Species with shells that are spherical or ovoid, *Protistology,* 9(1): 3-49.

Mieczan, T. and Adamczuk, M. (2015) Ecology of testate amoebae (Protists) in mosses: distribution and relation of species assemblages with environmental parameters (King George Island, Antarctica), *Polar Biology*, 38(2): 221–230.

Mitchell, E. A. D. (2004) Response of testate amoebae (Protozoa) to N and P fertilization in an Arctic wet sedge tundra. *Arctic Antarctic and Alpine Research,* 36:78–83.

Mitchell, E. A. D., Gilbert, D., Buttler, A., Amblard, C., Grosvernier, P. and Gobat, J.M. (2003) Structure of microbial communities in Sphagnum peatlands and effect of atmospheric carbon dioxide enrichment, *Microbial Ecology,* 46:187–199.

Mitchell, E.A., Charman, D.J. and Warner, B.G. (2008) Testate amoebae analysis in ecological and paleoecological studies of wetlands: past, present and future, *Biodiversity and conservation*, 17(9): 2115-2137.

Mitchell, E.A., Payne, R.J., van der Knaap, W.O., Lamentowicz, Ł., Gąbka, M. and Lamentowicz, M. (2013) The performance of single-and multi-proxy transfer functions (testate amoebae, bryophytes, vascular plants) for reconstructing mire surface wetness and pH, *Quaternary Research*, 79(1): 6-13.

Murray, J. (1908) “Scotia” collections - Note on microscopic life on Gough Island,

South Atlantic Ocean', in *Scottish National Antarctic Expedition. Report on the scientific results of the voyage of S.Y. 'Scotia' during the years 1902, 1903, and 1904, under the leadership of William S. Bruce. (1912), Vol. VI – Zoology:* 259-262.

Murray, J. (1910) Reports on the scientific investigations, Vol.1 Biology, In: *British Antarctic Expedition 1907-9 Under the command of Sir E. H. Shackleton, C.V.O.* Heinemann, London.

Newton, T. L. (2017) *Holocene sea-level changes in the Falkland Islands: new insights into accelerated sea-level rise in the 20th Century*. PhD Thesis. University of Plymouth, U.K.

Nicholls, K.H. and MacIsaac, H.J. (2004) Euryhaline, sand-dwelling, testate rhizopods in the Great Lakes, *Journal of Great Lakes Research*, 30(1): 123-132.

Ogden, C. G. and Coûteaux, M-M. (1988) The Effect of Predation on the Morphology of Tracheleuglypha dentata (Protozoa: Rhizopoda), *Archiv für Protistenkunde,* 136(1): 107-115.

Patterson, R.T. and Kumar, A. (2002) A review of current testate rhizopod (thecamoebian) research in Canada. *Palaeogeography, Palaeoclimatology, Palaeoecology*, 180(1-3): 225-251.

Payne, R.J. (2011) Can testate amoeba-based palaeohydrology be extended to fens?, *Journal of Quaternary Science,* 26(1): 15-27.

Payne, R.J., and Mitchell, E.A.D (2009) How Many Is Enough? Determining Optimal Count Totals for Ecological and Palaeoecological Studies of Testate Amoebae, *Journal of Paleolimnology* 42(4): 483–95.

Payne, R.J., Kishaba, K., Blackford, J.J. and Mitchell, E.A.D. (2006) Ecology of testate amoebae (Protista) in south-central Alaska peatlands: building transfer-function models for palaeoenvironmental studies, *The Holocene*, 16(3): 403-414.

Penard, E. (1890) Études sur les Rhizopodes d'eau douce. Mémoires de la Société de Physique d'Histoire Naturelle de Genève, 31:1–230.

Penard, E. (1902) Les Rhizopodes du bassin du Léman, Kündig, Genève.

Penard, E. (1911) Sarcodina. Rhizopodes d'eau Douce, In: *British Antarctic Expedition 1907-9. Reports on the Scientific Investigations. Vol.1. Biology*, edited by J. Murray, 203–62. London: Heinemann.

Penard, E. (1912) 'Further note on microscopic life on Gough Island, South Atlantic Ocean', in *Scottish National Antarctic Expedition. Report on the scientific results of the voyage of S.Y. 'Scotia' during the years 1902, 1903, and 1904, under the leadership of William S. Bruce. (1912), Vol. VI –*

Zoology: 265-269.

Penard, E. (1913) Rhizopodes d'eau douce. In: *Deuxieme Expedition Antarctique Francaise (1908-1910), Sciences Naturelles: Documents Scientifiques*.

Pendlebury, S. and Barnes-Keoghan, I.P. (2007) Climate and climate change in the sub-Antarctic. *Papers and Proceedings of the Royal Society of Tasmania*, 141(1): 67-81.

Pianka, E. R. (1989). Latitudinal gradients in species diversity. *Trends in Ecology and Evolution*, 4: 223.

Pither, J. (2003) Climate tolerance and interspecific variation in geographic range size, *Proceedings of the Royal Society of London. Series B: Biological Sciences*, 270: 475-481.

R Core Team (2017) R: A Language and Environment for Statistical Computing. R Foundation for Statistical Computing, Vienna, Austria, URL https://www.Rproject.org/.

Richters, F. (1904) Vorläufiger Bericht Über Die Antarktische Moosfauna. In: *Verhandlungen Der Deutschen Zoologischen Gesellschaft*, 236–39.

Richters, F. (1907) Die Fauna Der Moosrasen Des Gaussbergs Und Einiger Südlicher Inseln. In: *Deutsch Südpolar-Expedition 1901–1903. Zoologie 9*, 259–302.

Richters, F. (1908) Moosbewohner. In: *Wissenschaftliche Ergebnisse Der Schwedeschen Südpolar Expedition 1901- 1903.*

Rinnan, R., Rousk, J., Yergeau, E., Kowalchuk, G.A. and Bååth, E. (2009) Temperature adaptation of soil bacterial communities along an Antarctic climate gradient: predicting responses to climate warming, *Global Change Biology*, 15(11): 2615-2625.

Rintoul, S.R. (2011) The southern ocean in the earth system. *Science diplomacy: Antarctica, science, and the governance of international spaces*, 175-187.

Roe, H.M., Charman, D.J. and Roland Gehrels, W. (2002) Fossil testate amoebae in coastal deposits in the UK: implications for studies of sea-level change, *Journal of Quaternary Science*, 17(5-6): 411-429.

Roland, T. P., M. J. Amesbury, D. M. Wilkinson, D. J. Charman, P. Convey, D. A. Hodgson, J. Royles, S. Clauß, and E. Völcker (2017) Taxonomic Implications of Morphological Complexity Within the Testate Amoeba Genus Corythion from the Antarctic Peninsula, *Protist,* 168(5): 565–85.

Royles, J., Amesbury, M. J., Roland, T. P., Jones, G. D., Convey, P., Griffiths, H., Hodgson, D. A. and Charman, D. J. (2016) Moss stable isotopes (carbon-13, oxygen-18) and testate amoebae reflect environmental inputs and microclimate along a latitudinal gradient on the Antarctic Peninsula, *Oecologia,* 181(3): 931–945.

Royles, J., Amesbury, M.J., Convey, P., Griffiths, H., Hodgson, D.A., Leng, M.J. and Charman, D.J. (2013) Plants and soil microbes respond to recent warming on the Antarctic Peninsula, *Current Biology*, 23(17): 1702-1706.

Royles, J., Ogée, J., Wingate, L., Hodgson, D.A., Convey, P. and Griffiths, H. (2012) Carbon isotope evidence for recent climate-related enhancement of CO_2 assimilation and peat accumulation rates in Antarctica, *Global Change Biology*, 18(10): 3112-3124.

Ruzicka, E. (1982) Die subfossile Testacean des Krottensees (Salzburg, Oesterich), *Limnologica,* 1: 49-88.

Sandon, H. and Cutler, D. W. (1924) Some protozoa from the soils collected by the “Quest” expedition (1921-22), *Journal of the Linnean Society of London – Zoology*, 36: 1-2

Santibáñez, P.A., Kohshima, S., Scheihing, R.A., Silva, R., Jaramillo M, J.I., Labarca P, P.J. and Casassa R, G. (2011) First record of testate amoebae on glaciers and description of a new species *Puytoracia jenswendti* nov. sp. (Rhizaria, Euglyphida), *Acta Protozoologica*, 50(1): 1-14.

Saunders, K. M., Hodgson, D. A., McMurtrie, S. and Grosjean, M. (2015) A diatom conductivity transfer function for reconstructing past changes in the Southern Hemisphere westerly winds over the Southern Ocean, Journal of Quaternary Science, 30 (5): 464–77.

Saunders, K. M., Roberts, S. J., Perren, B., Butz, C., Sime, L., Davies, S., Van Nieuwenhuyze, W., Grosjean, M. and Hodgson, D. A. (2018) Holocene dynamics of the Southern Hemisphere westerly winds and possible links to CO_2 outgassing, Nature Geoscience, 11: 650-655.

Schönborn, W. (1992) Adaptive polymorphism in soil-inhabiting testate amoebae (Rhizopoda): its importance for delimitation and evolution of asexual species, *Archiv für Protistenkunde*, 142(3-4): 139-155.

Scott, D.B. and Asioli, A. (2014) A testate rhizopod assemblage in an extreme environment: the Antarctic permanently ice-covered lake Hoare (Taylor Valley), *The Journal of Foraminiferal Research*, 44(2): 177-186.

Smith, F. D., May, R. M. and Harvey, P. H. (1994) Geographical ranges of Australian mammals, *Journal of Animal Ecology*, 63: 441-450.

Smith, H. G. (1972) The terrestrial protozoa of Elephant Island, South Shetland Islands, *British Antarctic Survey Bulletin*, 31: 55–62.

Smith, H. G. (1986) ‘The testate rhizopod fauna of Drepanocladus moss carpet near Rothera station, Adelaide Island’, *British Antarctic Survey Bulletin*, 72: 77–79.

Smith, H. G. (1987) ‘A species-poor testate rhizopod fauna on Brabant Island’, *British Antarctic Survey Bulletin*, 77: 173–176.

Smith, H.G (1982) The terrestrial protozoan fauna of South Georgia, *Polar Biology,* 1:173-179.

Smith, H.G. (1969) A survey of the soil protozoa of Signy Island (Preliminary report, Unpublished), British Antarctic Survey document reference number: N8/1969/H.

Smith, H.G. (1970) Taxonomy and ecology of terrestrial protozoa (Interim report, unpublished). British Antarctic Survey document reference number: N7/1969-70/H.

Smith, H.G. (1973) The Signy Island terrestrial reference sites: II. The Protozoa, *British Antarctic Survey Bulletin*, 33&34: 83–87.

Smith, H.G. (1974) A Comparative Study of Protozoa Inhabiting Drepanocladus Moss Carpet in the South Orkney Islands, *British Antarctic Survey Bulletin,* 38: 1–16.

Smith, H.G. (1975) Protozoaires terricoles de l’le de la Possession, *Rev. Ecol. Biol. Sol.* 12(2): 523-530.

Smith, H.G. (1978) The Distribution and Ecology of Terrestrial Protozoa of Sub-Antarctic and Maritime Antarctic Islands. British Antarctic Survey Scientific Reports. No. 95. Natural Environment Research Council.

Smith, H.G. (1985) The colonization of volcanic tephra on Deception Island by protoza: Long-term trends, *British Antarctic Survey Bulletin*, 66: 19–33.

Smith, H.G. (1996) Diversity of Antarctic terrestrial protozoa, *Biodiversity & Conservation*, 5(11): 1379-1394.

Smith, H.G. and Headland, R. K. (1983) The population ecology of soil testate rhizopods on the sub-Antarctic island of South Georgia, *Rev. Ecol. Biol. Sol.* 20(2): 269-286.

Smith, H.G. and Wilkinson, D. M. (1986) Biogeography of testate rhizopods in the southern temperate and Antarctic zones, *Colloque sur les écosystémes terrestres subantarctiques,* C.N.F.R.A. 58: 83-96.

Smith, H.G. and Wilkinson, D. M. (2007) Not All Free-Living Microorganisms Have Cosmopolitan Distributions - The Case of Nebela (Apodera) Vas Certes (Protozoa: Amoebozoa: Arcellinida), *Journal of Biogeography*, 34(10): 1822–31.

Stevens, G. C. (1989) The latitudinal gradient in geographical ranger: how so many species coexist in the tropics, *The American Naturalist*, 133: 240-256.

Swindles, G. T., Amesbury, M. J., Turner, T. E., Carrivick, J. L., Woulds, C., Raby, C., Mullan, D., Roland, T. P., Galloway, J. M., Parry, L., Kokfelt, U., Garneau, M., Charman, D. J. and Holden, J. (2015a) Evaluating the use of testate amoebae for palaeohydrological reconstruction in permafrost peatlands, *Palaeogeography, Palaeoclimatology, Palaeoecology,* 424: 111–122.

Swindles, G. T., Morris, P. J., Mullan, D., Watson, E. J., Turner, E., Roland, T. P., Amesbury, M. J., Kokfelt, U., Schoning, K., Pratte, S., Gallego-Sala, A.,Charman, D. J., Sanderson, N., Garneau, M., Carrivick, J., Woulds, C., Holden, J., Parry, L., Galloway, J. M. (2015b) The long-term fate of permafrost peatlands under rapid climate warming, *Scientific Reports*, 1–6.

Swindles, G.T., Reczuga, M., Lamentowicz, M., Raby, C.L., Turner, T.E., Charman, D.J., Gallego-Sala, A., Valderrama, E., Williams, C., Draper, F. and Coronado, E.N.H. (2014) Ecology of testate amoebae in an Amazonian peatland and development of a transfer function for palaeohydrological reconstruction, *Microbial ecology*, 68(2): 284-298.

Thompson, A.R., Powell, G.S. and Adams, B.J. (2019) Provisional checklist of terrestrial heterotrophic protists from Antarctica, *Antarctic Science*, 31(6): 287-303.

Todorov, M. and Bankov, N. (2019) An Atlas of Sphagnum-dwelling Testate Amoebae in Bulgaria. Pensoft, Sofia.

Todorov, M. and Golemansky, V. (1996) Notes on Testate Amoebae (Protozoa: Rhizopoda) from Livingston Island, South Shetland Islands, Antarctic, *Bulgarian Antarctic Research Life Sciences*, 70–81.

Todorov, M. and Golemansky, V. (1999) Biotopic distribution of testate amoebae (Rhizopoda: Testacea) in continental habitats of the Livingston Island (the Antarctic), *Bulgarian Antarctic Research,* 2: 48-56.

Turner, J., Bindschadler, R., Convey, P., di Prisco, G., Fahrbach, E., Gutt, J., Hodgson, D., Mayewski, P. and Summerhayes, C. (2009). Antarctic Climate Change and the Environment (Cambridge: Scientific Committee on Antarctic Research).

van Bellen, S., Mauquoy, D., Hughes, P.D., Roland, T.P., Daley, T.J., Loader, N.J., Street-Perrott, F.A., Rice, E.M., Pancotto, V.A. and Payne, R.J. (2015) Late-Holocene climate dynamics recorded in the peat bogs of Tierra del Fuego, South America, *The Holocene*, 26(3): 489-501.

van Bellen, S., Mauquoy, D., Payne, R.J., Roland, T.P., Hughes, P.D., Daley, T.J., Loader, N.J., Street-Perrott, F.A., Rice, E.M. and Pancotto, V.A. (2017) An alternative approach to transfer functions? Testing the performance of a functional trait-based model for testate amoebae, *Palaeogeography, Palaeoclimatology, Palaeoecology,* 468: 173-183.

Van de Vijver, B. and Beyens, L. (1999) Biogeography and ecology of freshwater diatoms in Subantarctica: a review, *Journal of biogeography*, 26(5): 993-1000.

Van der Putten, N., Mauquoy, D., Verbruggen, C. and Björck, S. (2012a) Subantarctic peatlands and their potential as palaeoenvironmental and palaeoclimatic archives, *Quaternary International*, 268: 65-76.

Van der Putten, N., Verbruggen, C., Björck, S., de Beaulieu, J.L., Barrow, C.J. and Frenot, Y. (2012b) Is palynology a credible climate proxy in the Subantarctic?. *The Holocene*, 22(10): 1113-1121.

Vanhoffen, E. (1912) Tire und Pflanzen der Heard-Insel. *Deutsche Südpol Expédition*, 2: 267–271.

Veter, N. M., De Santis, L. R., Yann, L. T., Donohue, S. L., Haupt, R. J., Corapi, S. E. et al. (2013) Is Rapoport's rule a recent phenomenon? A deep time perspective on potential causal mechanisms, *Biology Letters*, 9: 20130398.

Vincke, S., Gremmen, N., Beyens, L. and van de Vijver, B. (2004c) The moss dwelling testacean fauna of Ile de la Possession, *Polar Biology,* 27: 753-766.

Vincke, S., Ledeganck, P., Beyens, L. and Van de Vijver, B. (2004a) Soil testate amoebae from sub-Antarctic Îles Crozet, *Antarctic Science*, 16(2): 165-174.

Vincke, S., van de Vijver, B., Gremmen, N. and Beyens, L. (2006a) The moss dwelling testacean fauna of the Stromness Bay (South Georgia), *Acta Protozoologica,* 45: 65-75.

Vincke, S., van de Vijver, B., Ledeganck, P., Nijs, I. and Beyens, L. (2007) Testacean communities in perturbed soils: the influence of the wandering albatross, *Polar Biology,* 30: 395-406.

Vincke, S., van de Vijver, B., Mattheeusen, R. and Beyens, L. (2004b) Freshwater testate amoebae communities from Ile de la Possession, Crozet Archipelago, Subantarctica, *Arctic, Antarctic and Alpine Research,* 36(4): 584-590.

Vincke, S., van de Vijver, B., Nijs, I. and Beyens, L. (2006b) Changes in the testatacean community structure along small soil profiles, *Acta Protozoologica,* 45: 395-406.

Vucetich, M.C. (1975) Tecamebianos muscicolas y esfagnicolas de Islas Malvinas (Argentina), *Neotropica*, 21: 11-16.

Wanner, M. (1995) Biometrical investigations of terrestrial testate amoebae (Protozoa: Rhizopoda) as a method for bioindication, *Acta Zoologica Fennica*, 196: 267-270.

Wanner, M. (1999) A review of the variability of testate amoebae: methodological approaches, environmental influences and taxonomic implications, *Acta Protozoologica,* 38:15–29.

Warner, B. G. and Charman, D. J. (1994) Holocene changes on a peatland in northwestern Ontario interpreted from testate amoebae (Protozoa) analysis, *Boreas*, 23(3): 270-279.

Whittle, A., Amesbury, M.J., Charman, D.J., Hodgson, D.A., Perren, B.B., Roberts, S.J. and Gallego-Sala, A.V. (2019) Salt-enrichment impact on biomass production in a natural population of peatland dwelling Arcellinida and Euglyphida (Testate Amoebae), *Microbial ecology*, 78(2): 534-538.

Wilkinson, D.M. (1994) A Review of the Biogeography of the Protozoan Genus Nebela in the Southern Temperate and Antarctic Zones, *Area* 26(2): 150–57.

Wilkinson, D.M., Koumoutsaris, S., Mitchell, E.A.D. and Bey, I. (2011) Modelling the effect of size on the aerial dispersal of microorganisms, *Journal of Biogeography,* 39(1): 89-97.

Woodland, W.A., Charman, D.J. and Sims, P.C. (1998) Quantitative estimates of water tables and soil moisture in Holocene peatlands from testate amoebae, *The Holocene*, 8(3): 261-273.

Yeates, G.W. and Foissner, W. (1995) Testate amoebae as predators of nematodes, *Biology and Fertility of Soils*, 20(1): 1-7.

Zhang, H., Piilo, S.R., Amesbury, M.J., Charman, D.J., Gallego-Sala, A.V. and Väliranta, M.M. (2018) The role of climate change in regulating Arctic permafrost peatland hydrological and vegetation change over the last millennium, *Quaternary Science Reviews*, 182: 121-130.

2.7. Supplementary Information

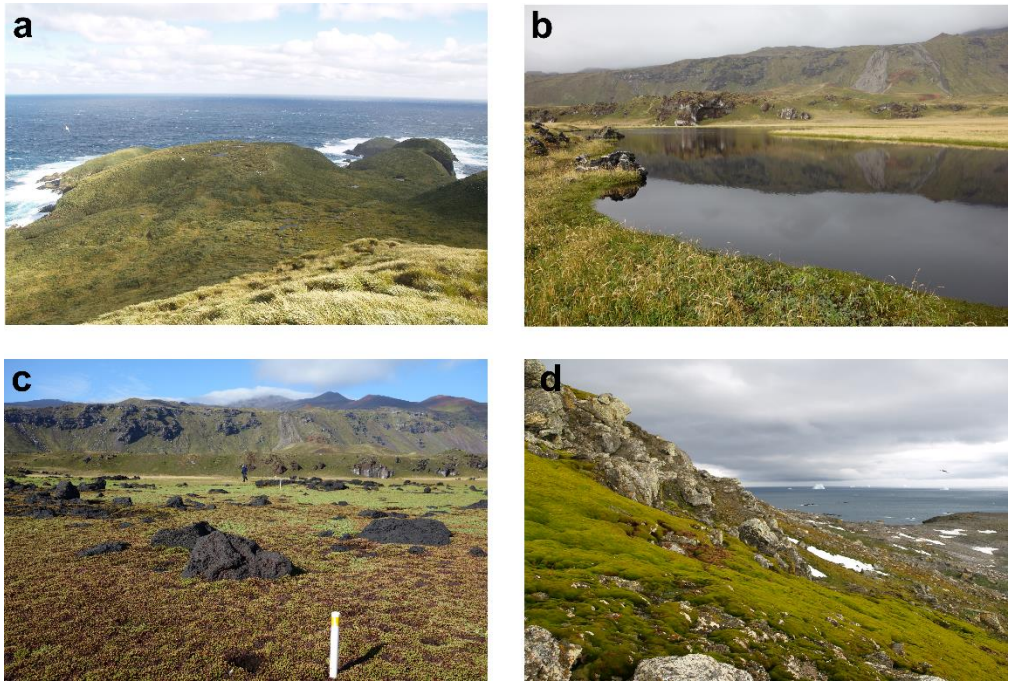

Supplementary Figure 2.1 | Examples of palaeoenvironmental archives in the Southern Ocean region. a) Peatland at Molly Meadows, Bird Island (South Georgia; Sub-Antarctic), b) coastal lake and peatland (c) at Kampkoppie, Marion Island (Sub-Antarctic), and d) moss bank, western coast of Signy Island (Maritime Antarctic). Photograph sources: Alex whittle (a,d), Dominic Hodgson (b,c).

Supplementary Table 2.1 | List of testate amoebae taxa currently reported from the sub-Antarctic region, and updates in taxonomic nomenclature made during the compilation of the database. Sub-location codes refer to specific locations (islands) in which the taxon has so far been reported: South Georgia – S, Heard Island – HI, Ile de la Possession (Crozet Archipelago) – IP, Kerguelen Island – KI, Marion Island – MA, Macquarie Island – MQ. ● denotes reported presence of species at sampling location. ○ Taxa reported from location. Bracketed numbers refer to the original report, shown in reference list below.

*** Order** **** Family** Original reported taxon name [Report]	Current taxon name/authority	Sub-location codes SG	HI	IP	KI	MA	MQ
***Arcellinida Kent 1880**							
**** Arcellidae Ehrenberg 1843**							
	Arcella arenaria	●		●	●	●	●
	Arcella bathystoma	●					
	Arcella catinus					●	
	Arcella discoides			●		●	
Arcella rotundata var. alta [1] (see [2])	*Arcella hemisphaerica*	●		●			
Arcella rotundata var. aplanata [3] [1] (see [2]) *Arcella rotundata var. scrobiculata* [1] (see [2]) *Arcella rotundata var. stenostoma f. undulata* [4][1] (see [2])							
	Arcella vulgaris	●	●	●	●	●	●
Arcella sp. 1 [3]				○			
Arcella sp.1 [4]		○					
Arcella sp.2 [4]		○					
Arcella sp.3 [4]		○					

**** Centropyxidae Jung 1942**											
Centropyxis aculeate [3]	*Centropyxis aculeata*	●		●		●					
Centropyxis aculeata var. ecornis [5]	*(complex)*										
Centropyxis aculeata var. minima [1] (see [6])											
Centropyxis aerophila var. minuta [4][1]	*Centropyxis aerophila*	●		●	●	●					
Centropyxis aerophila var. sphagnicola [7][8][9][4][1]	*(complex)*										
Centropyxis aerophila var. sylvatica [8][9][10][4]											
Centropyxis globulosa [7]											
	Centropyxis cassis	●		●	●	●					
Difflugia constricta [11][12][5][13]	*Centropyxis constricta*	●	●	●	●	●	●				
	Centropyxis deflandriana			●	●						
	Centropyxis ecornis	●									
	Centropyxis elongata	●									
Centropyxis gibba gibbosa [1]	*Centropyxis gibba*	●									
	Centropyxis hemisphaerica					●					
	Centropyxis hirsuta			●							
	Centropyxis laevigata	●									
	Centropyxis minuta	●				●					
	Centropyxis orbicularis	●									
Centropyxis cf. plagiostoma [7]	*Centropyxis plagiostoma*				●						
Centropyxis plagiostoma terricola [7]											
	Centropyxis platystoma	●		●		●					
	Centropyxis sacciformis			●		●					
Centropyxis sylvatica minor [7]	*Centropyxis sylvatica*				●	●					
Centropyxis sp.1 [4]		○									
**** Cryptodifflugiidae Jung 1942**											
	Cryptodifflugia compressa			●							
Difflugiella crenulata [8][3][9][10][4][14]	*Cryptodifflugia crenulata*	●		●		●					
Difflugiella crenulata var. globosa [4][15][3][9]											
Difflugiella minuta [3][9][10] (see [16])	*Cryptodifflugia minuta*			●							
Difflugiella oviformis [7][8][3][9][10][14]	*Cryptodifflugia oviformis*	●		●	●	●					
Difflugiella oviformis var. fusca [4][15][3][9][10]											
Difflugiella oviformis var. fusca f. major [14]											
Difflugiella pusilla [8][15][3][9][10]	*Cryptodifflugia pusilla*			●							
Difflugiella sacculus [3][9][10][14]	*Cryptodifflugia sacculus*			●		●					
Difflugiella sp. [17] *(Cryptodifflugia* sp.*)*		○									
Cryptodifflugia-Pseudodifflugia spp. [18]						○					
Difflugiella sp.1 [8] *(Cryptodifflugia* sp.*)*				○							
Difflugiella sp.2 [3] *(Cryptodifflugia* sp.*)*				○							
Difflugiella sp.3 [9] *(Cryptodifflugia* sp.*)*				○							
	Wailesella eboracensis					●					
**** Hyalospheniidae Schultze 1877**											
Nebela vas [7][8][3][9][10][12][17][14][13]	*Apodera vas*	●		●	●	●	●				
Nebela vas. longicollis [14]											
Nebela vas. obliqua [14]											
Nebela certesi [14]	*Certesella certesi*					●					
Nebela martiali [17][14][19][13]	*Certesella martiali*	●				●	●				
Certesella spp. [18]						○					
	Hyalosphenia minuta	●									
	Hyalosphenia papilio					●					
Hyalosphenia sp.1 [4]		○									
Hyalosphenia sp.1 [8]				○							
Hyalosphenia sp.1 [15]				○							
Hyalosphenia sp.1 [9]				○							
Hyalosphenia sp.1 [3]				○							
Hyalosphenia sp.1 [10]				○							
Hyalosphenia sp.2 [4]		○									
Hyalosphenia sp.2 [9]				○							
Hyalosphenia sp.3 [9]				○							
Hyalosphenia sp.4 [9]				○							
	Nebela collaris	●	●	●	●						
	Nebela minor			●							
	Nebela tincta			●		●					
Nebela sp.1 [3]				○							
Nebela sp.3 [3]				○							
Nebela sp.4 [3]				○							
Nebela lageniformis [7][1][13]	*Padaungiella lageniformis*	●			●	●	●				
Nebela tubulata [7][8][3][9][10]	*Padaungiella tubulata*			●	●						

Nebela wailesi [11][9][10][17][14]	*Padaungiella wailesi*	●		●		●	
	Porosia bigibossa					●	
	Quadrulella symmetrica					●	
**** Microchlamyiidae Ogden 1985**							
	Microchlamys patella	●		●		●	
** **Microcoryciidae de Saedeleer 1934**							
	Diplochlamys fragilis				●		
	Diplochlamys timida				●		
	Microcorycia flava					●	
Microcorycia sp. [1] (see subsequent description as a new species [20]).	*Microcorycia husvikensis*	●					
Microcorycia sp.1 [4]		○					
** **Netzeliidae Kosakyan et al. 2016**							
Difflugia oviformis [1]	*Netzelia oviformis*	●					
** **Paraquadrulidae Deflandre 1953**							
	Paraquadrula irregularis			●	●		
** **Phryganellidae Jung 1942**							
Phryganella hemisphaerica [13] (see [21])	*Phryganella acropodia*	●		●	●	●	●
	Phryganella paradoxa			●	●		
** **Plagiopyxiidae Bonnet & Thomas 1960**							
Bullinula indica [13]	*Bullinularia indica*						●
	Plagiopyxis callida			●			
	Plagiopyxis declivis			●	●		
	Plagiopyxis intermedia				●		
	Plagiopyxis labiata				●		
	Plagiopyxis minuta				●		
Protoplagiopyxis sp.1 [3]				○			
** **Trigonopyxidae Loeblich & Tappan 1964**							
Cyclopyxis aff. arcelloides [3]	*Cyclopyxis arcelloides*	●		●			
Cyclopyxis arcelloides var. minima [4]							
Cyclopyxis eurystoma parvula [4][7]	*Cyclopyxis eurystoma*	●			●	●	
	Cyclopyxis microstoma	●					
	Cyclopyxis puteus			●			
Cyclopyxis sp.1 [3]				○			
Cyclopyxis sp.1 [8]				○			
Cyclopyxis sp.1 [15]				○			
Cyclopyxis sp.1 [9]				○			
Cyclopyxis sp.2 [9]				○			
Difflugia arcula [22][13]	*Trigonopyxis arcula*	●				●	●
Trigonopyxis sp.1 [4]		○					
** **Incertae sedis**							
Nebela caudata [13]	*Argynnia caudata*	●				●	●
Nebela dentistoma [7][8][15][11][3][9][10][17][14][19][13]	*Argynnia dentistoma*	●		●	●	●	●
Nebela antarctica [14] (see [23])							
Nebela playfairi [14]	*Argynnia playfairi*					●	
Nebela playfairi var. elongata [14]							
Nebela playfairi var. lata [14]							
	Argynnia spicata					●	
Nebela teres [14]	*Argynnia teres*					●	
	Argynnia vitraea					●	
Difflugia aff. ampullula [3]	*Difflugia ampullula*			●			
Difflugia aff. angulostoma [3] (see [24])	*Difflugia angulostoma*			●			
	Difflugia avellana					●	
Difflugia longicollis [3][17][19] (see [25])	*Difflugia bryophila*	●		●	●		
Difflugia microstoma [3] (see [24])	*Difflugia difficilis*			●			
	Difflugia dujardini	●			●		
	Difflugia glans	●					
	Difflugia globularis	●					
	Difflugia globulosa	●	●	●	●	●	
	Difflugia globulus	●		●			
	Difflugia lacustris	●					
	Difflugia lanceolata	●					
	Difflugia lata	●					
Difflugia cfr. lucida [9]	*Difflugia lucida*	●		●	●		
	Difflugia molesta	●					
Difflugia bacillifera [7][8][15][3][9][10] (syn. see [25])	*Difflugia oblonga*	●		●	●		
Difflugia parva [4] (see [25])							

		Difflugia pecac	●									
Difflugia tenuis[4][3][9][10] (see [24])		*Difflugia penardi*	●			●						
Difflugia manicata [3] (see [24])												
Difflugia penardi var. ogiva [1]												
		Difflugia pristis				●						
		Difflugia pulex	●			●				●		
Difflugia piriformis [12]		*Difflugia pyriformis*	●		●	●	●	●				
		Difflugia serrata	●									
Difflugia sp.1 [3]						○						
Difflugia sp.1 [4]			○									
Difflugia sp.1 [15]						○						
Difflugia sp.2 [3]						○						
Difflugia sp.2 [4]			○									
Difflugia sp.3 [3]						○						
Difflugia sp.3 [8]						○						
Difflugia sp.3 [15]						○						
Difflugia sp.3 [9]						○						
Difflugia sp.3[10]						○						
Difflugia sp.4 [3]						○						
Difflugia sp.4 [9]						○						
Difflugia sp.5 [3]						○						
Difflugia sp.5 [9]						○						
Difflugia sp.6 [3]						○						
Difflugia sp.6 [4]			○									
Difflugia sp.6 [8]						○						
Difflugia sp.6 [15]						○						
Difflugia sp.6 [9]						○						
Difflugia sp.6 [10]						○						
Difflugia sp.7 [3]						○						
Difflugia sp.7 [8]						○						
Difflugia sp.7 [9]						○						
Difflugia sp.7 [10]						○						
Difflugia sp.8 [9]						○						
Difflugia sp.8 [10]						○						
Difflugia sp.9 [8]						○						
Difflugia sp.9 [9]						○						
Difflugia sp.9 [10]						○						
Difflugia sp.10 [8]						○						
Difflugia sp.10 [15]						○						
Difflugia sp.10 [9]						○						
Difflugia sp.10 [10]						○						
Difflugia sp.11 [9]						○						
		Heleopera petricola				●	●		●		●	
		Heleopera sphagni									●	
		Heleopera sylvatica	●			●	●				●	
		Microquadrula musciphila					●					
		Pyxidicula operculata							●			
Pyxidicula spp.1 [18]									○			
Pyxidicula spp.2 [18]									○			
Schwabia spp. [7]							○					
Difflugia minutissima [9]		*Sexangularia minutissima*				●						
* **Euglyphida Copeland 1956**												
** **Assulinidae Lara 2007**												
Assulina muscora [11]		*Assulina muscorum*	●			●	●		●		●	
Euglypha seminulum [12]		*Assulina seminulum*			●	●	●					
Assulina sp.1 [8]						○						
Assulina sp.1 [3]						○						
Assulina sp.1 [15]						○						
Assulina sp.1 [9]						○						
Assulina sp.1 [4]			○									
		Valkanovia elegans							●			
** **Cyphoderiidae De Sandeleer, 1934**												
Corythionella sp.1 [10]						○						
		Cyphoderia ampulla				●						
Cyphoderia sp.1 [10]						○						
Cyphoderia sp.2 [10]						○						
Cyphoderia sp.1 [3]						○						
Cyphoderia sp.1 [8]						○						
Cyphoderia sp.1 [15]						○						

Cyphoderia sp.1 [9]			○			
Cyphoderia sp.2 [15]			○			
** **Euglyphidae Wallich 1864**						
	Euglypha bryophila	●	●	●		
	Euglypha castrii			●		
Euglypha ciliata var. glabra [8][15][3][9][10]	*Euglypha ciliata*	●	●	●	●	●
Euglypha ciliata f. heterospina [14]						
Euglypha compressa var. glabra [8][9][10]	*Euglypha compressa*	●	●	●	●	●
Euglypha cristata var. turbo [14]	*Euglypha cristata*		●		●	
	Euglypha cuspidata		●	●		
	Euglypha denticulata			●		
	Euglypha filifera		●			
Euglypha alveolata [13] (see [26])	*Euglypha laevis*		●		●	●
	Euglypha polylepis	●	●			
	Euglypha rotunda	●	●	●	●	
Euglypha strigosa var. glabra [8][3]	*Euglypha strigosa*	●	●	●	●	
Euglypha tuberculata var. minor [9][10]	*Euglypha tuberculata*	●	●	●	●	
Euglypha sp. [5]		○				
Euglypha sp.1 [9]			○			
Euglypha sp.2 [9]			○			
Euglypha sp.2 [15]			○			
Euglypha sp.3 [9]			○			
Euglypha sp.4 [9]			○			
Euglypha acanthophora [3][10] (see [27])	*Scutiglypha crenulata*		●			
** **Sphenoderiidae Chatelain 2013**						
Corythion pulchellum [7]	*Trachelcorythion pulchellum*	●	●	●		
** **Trinematidae Hoogenraad and De Groot, 1940**						
	Corythion delamarei			●		
Corythion dubium aerophila [7]	*Corythion dubium*	●	●	●	●	●
Corythion sp.1 [8]			○			
	Trinema alofsi	●				
Trinema complanatum var. globulosa [10]	*Trinema complanatum*	●	●		●	
Trinema complanatum var. inflata [10]						
	Trinema enchelys	●	●	●	●	●
Trinema lineare f. minuscula [1]	*Trinema lineare*	●	●	●	●	
Trinema lineare var. globulosa [1]						
Trinema lineare var. truncatum [15]						
** **Incertae sedis**						
Tracheleuglypha acolla (see [28][29])	*Tracheleuglypha dentata*		●	●	●	●
Sphenoderia dentata [13] (see [26])						
Tracheleuglypha sp.1 [3]			○			
* **Stramenopila**						
** **Amphitremidae Poche, 1913**						
Archerella sp.1 [8]			○			
Archerella sp.1 [9]			○			
Archerella sp.1 [4]		○				
* **Other cercozoa**						
** **Psammonobiotidae Golemansky 1974**						
	Edaphonobiotus campascoides	●	●			
** **Pseudodifflugiidae De Sandeleer 1934**						
	Pseudodifflugia fulva	●	●		●	
Pseudodifflugia gracilis var. terricola [8][10]	*Pseudodifflugia gracilis*		●			
** **Incertae sedis**						
	Frenzelina reniformis		●			

References:

[1] L. Beyens, D. Chardez, D. De Baere, and C. Verbruggen (1995) The aquatic testate amoebae fauna of the Strømness Bay area, South Georgia, *Antarctic Science*, 7(1): 3-8.

[2] Lahr, D.J.G. and Lopes, S.G.B.C. (2009) Evaluating the taxonomic identity in four species of the lobose testate amoebae genus Arcella Ehrenberg, 1832, *Acta Protozoologica*, 48(2): 127–142.

[3] Vincke, S., Van De Vijver, B., Mattheeussen, R. and Beyens, L. (2004) Freshwater Testate Amoebae Communities from Île de la Possession, Crozet Archipelago, *Subantarctica, Arctic Antarctic and Alpine Research*, 36(4): 584-590.

[4] Vincke, S., Van De Vijver, B., Gremmen, N. and Beyens, L. (2006) The Moss Dwelling Testacean Fauna of the Strømness Bay (South Georgia), *Acta Protozoologica*, 45: 65-75.

[5] Sandon, H. and Cutler, D. W. (1924) Some protozoa from the soils collected by the “Quest” expedition (1921-22), *Journal of the Linnean Society of London – Zoology*, 36: 1-2

[6] Lahr, D.J., Bergmann, P.J. and Lopes, S.G. (2008) Taxonomic identity in microbial eukaryotes: a practical approach using the testate amoeba Centropyxis to resolve conflicts between old and new taxonomic descriptions. *Journal of Eukaryotic Microbiology*, *55*(5): 409-416.
[7] Bonnet, L. (1981) Thecamoeniens (Rhizopoda Testacea), *Bull. Com. Nat. Fran. Res. Antarct.* 48: 23–32.
[8] Vincke, S., van de Vijver, B., Nijs, I. and Beyens, L. (2006) Changes in the testatacean community structure along small soil profiles, *Acta Protozoologica,* 45: 395-406.
[9] Vincke, S., Gremmen, N., Beyens, L. and van de Vijver, B. (2004) The moss dwelling testacean fauna of Ile de la Possession, *Polar Biology,* 27: 753-766.
[10] Vincke, S., Ledeganck, P., Beyens, L. and Van de Vijver, B. (2004) Soil testate amoebae from sub-Antarctic Îles Crozet, *Antarctic Science*, 16(2): 165-174.
[11] Smith, H.G. (1975) Protozoaires terricoles de l'le de la Possession, *Rev. Ecol. Biol. Sol.* 12(2): 523-530.
[12] Richters, F. (1907) Die Fauna Der Moosrasen Des Gaussbergs Und Einiger Südlicher Inseln. In: *Deutsch Südpolar-Expedition 1901–1903. Zoologie 9*, 259–302.
[13] Penard, E. (1913) Rhizopodes d'eau douce. In: *Deuxieme Expedition Antarctique Francaise (1908-1910), Sciences Naturelles: Documents Scientifiques*.
[14] Grospietsch, T. (1971) 'Beitrag zur ökologie der Testaceen Rhizopoden von Marion Island', in Van Zinderen-Bakker, E. M., Winterbottom, J. M., and Dyer, R. A. (eds) *Marion and Prince Edward Island, Report on the South African Biological and Geological Expedition 1965-1966*. Cape Town: Balkema, pp. 411–423.
[15] Vincke, S., van de Vijver, B., Ledeganck, P., Nijs, I. and Beyens, L. (2007) Testacean communities in perturbed soils: the influence of the wandering albatross, *Polar Biology,* 30: 395-406.
[16] Bobrov, A. and Mazei, Y. (2017) A review of testate amoeba genus Cryptodifflugia Penard, 1890 (Phryganellina: Cryptodifflugiidae) with a key to species, *Zootaxa*, *4282*(2): 292-308.
[17] Smith, H.G (1982) The terrestrial protozoan fauna of South Georgia, *Polar Biology,* 1:173-179.
[18] Whittle, A., Amesbury, M.J., Charman, D.J., Hodgson, D.A., Perren, B.B., Roberts, S.J. and Gallego-Sala, A.V. (2019) Salt-enrichment impact on biomass production in a natural population of peatland dwelling Arcellinida and Euglyphida (Testate Amoebae), *Microbial ecology*, 78(2): 534-538.
[19] Smith, H.G. and Headland, R. K. (1983) The population ecology of soil testate rhizopods on the sub-Antarctic island of South Georgia, *Rev. Ecol. Biol. Sol.* 20(2): 269-286.
[20] Beyens, L. and Chardez, D. (1997) New testate amoebae taxa from the Polar Regions, *Acta Protozoologica,* 36: 137-142.
[21] Dumack, K., Kahlich, C., Lahr, D.J. and Bonkowski, M. (2018) Reinvestigation of Phryganella paradoxa (Arcellinida, Amoebozoa) Penard 1902, Journal of Eukaryotic Microbiology, 66(2): 232-243.
[22] Richters, F. (1908) Moosbewohner. In: *Wissenschaftliche Ergebnisse Der Schwedeschen Südpolar Expedition 1901-1903.*
[23] Heger, T.J., Mitchell, E.A., Ledeganck, P., Vincke, S., Van de Vijver, B. and Beyens, L. (2009) The curse of taxonomic uncertainty in biogeographical studies of free-living terrestrial protists: a case study of testate amoebae from Amsterdam Island, *Journal of Biogeography*, 36(8): 1551-1560.
[24] Mazei, Y. and Warren, A. (2015) A survey of the testate amoeba genus Difflugia Leclerc, 1815 based on specimens in the E. Penard and C.G. Ogden collections of the Natural History Museum, London. Part 3: Species with shells that are spherical or ovoid, *Protistology,* 9(1): 3-49.
[25] Mazei, Y. and Warren, A. (2014) A survey of the testate amoeba genus Difflugia Leclerc, 1815 based on specimens in the E. Penard and C.G. Ogden collections of the Natural History Museum, London. Part 2: Species with shells that are pyriform or elongate, *Protistology*, 8(4): 133-171.
[26] Todorov, M. and Bankov, N. (2019) An Atlas of Sphagnum-dwelling Testate Amoebae in Bulgaria. Pensoft, Sofia.
[27] Foissner, W. and Schiller, W. (2001) Stable for 15 million years: scanning electron microscope investigation of Miocene euglyphid thecamoebians from Germany, with description of the new genus Scutiglypha, *European Journal of Protistology*, *37*(2):167-180.
[28] Ogden, C. G. and Coûteaux, M-M. (1988) The Effect of Predation on the Morphology of Tracheleuglypha dentata (Protozoa: Rhizopoda), *Archiv für Protistenkunde,* 136(1): 107-115.
[29] Lüftenegger, G. and Foissner, W., 1991. Morphology and biometry of twelve soil testate amoebae (Protozoa, Rhizopoda) from Australia, Africa, and Austria. *Bulletin of the British Museum, Natural History. Zoology*, *57*(1): 1-16.

Supplementary note 2.1: Observations of seasonality in testate communities in the Southern Ocean region.

Seasonality is an important climatic feature of the Southern Ocean region. Many areas experience a short growing season in summer and sub-zero temperatures in winter when land becomes blanketed by snow and ice.

In the Maritime Antarctic, a general pattern of activity cessation in winter and rapid spring blooms followed by decline during summer as moisture is depleted, has been observed in studies monitoring testate amoebae populations within plots of *Polytrichum-Chorisodontium* moss peat (Smith, 1973; 1978). The most abundant species within these mosses, *Corythion dubium* and *Phryganella acropodia* have both been studied individually. Within samples from three soil horizons spanning 0-9 cm depth, Smith (1973) reported a marked variation in numbers of *C. dubium* between winter and summer. Populations in each horizon demonstrated a dramatic increase in numbers during September and November as surface layers thawed, and in possible correlation with increased yeast and bacterial abundance and nutrient availability. The bloom propagated downward through the soil surface layers during the summer, and numbers remained relatively high until the onset of thawing. *P. acropodia* showed a similar seasonal pattern to *C. dubium* within this environment (Smith, 1978). Initially high abundance in summer followed progressive mortality through the autumn and winter months, and close to zero live individuals were recorded in mid-winter (August) when average temperature fell to approximately -8˚C. A bloom then followed in September-October coinciding with the availability of moisture during the spring melt, when average temperatures rose above 0˚C. Throughout the summer, drying of the soil correlated with a decline in abundance before a second bloom of lesser magnitude occurred when wetter conditions temporarily returned in autumn (Smith, 1978).

The sub-Antarctic climate is less seasonal and similar analysis monitoring populations from four soil types on South Georgia revealed no consistent pattern to demonstrate any definite seasonality (Smith and Headland, 1983). Although all abundant species underwent blooms during the spring months, propagation to levels lower in the soil with time was not observed, and records of peak abundance beneath snow cover in winter were also made. This suggests that sub-Antarctic faunas although compositionally similar to the maritime Antarctic, are capable of maintaining some reproductive activity through the year, likely due to the absence of very low sub-zero temperatures during winter. It is suggested that fluctuations between/within populations correlate to growth and availability of organisms at lower trophic levels, such as bacteria and fungi, which are known to vary (Smith and Headland, 1983).

Chapter 3

Salt-enrichment impact on biomass production in a natural population of peatland dwelling Arcellinida and Euglyphida (testate amoebae)

Published in *Microbial Ecology* (2019)

Alex Whittle[1,2,*], Matthew J. Amesbury[1], Dan J. Charman[1], Dominic A. Hodgson[2], Bianca B. Perren[2], Stephen J. Roberts[2], Angela V. Gallego-Sala[1].

[1] Department of Geography, University of Exeter, Amory Building, Rennes Drive, Exeter, EX4 4RJ, UK.

[2] British Antarctic Survey, Natural Environment Research Council, High Cross, Madingley Road, Cambridge, CB3 0ET, UK.

Unicellular free-living microbial eukaryotes of the order Arcellinida (Tubulinea; Amoebozoa) and Euglyphida (Cercozoa; SAR), commonly termed testate amoebae, colonise almost every freshwater ecosystem on Earth. Patterns in the distribution and productivity of these organisms are strongly linked to abiotic conditions - particularly moisture availability and temperature - however the ecological impacts of changes in salinity remain poorly documented. Here we examine how variable salt concentrations affect a natural community of Arcellinida and Euglyphida on a freshwater sub-Antarctic peatland. We principally report that deposition of wind-blown oceanic salt-spray aerosols onto the peatland surface corresponds to a strong reduction in biomass and to an alteration in the taxonomic composition of communities in favour of generalist taxa. Our results suggest novel applications of this response as a sensitive tool to monitor salinisation of coastal soils and to detect salinity changes within peatland palaeoclimate archives. Specifically, we suggest that these relationships could be used to reconstruct millennial scale variability in salt-spray deposition - a proxy for changes in wind-conditions - from sub-fossil communities of Arcellinida and Euglyphida preserved in exposed coastal peatlands.

Testate amoebae | Sub-Antarctica | Salinity | Southern Hemisphere Westerly Winds | Bioindicators

Arcellinida and Euglyphida (AE) belong to a polyphyletic group of test-forming protozoans that are widely used in environmental biomonitoring and palaeoclimatology [1-2]. Despite the predominant association of most taxa with freshwater ecosystems (e.g., lakes, soils, peatlands) the distribution of active communities also extends into many moderately saline environments [3-8]. Nevertheless, like other microbial groups [9-10], physiological and metabolic challenges exerted by differing salinity conditions appear to be reflected in the global and local distribution of AE. Only a small percentage of taxa are known to occur in marine ecosystems [e.g. 11], and salinity conditions have been linked to patterns in the distribution of taxa within lakes contaminated by road-salt run-off [12-13], anchialine pools [14], and saltmarshes [3,15-16]. However, the importance of salinity in defining the distribution of taxa, community structure, and size of AE populations remains uncertain.

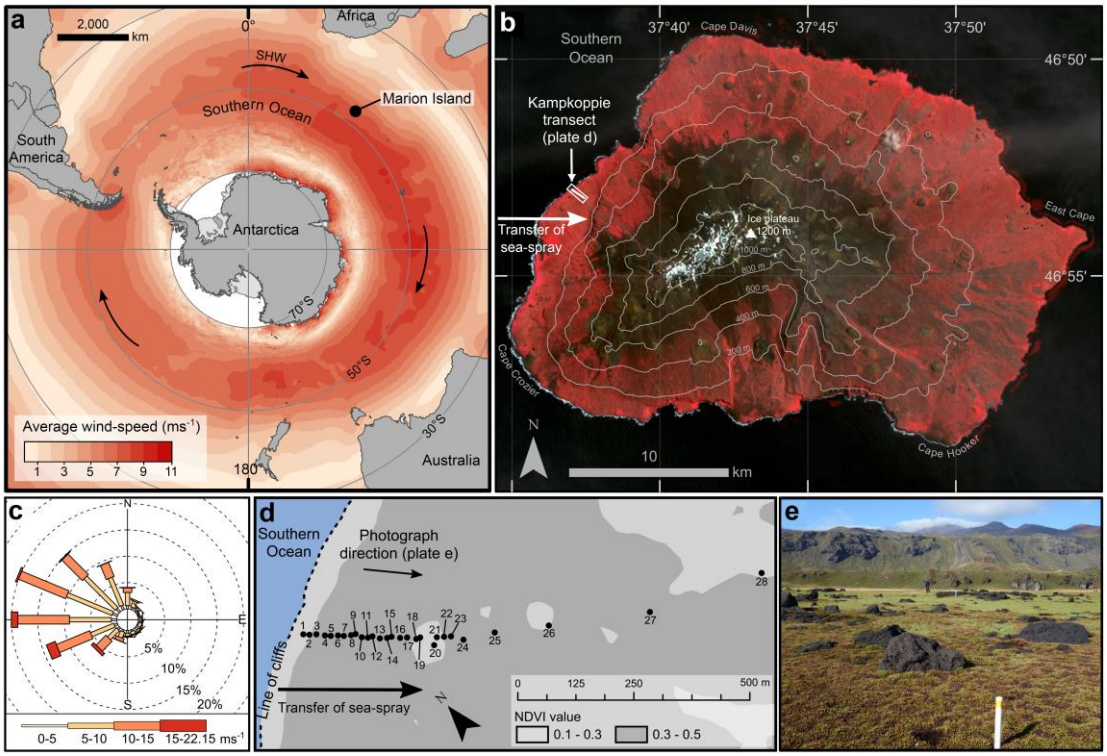

Figure 3.1 | a) Location of Marion Island in the Southern Indian Ocean province of sub-Antarctica and within the core belt of the Southern Hemisphere Westerly winds (SHW). Arrows indicate prevailing atmospheric circulation. Annual sea surface-level (10 m) mean wind speeds are based on NOAA blended high resolution (0.25 degree grid) vector data downloaded from (https://www.ncdc.noaa.gov/data-access/marineocean-data/blended-global/blended-sea-winds), and are calculated from monthly mean values for the period 1995-2005. b) False-colour satellite image indicating vegetation cover (red shading) and the peatland at Kampkoppie where samples were collected. Image courtesy of the U.S. Geological Survey (http://earthexplorer.usgs.gov/). c) Wind-rose derived from daily NOAA blended sea-winds data (source as Fig. 3.1a) for the period

2008-2018, indicating the prevailing winds from the west-north-west. Wind strengths and frequency were calculated for wind directions at 22.5 degree intervals. d) Locations of samples (marked 1-28) within the gradient of salt-enrichment at Kampkoppie. Normalised difference vegetation index (NDVI) values indicate minor changes in the vegetation cover at the peatland surface. e) Photograph of the peatland surface looking east from the coast and showing the lack of topographic variability along the sampled gradient. Vegetation is characteristic of exposed coastal areas with a salt-spray complex of *Cotula plumosa* and *Crassula moschata* (foreground) and exhibits a distinct succession with distance inland. Palaeocliffs visible in the background mark the most inland extent of the sampling transect (Photograph source: Dominic Hodgson).

We directly examined changes in a population of AE along an uninterrupted salinity gradient from brackish to freshwater conditions within a west-facing coastal peatland on sub-Antarctic Marion Island (Fig. 3.1). Correlation between salt-enrichment and coastal exposure is a characteristic feature of ecosystems on the sub-Antarctic islands which results from intense generation and deposition of oceanic salt-spray by strong prevailing westerly winds [17]. Soil-dwelling AE communities were described from twenty-eight samples exposed to varying levels of relative salt-enrichment which was quantified by measuring the conductivity of pore-water, a direct proxy for microhabitat salinity (Fig. 3.1; Supplementary methods). Principal component (PC) analysis confirmed that conductivity was the primary ecological gradient represented by the samples (Fig. 3.2a) and suggested that atmospheric deposition of oceanic salt-spray was the dominant cause of elevated salinity (see Supplementary methods). The peatland transect, which spanned a coastal terrace ~30 m above sea-level, represented a model system for assessing the ecological importance of salinity because; (1) the carbon and moisture rich substrate provides consistent conditions for colonisation, (2) confounding micro-environmental conditions thought to affect the distribution of AE in other salt-influenced systems were controlled, and (3) the low-energy depositional environment limits potential for contamination of assemblages by allochthonous tests.

We recorded a diverse fauna of 34 taxa from 21 genera, including 17 taxa not previously identified on Marion Island (Supplementary Figure 3.1; Supplementary Table 3.1). We also report the first known occurrence of *Quadrulella symmetrica* within the sub-, maritime- or continental Antarctic region. Taxa belonging to the third major group of testate amoebae, Amphitrematidae (Labyrinthulids; SAR), were not present in these samples.

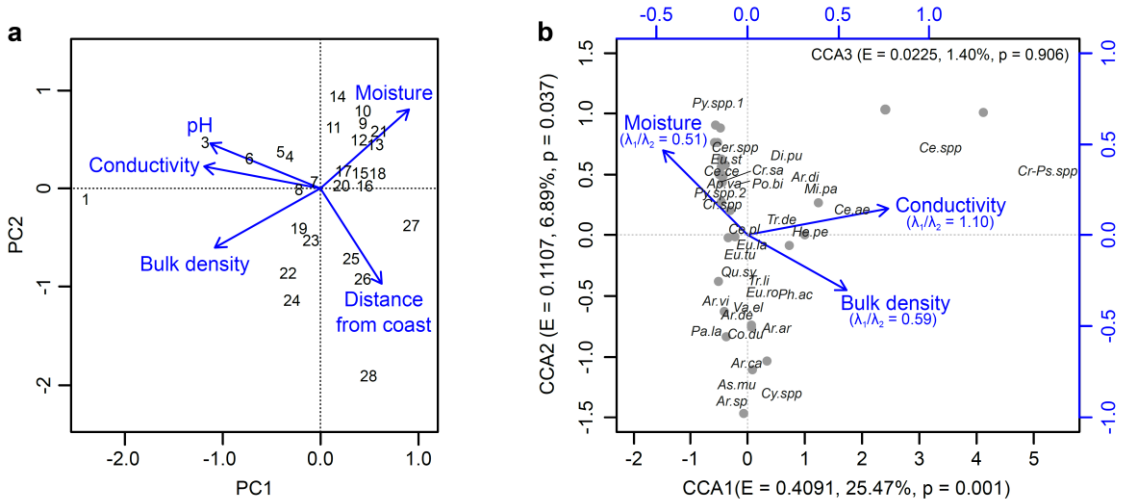

Figure 3.2 | a) Principal component (PC) analysis of environmental conditions represented in the sampled communities of Arcellinida and Euglyphida. Numbers indicate sample locations within the salinity gradient labelled sequentially with distance inland from the coastline (see Fig. 3.1d). High correlation between conductivity and pH of pore-water (R^2 = 0.82, p <0.001) and distance inland from the coast is indicative of oceanic salt-spray inputs, which cause a simultaneous increase in ionic strength and pH of the otherwise freshwater and acidic peatland ecosystem (i.e., both pH and conductivity act as proxies for salt-enrichment in this environment). b) Canonical correspondence analysis (CCA) tri-plot representing the relationship between key micro-environmental variables and taxonomic assemblages. The ratio >1 between the first constrained (λ_1) and unconstrained axis (λ_2) from a partial CCA run individually for each micro-environmental variable shows that conductivity is the main determinant of relative taxon abundance. pH and distance from the coast were removed from analysis due to their high correlation with conductivity. Eigenvalues (E) and percentage of variance in assemblage data explained by each axis is shown. Values of each environmental variable increase in the direction of the arrow. Abbreviations of individual taxa are given in Supplementary Table 3.1. Grey markers designate the distribution of samples. Full summaries of analysis are given in Supplementary Table 3.2 and 3.3.

Marked differences in the AE fauna were observed between samples. Canonical correspondence analysis (CCA) indicated that measured conductivity is (or is linearly related to) the main determinant of assemblages (i.e., relative taxon abundance) in the sampled communities denoting a connection between AE fauna and magnitude of salt-enrichment (Fig. 3.2b). In total, conductivity accounted for ~48% of explained variance in the assemblages, and also explained the largest independent portion of variance after removing the contributions of confounding microhabitat variables (Supplementary Table 3.4). Despite major differences in habitat, this relationship corroborates the role of

salinity as a driver of assemblage changes suggested from observations of freshwater lakes exposed to salt addition of a comparable magnitude [12-13].

Although the distribution of samples is skewed toward lower salinity conditions, tight clustering at the centre of CCA axis 1 indicates that saline conditions are sub-optimal for the majority of taxa. Accordingly, communities exposed to high concentrations of salt-spray deposition generally presented lower taxonomic-richness and evenness, implying that many taxa are selectively excluded by high salinity conditions (Fig. 3.3). Opportunistic generalist taxa from the genus *Centropyxis* [16] which have been suggested to exhibit moderately euryhaline ecology [13-14] are a notable exception. These taxa dominated high salinity communities and possibly benefit from reduced competition caused by exclusion of other taxa (Supplementary Figure 3.2).

To test whether salinity elicits quantifiable changes beyond the distribution of individual taxa, we examined variability in total biomass ([18-19]; Supplementary methods). Biomass co-varied with alpha-diversity, and denotes a major distinction between productive freshwater communities and depauperate, less productive salt-enriched communities (Fig. 3.3). Specifically, biomass and conductivity are linked by a highly significant, negative logarithmic relationship (R^2 = 0.6394, p = <0.001). Arcellinida and Euglyphida responded consistently (R^2 = 0.6283 / 0.6234 respectively, both p = <0.001); although, as a more diverse taxonomic group, Arcellinida contributed a larger portion to total biomass. This relationship held when communities in samples exhibiting high conductivity values - i.e. >2 millisiemens per cm (mS/cm) - were sequentially excluded (Supplementary Figure 3.3). Our data therefore indicates that AE are highly sensitive even to small perturbations in salinity; for the least saline sample included in this study, an increase in microhabitat conductivity of only 0.25 mS/cm (from 0.58 to 0.83 mS/cm) was estimated to result in a 50% biomass reduction.

AE are important heterotrophs in peatlands [18, 20-21] and consume a wide range of microbial prey (i.e., bacteria, other protozoa, fungi, algae [22]). Following this, it is possible that the observed variability in AE biomass reflects unmeasured differences in the availability of these prey microorganisms. To test this, we examined correlations between conductivity conditions and the prevalence of functional-traits linked to feeding ecology. However, no significant relationships were found to support this interpretation (Supplementary Table 3.5). Additionally,

we did not observe the presence of foraminifera which can coexist with AE in brackish environments [8,14,16] and may compete for resources. Abiotic factors, therefore, appear to be more influential than feeding interactions in governing the distribution and abundance of AE under these conditions, although more research is needed into potential variability in predation pressure.

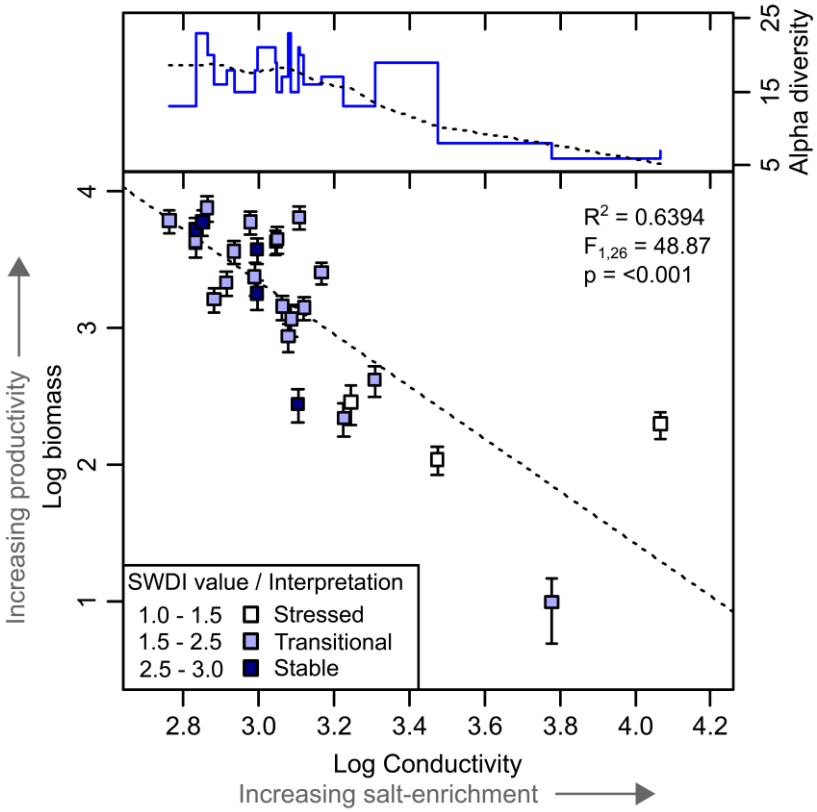

Figure 3.3 | Relationship between pore-water conductivity, and AE alpha-diversity, Shannon-Weaver diversity index (SWDI) and community biomass. Conductivity of pore-water was used as an indicator of salt-enrichment level in each community. Higher diversity, SWDI value and biomass are indicative of more productive AE communities. Interpretation of SWDI values indicate the favourability of environmental conditions for AE colonisation; healthy faunas in stable environments are characterised by high values, whereas low values represent faunas dominated by a small number of taxa under stressed environmental conditions [16,27]. Conductivity (microsiemens/cm) and biomass (g C g dry-soil^{-1}) were $\log_{10}(x)$ transformed. Error bars represent uncertainty in community biomass calculated using upper and lower estimates of AE concentration and standardised values for taxon specific biovolume (Supplementary methods).

The relationship between AE biomass and salinity was largely independent from patterns in species turnover. Variability in biomass was driven primarily by the abundance of individuals (population size) despite large differences in the sizes

of the individual assemblage constituents (Supplementary Table 3.6). Accordingly, population size was strongly correlated with conductivity (R^2 = 0.6631, $p < 0.001$), which is consistent with observations linking reduced concentrations of AE to greater marine influence in coastal marshes [e.g., 6, 23].

AE taxa perform reproduction either; (1) via asexual binary fission, (2) as a result of sexual life-cycles, or (3) as a combination of both strategies [24]. Test dimensions are set either during or shortly after reproduction and so it is assumed that cells maintain a fixed biovolume throughout their lifetime [but see 25]. Therefore, if both a constant rate of predation pressure and constant decay rate of empty tests is assumed, observed biomass is related directly to the rate of reproduction. Consequently, we suggest that reduced biomass is partly the result of an increased energetic cost associated with osmoregulation which is progressively traded-off against reproduction under increasing salinity. Most taxa appear not to be adapted to conditions where pore-water conductivity exceeds ~3.0 mS/cm which may mark the transition to a prevailing hypertonic environment (Fig. 3.3). This explanation linking the ionic strength of the AE microhabitat with community-level biomass is also consistent with a reduction in biomass observed after artificial nutrient addition to an Arctic fen-dwelling community [19].

The highly sensitive response of AE biomass, combined with patterns in the diversity and distribution of taxa, offer substantive potential for the use of these organisms as a bioindicator of environmental salinity. Application of these relationships to sub-fossil AE communities could considerably advance palaeoclimatology by providing, for the first time, millennial scale records of changes in atmospheric circulation recorded by salt-spray aerosol deposition onto coastal peatlands. Additionally, AE could play an important role in monitoring salinisation of coastal peatland ecosystems that are vulnerable to increased inundation under projected sea-level rise [see 26]. Biomass especially appears to offer a highly sensitive proxy for relative salt-enrichment, with the benefit of increased analytical efficiency over traditional approaches which require identification of individual taxa. More research should be conducted to confirm that comparable responses are observed under both experimental laboratory conditions and in other salt-stressed soil ecosystems.

Our results indicate for the first time that the effects of salt-enrichment on AE communities extend beyond previously documented changes in taxonomic

composition to include strong effects on biomass production. AE offer potential as bioindicators of salinity with the capability to resolve low magnitude changes in salt-enrichment, such as deposition of wind-blown oceanic salt-spray.

References

[1] Charman DJ (2001) Biostratigraphic and palaeoenvironmental applications of testate amoebae. Quaternary Science Reviews 20: 1753-1764.

[2] Kosakyan A, Gomaa F, Lara E, Lahr DJ (2016) Current and future perspectives on the systematics, taxonomy and nomenclature of testate amoebae. European Journal of Protistology 2016. 55: 105-117.

[3] Charman DJ, Roe HM, Gehrels WR (1998) The use of testate amoebae in studies of sea-level change: a case study from the Taf Estuary, south Wales, UK. The Holocene 8: 209-218.

[4] Golemansky V (1998) Interstitial testate amoebae (Rhizopoda: Testacea) from the Italian coast of the Mediterranean Sea. Acta Protozoologica 37: 139-143.

[5] Heger TJ, Mitchell EAD, Todorov M, Golemansky V, Lara E, Leander BS et al (2010) Molecular phylogeny of euglyphid testate amoebae (Cercozoa: Euglyphida) suggests transitions between marine supralittoral and freshwater/terrestrial environments are infrequent. Molecular Phylogenetics and Evolution 55: 113-122.

[6] Ooms M, Beyens L, Temmerman S (2012) Testate amoebae as proxy for water level changes in a brackish tidal marsh. Acta Protozoologica 51: 271-289.

[7] Camacho S, Connor S, Asioli A, Boski T, Scott D (2015) Testate amoebae and tintinnids as spatial and seasonal indicators in the intertidal margins of Guadiana estuary (southeastern Portugal). Ecological Indicators 58: 426-444.

[8] Barnett RL, Newton TL, Charman DJ, Gehrels WR (2017) Salt-marsh testate amoebae as precise and widespread indicators of sea-level change. Earth-science reviews 164: 193-207.

[9] Lozupone CA, Knight R (2007) Global patterns in bacterial diversity. Proceedings of the National Academy of Sciences 104: 11436-11440.

[10] Logares R, Bråte J, Bertilsson S, Clasen JL, Shalchian-Tabrizi K, Rengefors, K (2009) Infrequent marine-freshwater transitions in the microbial world. Trends in Microbiology 17: 414-422.

[11] Nicholls KH. Six new marine species of the genus Paulinella (Rhizopoda: Filosea, or Rhizaria: Cercozoa) (2009) Journal of the Marine Biological Association of the United Kingdom 89: 1415-1425.

[12] Roe HM, Patterson RT, Swindles GT (2010) Controls on the contemporary distribution of lake thecamoebians (testate amoebae) within the Greater Toronto Area and their potential as water quality indicators. Journal of Paleolimnology 43: 955-975.

[13] Roe HM, Patterson RT. Arcellacea (testate amoebae) as bio-indicators of road salt contamination in lakes (2014). Microbial Ecology 68: 299-313.

[14] Van Hengstum PJ, Reinhardt EG, Beddows PA, Huang RJ, Gabriel JJ (2008) Thecamoebians (testate amoebae) and foraminifera from three anchialine cenotes in Mexico: Low salinity (1.5-4.5 psu) faunal transitions. Journal of Foraminiferal Research 38: 305-317.

[15] Charman DJ, Roe HM, Gehrels WR (2002) Modern distribution of saltmarsh testate amoebae: regional variability of zonation and response to environmental variables. Journal of Quaternary Science 17: 387-409.

[16] Riveiros NV, Babalola AO, Boudreau REA, Patterson RT, Roe HM, Doherty C (2007) Modern distribution of salt marsh foraminifera and thecamoebians in the Seymour-Belize Inlet Complex, British Columbia, Canada. Marine Geology 242: 39–63.

[17] Saunders KM, Hodgson DA, McMurtrie S, Grosjean M (2015) A diatom-conductivity transfer function for reconstructing past changes in the Southern Hemisphere westerly winds over the Southern Ocean. Journal of Quaternary Science 30: 464-477.

[18] Royles J, Amesbury MJ, Roland TP, Jones GD, Convey P, Griffiths H et al (2016) Moss stable isotopes (carbon-13, oxygen-18) and testate amoebae reflect environmental inputs and microclimate along a latitudinal gradient on the Antarctic Peninsula. Oecologia 181: 931-945.

[19] Mitchell EAD (2004) Response of testate amoebae (Protozoa) to N and P fertilization in an Arctic wet sedge tundra. Arctic, Antarctic, and Alpine Research 36: 78-83.

[20] Jassey VEJ, Chiapusio G, Binet P, Buttler A, Laggoun-Défarge F, Delarue F, Bernard N, Mitchell EAD, Toussaint M-L, Francez A-J, Gilbert D (2013) Above- and belowground linkages in *Sphagnum* peatland: climate warming affects plant-microbial interactions. Global Change Biology 19: 811-823.

[21] Gilbert D, Amblard C, Bourdier G, Francez A-J (1998) The microbial loop at the surface of a peatland: structure, function, and impact of nutrient input. Microbial Ecology 35: 83-93.

[22] Gilbert D, Amblard C, Bourdier G, Francez A-J, Mitchell EAD (2000) Le régime alimentaire des thécamoebiens (Protista, Sarcodina) L'Année Biologique 39: 57-68.

[23] Barnett RL, Charman DJ, Gehrels WR, Saher MH, Marshall WA (2013) Testate amoebae as sea-level indicators in Northwestern Norway: developments in sample preparation and analysis. Acta Protozoologica 52: 115-128.

[24] Lahr DJG, Parfrey, LW, Mitchell EAD, Katz LA, Lara E (2011) The chastity of amoebae: re-evaluating evidence for sex in amoeboid organisms. Proceedings of the Royal Society B-Biological Sciences 278: 2081-2090.

[25] Pchelin IM (2011) Testate amoeba *Arcella vulgaris* (Amoebozoa, Arcellidae) is able to survive without the shell and construct a new one. Protistology 6: 251-257.

[26] Whittle A, Gallego-Sala, AV (2016) Vulnerability of the peatland carbon sink to sea-level rise. Scientific reports 6: 28758.

[27] Patterson RT, Kumar A (2002) A review of current testate rhizopod (thecamoebian) research in Canada. Palaeogeography, Palaeoclimatology, Palaeoecology 180: 225-251.

Acknowledgements

We thank Prof. Steven L. Chown for sponsoring our visits to Marion Island with the South African National Antarctic Program. Dominic Hodgson carried out fieldwork with support from Dr. Bernard Coetzee, Mashudu Mashau and Rashawi Kgopong of the University of Stellenbosh, RSA. Dr Elie Verleyen and Dr Wim Van Nieuwenhuyze of the University of Ghent, Belgium, carried out initial site reconnaissance. Members of the Marion Island wintering teams M69 and M70, and Starlight Aviation provided local support and access to the field sites. Alex Whittle was supported by a Natural Environment Research Council GW4+ DTP studentship, grant number NE/L002434/1. We are thankful for the constructive suggestions made by Edward Mitchell and two anonymous reviewers.

Supplementary Information

Supplementary Methods

Study site and salinity gradient. Marion Island (46°54'S, 37°45'E) is an extremely isolated landmass of 290 km^2, located in the South Indian Ocean province of the sub-Antarctic biome (see Fig. 3.1 in main text). Climatic conditions are oceanic; mean annual temperature is 6.4°C, and mean annual precipitation is c.2000 mm (Le Roux & McGeoch, 2008a). Temperatures are stable with only 3.6°C difference between the warmest and coldest months, and a mean diurnal variability of 1.9°C (Smith, 2002). Southern Hemisphere westerly winds (SHW) are a dominant feature of the climate; mean annual wind-speed is 9.5 ms^{-1} (34.2 km hr^{-1}) (based on daily NOAA blended seawinds data for the period 2008-2018 (see Fig. 3.1 in main text for source)), and gale force winds (>18.3 m s^{-1}, 65.9 km hr^{-1}) occur more than 100 times per year (Gremmen et al. 1998) often lasting for 10 hours (Hedding et al. 2015).

Samples were collected during an expedition to Marion Island in April-May 2013. A transect aligned to the direction of the prevailing wind (i.e. East to West) was established across an area of low elevation coastal peatland at Kampkoppie on the west coast of the island (see Fig. 3.1 in main text). The transect stretched ~1 km inland of low sea-cliffs (~20 m above sea level) and spanned a coastal plateau with an altitudinal range of <50 m. No direct contact occurs between the peatland and ocean, although atmospheric transport and subsequent deposition of oceanic salt-spray is an important feature of coastal areas (e.g., Smith, 1978; Hänel & Chown, 1998; Le Roux and McGeoch, 2008b; Yeloff et al, 2007).

Peat forming vegetation at Kampkoppie consisted of a graminoid rich flora (e.g., *Agrostis magellanica, Uncinia compacta, Juncus scheuchzerioides*), and notably did not include *Sphagnum* mosses. The surface of the peatland is flat without a microtopography of hummocks and hollows which allowed the depth to water-table - a major influence on the distribution of Arcellinida and Euglyphida in other ecosystems – to be controlled.

Samples of the peatland surface (monoliths of 10 x 10 x 10 cm) were collected along the transect at 28 locations at 10 m intervals, with greater intervals for

samples 24-28. Sample numbers were allocated sequentially (i.e. 1 = most coastal, 28 = furthest inland).

All samples were stored frozen and sealed within plastic bags prior to analysis. Conductivity and pH was recorded using a calibrated Hanna Instruments HI98129 meter from pore-water extracted by applying a compressive force to sub-samples of the surface 5 cm of each monolith. The relative level of salt-enrichment received by each sample was quantified by proxy of pore-water conductivity which is linearly related to salinity under these measurement conditions (Wagner et al, 2006). Physical properties of the substrate were measured in a separate sub-sample of 2 cm^3 (also from the surface 5 cm); bulk density was calculated by dividing the dry mass of each sample by its volume, and the change in sample mass after drying determined the moisture content (%).

Enumeration of Arcellinida and Euglyphida populations. Tests (shells) of Arcellinida and Euglyphida were isolated from 1 cm^3 sub-samples collected from the surface (1 cm) of each monolith, and were concentrated for direct observation using a standard water-based protocol (Charman et al, 2000; Booth et al, 2010). One tablet of *Lycopodium* spores (Lund University; Batch number 1031) was added as an exotic marker in each sample (Stockmarr, 1971). Samples were boiled in 100 ml of de-ionised (DI) water for 10 minutes to disaggregate tests from the substrate, and allowed to cool to room temperature. The samples were then rinsed through sieves with DI water, and residues of the 15-300 µm fraction were retained for analysis. Supernatant water was removed by centrifuge (3000 rpm for 5 minutes).

Slides were prepared by diluting the residue with glycerol, and counts of taxon abundance were made at x200-400 magnification on a Zeiss AxioImager A1 light microscope. A minimum of two slides were analysed from each sample.

Counts included all individuals (i.e. living, encysted, and empty tests) to minimise possible assemblage bias caused by seasonal blooms (Barnett et al, 2013). A minimum of 200 individual tests were counted in each sample to detect subtle assemblage changes and to ensure that total diversity was accounted for (Payne & Mitchell, 2009). This threshold could not be reached for samples 2 and 3, where 12 and 50 individuals were observed respectively. A lower count total was considered sufficient because of the low diversity of taxa in the assemblage of

sample 3 (Payne & Mitchell. 2009), and so these data were included in analysis. We also consider the low concentration of tests in sample 2 to be a valid result since the occurrence of *Lycopodium* spores rules out error in sample preparation, however these data were omitted from species-level analysis since the count total was deemed insufficient to accurately represent the taxonomic composition of the community.

Measurements of test dimensions were made using AxioVision software (version 4.8.2.0) coupled to a AxioCamHR3 camera. Tests are most commonly observed in broad lateral view during routine counting so measurements of test height (i.e. in the plane perpendicular to width and length) were made using a stereomicroscope. Literature values were used to supplement the data where it was not possible to obtain a sufficient number of measurements (Supplementary Table 3.6).

Concentration of tests per cubic centimetre was calculated from the ratio of tests to *Lycopodium* spores, and converted to tests per dry gram using substrate bulk density (see Royles et al, 2016). Average biovolume of each taxon (Supplementary Table 3.6) was calculated assuming standard geometric test shapes (Mitchell, 2004), and converted to biomass using the factor 1 μm^3 = 1.1 $\times$ 10^{-7} µg C (Mitchell, 2004). For each sample, total biomass was calculated by multiplying these values by taxon abundance. Error in biomass estimates was quantified by comparing maximum and minimum estimates, each based on upper (75%) and lower quartile (25%) ideal individual test dimensions and maximum and minimum test concentration values, respectively.

Shannon-Weaver diversity index values (Sageman & Bina, 1997) were calculated for each sample using the equation:

$$SWDI = -\sum_{i=1}^{S}\left(\frac{Xi}{Ni}\right) \times \ln\left(\frac{Xi}{Ni}\right)$$

Where S is richness of taxa (alpha-diversity), X_i is the abundance of each taxon, and N_i is the total abundance of Arcellinida and Euglyphida within the sample. We assumed that values; 2.5-3.5, represent stable environmental conditions, 1.5-2.5, transitional, and 0.1-1.5 are indicative of stressed conditions dominated by a small number of taxa (Patterson & Kumar, 2002).

Morphological trait values associated with feeding ecology were measured for each taxon (Supplementary Table 3.5). Community weighted means for trait prevalence in each sample were calculated by multiplying these values by taxon abundance using the add-on package 'FD' for 'R' (Laliberté et al, 2014). Relationships between the community weighted mean value for each trait and conductivity were then assessed.

Taxonomy. Identification of taxa was based on Ogden and Hedley (1980), Charman et al, (2000), Mazei and Tsyganov (2006), and Meisterfeld (2002a,b) with additional use of photographs and descriptions of southern hemisphere taxa (Fernández et al, 2015; Zapata & Fernández, 2008; van Bellen et al, 2014) and saltmarsh taxa (Charman et al, 2002; Gehrels et al, 2006). For standardisation with existing studies, identification used morphological features of the test, including; composition, shape, ornamentation, size and colour. We adopted a conservative approach to taxonomy to ensure that taxa represent biological species as closely as possible, and to produce an accurate estimation of diversity. Following Charman et al (2002), complexes of taxa (e.g., the genus *Centropyxis*) that are difficult to identify by test morphology were divided to the lowest possible level whilst maintaining clear, consistent and convenient morphological criteria. Microphotographs of all observed taxa are shown in Supplementary Figure 3.1, and a list of taxa is given in Supplementary Table 3.1.

Analysis of community assemblages. All observed taxa were included in statistical analysis. Prior to analysis, assemblage counts were converted to relative abundance (percent) and square-root transformed to reduce the influence of dominant taxa (see Vincke et al, 2004). Detrended correspondence analysis (DCA) was used to estimate the overall gradient length of the assemblage data by determining whether species responses were primarily unimodal (gradient length > 2 standard deviations) or monotonic (gradient length < 2) (Legendre & Birks, 2012). Gradient lengths exceeded 3.0 standard deviations (3.07 for square-root transformed assemblage data), and therefore unimodal ordination methods were used to analyse the relationship between assemblages and corresponding environmental variables (ter Braak & Prentice, 1988).

Principal component analysis (PCA) was used to determine the major gradients in the environmental data. Prior to analysis environmental variables were

checked for skewness, centred and standardised. Skewness of conductivity was reduced by applying a $\log_{10}$ transformation. Both conductivity and pH were shown to correlate with distance inland from the coast (R^2 = -0.45, p = 0.05, and R^2 = -0.56, p = 0.01 respectively), which confirms that the salinity gradient is produced by spatially variable deposition of oceanic salt-spray (i.e. levels decrease with distance inland from the coast). pH and conductivity therefore did not represent independent ecological signals in this dataset. Instead, both reflect salt-enrichment of an otherwise low-pH freshwater environment. Since conductivity is linearly related to salinity, unlike pH, it was retained for further analysis as an indicator of salt-enrichment level while pH was removed. Distance inland of coast was also removed from subsequent analysis since it is a synthetic (i.e. non-ecological) variable.

Canonical correspondence analysis (CCA) with Monte Carlo permutation tests was applied to assess the statistical significance of the measured microhabitat variables in explaining variations in assemblages between samples. Partial-CCA where each environmental variable was included as the only explanatory variable, against the assemblage dataset, was used to measure the significance of each environmental variable. Interaction between variables was estimated by sequentially including each as a co-variable in successive iterations (Supplementary Table 3.4). To measure the strength of each environmental variable, in explaining changes in assemblages between samples, we calculated the ratio between the first constrained (CCA1) and first un-constrained (CA1) axis. A value > 1 indicates that the variable represents an important ecological gradient (Juggins, 2013).

All analyses were performed in R (version 3.4.1) (R core development team, 2017), and add-on package vegan (Oksanen et al, 2017).

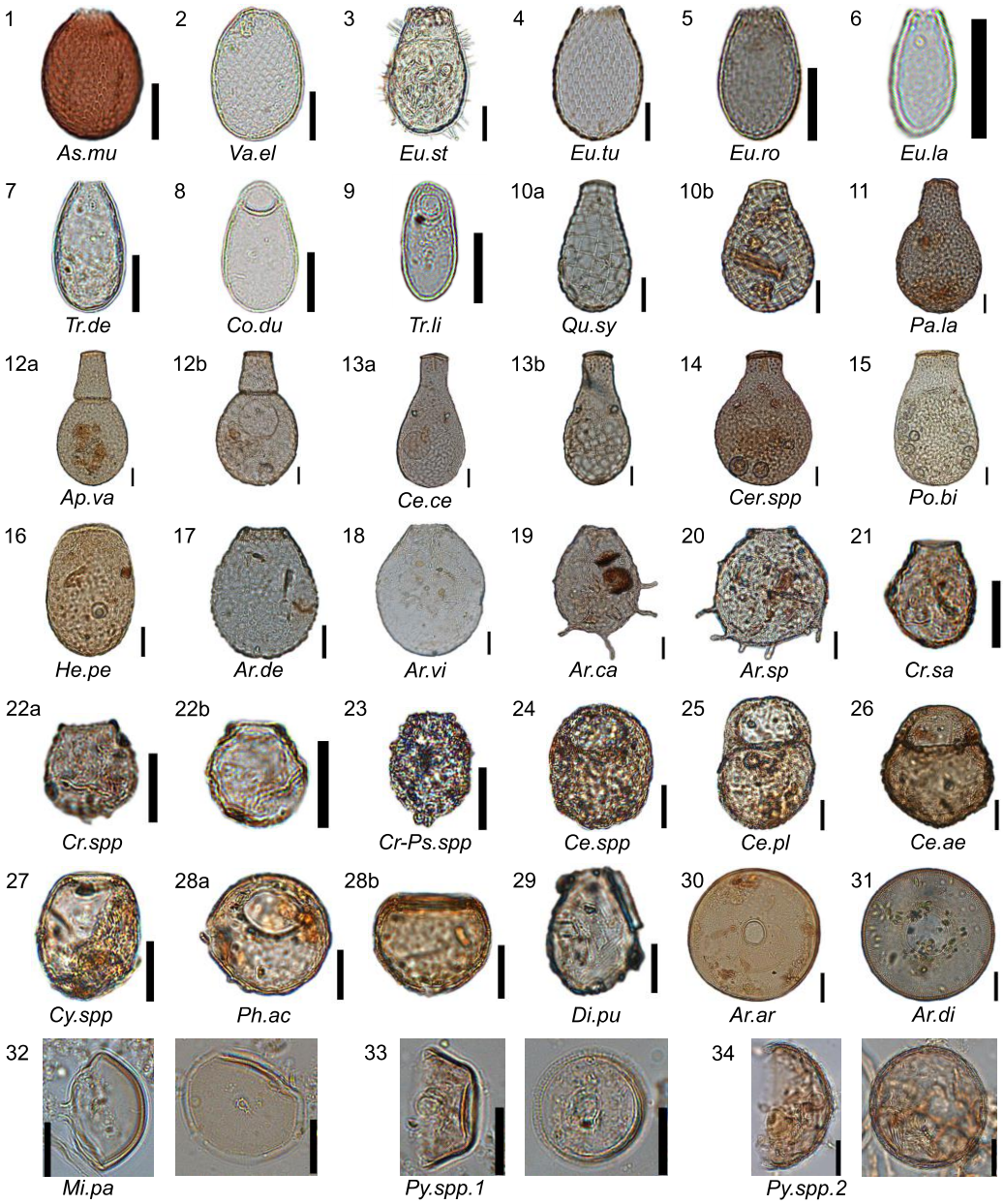

Supplementary Figure 3.1 | Arcellinida and Euglyphida taxa (collectively testate amoebae) identified in this study. Abbreviations for taxon name correspond to those used in Fig. 3.2 (in main text). Reference numbers correspond to the full list of taxa given in Supplementary Table 3.1. Images were obtained using a Zeiss AxioImager A1 light microscope coupled with an AxioCamHR3 camera. Scale bars represent 20 µm in all images.

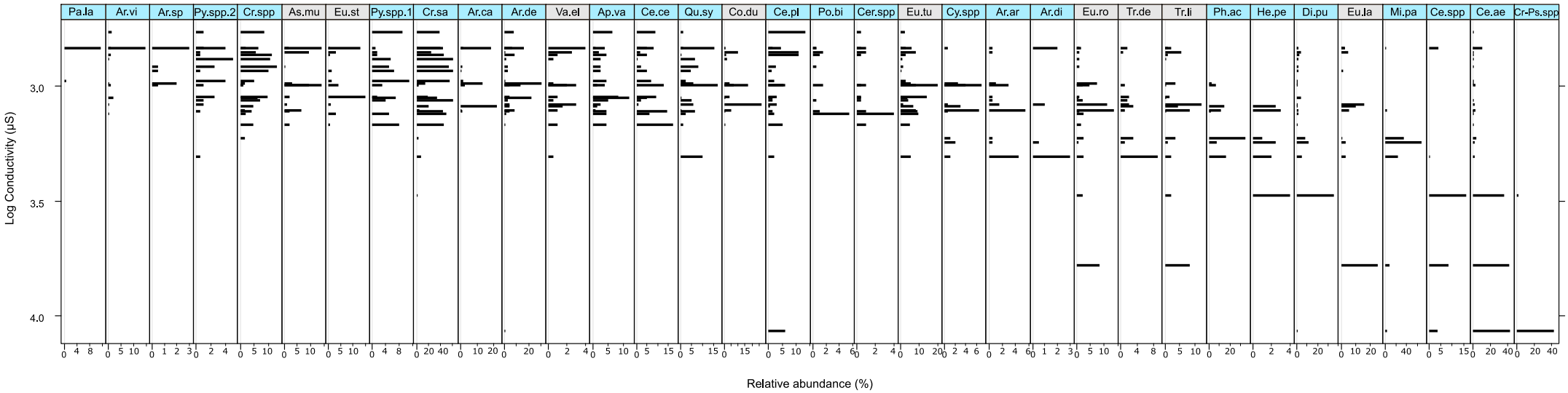

Supplementary Figure 3.2 | Percentage abundance of Arcellinida (blue shading) and Euglyphida (grey shading) taxa from the Kampkoppie peatland plotted against sample pore-water conductivity. Low conductivity values represent low levels of salt-enrichment. Taxa are ordered by conductivity optima calculated by weighted average. Taxon abbreviations refer to those given in Supplementary Table 3.1.

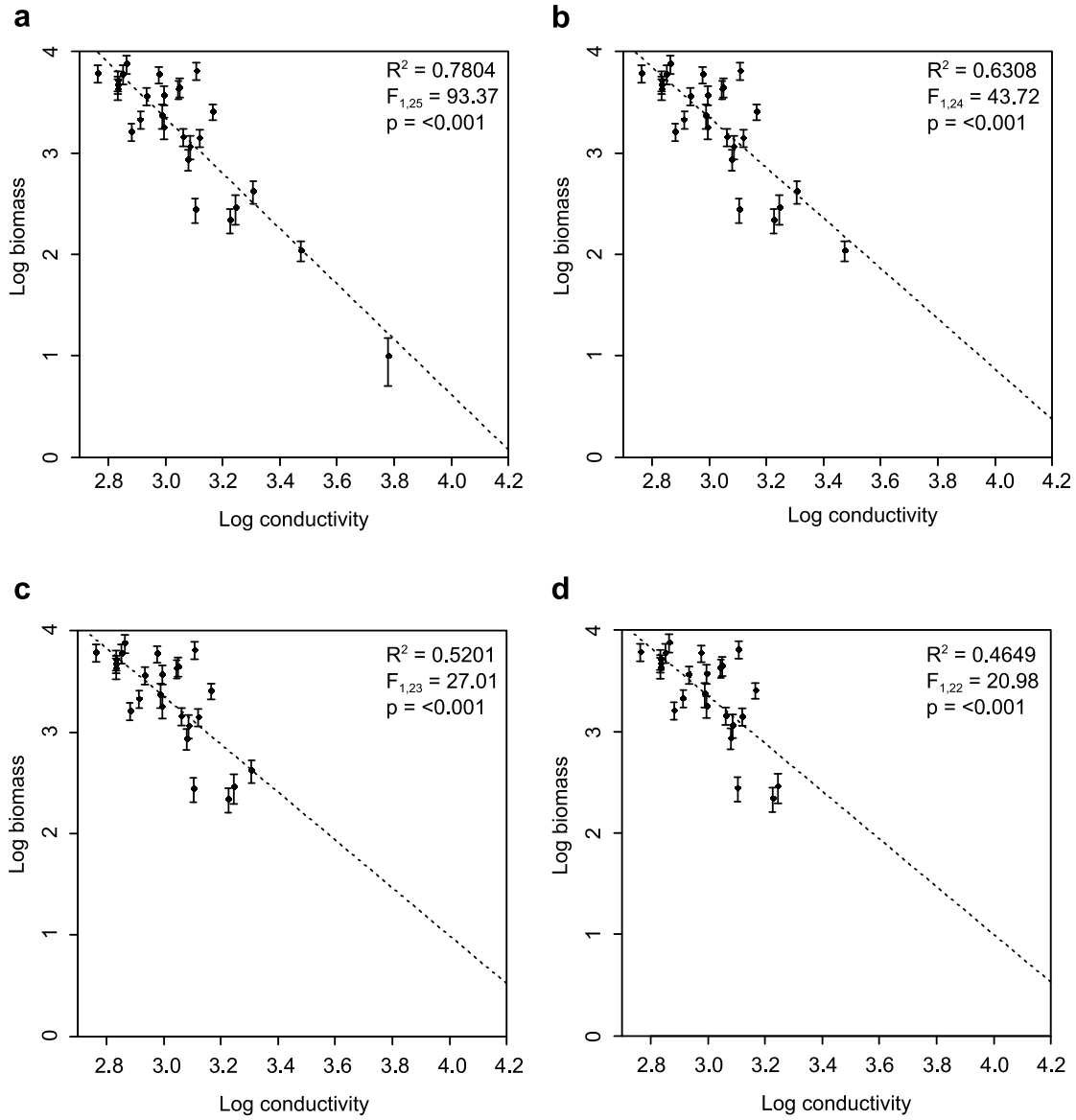

Supplementary Figure 3.3| Relationship between pore-water conductivity (µS; microsiemens/cm) and testate amoebae biomass (g C g dry-soil^{-1}) after sequential removal of highly salt enriched samples (i.e. those with conductivity values > 2000 µS). Relationship for the range 580-6000 µS (a), 580-2980 µS (b), 580-2030 µS (c) and 580-1760 µS (d). Conductivity and biomass were $\log_{10}(x)$ transformed.

Supplementary Table 3.1 | List of all Arcellinida and Euglyphida taxa observed from the Kampkoppie peatland on Marion Island and corresponding abbreviations used in Fig. 3.2 (in main text). Taxonomy follows Krashevska et al (2016). One taxon could not be identified accurately to genus level and has been termed Cr-Ps.spp to reflect this uncertainty. 'Spp.' was used where taxa could only be confidently identified to the genus level, and 'type' for taxa exhibiting several morphotypes that possibly represent distinct species. Microphotographs of each taxa are shown in Supplementary Figure 3.1. ● Indicates taxa not previously identified on Marion Island in the existing study of testate amoebae by Grospietsch (1971).

*Order / **Family	Taxon name / authority	Taxon abbreviation	Supplementary Figure 3.1 reference number
*Arcellinida Kent 1880			
	**Arcellidae Ehrenberg 1843		
	Arcella arenaria Greeff, 1866 ●	Ar.ar	30
	Arcella discoides Ehrenberg, 1843 ●	Ar.di	31
	**Hyalospheniidae Schultze 1877		
	Quadrulella symmetrica (Wallich, 1863) Schulze, 1875 ●	Qu.sy	10 a-b
	Apodera vas Certes, 1889	Ap.va	12 a-b
	Certesella certesi Penard, 1911	Ce.ce	13 a-b
	Certesella spp. ●	Cer.spp	14
	Porosia bigibossa (Penard, 1890) Jung, 1942 ●	Po.bi	15
	Padaungiella lageniformis (Penard, 1902) Lara and Todorov, 2012 ●	Pa.la	11
	**Microchlamyiidae Ogden 1985		
	Microchlamys patella (Claparède & Lachmann, 1859) Cockerell, 1911	Mi.pa	32
	**Cryptodifflugiidae Jung 1942		
	Cryptodifflugia sacculus Penard, 1902	Cr.sa	21
	Cryptodifflugia spp. ●	Cr.spp	22 a-b
	Cryptodifflugia-Pseudodifflugia spp. ●	Cr-Ps.spp	23
	**Centropyxidae Jung 1942		
	Centropyxis platystoma type (Penard, 1890) Deflandre, 1929	Ce.pl	25
	Centropyxis aerophila Deflandre, 1929	Ce.ae	26
	Centropyxis spp.	Ce.spp	24
	**Phryganellidae Jung 1942		
	Phryganella acropodia (Hertwig and Lesser, 1874) Hopkinson, 1909	Ph.ac	28 a-b
	**Trigonopyxidae Loeblich and Tappan 1964		
	Cyclopyxis spp. ●	Cy.spp	27
	** Incertae sedis Arcellinida		
	Argynnia dentistoma Penard, 1890	Ar.de	17
	Argynnia vitraea Penard, 1899 ●	Ar.vi	18
	Argynnia caudata Leidy, 1879	Ar.ca	19
	Argynnia spicata Wailes, 1913 ●	Ar.sp	20
	Difflugia pulex Penard, 1902 ●	Di.pu	29
	Heleopera petricola Leidy, 1879 ●	He.pe	16
	Pyxidicula spp.1 ●	Py.spp1	33
	Pyxidicula spp.2 ●	Py.spp2	34
* Euglyphida Copeland 1956			
	** Euglyphidae Wallich 1864		
	Euglypha strigosa (Ehrenberg, 1871) Leidy, 1878	Eu.st	3
	Euglypha tuberculata Dujardin, 1841 ●	Eu.tu	4
	Euglypha rotunda Wailes, 1915	Eu.ro	5
	Euglypha laevis (Ehrenberg, 1832) Perty, 1849	Eu.la	6
	**Trinematidae Hoogenraad and De Groot 1940		
	Trinema lineare Penard, 1890	Tr.li	9
	Corythion dubium Taránek, 1881	Co.du	8
	** Assulinidae Lara 2007		
	Assulina muscorum Greeff, 1888	As.mu	1
	Valkanovia elegans Schönborn, 1964 ●	Va.el	2
	** Incertae sedis euglyphid testate amoebae		
	Tracheleuglypha dentata Deflandre, 1928	Tr.de	7

Supplementary Table 3.2 | Principal Component (PC) analysis (a) axis scores, and (b) scores for each microhabitat variable.

		PC1	PC2	PC3	PC4	PC5	Sum of Eigenvalues
a)	Standard deviation	1.7142	1.1501	0.6342	0.4285	0.3911	5
	Eigenvalues	2.9383	1.3228	0.4022	0.1837	0.1530	
	Percentage of explained variance	58.77	26.46	8.05	3.67	3.06	
	Cumulative percentage of explained variance	-	85.22	93.27	96.94	100	
		PC1	PC2	PC3			
b)	Conductivity	-0.5243	0.1460	-0.4501			
	pH	-0.4970	0.3059	-0.4006			
	Moisture content	0.4091	0.5435	-0.3326			
	Bulk density	-0.4790	-0.4022	0.2112			
	Distance from coast	0.2850	-0.6542	-0.6940			

Supplementary Table 3.3 Canonical correspondence analysis (CCA) of community assemblages and ecological microhabitat variables (pore-water conductivity, bulk density and moisture content).

Axes	CCA1	CCA2	CCA3	Sum of canonical Eigenvalues	Sum of Eigenvalues
Eigenvalues	0.4091	0.1107	0.0225	0.5423	1.6059
p-value	0.001	0.037	0.906		
Percentage of variance of species data explained	25.47	6.89	1.40		
Cumulative percentage variance of species data explained	-	32.36	33.76		

Supplementary Table 3.4 a) Individual canonical correspondence analysis results. CCA1/CA1 is used to measure the strength of each explanatory variable in explaining changes in assemblages between samples, where a value >1 indicates that the corresponding variable represents an important ecological gradient (Juggins, 2013). b) Variance partitioning results. C – pore-water conductivity, M – moisture content, and BD – bulk density.

	Variable	Co-variable	CCA1	CCA1/CA1	Sum of Eigenvalues	Variance explained by variable (%)	Interaction between variable and co-variable(s) (%)	*p*-value
a)	C	none	0.3892	1.10	1.6059	24.24	-	0.001
	M	none	0.2123	0.51		13.22	-	0.01
	BD	none	0.2224	0.59		13.85	-	0.001
b)	C	M	0.3066		1.6059	19.09	5.15	
		BD	0.2567			15.98	8.26	
		All	0.258			16.07	8.17	
					Total interaction:		**13.41**	
	M	BD	0.0619		1.6059	3.86	9.37	
		C	0.1297			8.08	5.15	
		All	0.0633			3.94	9.28	
					Total interaction:		**14.51**	
	BD	M	0.0720		1.6059	4.48	9.37	
		C	0.0899			5.60	8.26	
		All	0.0234			1.46	12.39	
						Total interaction:	**17.62**	

Supplementary Table 3.5 Selected morphological traits associated with the feeding ecology of Arcellinida and Euglyphida. None of the relationships between the prevalence of traits and conductivity conditions were found to be statistically significant at the $p \leq 0.05$ level. CWM – community weighted mean, C – pore-water conductivity.

Trait	Unit	Ecological interpretation	Reference	Correlation of trait CWM and C (R^2)	*p*-value
Pseudopod type	Lobose or Filose	Filose taxa (Euglyphida) are mainly bacterivores and are considered to be r-strategists, whereas Lobose taxa (Arcellinida) are assumed to be K-strategists.	Fournier et al (2012) Fournier et al (2016)	0.05	0.80
Test width 'Body Size'	µm	Test size is assumed to relate to foraging characteristics, although the exact link between size and trophic level is unclear. Larger taxa appear to have longer generation times.	Lamentowicz et al (2015) Fournier et al (2015) Krashevska et al (2016)	-0.17	0.38
Test length 'Body Size'	µm			-0.24	0.22
Aperture width	µm	Aperture dimensions are linked directly to the maximum size of food items which can be consumed. Taxa with a shell size >60 µm and aperture >15 µm are capable of consuming large prey items and hence it has been assumed that they occupy a high trophic level.	Lamentowicz et al (2015) Fournier et al (2015)	-0.10	0.61
Aperture width / Body length	Ratio	Low ratios are indicative of taxa which occupy a low trophic position (i.e. bacterivores and algivores), whereas a high ratio suggests a higher trophic position (i.e. taxa which predate other protists and micro-metazoan).	Jassey et al (2013) Krashevska et al (2016)	-0.17	0.38

Supplementary Table 3.6 Biovolume and biomass estimates for each taxon based on ideal individuals calculated from measurements of test dimensions. Bold values are derived from literature averages. Test shape classifications are based on the criteria defined by Mitchell (2004). Full names corresponding to the taxon codes are given in Supplementary Table 3.1.

Taxon code / **Test shape classification**								Individual biovolume (μm^3)	Individual biomass ($\mu gC\ g^{-1}$)	Literature data source
Ovoid	Test length (µm)			Test width (µm)			Test height (µm)			
	Mean	Std.Dev	*n*	Mean	Std.Dev	*n*				
Ap.va	151.80	9.79	*100*	80.12	7.90	*100*	**47.55**	385,500	0.0424	Mean calculated from data presented by Zapata and Fernández (2008)
Ar.ca	88.05	8.60	*62*	69.31	8.48	*62*	**49.50**	201,400	0.0222	Height based on *Ar.de* in Ogden and Hedley (1980)
Ar.de	88.17	9.02	*190*	73.47	11.55	*190*	**49.50**	213,800	0.0235	Ogden and Hedley (1980)
Ar.sp	90.81	8.13	*6*	79.92	5.25	*6*	**49.50**	239,500	0.0263	Height based on *Ar.de,* from Ogden and Hedley (1980)
Ar.vi	108.41	21.10	*14*	91.91	13.45	*14*	**75.00**	498,200	0.0548	Ogden and Hedley (1980)
As.mu	47.45	6.79	*92*	37.58	5.37	*91*	**20.00**	23,800	0.0026	Ogden and Hedley (1980)
Ce.ae	65.70	5.75	*81*	54.46	6.14	*78*	28.00	66,800	0.0073	
Ce.ce	138.95	8.18	*108*	75.17	6.53	*106*	49.87	347,300	0.0382	
Cer.spp	138.27	8.96	*11*	87.45	8.32	*11*	49.87	402,000	0.0442	
Ce.pl	86.00	8.05	*77*	62.82	7.30	*74*	48.95	176,300	0.0194	
Ce.spp	58.41	7.24	*14*	56.81	9.16	*14*	45.23	100,100	0.0110	
Co.du	38.56	5.64	*93*	25.39	3.25	*92*	**16.00**	10,400	0.0011	Cash and Hopkinson (1909)
Eu.la	26.28	5.21	*56*	13.78	3.22	*53*	6.89	1,700	0.0002	Test height estimated as width x 0.5 for all *Euglypha* spp.
Eu.ro	39.79	5.33	*83*	24.65	5.08	*83*	12.33	8,100	0.0009	
Eu.st	72.56	8.14	*45*	43.13	7.78	*43*	21.56	45,000	0.0050	-
Eu.tu	71.81	10.47	*194*	43.68	8.77	*175*	21.84	45,700	0.0050	-
He.pe	78.48	7.67	*16*	53.19	4.48	*16*	**45.00**	125,200	0.0138	Ogden and Hedley (1980)
Pa.la	139.54	8.43	*4*	82.71	7.76	*4*	**47.55**	365,900	0.0402	Based on *Ap.va*
Po.bi	145.48	10.33	*18*	80.40	8.93	*18*	49.87	388,900	0.0428	
Qu.sy	72.88	6.96	*94*	42.28	5.02	*87*	**29.61**	60,800	0.0067	
Va.el	44.08	6.02	*19*	29.41	4.12	*19*	**20.00**	17,300	0.0019	Based on *As.mu* following Royles et al. (2016)

Saucer	Test diameter (µm)			Test height (µm)					
	Mean	Std.Dev	*n*	Mean	Std.Dev	*n*			
Ar.ar	85.41	12.22	*30*	17.49	4.97	*5*	50,100	0.0055	
Ar.di	84.21	13.36	*7*	31.52	3.43	*2*	87,800	0.0097	
Mi.pa	42.41	6.89	*115*	14.71	4.28	*18*	10,400	0.0011	
Py.spp1	33.48	3.11	*34*	17.40	1.04	*2*	7,700	0.0008	
Py.spp2	70.52	7.30	*72*	43.18	15.15	*6*	84,300	0.0093	
Cylindrical-ovoid	Test length (µm)			Test diameter (µm)					
	Mean	Std.Dev	*n*	Mean	Std.Dev	*n*			
Di.pu	37.67	6.74	*73*	26.27	5.26	*71*	20,800	0.0023	
Tr.de	47.13	5.36	*35*	26.61	2.88	*35*	26,700	0.0029	
Tr.li	33.27	7.86	*52*	15.39	3.24	*40*	6,300	0.0007	
Hemispheric	Test diameter (µm)								
	Mean	Std.Dev	*n*						
Cr.sa	29.48	3.66	*306*				5,200	0.0006	
Cr.spp	27.76	2.50	*72*				5,000	0.0006	
Cy.spp	42.26	6.41	*50*				19,800	0.0022	
Ph.ac	40.74	4.45	*72*				16,100	0.0018	
Cr-Ps.spp	32.77	3.04	*37*				6,300	0.0007	

Supplementary References

Barnett, R. L., Charman, D. J., Gehrels, W. R., Saher, M. H. and Marshall, W. A. (2013) Testate amoebae as sea-level indicators in Northwestern Norway: developments in sample preparation and analysis. *Acta Protozoologica* 52(3): 115-128.

Booth, R. K., Lamentowicz, M. and Charman, D. J. (2010) Preparation and analysis of testate amoebae in peatland palaeoenvironmental studies. *Mires and Peat* 7: 1-11.

Cash, J. and Hopkinson, J. (1909) The British freshwater Rhizopoda and Heliozoa. Volume II. Ray Society, London.

Charman, D. J., Hendon, D. and Woodland, W. A. (2000) The identification of testate amoebae (Protozoa: Rhizopoda) in peats. Quaternary Research Association, London.

Charman, D. J., Roe, H. M. and Gehrels, W. R. (2002) Modern distribution of saltmarsh testate amoebae: regional variability of zonation and response to environmental variables. *Journal of Quaternary Science* 17(5-6): 387-409.

Fernández, L. D., Lara, E. and Mitchell, E. A. D. (2015) Checklist, diversity and distribution of testate amoebae in Chile. *European Journal of Protistology* 51(5): 409-424.

Fournier, B., Coffey, E. E. D., van der Knaap, W. O., Fernández, L. D., Bobrov, A. and Mitchell, E. A. D. (2016) A legacy of human-induced ecosystem changes: spatial processes drive the taxonomic and functional diversities of testate amoebae in Sphagnum peatlands of the Galápagos. *Journal of Biogeography* 43(3): 533-543.

Fournier, B., Lara, E., Jassey, V. E. and Mitchell, E. A. D. (2015) Functional traits as a new approach for interpreting testate amoeba palaeo-records in peatlands and assessing the causes and consequences of past changes in species composition. *The Holocene* 25(9): 1375-1383.

Fournier, B., Malysheva, E., Mazei, Y., Moretti, M. and Mitchell, E. A. D. (2012) Toward the use of testate amoeba functional traits as indicator of floodplain restoration success. *European Journal of Soil Biology* 49: 85-91.

Gehrels, W. R., Hendon, D. and Charman, D. J. (2006) Distribution of testate amoebae in salt marshes along the North American East Coast. *Journal of Foraminiferal Research* 36(3): 201-214.

Gremmen, N. J. M., Chown, S. L. and Marshall, D. J. (1998) Impact of introduced grass Agrostis stolonifera on vegetation and soil fauna communities at Marion Island, sub-Antarctic. *Biological Conservation* 85(3): 223-231.

Grospietsch, T. (1971) Beitrag zur ökologie der Testaceen Rhizopoden von Marion Island. In: Marion and Prince Edward Island, Report on the South

African Biological and Geological Expedition 1965-1966, eds. Van Zinderen-Bakker, E. M., Winterbottom, J. M. and Dyer, R. A. Balkema, Cape Town: 411-423.

Hänel, C. and Chown, S. L. (1998) The impact of a small, alien invertebrate on a sub-Antarctic terrestrial ecosystem: Limnophyes minimus (Diptera, Chironomidae) at Marion Island. *Polar Biology* 20(2): 99-106.

Hedding, D. W., Nel, W. and Anderson, R. L. (2015) Aeolian processes and landforms in the sub-Antarctic: Preliminary observations from Marion Island. *Polar Research* 34(1): 26365.

Jassey, V. E. J., Chiapusio, G., Binet, P., Buttler, A., Laggoun-Défarge, F., Delarue, F., Bernard, N., Mitchell, E. A. D, Toussaint, M- L., Francez, A-J., Gilbert, D. (2013) Above-and belowground linkages in *Sphagnum* peatland: climate warming affects plant-microbial interactions. *Global Change Biology* 19(3): 811-823.

Juggins, S. (2013) Quantitative reconstructions in palaeoclimatology: new paradigm or sick science? *Quaternary Science Reviews* 64: 20-32.

Krashevska, V., Klarner, B., Widyastuti, R., Maraun, M. and Scheu, S. (2016) Changes in structure and functioning of protist (testate amoebae) communities due to conversion of lowland rainforest into rubber and oil palm plantations. *PLoS ONE* 11(7): e0160179.doi:10.1371/journal.pone.0160179

Laliberté, E., Legendre, P. and Shipley, B. (2014) FD: measuring functional diversity from multiple traits, and other tools for functional ecology. R package version 1.0-12. https://cran.r-project.org/web/packages/FD/index.

Lamentowicz, M., Gałka, M., Lamentowicz, Ł., Obremska, M., Kühl, N., Lücke, A. and Jassey, V. E. (2015) Reconstructing climate change and ombrotrophic bog development during the last 4000 years in northern Poland using biotic proxies, stable isotopes and trait-based approach. *Palaeogeography, Palaeoclimatology, Palaeoecology* 418: 261-277.

Le Roux, P. C. and McGeoch, M. A. (2008a) Changes in climate extremes, variability and signature on sub-Antarctic Marion Island. *Climatic Change* 86(3-4): 309-329.

Le Roux, P. C. and McGeoch, M. A. (2008b) Rapid range expansion and community reorganization in response to warming. *Global Change Biology* 14(12): 2950-2962.

Legendre, P. and Birks, H. J. B. (2012) From classical to canonical ordination. In: Birks, H. J. B., Lotter, A. F., Juggins, S., Smol, J. P. (Eds) Tracking environmental change using lake sediments Developments in Paleoenvironmental Research 5, Springer, Dordrecht.

Mazei, Y. and Tsyganov, A. (2006) Freshwater Testate Amoebae. KMK, Moscow (In Russian).

Meisterfeld, R. (2002a) Order Arcellinida Kent, 1880. In: Lee, J.J., Leedale, G.F., Bradbury, P. (Eds.), An illustrated guide to the protozoa, 2, second ed. Society of Protozoologists, Lawrence, Kansas, USA, pp. 827–860.

Meisterfeld, R. (2002b) Testate Amoebae with Filopodia. In: Lee, J. J., Leedale, G. F., Bradbury, P. (Eds.), An illustrated guide to the protozoa, 2, second ed. Society of Protozoologists, Lawrence, Kansas, USA, pp. 1054–1084.

Mitchell, E. A. D. (2004) Response of testate amoebae (Protozoa) to N and P fertilization in an Arctic wet sedge tundra. *Arctic, Antarctic, and Alpine Research* 36(1): 78-83.

Ogden, C. G. and Hedley, R. H. (1980) An atlas of freshwater testate amoebae. Oxford University Press, Oxford.

Oksanen, J., Blanchet, F. G., Friendly, M., Kindt, R., Legendre, P., McGlinn, D., Minchin, P. R., O'Hara, R. B., Simpson, G. L., Solymos, P., Stevens, M. H. H., Szoecs, E. and Wagner, H. (2017). vegan: Community Ecology Package. R package version 2.4-4. https://CRAN.R-project.org/package=vegan.

Patterson, R. T. and Kumar, A. (2002) A review of current testate rhizopod (thecamoebian) research in Canada. *Palaeogeography, Palaeoclimatology, Palaeoecology* 180(1-3): 225-251.

Payne, R. J. and Mitchell, E. A. D. (2009) How many is enough? Determining optimal count totals for ecological and palaeoecological studies of testate amoebae. *Journal of Paleolimnology* 42: 483-495.

R Core Team (2017) R: A Language and Environment for Statistical Computing. R Foundation for Statistical Computing, Vienna, Austria, URL https://www.R-project.org/.

Royles, J., Amesbury, M. J., Roland, T. P., Jones, G. D., Convey, P., Griffiths, H., Hodgson, D. A. and Charman, D. J. (2016) Moss stable isotopes (carbon-13, oxygen-18) and testate amoebae reflect environmental inputs and microclimate along a latitudinal gradient on the Antarctic Peninsula. *Oecologia* 181(3): 931-945.

Sageman, B. B. and Bina, C.R. (1997) Diversity and species abundance patterns in Late Cenomanian black shale biofacies, Western Interior, USA. *Palaios* 12(5):449–466.

Smith, V. R. (1978) Animal-plant-soil nutrient relationships on Marion Island (Subantarctic). *Oecologia* 32(2): 239-253.

Smith, V. R. (2002) Climate change in the sub-Antarctic: an illustration from Marion Island. *Climatic Change* 52(3): 345-357.

Stockmarr, J. (1971) Tablets with spores used in absolute pollen analysis. *Pollen et Spores* 13: 615–621.

ter Braak, C. J. F. and Prentice, I. C. (1988) A theory of gradient analysis. *Adv Ecol Res* 18:271–317.

van Bellen, S., Mauquoy, D., Payne, R.J., Roland, T.P., Daley, T.J., Hughes, P.D., Loader, N.J., Street-Perrott, F.A., Rice, E.M. and Pancotto, V.A. (2014) Testate amoebae as a proxy for reconstructing Holocene water table dynamics in southern Patagonian peat bogs. *Journal of Quaternary Science*, 29(5): 463-474.

Vincke, S., Ledeganck, P., Beyens, L. and van de Vijver, B. (2004) Soil testate amoebae from sub-Antarctic Îles Crozet. *Antarctic Science* 16(2): 165-174.

Wagner, R. J., Boulger, R. W. Jr., Oblinger, C. J. and Smith, B. A. Guidelines and standard procedures for continuous water-quality monitors: station operation, record computation, and data reporting: U.S. Geological survey techniques and methods 1-D3. (2006) Available at: https://pubs.usgs.gov/tm/2006/tm1D3/. (Accessed: 6th June 2018).

Yeloff, D., Mauquoy, D., Barber, K., Way, S., van Geel, B. and Turney, C. S. M. (2007) Volcanic ash deposition and long-term vegetation change on subantarctic Marion Island. *Arctic, Antarctic and Alpine Research* 39(3): 500-511.

Zapata, J. and Fernández, L. (2008) Morphology and morphometry of *Apodera vas* (Certes, 1889) (Protozoa: Testacea) from two peatlands in Southern Chile. *Acta Protozoologica.* 47(4): 389-395.

Chapter 4

Low-salinity transitions drive abrupt microbial response to sea-level change

Alex Whittle[1,2*], Robert L. Barnett[1,3*], Dan J. Charman[1], Angela V. Gallego-Sala[1]

[1] Geography, College of Life and Environmental Sciences, University of Exeter, Exeter, UK

[2] British Antarctic Survey, Natural Environment Research Council, Cambridge, UK

[3] Département de biologie, chimie et géographie et Centre d'études nordiques, Université du Québec à Rimouski, Rimouski, Canada

The salinization of many coastal ecosystems is underway and will continue into the future because of sea-level rise and storm intensification due to climate change. However, the response of soil microbes to increasing salinity conditions within coastal ecologies is poorly understood, despite their importance for nutrient cascading, carbon sequestration and wider ecosystem functioning. Here we demonstrate the deterioration in productivity of a top tier microbial group (testate amoebae) to increasing coastal salinity, which we show to be consistent across phylogenetic groups, salinity gradients, environment types and latitude. Our results show that microbial changes occur in the very early stages of marine inundation, presaging more radical changes in soil and ecosystem function, and providing early warning of coastal salinization that could be used to improve coastal planning and adaptation.

coastal ecology | microbial | testate amoebae | productivity | biomass | salinity | sea level | climate change

Increasing rates of sea-level rise, frequency of extreme sea-level events, and intensification of cyclone activity (IPCC 2019) during the present century are driving changes to coastal environments worldwide; contributing to the submergence of low-lying islands (Storlazzi et al. 2018), increased coastal flooding (Vitousek et al. 2019), contamination of groundwater (Taylor et al. 2013)

and significant changes to coastal wetlands (Schuerch et al. 2018). As salt-water encroaches, sodium chloride and other salts (such as sulphates) are deposited further inland, increasing ionic concentrations and altering redox conditions (Jansson et al. 2020). Coastal soil ecosystems that have previously been dominated by freshwater are especially vulnerable to such salt-enrichment because few of the organisms they contain possess suitable physiological adaptions to thrive under more saline conditions. While studies of salt-stressed soil communities remain scarce, salinization has been shown to drive ecosystem changes ranging from negative and deleterious effects on individual microbial (Roe and Patterson 2014), plant and invertebrate communities (Pereira et al. 2018) to wholesale ecosystem reorganisations, such as the formation of ghost forests on submerging coasts of North America (Kirwan et al. 2019).

Salinization driven changes in the microbial productivity of coastal soils is both pertinent to future greenhouse gas production and carbon cycling (Pereira et al. 2018), and may also serve as an early indicator of impending 'state-shift' ecosystem change. Yet crucially, beyond shifting patterns in the species composition of communities, understanding of microbial community-level responses to salinization remains elusive, especially in terms of productivity. Initial measurements of prokaryotic biomass in soils exposed to high salt-enrichment levels have indicated strong (albeit apparently inconsistent) responses, which differ by community and environment type (Pereira et al. 2018), while in spite of the narrow salt-tolerances of many eukaryotic lineages, comparable quantifications of their productivity are lacking. Understanding how microbial productivity responds to changes in coastal salinity gradients prior to and during inundation will be critical for informing predictions of ecosystem evolution and greenhouse gas fluxes in coastal soils, as well as for supporting resilience strategies within environmental change biology.

Here we use testate amoebae (TA) to evaluate the hypothesis that heterotrophic eukaryote productivity in fresh- and brackish-water coastal soils responds to low-magnitude increases in salt exposure. To represent the conditions that occur early within marine-transgressions we define low-magnitude increases as less-than 10% of sea-water salinity-level. TA provide a model system as they occupy the highest levels of microbial food-webs throughout almost all freshwater and brackish ecosystems on Earth (Jassey et al. 2013; Dumack et al. 2018; Geisen

et al. 2018;) and represent a considerable component of soil-microbial nutrient and carbon cascading (Potapov et al. 2019). Crucially, they produce decay-resistant shells which has led to their widespread establishment as a bio-indicator for monitoring ecosystem health (Karimi et al. 2016) and past environmental conditions (Mitchell et al. 2008), and permits highly precise determination of changes in their productivity through time (Methods).

We drew together records of natural TA communities present within overlapping salinity gradients from coastal environments exposed to differing salt deposition regimes (salt-marsh, brackish marsh and coastal peatland). The data search resulted in 85 records of TA communities where concentrations of tests (tests/cm^3 of material) and conductivity (µS) were both available and used as approximations of productivity and salinity respectively. Samples originated from either sub-Arctic or sub-Antarctic coastal sites, which avoided confounding signal effects from anthropogenic activity and provided a geographically diverse dataset; although the unavailability of samples from temperate latitudes following the data search is recognised by the study. Combined, the sampled TA communities are representative of salinity conditions spanning from predominantly freshwater to diurnal tidal inundation (Fig.4.1a).

In this study, total test concentrations were used as an indicator of productivity over time. Total TA production is a function of the accumulation of dead (empty) tests plus generation of new live tests during a given period (Schönborn 1982, 1986; Wilkinson and Mitchell 2010). Our test concentration data originate from the top 1 cm of surface sediment, representing a time-averaged period of approximately a decade and thus many hundreds of TA generational cycles. Over such a time-averaged period, the accumulation of dead tests would be expected dominate the total (i.e., dead plus live) production signal, allowing our inference of productivity from test concentration to be robust. However, we recognise that total TA production requires an assessment of live tests (unavailable for this study) and that population specific production varies across species (Schönborn 1983; Wilkinson and Mitchell 2010).

Results and Discussion

We found a highly significant (negative exponential) decline in the productivity (R^2 = 0.5611; p<0.001; Fig. 4.1b) and biomass (R^2 = 0.4349; p<0.001; Fig. 4.1c)

of TA communities with increasing microhabitat salinity conditions, a response that remained consistent throughout different locations and coastal environment types. The productivity of populations from both major TA lineages also exhibited consistent trends; Arcellinida (R^2 = 0.4369; p<0.001) and Euglyphida (R^2 = 0.4769; p<0.001) (Supplementary Fig. 4.1). Productivity of Euglyphid species underwent comparatively steeper decline, suggesting generally lower salt-tolerance compared to species within the Arcellinida order.

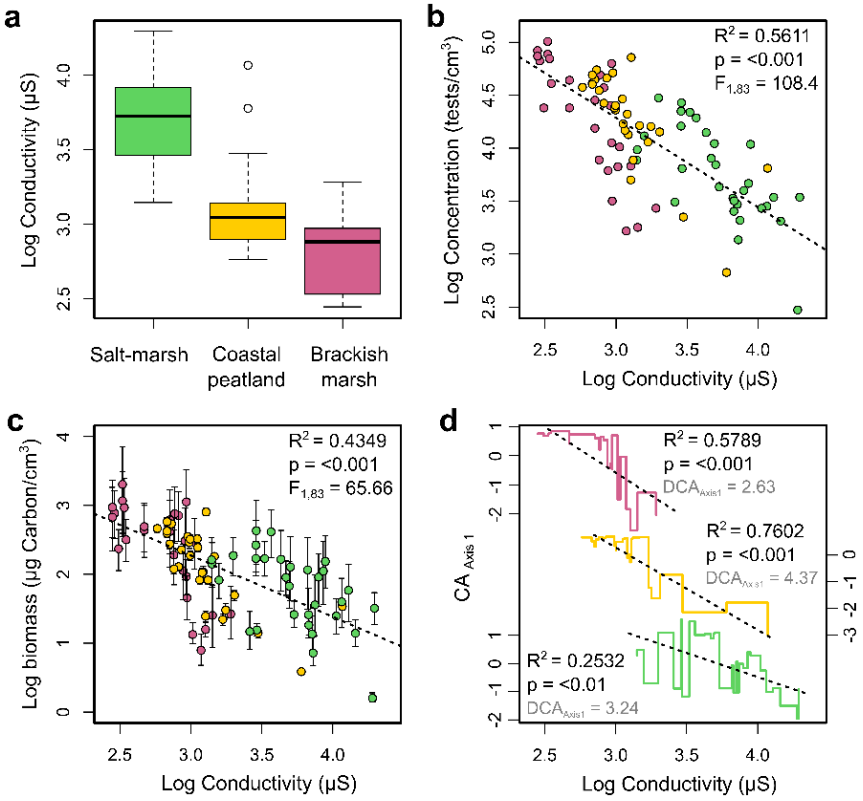

Figure 4.1 | Salinity conditions represented by sampled transects within salt-enriched environments (a) and the response of testate amoeba productivity (b), biomass (c) and species turnover (d). Conductivity, measured from pore-water in the testate amoeba microhabitat, provides a direct proxy for the degree of salinization where higher values indicate higher salinity. The total salinity gradient, compiled from transects sampled within each environment, spans 280-20,000 µS. Points in panel (b, c) and lines in (d) are coloured by environment type in (a). Correspondence analysis (CA) Axis 1 score (d) for each sampling station (Supplementary Fig. 4.3) provides an indication of the extent of species turnover, where similar values indicate more similar composition of species assemblages. Detrended correspondence analysis (DCA) Axis 1 scores (grey) > 2 standard deviations (std) indicate that the overall species response to salinity is unimodal within all environment types (Methods).

This remarkably consistent relationship also indicates that the productivity of natural TA communities throughout brackish and freshwater ecosystems is highly sensitive to small perturbations in salinization regime. For example, the modelled trajectory for the community within the lowest recorded salinity conditions suggested that an enrichment of only 357 µS (equivalent to ~0.7% of the salinity of sea-water) would reduce community size by 50%, while 4000 µS (~8% sea-water equivalent) would lead to a 90% reduction (Fig. 4.1b). Accordingly, a statistically significant and slightly shallower rate of productivity decline was observed in communities from environments exposed to higher average salinization levels (i.e. salt-marsh and coastal peatland) indicating comparatively greater resistance of pre-exposed communities to further salinity changes (Supplementary Fig. 4.2; Supplementary Table 4.1).

Changes in the species composition of communities, derived from a correspondence analysis (CA) of species relative abundance data occurred in concert with increasing microhabitat salinity, indicating reorganisation throughout the salinity gradient in favour of more salt-tolerant species (Fig. 4.1d; Supplementary Table 4.2). Compositional turnover, which reflects the optima and tolerance of individual populations (Roe and Patterson, 2014; Barnett et al. 2017a; Whittle et al. 2019), is therefore expected to be responsible for partially offsetting declining productivity as salinity levels become sub-optimal for certain species and more favourable to others. In support of this we observed a statistically independent and steeper rate of productivity decline when the effect of turnover was minimised by including only common species, which we define as those shared between all three environment-types (Supplementary Fig. 4.4). Nevertheless, our data highlights that despite the presence of moderately salt-tolerant species within the available pool (Supplementary Fig. 4.5), turnover is insufficient to maintain large TA communities as salinity levels increase. This is to say, species tolerant of more saline conditions are less productive under higher-salinity conditions than their freshwater counterparts are under very low-salinity conditions.

Whilst our use of TA as a model organism does not represent the entire microbial community, we show that the effective removal of this important group of heterotrophic microbial-eukaryotes from the coastal soil microbiome is initiated following even very low-levels of salt-enrichment. This emphasises the potential

risk that coastal salinization poses to broader soil microbial functioning, strongly indicating that changes in microbial productivity are likely to occur early within salt-stress induced ecosystem transitions (e.g. increased frequency coastal flooding events).

To test this conclusion we examined the response of TA communities to historical changes in salinization. We used co-located but independently derived sea-level reconstructions (Barnett et al. 2017b) from the salt-marsh and brackish-marsh sites included in this study to compare local sea-level changes against salinity derived from trends in sub-fossil TA productivity. Both sequences chart an ecosystem evolution with a clear trend toward higher salinity regimes (i.e. rising sea-level), and are punctuated with spatially and temporally consistent 'state-shift' events (e.g. the transition from high to mid-marsh conditions). Directional trends in salinity interpreted from the productivity of sub-fossil TA communities occur synchronously with these recorded changes (Fig. 4.2; Supplementary Fig. 4.6), and statistical changepoints within the resultant time-series show coherent timings with the significant environmental state-shifts defined from independent indicators, such as foraminifera assemblages and sedimentology (Fig 4.2; Methods). Taken together, the consistent timings and direction of the TA response to rising sea levels confirms that communities respond sensitively and rapidly to these environmental transitions. Combined with the low-levels of salinity observed to initiate these changes, our data show that TA can serve as early indicators of future ecosystem evolution in response to salinization, with great potential to detect environmental perturbations (Trevathan-Tackett et al. 2019) and support Earth monitoring systems (Ward et al. 2020; Ranasinghe 2020).

The cause of productivity decline under higher salinity regimes remains unclear from our field-based study. However, we suggest that the remarkable consistency of the relationship throughout differing environments, varying species assemblages, and time, points toward an intrinsic physiological property shared among many TA species. Although salt-tolerant species are known to occur (Barnett et al. 2017a), TA are most abundant and diverse in predominantly water-logged freshwater environments, including ombrotrophic peatlands where ionic concentrations can be extremely low. High concentrations of solute ions are therefore likely to initiate amoebic osmoregulation mechanisms in order to

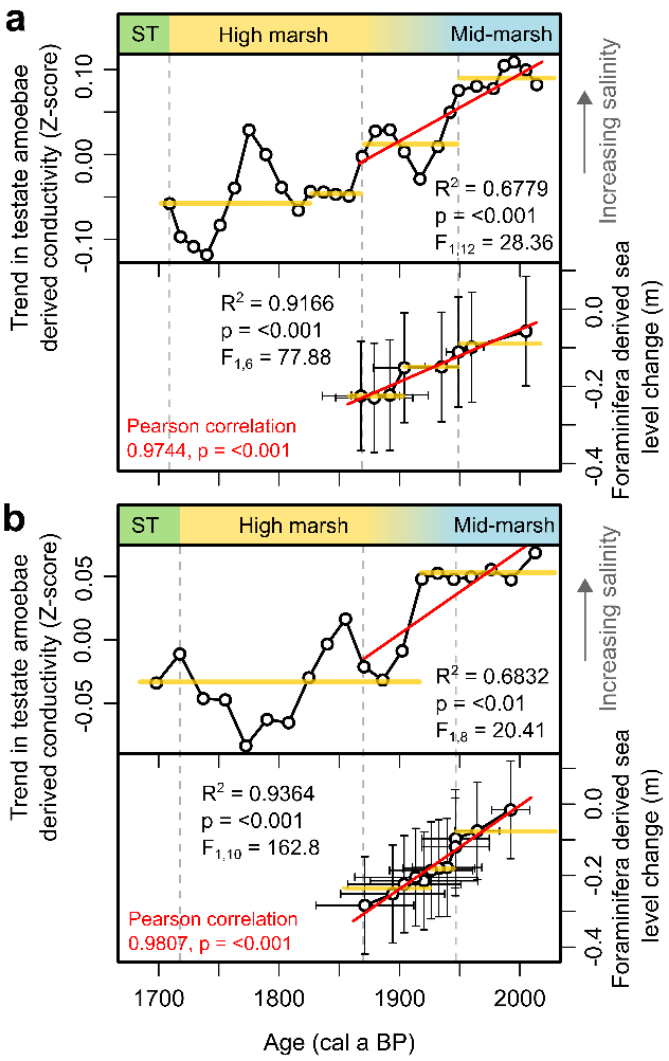

Figure 4.2 | Response of testate amoeba population size to ecosystem state-shifts induced by past sea-level change in brackish marsh (a) and salt-marsh (b) environments. TA derived conductivity reconstructions (top panels) calculated from sub-fossil testate amoeba population sizes and the salinity relationship (Fig. 4.1b); sea-level reconstructions (bottom panels) are calculated from foraminifera-derived transfer function model predicted marsh surface elevations[19] and both reconstructions apply age-depth models from the original study[19] for temporal constraints. Environmental transitions (top bars) are based on self-consistent sedimentological and biostratigraphical interpretations of the sediment-core data and are independent from TA populations. In both records, the conversion from supratidal (ST; green) to intertidal occurs with the first tidal submergence around 1710 CE, with high-marsh (yellow) conditions persisting until ~1870 CE when the transition towards mid-marsh (blue) begins. The present day mid-marsh state of both ecosystems is reached by ~1950 CE. Red lines indicate linear regressions over time-spans equivalent to the length of the sea-level reconstructions. Yellow lines indicate statistically derived change points in the reconstructed trends. Pearson correlation coefficients reflect the correlation between TA derived conductivity and Foraminifera sea-level estimates for each environment.

balance osmotic pressure across cell membranes and prevent (or at least delay) cytolysis. Nevertheless, high salinity conditions do not necessarily cause cell mortality. Experimental exposure of Euglyphid TA to hyperosmotic stress indicates that certain species can withstand temporary stress by forming dormant pre-cysts, albeit at the cost of reproductive function and therefore a reduced rate of productivity (Wanner et al. 2020). Both pre-cyst formation and the subsequent recovery (assuming conditions quickly return to more optimal salinity-levels) occurs very rapidly (Wanner et al. 2020) meaning that changes in community size through time more strongly reflect longer-term or average salinity-conditions than 'one-off' short-lived events, such as salt-spray deposition from the atmosphere during an individual storm.

Indirect impacts are also expected to contribute to declining productivity levels. As predominantly high trophic level microbial-consumers (Jassey et al. 2013; Dumack et al. 2018), TA are also vulnerable to underlying changes in resource availability; specifically the presence of, and competition for, the lower order microbial populations that partially comprise their prey. Reduced growth rates and shifts in species composition of prey organisms (e.g. soil fungi and bacterial communities) and the expansion of foraminifera populations, which are seen to occupy an overlapping niche with TA (e.g. Kemp et al. 2017) and may compete for resources, have been observed in response to salinization (Rath et al. 2019; Wanner et al. 2020). Importantly, such changes in microbial predator-prey mass ratios as a result of environmental stress has wider implications for total microbial activity across trophic levels (Reczuga et al. 2018), nutrient cycling, including carbon (Jassey et al. 2015), nitrogen (Geisen et al. 2018) and silica (Wanner et al. 2020) and plant functioning (Gao et al. 2019). As a key microbial group in soil ecosystems (Geisen et al. 2017; Gao et al. 2019), the effects of salinization on TA, whether directly or indirectly driven, will therefore play an important role in determining food web structures, nutrient cascading and carbon budgets at the coast.

This study set out to define a first-order relationship between salinity and communities of TA in coastal brackish and freshwater systems. The striking consistency of the relationship we observed across different coastal environments and through time indicates substantial applications of TA for (1) forecasting the microbial response to future coastal salinization under different

scenarios (e.g., from salt-spray aerosol deposition to inundation), and (2) providing a novel tool to derive records of past salinity changes from coastal sediments, useful for palaeoenvironmental analysis (e.g. in developing reconstructions of sea-level and wind-driven salt-spray deposition) and for informing coastal management decisions. Considering that TA are representative microbial eukaryotes, top-tier microbial heterotrophs and drivers of microecological ecosystem functioning, the sensitivity we observe potentially alludes to the vulnerability of the wider microbiome of coastal soils to low-level salinization, not considered by previous research efforts. Further research is now needed to better understand the context of this response within wider ecosystem changes, and to quantify the impact of entire community changeover (i.e., towards fully halophytic taxa across trophic levels) on nutrient availability for plant functioning and carbon cycling for sequestration potential.

Methods

Data compilation: We compiled records of natural soil-dwelling TA communities representative of different coastal environments from published literature. To be accepted for analysis, we required that TA communities (i.e., relative abundance data calculated from census counts) had constrained total concentrations (i.e., tests per unit volume of sediment), and also paired conductivity estimates (µS) from their precise locations. This search yielded 85 samples from four distinct transects of variable coastal salt-deposition at three independent coastal environment sites. The dataset comprised 31 samples from two transects across a Canadian sub-Arctic salt-marsh in the Magdalen Islands (47.4°N 61.9°W) (Barnett et al. 2017b); 26 samples from one transect across a brackish, tidal marsh also in the Magdalen Islands (Barnett et al. 2017b); and 28 samples from one transect across a sub-Antarctic coastal peatland on Marion Island (46.9°S 37.6°E) (Whittle et al. 2019). Full site descriptions are available in the original sources.

Communities of TA were enumerated from samples of denuded surface sediment (defined as the topmost 1 cm layer) which were hermetically stored after collection. TA were isolated from the sediment matrix following the standard water-based protocol for peat-soils provided in Charman et al. (2000), however modifications suitable for salt-marsh sediments (after Barnett et al. 2013) were applied for samples from the Canadian sites. Identification was conducted directly

by light-microscope at x200-400 magnification and was based on morphological features of the tests (composition, shape, ornamentation, size and colour). Taxonomy primarily followed Charman et al. (2000), although supplementary references were used for the identification of regional and environment specific taxa (Barnett et el. 2016, 2017a,b; Whittle et al. 2019).

The salinity of each microhabitat was measured at the TA sampling stations, spaced within each transect, by using pore-water conductivity, which is linearly related to salinity under the environmental conditions present (Wagner et al. 2006). A calibrated Hanna Instruments probe (HI98129/HI98130) was used to measure pore-water conductivity from groundwater recharge within small boreholes (Canadian sites), and from water extracted from sub-samples of surface (5 cm) material under laboratory conditions, where in situ measurements were not possible (Marion Island sites). The dominant source of oceanic salts to the brackish and saltmarsh sites is via coastal flooding and tidal inundation, whereas the coastal peatland sites receive salt solely from atmospheric deposition (i.e., wind-blown salt-spray and precipitation).

Sub-fossil TA communities from sediment cores collected at the salt marsh and brackish marsh environments in the Magdalen Islands (Barnett et al. 2017b) were compiled to explore TA responses to salinity changes through time. Communities were enumerated at contiguous intervals through the top ~30 cm of each core (approximately equivalent to the past 300 years). Relative changes in salinity were reconstructed by standardising (using z-scores) derived conductivity values that were calculated using the relationship between TA productivity and conductivity (Fig. 4.1b). The reconstructed salinity trend was compared against independent foraminifera-derived relative sea-level reconstructions from the same locations and sedimentological descriptions from the original study (Barnett et al. 2017b).

Taxonomic standardisation: Original taxonomic designations (presented in Whittle et al. 2019 and Barnett et al. 2017b) were updated and harmonised to ensure that included taxa were consistent and closely representative of biological species (Supplementary Table 4.3). Specifically, we combined *Phryganella acropodia* and *Difflugia globulosa* (maintaining the designation of *P. acropodia*) since separation requires observation of living-cells which were not differentiated during creation of the records; *Cyclopyxis* spp. (in Whittle et al. 2019) was re-

designated as *C. eurystoma,* and; *Corythion dubium* (in Whittle et al. 2019) was merged with *Corythion-Trinema* type.

Biomass and productivity: Census counts of each sample included all individuals (i.e., living and encysted cells, and empty tests) to minimise bias in assemblages caused by seasonal blooms (Barnett et al. 2013). Productivity (community size), as a product of sediment volume (i.e. tests cm^{-3}), was estimated from the ratio of tests to parallel counts of an exotic marker of known concentration (*Lycopodium clavatum*; Stockmarr et al. 1971). Average biovolume of each taxon was calculated assuming standard geometric test shapes (Mitchell et al. 2004) and average test dimensions (Supplementary Table 4.4). Biovolume was converted to biomass using the factor 1 $\mu m^3 = 1.1 \times 10^{-7}$ µg Carbon (Mitchell et al. 2004). Total biomass of the TA community at each sampling station was then quantified by multiplying these values by taxon abundance.

Statistical analyses: Linear regressions of log transformed productivity and biomass data against conductivity measurements were performed in R (version 3.6.3) (R Core Team 2020). Detrended correspondence analysis (DCA) Axis 1 scores, calculated from relative abundance (%) data for each sampling station were used to classify the overall species response to salinity; where values > 2 standard deviations suggest a unimodal response (ter Braak and Prentice 1988; Birks 1995; Šmilauer and Lepš 2014). Correspondence analysis (CA) based on un-transformed species relative abundance (%) data, including all observed taxa, was used to summarise variation in community composition between sampling stations. All multi-variate analyses were performed in the statistical package 'vegan' (Oksanen 2017) within R (R Core Team 2020). Analysis of covariance (ANCOVA) was used to test the homogeneity of regression slopes (gradients) for the relationship between conductivity and TA concentrations for each of the salt-enriched environment types, and was conducted using the R package 'car' (Fox et al. 2012). Identification of statistically significant changepoints within the TA derived conductivity and foraminifera inferred sea-level time-series' was conducted using the cpt.meanvar function of the 'changepoint' (Killick and Eckley 2013) R package, to find concurrent changes in the mean and variance for each time series (default settings were adopted). Pearson correlation between TA derived conductivity and foraminifera inferred sea-level was conducted using 2nd

order polynomial LOESS smoothed data, re-sampled to consistent 25 year intervals.

References

Barnett, R.L., Charman, D.J., Gehrels, W.R., Saher, M.H., Marshall, W.A. (2013). Testate amoebae as sea-level indicators in northwestern Norway: developments in sample preparation and analysis. *Acta Protozool.,* 52, 115-128.

Barnett, R.L., Garneau, M.G., Bernatchez, P. (2016). Salt-marsh sea-level indicators and transfer function development for the Magdalen Islands in the Gulf of St Lawrence, Canada. *Mar. Micropaleontol*., 122, 13-26.

Barnett, R.L., Newton, T.L., Charman, D.J., Gehrels, W.R. (2017a). Salt-marsh testate amoebae as precise and widespread indicators of sea-level change. *Earth Sci. Rev.*, 164, 193-207.

Barnett, R.L., Bernatchez, P., Garneau, M., Juneau, M.-N. (2017b). Reconstructing late Holocene relative sea-level changes at the Magdalen Islands (Gulf of St. Lawrence, Canada) using multi-proxy analyses. *J. Quat. Sci.*, 32(3) 380-395.

Birks, H.J.B. (1995). Quantitative palaeoenvironmental reconstructions. In: Statistical Modelling of Quaternary Science Data, (eds. Maddy, D., Brew, J.S.), Quaternary Research Association, Cambridge, 161–253.

Charman, D.J., Hendon, D., Woodland, W.A. (2000). The Identification of Peatland Testate Amoebae. Technical Guide 9, Quaternary Research Association, London.

Dumack, K., Kahlich, C., Lahr, D.J.G., Bonkowski, M. (2018). Reinvestigation of *Phryganella paradoxa* (Arcellinida, Amoebozoa) Penard 1902. *J. Eukaryot. Microbiol.*, 0, 1-12.

Fox, J., Weisberg, S., Adler, D., Bates, D., Baud-Bovy, G., Ellison, S., Firth, D., Friendly, M., Gorjanc, G., Graves, S., Heiberger, R. (2012) car: Companion to Applied Regression. R package – version 3.0-10. https://cran.r-project.org/web/packages/car/index.html

Gao, Z., Karlsson, I., Geisen, S., Kowalchuk, G., Jousset, A. (2019). Protists: Puppet masters of the rhizosphere microbiome. *Trends Plant Sci.*, 24(2), 165-176.

Geisen, S. *et al.* (2017). Soil protistology rebooted: 30 fundamental questions to start with. *Soil Biol. Biochem.*, 111, 94-103.

Geisen, S. *et al.* (2018). Soil protists: a fertile frontier in soil biology research. *FEMS Microbiol. Rev.,* 42, 293-323.

IPCC (2019). IPCC Special Report on the Ocean and Cryosphere in a Changing Climate [eds. Pörtner, H.-O., Roberts, D.C., Masson-Delmotte, V., Zhai, P., Tignor, M., Poloczanska, E., Mintenbeck, K., Alegría, A., Nicolai, M., Okem, A., Petzold, J., Rama, B., Weyer, N.M.]. In press.

Jansson, J.K., Hofmockel, K.S. (2020). Soil microbiomes and climate change. *Nat. Rev. Microbiol.*, 18, 35-46.

Jassey, V.E.J. *et al*. (2013). To what extent do food preferences explain the trophic position of heterotrophic and mixotrophic microbial consumers in a Sphagnum peatland? *Microb. Ecol.*, 66(3), 571-580.

Jassey, V.E.J. *et al.* (2015). An unexpected role for mixotrophs in the response of peatland carbon cycling to climate warming. *Sci. Rep.*, 5, 16931.

Karimi, B., Meyer, C., Gilbert, D., Bernard, N. (2016). Air pollution below WHO levels decreases by 40 % the links of terrestrial microbial networks. *Environ. Chem. Lett.*, 14, 467-475.

Kemp, A.C. *et al.* (2017). Utility of salt-marsh foraminifera, testate amoebae, and bulk-sediment d13C values as sea-level indicators in Newfoundland, Canada. *Mar. Micropaleontol*, 130, 43-59.

Killick, R. and Eckley, I. (2013). Changepoint: an R Package for changepoint analysis. *J. Stat. Softw.,* 58, 1-15.

Kirwan, M.L., Gedan, K.B. (2019). Sea-level driven land conversion and the formation of ghost forests. *Nat. Clim. Chang.,* 9, 450-457.

Mitchell, E.A.D. (2004). Response of testate amoebae (Protozoa) to N and P fertilization in an Arctic wet sedge tundra. *Arct., Antarct. Alp. Res.*, 36(1), 78-83.

Mitchell, E.A.D., Charman, D.J., Warner, B.G. (2008). Testate amoebae analysis in ecological and paleoecological studies of wetlands: past, present and future. *Biodivers. Conserv*., 17, 2115-2137.

Oksanen, F.J. (2017). Vegan: Community Ecology Package. R Package Version 2.5-6 [https://CRAN.R-project.org/package=vegan]

Pereira, C.S. *et al*. (2018). Salinization effects on coastal ecosystems: a terrestrial model ecosystem approach. *Phil. Trans. R. Soc. B*, 374, 20180251.

Potapov, A.M., Tiunov, A.V., Scheu, S. (2019). Uncovering trophic positions and food resources of soil animals using bulk natural stable isotope composition. *Biolog. Rev.*, 94, 37-59.

R Core Team. (2020). R: A Language and Environment for Statistical Computing. R Foundation for Statistical Computing, Vienna, Austria [https://www.R-project.org].

Ranasinghe, R. (2020). On the need for a new generation of coastal change models for the 21st century. *Sci. Rep.*, 10, 2010.

Rath, K.M., Maheshwari, A., Bengtson, P., Rousk, J. (2016). Comparative toxicities of salts on microbial processes in soil. *Appl. Environ. Microbiol.,* 82, 2012-2020.

Rath, K.M., Fierer, N., Murphy, D.V., Rousk, J. (2019). Linking bacterial community composition to soil salinity along environmental gradients. *ISME J.*, 12, 836-846.

Reczuga, M.K. *et al*. (2018). Predator-prey mass ratio drives microbial activity under dry conditions in *Sphagnum* peatlands. *Ecol. Evol.*, 8, 5752-5764.

Roe, H.M., Patterson, R.T. (2014). Arcellacea (testate amoebae) as bioindicators of road salt contamination in lakes. *Microb. Ecol.*, 68, 299-313. [10.1007/s00248-014-0408-3]

Schönborn, W. (1982). Estimates of annual production of Testacea (Protozoa) in mull and moder (II). *Pedobiologia*, 23, 383-393.

Schönborn, W. (1983). Relationships between the characteristics of the production of testacean (Protozoa) communities in soil. *Pedobiologia*, 25, 403-412.

Schönborn, W. (1986). Comparisons between the characteristics of the production of testacea (protozoa, Rhizopoda) in different forms on humus. *Symposia Biologica Hungarica*, 33, 275-284.

Schuerch, M. *et al*. (2018). Future response of global coastal wetlands to sea-level rise. *Nature*, 561, 231-234.

Šmilauer, P., Lepš, J. (2014). Multivariate Analysis of Ecological Data Using Canoco 5, Cambridge University Press.

Stockmarr, J. (1971) Tablets with spores used in absolute pollen analysis. *Pollen Spores*, 13, 615-621.

Storlazzi, C.D. *et al*. (2018). Most atolls will be uninhabitable by the mid-21st century because of sea-level rise exacerbating wave-driven flooding. *Sci. Adv.*, 4, eaap9741.

Taylor, R.G. *et al.* (2013). Ground water and climate change. *Nat. Clim. Chang.*, 3, 322-329.

ter Braak, C.J.F., Prentice, I.C. (1988). A theory of gradient analysis. *Adv. Ecol. Res.*, 18:271–317.

Trevathan-Tackett, S.M. (2019). A horizon scan of priorities for coastal marine microbiome research. *Nat. Ecol. Evol.*, 3, 1509-1520.

Vitousek, S. *et al*. (2017). Doubling of coastal flooding frequency within decades due to sea-level rise. *Sci Rep.*, 7,1399.

Wagner, R.J., Boulger, R.W.Jr., Oblinger, C.J., Smith, B. A. Guidelines and standard procedures for continuous water-quality monitors: station operation, record computation, and data reporting: U.S. Geological survey techniques and methods 1-D3. (2006) Available at: https://pubs.usgs.gov/tm/2006/tm1D3/. (Accessed: 28th May 2021).

Wanner, M., Birkhofer, K., Puppe, D., Shimano, S.D., Shimizu, M. (2020). Tolerance of testate amoeba species to rising sea levels under laboratory conditions in the South Pacific. *Pedobiologia – J. Soil Ecol.*, 79, 150610.

Ward, N.D. *et al*. (2020). Representing the function and sensitivity of coastal interfaces in Earth system models. *Nat.Commun.*, 11, 2458.

Whittle, A. *et al*. (2019). Salt-enrichment on biomass production in a natural population of peatland dwelling Arcellinida and Euglyphida (testate amoebae). *Microb. Ecol.*, 78, 534-538.

Wilkinson, D.M., Mitchell, E.A.D. (2010) Testate amoebae and nutrient cycling with particular reference to soils. *Geomicrobiol. J.,* 27, 520-533. [10.1080/01490451003702925].

Acknowledgements

The research was supported by a Natural Environment Research Council GW4+ DTP studentship (NE/L002434/1) to AW and a postdoctoral research fellowship between the Sécurité publique du Québec (CPS 16-17-04) and the University of Exeter to RLB.

Author Statement

All authors conceptualised the study. AW and RLB led on data curation and methodological design. AW led on formal analysis and visualisation with support from RLB. RLB led on the original manuscript draft with support from AW. All authors reviewed and edited the manuscript. DJC and AGS provided project supervision and funding acquisition.

.

Supplementary Information

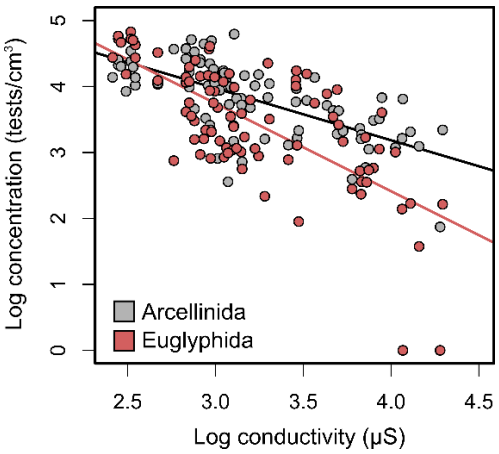

Supplementary Figure 4.1 | Relationship between conductivity and the productivity (concentration) of testate amoebae belonging to the two major orders. Arcellinida (light grey; R^2=0.4369, $F_{1,83}$= 66.17) and Euglyphida (red; R^2=0.4769, $F_{1,83}$=77.59), both p = <0.001. Statistical difference in slope gradients tested using analysis of covariance (ANCOVA) shows that regression slopes are not homogenous between the orders (F = 7.840, p= <0.01).

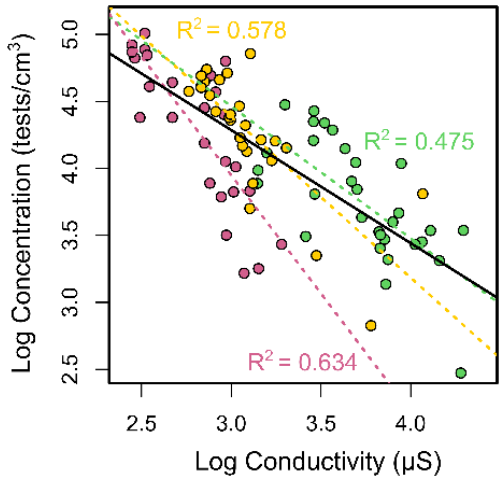

Supplementary Figure 4.2 | Regression gradients for each environment type. Salt-marsh (green), coastal peatland (yellow) and brackish marsh (red). Gradient for combined data indicated by solid black line. All relationships significant p = <0.001.

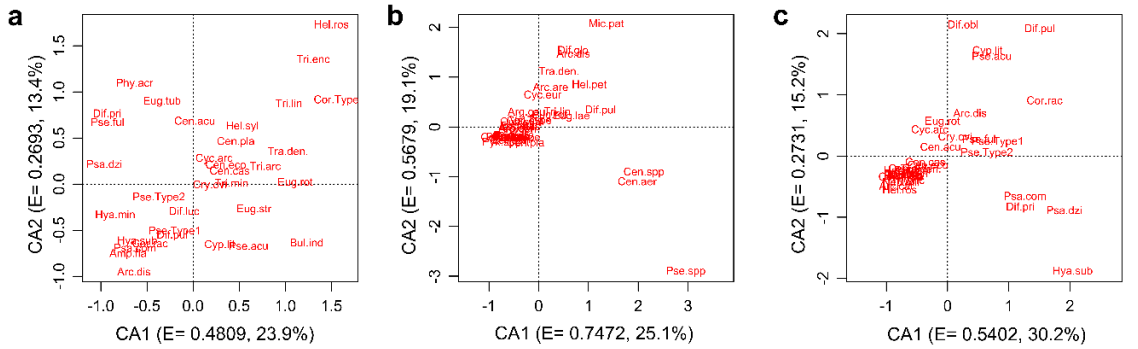

Supplementary Figure 4.3 | Correspondence analysis (CA) of species abundance data with percentage of variance explained by each axes. a) salt-marsh, b) coastal peatland, and c) brackish marsh. E denotes the axis Eigenvalue. Full species names are given in Supplementary Table 4.4.

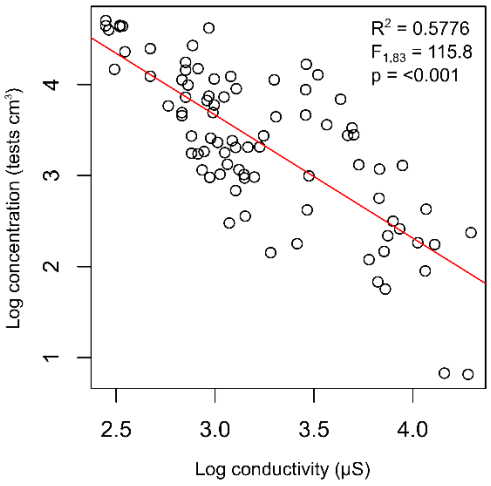

Supplementary Figure 4.4 | Salinity response of generalist species that are present within all three environment types. Gradient of the response is statistically distinct from the response when all species are included (ANCOVA; F = 11.57, p<0.001). A list of the included species is presented in Supplementary Table 4.3.

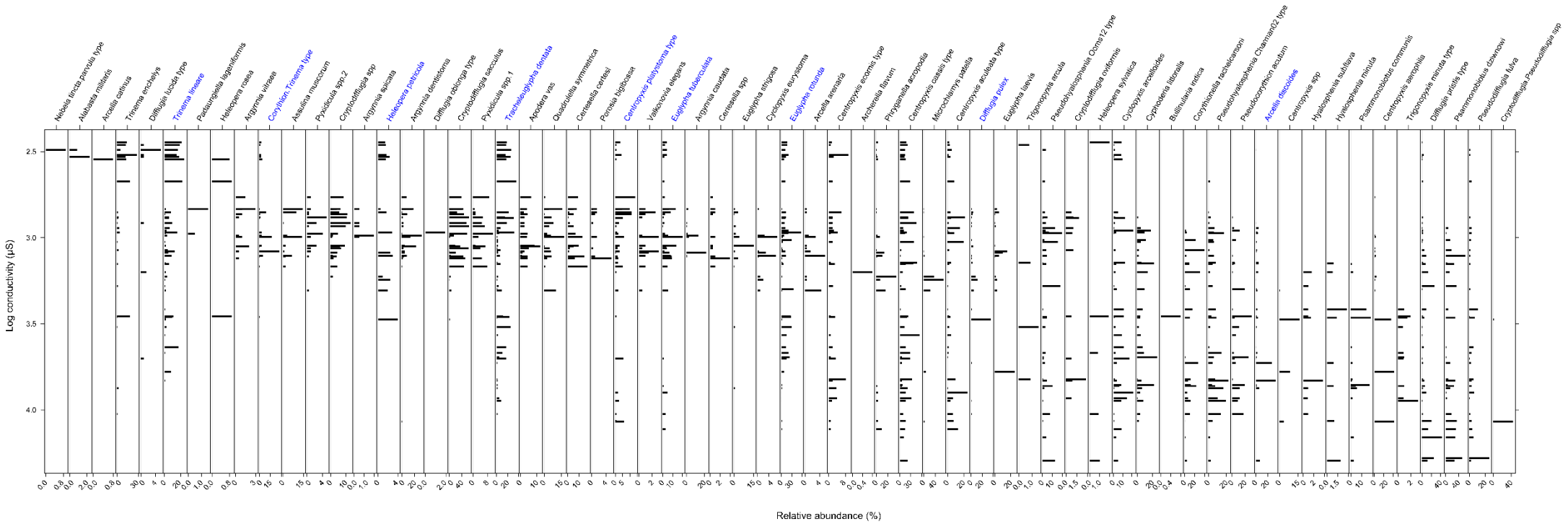

Supplementary Figure 4.5 | Relative abundance (percent) of species identified within communities plotted against environmental salinity (conductivity) conditions. Species are ordered by conductivity optima calculated by weighted averaging. High conductivity values represent high levels of salt-enrichment. Generalist species present in all of the sampled environments are highlighted in blue.

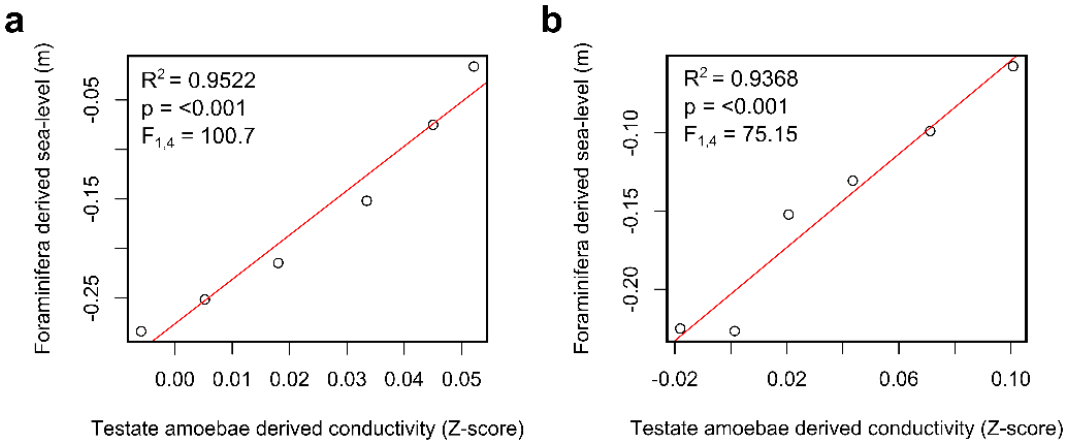

Supplementary Figure 4.6 | Correlation between conductivity Z-scores derived from the productivity of testate amoebae and sea-level reconstructions for Les Sillons (a) and Bassin (b).

Supplementary Table 4.1 | Analysis of covariance (ANCOVA), with environment type included as an interaction term, used to examine the heterogeneity of regression slopes (gradients) for the responses of testate amoeba concentration (productivity) to environmental conductivity (salinity) conditions. CP – coastal peatland, BM – brackish marsh, SM – salt-marsh. Indicates that site does affect the relationship, with values implying that the rate of productivity decline within brackish marsh is statistically different (faster) than within the salt-marsh environment. See Supplementary Fig. 4.2.

Model	Gradient F-value	*p*	Interpretation
CP – BM	3.016	0.089 .	No statistical difference in the rate of productivity decline between CP and BM dwelling testate amoeba communities.
CP - SM	0.642	0.426	No statistical difference in the rate of productivity decline between CP and SM dwelling testate amoeba communities.
BM – SM	5.920	0.018 * (p=<0.05)	Statistically significant difference in the rate of productivity decline between BM and SM dwelling testate amoeba communities. Productivity of BM communities decline at a faster rate as salinity level increases.
All environment types	3.187	0.047 * (p=<0.05)	

Supplementary Table 4.2 | Pearson correlation coefficient for correspondence analysis (CA) axis 1 sample scores and microhabitat conductivity conditions (log conductivity). n= number of samples.

Transect/Site	Pearson correlation coefficient	*p*	*n*
Salt-marsh	0.53	0.0023	31
Brackish marsh	0.77	<0.001	26
Coastal peatland	0.88	<0.001	28

Supplementary Table 4.3 | List of species present within the compiled dataset with details of actions taken to standardise taxonomies applied by individual records. BM – Brackish marsh, CP – Coastal peatland, and SM – Salt-marsh. Type is used to indicate where designations include additional species (see Charman et al. 2000).

* Order / ** Family	Taxon name	Authority	BM	CP	SM	Shared species
***Arcellinida Kent 1880**						
**Arcellidae Ehrenberg1843						
	Arcella arenaria	Greef 1866		●		
	Arcella catinus type	Penard 1890	●		●	
	Arcella discoides type	Ehrenberg 1843	●	●	●	●
**Hyalospheniidae Schultze 1877						
	Apodera vas	(Certes 1889) Loeblich and Tappan, 1961		●		
	Certesella certesi	(Penard 1911) Loeblich and Tappan, 1961		●		
	Certesella spp	See Whittle et al. (2019)		●		
	Alabasta (Nebela) militaris type	(Penard 1890) Duckert et al. 2018	●		●	
	Nebela tincta-parvula type	See Charman et al. (2000)	●		●	
	Padaungiella lageniformis	(Penard 1902) Lara and Todorov 2012		●		
	Porosia bigibbosa	(Penard 1890) Jung 1942		●		
	Quadrulella symmetrica	(Wallich 1863) Schulze 1875		●		
**Microchlamyiidae Ogden 1985						
	Microchlamys patella	(Claparède and Lachmann 1859) Cockerell 1911		●		
**Cryptodifflugiidae Jung1942						
	Cryptodifflugia oviformis	Penard 1890	●		●	
	Cryptodifflugia sacculus	Penard 1902		●		
	Cryptodifflugia spp	See Whittle et al. (2019)		●		
	Cryptodifflugia-Pseudodifflugia spp	See Whittle et al. (2019)		●		
**Centropyxidae Jung1942						
	Centropyxis aculeata type	(Ehrenberg 1838) Stein 1857	●		●	
	Centropyxis aerophila	Deflandre 1929		●		
	Centropyxis cassis type	(Wallich 1864) Deflandre 1929	●		●	
	Centropyxis ecornis type	(Ehrenberg 1841) Leidy 1879	●		●	
	Centropyxis platystoma type	(Penard 1890) Deflandre 1929	●	●	●	●
	Centropyxis spp	See Whittle et al. (2019)		●		
**Phryganellidae Jung1942						
	Phryganella acropodia (merged with *Difflugia globulosa* (Dujardin, 1837) Penard, 1902)	Hertwig and Lesser 1874 (Hopkinson 1909)	●	●	●	
**Plagiopyxiidae Bonnet and Thomas 1960						
	Bullinularia indica	(Penard 1911) Deflandre 1953			●	
**Trigonopyxidae Loeblich and Tappan 1964						
	Cyclopyxis arcelloides	(Penard 1902) Deflandre 1929	●		●	
	Cyclopyxis eurystoma (merged with C*yclopyxis* spp from Whittle et al. 2019)	Deflandre 1929		●		
	Trigonopyxis arcula	(Leidy 1879) Penard 1912	●		●	
	Trigonopyxis minuta type	Shönborn and Peschke 1988			●	
** Incertae sedis Arcellinida						
	Argynnia caudata	(Leidy 1879) Vucetich, 1974		●		
	Argynnia dentistoma	(Penard 1890) Vucetich, 1974		●		
	Argynnia spicata	(Wailes 1913) Vucetich, 1974		●		
	Argynnia vitraea	(Penard 1899) Vucetich, 1974		●		
	Difflugia lucida type	Penard 1890	●		●	
	Difflugia oblonga type	Ehrenberg 1838	●			
	Difflugia pristis type	Penard 1902	●		●	
	Difflugia pulex	Penard 1902	●	●	●	●

	Heleopera petricola	Leidy 1879	●	●	●	●
	Heleopera rosea	Penard 1890	●		●	
	Heleopera sylvatica	Penard 1890	●		●	
	Pseudohyalosphenia Charman 02 type		●		●	
	Pseudohyalosphenia Ooms12 type		●		●	
	Pyxidicula spp 1	See Whittle et al. (2019)		●		
	Pyxidicula spp 2	See Whittle et al. (2019)		●		
** Hyalospheniidae Schultze 1877						
	Hyalosphenia minuta	Cash 1891			●	
	Hyalosphenia subflava	Cash 1909	●		●	
* Euglyphida Copeland 1956						
** Cyphoderiidae De Sandeleer, 1934						
	Corythionella rachelcarsoni	Nicholls 2007	●		●	
	Cyphoderia littoralis	Golemansky, 1973	●		●	
	Pseudocorythion acutum	Wailes 1927	●		●	
** Euglyphidae Wallich 1864						
	Euglypha laevis	(Ehrenberg 1832) Perty 1849		●		
	Euglypha rotunda	Wailes 1915	●	●	●	●
	Euglypha strigosa	(Ehrenberg 1871) Leidy 1878		●	●	
	Euglypha tuberculata	Dujardin 1841	●	●	●	●
**Trinematidae Hoogenraad and De Groot 1940						
	Corythion-Trinema type (merged with Corythion dubium Taránek 1881)	See Charman et al. 2000	●	●	●	●
	Trinema enchelys	(Ehrenberg 1838) Leidy 1878	●		●	
	Trinema lineare	Penard 1890	●	●	●	●
** Assulinidae Lara 2007						
	Assulina muscorum	Greef 1888		●		
	Valkonovia elegans	Schönborn 1964		●		
** Incertae sedis euglyphid testate amoebae						
	Tracheleuglypha dentata	(Vejdovsky, 1882) Deflandre 1928	●	●	●	●
*** Stramenopila**						
**Amphitremidae Poche 1913						
	Archerella (Amphitrema) flavum	(Archer, 1877) Loeblich and Tappan, 1961			●	
*** Other cercozoa**						
** Psammonobiotidae Golemansky 1974						
	Psammonobiotus communis	Golemansky 1970	●		●	
	Psammonobiotus dziwnowi	Nicholls 2005	●		●	
**Pseudodifflugiidae De Sandeleer 1934						
	Pseudodifflugia fulva	Archer 1870	●		●	

Supplementary Table 4.4 | Biovolume and Biomass estimates for each species based on measurements of an ideal individual collated from published test dimensions. Test shape classifications are based on the criteria defined by Mitchell (2004); O – ovoid, S – spherical, C-O – cylindrical-ovoid, H – hemispheric. Values in bold denote those previously published in Whittle et al. (2019), see original source for full details.

ID code	Species name	Test shape	Length (µm)		Width (µm)		Height (µm)		Diameter (µm)		Literature sources	Biovolume (µm³ per individual)			Biomass (µg Carbon per individual)		
			+ve	-ve	+ve	-ve	+ve	-ve	+ve	-ve		Mean	+ve	-ve	Mean	+ve	-ve
Amp.fla	*Archerella (Amphitrema) flavum*	O	77	45	45	23	25	15			Cash et al. (1915)	27653	57750	10350	0.003042	0.006353	0.001139
Apo.vas	***Apodera vas***	**O**	**159**	**146**	**84**	**76**	**48**	**48**				**385542**	**421629**	**35228**	**0.04241**	**0.04638**	**0.03880**
Arg.cau	***Argynnia caudata***	**O**	**95**	**82**	**78**	**63**	**50**	**50**			***Based on Arg.den***	**201391**	**243539**	**168470**	**0.02215**	**0.02679**	**0.01854**
Arg.den	***Argynnia dentistoma***	**O**	**96**	**80**	**83**	**64**	**50**	**50**				**213769**	**261127**	**170157**	**0.02352**	**0.02872**	**0.01872**
Arg.spi	***Argynnia spicata***	**O**	**96**	**87**	**82**	**79**	**50**	**50**			***Based on Arg.den***	**239499**	**259737**	**226354**	**0.02635**	**0.02857**	**0.02490**
Arg.vit	***Argynnia vitraea***	**O**	**112**	**102**	**94**	**83**	**75**	**75**				**498198**	**526438**	**420758**	**0.05480**	**0.05790**	**0.04629**
Ass.mus	***Assulina muscorum***	**O**	**51**	**44**	**41**	**35**	**20**	**20**				**23776**	**27765**	**20461**	**0.00262**	**0.00306**	**0.00226**
Bul.ind	*Bullinaria indica*	O	148	138	172	165	99	94			Ogden and Hedley (1980)	1550144	1680096	1426920	0.170516	0.184811	0.156961
Cen.acu	*Centropyxis aculeata type*	O	178	92	137	77	72	40			Ogden and Hedley (1980)	539280	1170528	188907	0.059321	0.128758	0.020780
Cen.aer	***Centropyxis aerophila***	**O**	**70**	**62**	**58**	**51**	**28**	**28**				**66790**	**76193**	**59164**	**0.00735**	**0.00838**	**0.00651**
Cen.cas	*Centropyxis cassis type*	O	117	79	90	57	63	41			Ogden and Hedley (1980)	249704	442260	123082	0.027467	0.048649	0.013539
Cen.eco	*Centropyxis ecornis type*	O	380	100	380	100	80	20			Lahr et al. (2008)	1920000	7701333	133333	0.211200	0.847147	0.014667
Cen.pla	*Centropyxis platystoma type*	O	81	62	48	34	31	25			Ogden and Hedley (1980)	54721	80352	35133	0.006019	0.008839	0.003865
Cen.spp	***Centropyxis spp***	**O**	**63**	**55**	**62**	**15**	**45**	**45**				**100057**	**118864**	**84544**	**0.01101**	**0.01308**	**0.00930**
Cer.cer	***Certesella certesi***	**O**	**144**	**134**	**80**	**72**	**50**	**50**			***Based on Apo.vas***	**347278**	**384037**	**319312**	**0.03820**	**0.04224**	**0.03512**
Cer.spp	***Certesella spp***	**O**	**142**	**131**	**92**	**81**	**50**	**50**			***Based on Apo.vas***	**402033**	**433358**	**350483**	**0.04422**	**0.04767**	**0.03856**
Cor.rac	*Corythionella rachelcarsoni*	O	36	36	20	20	15	15			Nicholls (2009)	7200	7200	7200	0.000792	0.000792	0.000792
Cor.type	*Corythion-Trinema type*	O	55	33	33	24	17	9			Ogden and Hedley (1980)	10868	20570	4752	0.001195	0.002263	0.000523
Dif.luc	*Difflugia lucida type*	O	100	80	55	25	37	16			Charman et al. (2000)	63600	135667	21333	0.006996	0.014923	0.002347
Dif.obl	*Difflugia oblonga type*	O	237	190	146	92	146	92			Ogden and Hedley (1980)	2015582	3367928	1072107	0.221714	0.370472	0.117932
Dif.pri	*Difflugia pristis type*	O	58	51	45	36	45	36			Charman et al. (2000)	59596	78300	44064	0.006556	0.008613	0.004847
Eug.lae	***Euglypha laevis***	**O**	**29**	**22**	**15**	**12**	**8**	**6**				**1662**	**2165**	**984**	**0.00019**	**0.00024**	**0.00011**
Eug.rot	*Euglypha rotunda type*	O	52	22	34	14	22	9			Cash et al. (1915)	9176	25931	1848	0.001009	0.002852	0.000203
Eug.str	*Euglypha strigosa*	O	100	45	60	30	30	20			Cash et al. (1915)	54375	120000	18000	0.005981	0.013200	0.001980
Eug.tub	*Euglypha tuberculata type*	O	100	45	50	24	25	12			Cash et al. (1915)	33084	83333	8640	0.003639	0.009167	0.000950
Hel.pet	*Heleopera petricola*	O	84	76	57	51	50	40			Ogden and Hedley (1980)	129600	159600	103360	0.014256	0.017556	0.011370
Hel.ros	*Heleopera rosea*	O	128	117	107	94	57	51			Ogden and Hedley (1980)	443205	520448	373932	0.048753	0.057249	0.041133
Hel.syl	*Heleopera sylvetica*	O	75	50	30	25	15	12			Cash and Hopkinson (1909)	15469	22500	10000	0.001702	0.002475	0.001100
Hya.min	*Hyalosphenia minuta*	O	41	26	25	16	12.5	8			Mazei (2006)	4693	8542	2219	0.000516	0.000940	0.000244
Hya.sub	*Hyalosphenia subflava*	O	62	56	38	37	25	24			Ogden and Hedley (1980)	36138	39267	33152	0.003975	0.004319	0.003647
Neb.mil	*Alabasta (Nebela) militaris type*	O	70	59	41	33	23	21			Ogden and Hedley (1980)	35002	44007	27258	0.003850	0.004841	0.002998

Neb.tin	*Nebela tincta-parvula type*	O	94	76	71	51	58	35			Ogden and Hedley (1980)	160735	258061	90440	0.017681	0.028387	0.009948
Pad.lag	***Padaungiella lageniformis***	**O**	**145**	**133**	**86**	**79**	**48**	**48**			***Based on Apo.vas***	**365861**	**396133**	**332104**	**0.04025**	**0.04357**	**0.03653**
Por.big	***Porosia bigibbosa***	**O**	**152**	**139**	**86**	**74**	**50**	**50**			***Based Apo.vas***	**388896**	**432106**	**340969**	**0.04278**	**0.04753**	**0.03751**
Psa.dzi	*Psammonobiotus dziwnowi*	O	27	21	14	9	12	9			Nicholls (2005)	1932	3024	1134	0.000213	0.000333	0.000125
Psa.com	*Psammonobiotus communis*	O	52	23	19	19	15	15			Siemensma (2019)	7125	9880	4370	0.000784	0.001087	0.000481
Pse.acu	*Pseudocorythion acutum*	O	55	50	23	23	20	20			Siemensma (2019)	16100	16867	15333	0.001771	0.001855	0.001687
Pse. Type1	*Pseudohyalosphenia Charman02 type*	O	50	50	40	40	40	40			Charman et al. (2002), Barnett et al. (2016) (*est.*)	53333	53333	53333	0.005867	0.005867	0.005867
Pse. Type2	*Pseudohyalosphenia Ooms12 type*	O	50	50	40	40	40	40			Charman et al. (2002), Barnett et al. (2016) (*est.*)	53333	53333	53333	0.005867	0.005867	0.005867
Qua.sym	***Quadrulella symmetrica***	**O**	**76**	**70**	**44**	**40**	**30**	**30**				**60816**	**66504**	**54688**	**0.00669**	**0.00732**	**0.00602**
Val.ele	***Valkonovia elegans***	**O**	**47**	**41**	**33**	**27**	**20**	**20**				**17285**	**20383**	**14922**	**0.00190**	**0.00224**	**0.00164**
Arc.are	***Arcella arenaria***	**S**					**18**	**14**	**85**	**85**		**50103**	**52682**	**40650**	**0.005511**	**0.005795**	**0.004471**
Arc.cat	*Arcella catinus type*	S					29	22	114	73	Ogden and Hedley (1980)	87543	148002	46039	0.009630	0.016280	0.005064
Arc.dis	*Arcella discoides type*	S					30	23	104	83	Ogden and Hedley (1980)	90976	127423	62222	0.010007	0.014017	0.006844
Mic.pat	***Microchlamys patella***	**S**					**17**	**12**	**50**	**40**		**10390**	**14914**	**7145**	**0.00114**	**0.00164**	**0.00078**
Pyx.spp.1	***Pyxidicula* spp 1**	**S**					**18**	**17**	**35**	**31**		**7659**	**8691**	**6410**	**0.00085**	**0.00096**	**0.00070**
Pyx.spp.2	***Pyxidicula* spp 2**	**S**					**42**	**35**	**74**	**67**		**84327**	**90835**	**60400**	**0.00927**	**0.00999**	**0.00664**
Cry.ovi	*Cryptodifflugia oviformis*	C-O	18	15	15	8			15	8	Mazei (2006)	1746	3240	768	0.000192	0.000356	0.000084
Tri.enc	*Trinema enchelys*	C-O	78	47	34	19			34	19	Ogden and Hedley (1980)	35113	72134	13574	0.003862	0.007935	0.001493
Tri.lin	*Trinema lineare*	C-O	35	25	19	14			19	14	Ogden and Hedley (1980)	6534	10108	3920	0.000719	0.001112	0.000431
Tra.den	*Tracheleuglypha dentata*	C-O	47	47	27	27			27	27	Whittle et al. (2019)	27410	27410	27410	0.003015	0.003015	0.003015
Dif.pul	*Difflugia pulex*	C-O	43	28	30	16			30	16	Penard (1902)	15024	30960	5734	0.001653	0.003406	0.000631
Cyp.lit	*Cyphoderia littoralis*	C-O	53	46	27	22			27	22	Todorov et al. (2009)	23770	30910	17811	0.002615	0.003400	0.001959
Pse.ful	*Pseudodifflugia fulva*	C-O	36	15	30	12			30	12	Mazei (2006)	8996	25920	1728	0.000990	0.002851	0.000190
Phr.acr	*Phryganella acropodia*	H					80	20	110	35	Mazei (2006)	99766	348455	11225	0.010974	0.038330	0.001235
Cyc.arc	*Cyclopyxis arcelloides type*	H							107	35	Charman et al. (2000)	93701	320716	11225	0.010307	0.035279	0.001235
Cyc.eur	***Cyclopyxis eurystoma***	**H**							**46**	**38**		**19794**	**26031**	**14565**	**0.00218**	**0.00286**	**0.00161**
Cry.sac	***Cryptodifflugia sacculus***	**H**							**28**	**26**		**5170**	**5833**	**4429**	**0.00057**	**0.00064**	**0.00048**
Cry.spp	***Cryptodifflugia spp***	**H**							**28**	**25**		**4961**	**5957**	**4164**	**0.00055**	**0.00066**	**0.00046**
Pse.spp	***Cryptodifflugia-Pseudodifflugia spp***	**H**							**30**	**27**		**6322**	**7420**	**5190**	**0.00069**	**0.00081**	**0.00057**
Tri.min	*Trigonopyxis minuta type*	H					56	43	88	69	Mazei (2006)	126642	178409	86003	0.013931	0.019625	0.009460
Tri.arc	*Trigonopyxis arcula type*	H					68	56	112	93	Mazei (2006)	281929	367809	210580	0.031012	0.040459	0.023164

Supplementary References

Barnett, R.L., Garneau, M., Bernatchez, P. (2016). Salt-marsh sea-level indicators and transfer function development for the Magdalen Islands in the Gulf of St. Lawrence, Canada. Marine Micropaleontology, 122, 13-26.

Cash, J., Hopkinson, J. (1909). The British Freshwater Rhizopoda and Heliozoa, vol. II. The Ray Society, London.

Cash, J., Wailes, G., Hopkinson, J. (1915). The British Freshwater Rhizopoda and Heliozoa, vol. III. The Ray Society, London.

Charman, D.J., Hendon, D., Woodland, W.A. (2000). The identification of testate amoebae (Protozoa: Rhizopoda) in peats. Quaternary Research Association, London.

Charman, D.J., Roe, H.M., Gehrels, W.R. (2002). Modern distribution of saltmarsh testate amoebae: Regional variability of zonation and response to environmental variables. Journal of Quaternary Science, 17(5–6), 387–409.

Lahr, D.J.G., Bergmann, P.J., Lopes, S.G.B.C. (2008). Taxonomic identity in microbial eukaryotes: A practical approach using the testate amoeba Centropyxis to resolve conflicts between old and new taxonomic descriptions. Journal of Eukaryotic Microbiology, 55(5), 409–416.

Mazei, Y., Tsyganov, A.N. (2006). Freshwater testate amoebae (In Russian). KMK, Moscow 302.

Nicholls, K.H. (2005). Psammonobiotus dziwnowi and Corythionella georgiana, Two new freshwater sand-dwelling testate amoebae (Rhizopoda: Filosea). Acta Protozoologica, 44(3), 271–278.

Nicholls, K.H. (2009). A multivariate statistical evaluation of the “acolla-complex” of Corythionella species, including a description of C. darwini n. sp. (Rhizopoda: Filosea or Rhizaria: Cercozoa). European Journal of Protistology, 45, 183–192.

Ogden, C.G., Hedley, R.H. (1980). An atlas of freshwater testate amoebae. Oxford University Press, Oxford.

Penard E. (1902). Faune rhizopodique du Bassin du Léman. Henry Kündig, Genève.

Siemensma, F.J. (2019). Microworld, world of amoeboid organisms. World-wide electronic publication, Kortenhoef, the Netherlands. https://www.arcella.nl.

Todorov, M.T., Golemansky, V., Mitchell, E.A.D., Heger, T.J. (2009). Morphology, biometry, and taxonomy of freshwater and marine interstitial Cyphoderia (Cercozoa: Euglyphida). Journal of Eukaryotic Microbiology, 56(3), 279–289.

Whittle, A., Amesbury, M. J., Charman, D. J., Hodgson, D. A., Perren, B. B., Roberts, S. J. and Gallego-Sala, A. (2019) Salt-enrichment impact on biomass production in a natural population of peatland dwelling Arcellinida and Euglyphida (testate amoebae). Microbial Ecology, 78(2), 534–538.

Chapter 5

Recent intensification of the Southern Hemisphere westerly winds as detected in the response of terrestrial testate amoebae in the sub-Antarctic

5.1. Introduction

The Southern Hemisphere westerly winds (SHWs) circulate between areas of high-pressure over the subtropics and low-pressures over the Antarctic (Toggweiler, 2009), and reach maximum intensity within a latitudinal belt between 50-55^{o}S (Lamy et al. 2010). Between these latitudes airflow can complete a full circumpolar rotation virtually unhindered by topographic obstacles, and therefore develops into a circulation consisting of the strongest time-averaged oceanic winds anywhere in the world (Hodgson and Sime, 2010). Variability in the latitudinal position and intensity of the SHWs plays a critical role in both the regional and global climate (Sime et al. 2013). However, depletion of stratospheric ozone since the 1960s, caused by anthropogenic emissions of CFCs, alongside warming from rising concentrations of atmospheric carbon dioxide, have caused the wind-belt to intensify and migrate southwards over the past 50 years (Thompson and Solomon, 2002; Cai, 2006; Thompson et al. 2011). The wind belt now extends ~3.5 degrees further South in winter and ~2 degrees in summer, and has intensified by up to 6% between 2001-2010 compared to 1981-1990 (Mayewski et al. 2013).

As a result of the changing wind-behaviour, storm-tracks that would normally carry moisture to the continental regions surrounding the Southern Ocean, have been diverted further poleward (Abram et al. 2014). Precipitation in New Zealand has consequently reduced (Ummenhofer and England, 2007; Ummenhofer et al. 2009), and droughts and wildfires have occurred in south-western Australia (Cai et al. 2011), South Africa (Reason and Rouault, 2005), and southern South America (Holz et al. 2017; Garreaud, 2018). Beyond moisture supply, these changes have also been linked to widespread environmental change throughout the southern high latitudes, including: 1) perturbation of the Southern Ocean circulation (Lovenduski et al. 2008; Anderson et al. 2009; Marshall and Speer, 2012) which modifies the upwelling of carbon-rich deep-water and affects the exchange of carbon dioxide between ocean and atmosphere (Toggweiler et al.

2006; Le Quéré et al. 2007; Hodgson and Sime, 2010; Landschützer et al. 2015), 2) increased basal melting of ice-shelves surrounding the West Antarctic ice-sheet and Antarctic Peninsula (Marshall et al. 2006; Pritchard et al. 2012; Smith et al. 2017; Holland et al. 2019), 3) changing sea-ice extent (Purich et al. 2016), 4) climatic warming along the Antarctic Peninsula (Vaughan et al. 2003), and 5) enhanced Agulhas leakage (Biastoch et al. 2009).

Recovery of ozone during the coming decades could partially reverse these trends, however under most emission scenarios, climate models estimate that rising greenhouse gas concentrations will cancel out this recovery, at least in summer when the effect of depleted ozone at the surface is greatest (Mayewski et al. 2015). Climatic warming associated with greenhouse gas emissions is then projected to dominate under high emission scenarios leading to an overall increase in strength and maintained southward displacement of the wind-belt by 2100 (Bracegirdle et al. 2013).

The changes in SHW behaviour (and by association the Southern Annular Mode index (Marshall, 2003)) over recent decades have been documented from satellite observations (e.g. Swart and Fyfe (2012); Bracegirdle (2018)) and a sparse network of station-based records from locations within the Southern Ocean (e.g. Marshall (2003)). However, as a consequence of the differing periods that research bases have remained permanently occupied, most records are discontinuous and short (see Adams (2009); BAS Reader (2020)). Many are also difficult to interpret owing to the locations of measurement sites in more sheltered sites close to research bases. As a result, understanding of long-term climatic evolution, particularly prior to the 1950s, remains elusive (Thomas et al. 2018).

In the absence of a long-term observational record, particularly within the core wind-belt region, palaeoenvironmental reconstructions represent a powerful opportunity to extend our understanding of changes in wind-behaviour over decadal, centennial and millennial timescales, and thereby improve our ability to predict future climatic implications. Locations of the archives used to develop SHW reconstructions are currently biased to either Patagonia (e.g. Lamy et al. (2010); Moreno et al. (2018)), or the other continental landmasses surrounding the Southern Ocean (e.g. Knudson et al. (2011); Saunders et al. (2012); Stager et al. (2012); Chase et al. (2013); Hinojosa et al. (2017)). In addition to this lack of spatial resolution, many of the reconstructions have relied on indirect and

sometimes convoluted proxies for assessing changes in wind strength. Many inferences of past wind changes are reliant on complex correlation between wind-intensity and precipitation (Kohfeld et al. 2013), for which there are many established palaeo-proxies (e.g. sub-fossil pollen assemblages and sediment geochemistry (e.g. Lamy et al. (2001); Knudson et al. (2011)). Few of these records are highly resolved.

Vast areas of the southern high latitudes have lacked reliable palaeo-wind reconstructions until recent years, when this has been partially addressed with the development of new approaches (Saunders et al. 2018; Perren et al. 2020). These research efforts have sought to access previously unused palaeo-environmental archives located on the sub-Antarctic islands, which lie within the Southern Ocean and inside the core wind-belt. These include reconstructions based on changes in tree-line altitude (Turney et al. 2016a) and deposition of wind-transported foreign aerosols such as charcoal (Turney et al. 2016b), and pollen (Strother et al. 2015). Nevertheless, these proxies are limited in applicability, for example few sub-Antarctic islands support trees, and influx of foreign aerosols is often complicated by concurrent changes in the source region which might not be directly related to winds.

One emerging methodological approach holds particular potential in allowing direct reconstruction of the SHW: that of using diatoms to track variations in the deposition of wind-blown sea-salt aerosols into otherwise freshwater sub-Antarctic lakes (Saunders et al. 2009; Saunders et al. 2015; 2018; Perren et al. 2020). Although lakes are common on the sub-Antarctic islands, wider application of the method is constrained by the availability of suitable lakes with sedimentary archives and conditions conducive to the preservation of diatoms. A possible solution to this problem is to use the archives afforded by peatlands which are also universally present throughout the sub-Antarctic (Van der Putten et al. 2012). Testate amoebae are unicellular microbial eukaryotes which are particularly abundant in freshwater mosses and soils worldwide, and produce shells (tests) that preserve in peat archives (Mitchell et al. 2008). Recent studies have demonstrated that the productivity of their populations is highly-sensitive to changes in surface-water salinity conditions, indicating that similarly to diatoms they could provide a proxy for wind-blown salt-spray deposition (Whittle et al. 2019; Chapter 4). Located within the core SHW belt in the South Atlantic sector

of the Southern Ocean, Bird Island (54˚00'S, 38˚02'W) represents an ideal site to explore the application of peat-dwelling testate amoeba for westerly wind reconstructions (Whittle et al. 2019; Chapter 4). However, the use of wind-blown salt-spray as a proxy relies on a direct linkage between terrestrial salinity and westerly wind conditions, which has not been tested previously on the island. In this paper: 1) we carried out detailed mapping of surface-water conductivity (salinity) in order to identify the major determinants of this variation and confirm that terrestrial salinity conditions relate directly to westerly wind strength; and 2) we use testate amoeba productivity to provide the first sub-decadal and direct reconstruction documenting the increasing SHW intensity over the past decades.

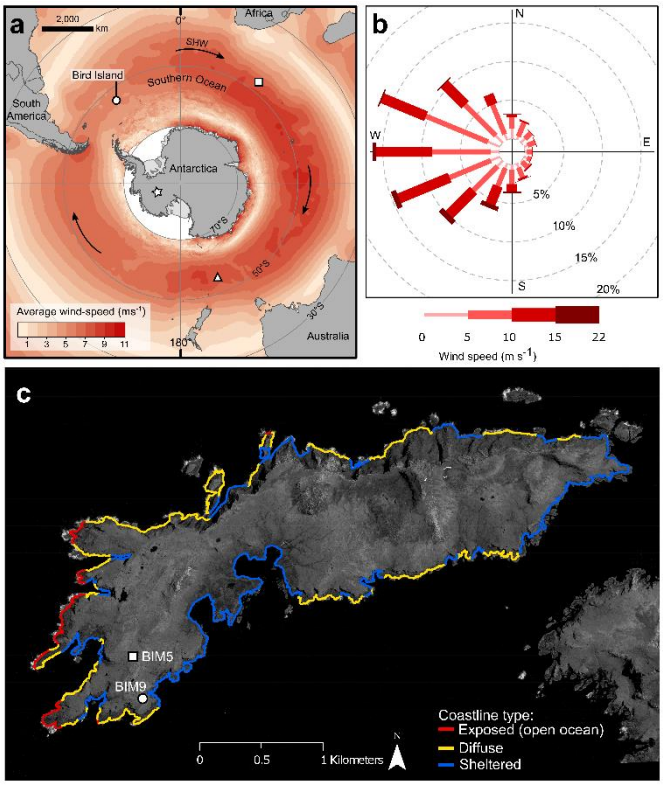

Figure 5.1 | a) Location of the modern-day core of the Southern Hemisphere Westerly Winds (SHW) over the Southern Ocean, in relation to the study site on Bird Island. Arrows indicate the prevailing direction of wind circulation. Red shading shows sea-surface level (10 m) mean annual wind intensity based on NOAA blended high-resolution (0.25 degree grid) vector data downloaded from (https://www.ncdc.noaa.gov/data-access/marineocean-data/blended-global/blended-sea-winds). Locations of other wind-records referred to in the text are denoted by the white triangle, Macquarie Island; white square, Marion Island; and white star, West Antarctic ice-sheet divide ice-core (WDC06A). b) wind-rose summarising the dominant airflow direction, intensity and frequency over Bird Island at 22.5˚ resolution, compiled from NOAA daily re-analysis data for the period 2012-2018. c) Map of Bird Island indicating the location of the coring site at Morris Point (BIM9, white circle), and wind-fetch categorisation of the islands coastline, calculated using wind-direction and frequencies shown in (b). The location of the BIM5 core, referred to in text is indicated by the white square.

5.2. Study Site

Bird Island lies approximately 1000 km south-east of the Falkland Islands, and is separated from nearby South Georgia by a 500 m channel which has allowed it to remain free of the invasive species, most notably rats, that are present there. Approximately 5 km long and 1 km wide, the island has a hilly topography consisting of a ridge that forms a backbone running east to west, and a maximum elevation of 350 m (Fig. 5.1). The northern coast forms precipitous cliffs, while to the south the land slopes more gradually to a series of inlets and tussock-grass covered hillocks. The island is extensively vegetated, and while snow and ice build-up during winter (between July-October), there is no permanent snow cover (Hunter et al. 1982). Winds blow almost exclusively from the west (Fig. 5.1) and climate is cool and wet, with temperatures of ~0˚C in winter and 4˚C in summer. The island represents an important breeding ground for seabirds and seals in summer, the largest of which are colonies of ~50,000 pairs of Macaroni and Gentoo penguins, 14,000 pairs of albatrosses, and 65,000 Antarctic fur-seals (Schmale et al. 2013).

5.3. Methods

5.3.1. Drivers of terrestrial salinity on Bird Island

Surface-water conductivity measurements

Spatial patterns in surface water salinity across Bird Island were mapped by measuring the electrical conductivity of 453 lakes, pools, streams or shallow soil-water recharge wells using a calibrated Hanna Instruments HI98129 meter. Under these conditions conductivity is linearly related to salinity (Wagner et al. 2006) and therefore can provide a direct proxy for the relative level of salt-spray deposition received at a particular location (Whittle et al. 2019). To control for differences in the dilution of salt inputs into waterbodies of significantly different volume, measurement locations were categorised into four types; 1) lake or pool (>5 m^2 in area), 2) flowing water, 3) terrestrial (including pore-water recharge), and 4) small surface pools or puddles (<5 m^2 in area). Disturbances caused by birds or seals close to measurement locations were also noted. All measurements were recorded during a five-week period between January and March 2017. Owing to the length of this period it was not possible to control against potentially confounding variables such as changes in ambient temperature, evaporation, precipitation or short-term fluctuations in salt-deposition (e.g. increases directly after a passing storm) which could lead to distortion of the pattern.

Salt-spray exposure variables

To identify whether the patterns of surface-water salinity were associated with wind-blown salt-spray, values for variables that we hypothesised to be related to a particular locations exposure were calculated on a 25 m resolution grid covering Bird Island (summarised in Table 5.1 and Fig. 5.2). Where relevant, these were weighted to reflect the average frequency of winds >10 ms^{-1} blowing from directions at 22.5˚ intervals. Wind speeds >10 ms^{-1} were used since they have been shown to be particularly important for salt-spray generation and transport (Schmale et al. 2013). Averages were calculated from NCEP/NCAR reanalysis data for the period 2012-2018. While ground-based observations are also available during this period they are prone to indicating erroneous wind-direction caused by the relatively sheltered location of the measurement site and turbulence as airflow is obstructed by local topography on Bird Island (Schmale et al. 2013).

Wind fetch of coastlines was calculated in the 'fetchR' software package in R (R core team, 2013; Seers, 2018). Fetch provides an estimate of the distance wind travels unhindered by land before reaching the coast, and can be considered a measure of overall wind exposure for a stretch of coastline (Seers, 2018). Higher levels of fetch in a particular direction indicates that more energy will be imparted on the sea surface, resulting in larger sea states and greater salt-spray generation when waves break against the coastline. Fetch was calculated for each direction at 22.5˚ intervals in order to calculate an average exposure for points surrounding the island. Averaged values were weighted to reflect the frequency of wind from different directions, and were subsequently divided into three categories; sheltered, diffuse and coastlines predominantly exposed to the open ocean.

Model development and testing

A training set of 67 samples was compiled to examine the relationship between observed surface water conductivity measurements and the variables which we hypothesised could explain them. To control the potentially confounding influence of greater dilution of deposited salts in larger volume water bodies, measurements taken from aquatic environments (pools, lakes and running water) were excluded from the training set. Samples included in the training set were

chosen to be most representative of locations across the island and the heterogeneity of different land-cover types.

Values of each gridded explanatory variable (Fig. 5.2) were extracted from locations corresponding to training set observation points. The relationship between these values and observations were used to develop two regression models, one generalised additive model (GAM) and one multiple linear regression. The model best representing the data was subsequently used to predict surface water conductivity values over the whole island. A subset of 192 observations, also solely from terrestrial environments, was used to ground-truth and test the accuracy of this prediction.

5.3.2. Reconstructing surface water salinity conditions

Core sampling

To address the second aim of this paper, a 33 cm long peat core was collected from a small (~50 m^2) area of valley floor mire close to the western tip of Bird Island at Morris Point (Fig. 5.1) during an expedition in 2017. The peat accumulation and peat forming vegetation is most closely associated with the 'Tussock peat' classification defined by Lewis Smith (1981), with vegetation consisting of predominantly tussock grass (*Poa flabellata)* with an understorey of mosses, including *Chorisodontium aciphyllum* and *Polytrichum alpestre*. The site lies ~30 m above sea-level and is surrounded to the North and South by small slopes vegetated with *Poa flabellata* and rising 5-10 m above the coring location. There are currently few birds and no seal colonies in the immediate vicinity of the coring location. The valley opens directly to the coast within <100 m, meaning that the core site is ideally situated to accumulate sea-salt aerosols from the prevailing wind. Surface water conductivity conditions in the area of coring were the highest recorded within a peat forming system (~700 µS) on the island, reflecting the high exposure of the site. Such conditions were chosen to ensure the record included both possible increases and decreases in salinity relative to modern conditions, while remaining within the zone of salinity conditions tolerated by testate amoebae (see Whittle et al. 2019; Chapter 4).

The core consisted of a single sequence sampled using a monolith tin. The monolith tin was inserted and cut free to avoid either compaction of the 'spongy' surface layers or contamination of the base of the core. Approximately 5 m of

Table 5.1 | Variables hypothesised to be linked to wind-blown salt-spray deposition on Bird Island. All variables were scaled between 0-1 prior to analysis in order to remove units and allow direct comparison.

Variable	Interpretation	Method/Source	Inputs used for calculation	Hypothesis
Coastal isolation index (weighted by fetch of the nearest down-wind coastline) (Fig. 5.2a)	Provides a proxy for the average downwind distance that a measurement point lies inland of the nearest coastline, while accounting for the relative exposure (or energy) of that coastline.	Coastal isolation was calculated by measuring the straight-line distance from points on a 25 x 25 m grid covering Bird Island, to the nearest coastline. Distance to the nearest coastline was measured for each direction at 22.5˚ intervals in order to calculate an average distance for each point. Since coastlines with greater fetch (exposure) will produce greater magnitudes of salt-spray, these values were also weighted by the fetch category of the nearest downwind coastline in each case.	1)Average wind direction 2)Coastline fetch category	H_1 Surface water conductivity levels will be lower in locations more isolated from the coast
Wind shelter coefficient (Fig. 5.2b)	Provides an indication of the sheltering effect of downwind topography on wind-speed, expressed as a fraction of wind-speed in an unobscured location (i.e. whether a location is sheltered by topography or exposed directly to passing airflow).	Wind shelter and Wind shelter coefficient$_{\text{westerly winds}}$ was calculated using the coefficient described by Ryan (1977) in the software package 'microclima' (Maclean et al. 2018) for R.	1)Topography (derived from the digital elevation model used for altitude) 2)Average wind direction	H_2 Surface water conductivity levels will be lower in locations sheltered from winds by surrounding topography
Wind shelter coefficient$_{\text{westerly winds}}$ (Fig. 5.2c)	Indicates the sheltering effect of topography on overland airflow for the prevailing wind direction on Bird Island (i.e. winds blowing west-to-east from the Westerly quadrant).		1)Topography (derived from the digital elevation model used for altitude) 2) Average frequency of winds from the westerly quadrant (247.5-292.5˚)	H_3 Surface water conductivity levels will be lower in locations sheltered from westerly winds by surrounding topography
Altitude (Fig.5.2d)	Height above sea level	5 m resolution digital elevation model provided by the British Antarctic Survey		H_4 Areas closer to sea-level will have higher surface water conductivity levels
Aspect (Fig. 5.2e)	Provides an indication of whether a location lies on a slope facing into or away from average wind conditions.	Using the digital elevation model a hill-shade model was calculated to simulate wind exposure by selecting a low (5˚ elevation angle and replacing sun azimuth with wind direction, in ArcGIS (Bricher et al. 2008). Calculations were repeated for each direction at 22.5˚ intervals in order to derive an average index of windward/leewardness.	1)Topography (derived from the digital elevation model used for altitude) 2) Average	H_5 Locations facing into the prevailing winds will have higher surface water conductivity levels

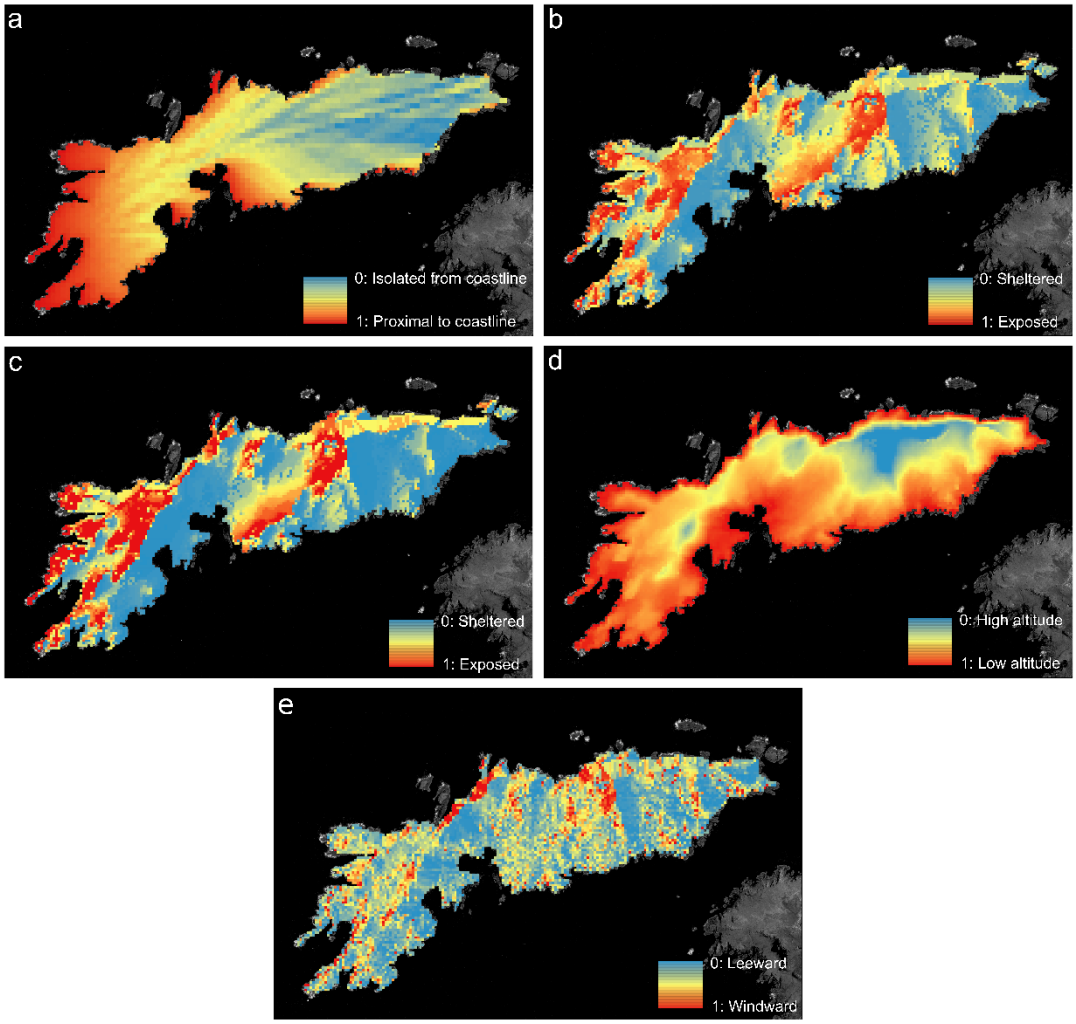

Figure 5.2 | Coastal isolation weighted by fetch of the nearest down-wind coastline (a), wind-shelter coefficient calculated based on 2012-2018 average wind-direction frequency (b), wind-shelter coefficient for winds from the westerly direction only (c), altitude (d) and aspect (e).

further peat sediment underlies the monolith (see Chapter 6). The monolith core was wrapped and transported to the Bird Island research station. Material was stored frozen prior to subsampling at 0.5 cm resolution.

Core chronology

The sequence was radiometrically dated with four ^{14}C dates from hand-picked samples of identifiable plant macrofossils taking particular care to avoid the inclusion of root material, mineral grains and fragments of fish and bird bones. Dates were calibrated using SHCAL 2013 terrestrial and post bomb calibration curves (Hogg, 2013; Hua et al. 2013), and a Bayesian age-depth model was generated using the BACON software package for R (Blaauw, 2010; Blaauw and Christen, 2011).

Expected accumulation rates were calculated from a ^{210}Pb profile (Supplementary Fig. 5.1) of the nearby core BIM5 (Fig. 5.1), which were used to compared and validate the age-depth model.

Isolation, enumeration and analysis of testate amoeba assemblages

To reconstruct changes in terrestrial salinity conditions through time we measured the productivity of the testate amoeba community at Morris Point (Whittle et al. 2019; Chapter 5), alongside alpha-diversity and Shannon-Weaver index. Testate amoebae were isolated from sub-samples collected from the core using a standard water based protocol for peatlands by wet sieving disaggregated material to retain particles in the size fraction 15-300 µm (Charman et al. 2000; Booth et al. 2010). Each sub-sample was gently homogenised and 1 cm^3 of material was used to obtain testate amoebae for analysis. Exotic *Lycopodium* pollen spore tablets (Lund University) were added to quantify the concentration (productivity) of testate amoebae within each sample (Stockmarr, 1971). Populations were enumerated by direct counting conducted at 200-400x magnification on a Zeiss AxioImager A1 light microscope, with the aim of reaching a total of 100 individuals per sample (Payne and Mitchell, 2009). For 8 samples this was not possible because of low test concentrations and a large quantity of obscuring mineral particles. Within these samples counts of >50 individuals were deemed sufficient. Identification of taxa was based on (Ogden and Hedley, 1980; Charman et al. 2000; Meisterfeld, 2002a; 2002b; Mazei and Tsyganov, 2006).

Taxa were filtered into 'minor' or 'major' groups by relative abundance and frequency, where major taxa were defined as those with >2% mean relative abundance, and presence within >25% of samples.

The size of the testate amoeba population corrected for changes in peat accumulation rate and variable compression of the peat through time (i.e. tests cm^2 $year^{-1}$) was calculated by dividing the concentration of tests, as derived from parallel counts with *Lycopodium* spores (cm^3), by the age-span of the sample indicated by the age-depth model. We do not convert the data to tests dry g $year^{-1}$ (Royles et al. 2016) as this leads to underestimation of concentrations in samples containing significant quantities of minerogenic material. To calculate population growth rate (tests $year^{-1}$) the change in the concentration of testate amoebae between two consecutive samples was divided by the corresponding age-span between them.

Shannon-Weaver diversity index (SWDI) (Shannon and Weaver, 1949) values were calculated in the R package 'vegan' (Oksanen et al. 2016) using the equation:

$$SWDI = -\sum_{i=1}^{S}\left(\frac{Xi}{Ni}\right) \times \ln\left(\frac{Xi}{Ni}\right)$$

Where X_i is the abundance of each taxon, N_i is the total number of tests present in the sample, and S is the species richness of the sample. SWDI provides a broad indication of the relative 'health' of the sampled community of testate amoebae and therefore the suitability of environmental conditions. For soil microorganism communities, values 0.5-1.5 generally characterize harsh and unfavourable conditions, 1.5-2.5 indicate intermediate conditions, and favourable conditions are represented by values >2.5 (Patterson and Kumar, 2002; Riveiros et al. 2007; Neville et al. 2010).

Faunistic zones within the testate amoeba relative abundance data were defined by constrained incremental sum of squares (CONISS) stratigraphically constrained cluster analysis, with broken stick analysis to identify the number of statistically significant groups, in the software packages 'vegan' (Oksanen et al. 2016) and 'rioja' for R (Juggins, 2015; R core development team, 2013). Correspondence analysis (CA) on centred relative percentage abundance testate amoeba data from the core was preformed using the R package 'vegan'.

The level of test preservation was estimated for individual taxa by recording the relative proportion of well-preserved to poorly-preserved specimens during counting. This method allows the identification of general trends in preservation, although it is not possible to quantify whether tests were completely lost through degradation. Poorly preserved specimens were defined as those exhibiting damage, such as cracks to the test, missing ornamentation, or a generally degraded appearance. We defined well-preserved taxa as those appearing similar to modern specimens at the surface. Example pictures of specimens included in each category are provided in Supplementary Fig. 5.2.

Peat properties

Changes in minerogenic deposition and carbon accumulation were also measured as possible wind-proxies. Bulk density and loss on ignition (LOI) were measured contiguously for each 0.5 cm sub-sample throughout the core. Dimensions of each

subsample was measured to derive volume (~2 cm^3) before freeze-drying and weighing to calculate bulk density (dry g cm^3). Organic matter content was determined from loss on ignition; the difference between the weight of dry samples and ash-residues remaining after incineration at 550°C for 4 hours (Chambers et al. 2011). Carbon content was assumed to be half of the organic matter content (Loisel et al. 2014). The rate of carbon accumulation (g C m^{-2} y^{-1}) was calculated by combining peat accumulation rate (derived from the age-depth model), with measured bulk density and Carbon content (Tolonen and Turunen, 1996). Mineral grains >2 mm in diameter were separated from LOI residues by wet sieving. Isolated grains were then freeze-dried and weighed allowing changes in grain abundance to be expressed as a percentage of the total dry sample weight.

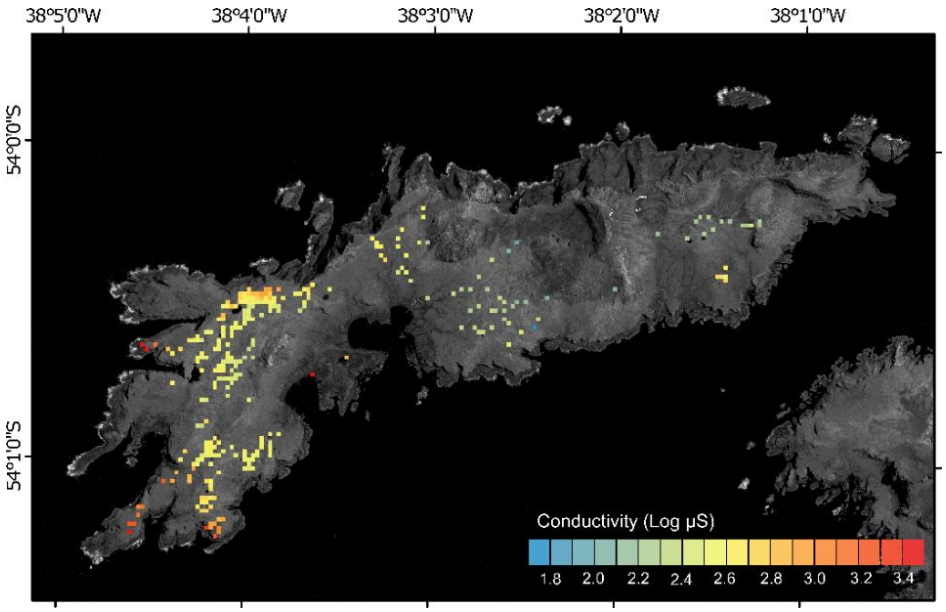

Figure 5.3 | Observed surface-water conductivity showing the broad gradient from west to east across Bird Island. Data presented on a 25x25 m grid, with values averaged where two or more measurements fell within the same grid square.

5.4. Results and Discussion

5.4.1. Determinants of salt-spray deposition on Bird Island

Measurements of electrical conductivity from 453 lakes, pools, streams or shallow soil-water recharge wells, indicate a broad spatial trend of salt-enrichment across Bird Island, with generally higher levels encountered on the west coast relative to the eastern portion of the island (Fig. 5.3). To investigate whether the determinants of this pattern were consistent with other sub-Antarctic islands, we tested hypothesised

relationships (Table 5.1) between landscape variables related to exposure and surface-water conductivity measurements (included in the training set).

Our data supports the acceptance of hypotheses H_1 and H_4 that surface-water conductivity conditions on Bird Island decline with increasing altitude and isolation from the coast (Pearson coefficient 0.77 and 0.68 respectively, both $p < 0.001$) (Fig. 5.4; Table 5.2). A weaker but statistically significant relationship (Pearson coefficient 0.23, $p = 0.05$) also supports hypothesis H_3, that greater topographic shelter from westerly winds is associated with lower levels of conductivity; however, we identified no statistically significant link between conductivity and shelter from average winds, leading to the rejection of H_2. Additionally, our data does not support hypothesis H_5 that conductivity levels are higher on more windward facing slopes, and instead indicates no overall relationship.

Comparison of a multi-linear regression and generalised additive model (GAM) for surface-water conductivity, including variables with a statistically significant (at the 0.05 level) link with conductivity measurements, indicated that coastal isolation and wind-shelter$_{\text{westerly winds}}$ were non-linear effects, and therefore were best represented in the GAM (Table 5.3). Performance of the GAM was good; comparison of observed and predicted training set values were very closely correlated and had a near 1:1 relationship (Fig. 5.5a; $R^2 = 0.84$, $p < 0.001$). Ground-truthing of values predicted by the GAM using the independent subset of surface observations, also showed very strong model performance (Person coefficient between observed and predicted values 0.66, $p = <0.001$; Fig. 5.5b). Overall the strong model performance indicates that together these variables are sufficient to account for much of the variability in surface-water conductivity conditions.

5.4.2. Model predicted surface water conductivity

The model predicts that the highest levels of terrestrial salinity occur directly inland of exposed coastlines (Fig. 5.6). Enrichment levels are comparatively lower for areas inland of the coastline in the eastern portion of the island. Western coasts are characterised by very steep gradients of salinity generally within 200-300 m of the coast. Lowest salinity levels coincide with areas of high altitude, which also correspond to the areas most isolated from the coastline (Fig. 5.2).

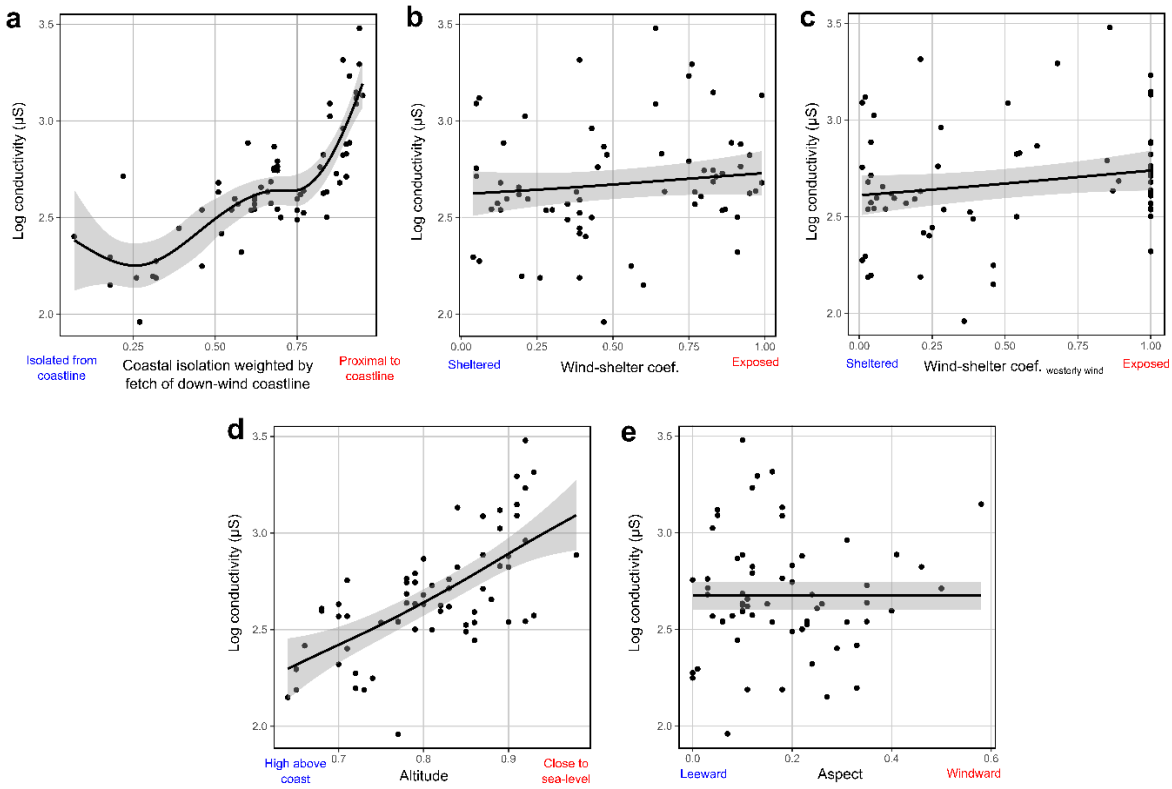

Figure 5.4 | Relationship between measurements of surface-water conductivity - a proxy for exposure to sea-spray deposition – and exposure-related landscape variables hypothesised to explain them. Coastal isolation index, weighted by fetch of the nearest down-wind coastline (a), provides a proxy for the distance that a measurement point lies inland of the nearest coastline, while accounting for the variable magnitude of salt-spray generated by that coastline. Wind-shelter coefficient (b), calculated using the R package 'microclima' (), indicates whether a measurement point lies on a windward or leeward facing slope, (i.e. facing into or away from passing airflow). Wind-shelter coefficient $_{\text{westerly wind}}$, was calculated similarly to (b) but weighted using the frequency of winds from westerly angles only (defined as 247.5˚ to 292.5˚). Altitude (d) was derived from a high-resolution (5m grid) digital elevation model supplied by the British Antarctic Survey. Aspect (e) indicating whether slopes predominantly face into or away from the prevailing wind. Surface-water conductivity measurements were Log transformed prior to analysis. Exposure-related landscape variables were scaled from 0-1 to remove original measurement units and allow for comparability. In each case, values closer to 1 are indicative of higher hypothesised exposure level. Values for all variables, excluding altitude, were weighted by prevailing wind conditions over Bird Island using the wind-speed, direction and frequency data for the period 2012-2018, as shown in Fig. 5.1b. Map outputs for each variable are shown in Fig. 5.2. Grey shaded areas indicate the 95% confidence interval.

Table 5.2 | Pearson correlation coefficients and p-values for exposure-related landscape variables and observed surface-water conductivity measurements.

Variable	Pearson coef.	p-value
Coastal isolation weighted by fetch of the nearest down-wind coastline	0.77	5.41 e^{-14}
Altitude	0.68	5.13 e^{-10}
Wind-shelter coefficient $_{\text{westerly wind}}$	0.23	0.05
Wind-shelter coefficient	0.19	0.12
Aspect	0.04	0.78

Table 5.3 | Comparison between multi-linear and GAM models used to predict surface-water conductivity conditions on Bird Island.

	Generalised cross validation (GCV)	AIC	R^2
Linear model	0.04	-31.45	0.63
GAM model	0.02	-67.86	0.81

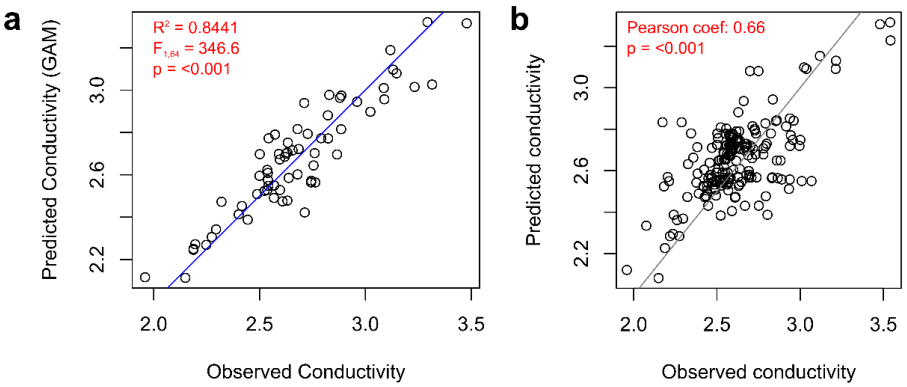

Figure 5.5 | a) Predicted and observed surface water conductivity from the generalized additive model for the training subset of observations. Blue line is a linear regression. b) Comparison between model predicted surface-water conductivity and separate ground-truthing observation subset. Grey line is a 1:1 line. Conductivity units are Log µS cm^{-1}.

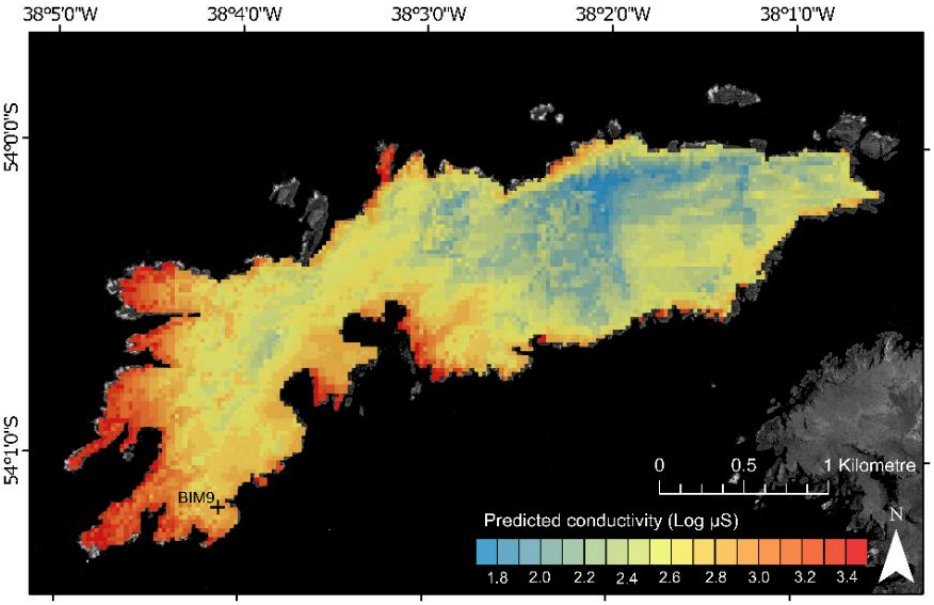

Figure 5.6 | Surface-water conductivity conditions on Bird Island predicted by the generalized additive model using exposure-related landscape variables (coastal isolation index, altitude, and $windshelter_{westerly\ wind}$). Data is presented on a 25 x 25 m grid.

5.4.3. Core chronology

The peat core collected within the area of high surface water salinity at Morris Point presents an unbroken record dating back to ~1920 CE, based on a model including all four ^{14}C dates, of which three were postbomb-peaks (Supplementary Fig. 5.3). Details of the individual ^{14}C dates are given in Supplementary Table 5.1. One date taken close to the base of the core (Beta-572832) was pre-bomb, and is indicated as a partial outlier by the age-depth model. Although the error range does overlap with the model, this date was considerably older than expected. Beyond contamination of the sample, one possible explanation is that the transition between the acrotelm and catotelm of the peatland lies close to this depth, resulting in a steep gradient from partially decayed recent material to relatively older and more compressed accumulations of organic matter. Mean peat accumulation throughout the record is ~3.4±0.16 mm $year^{-1}$, providing close to annual resolution for our peat core subsampled at 5 mm intervals.

5.4.4. Peat properties

Results of carbon accumulation, bulk density, loss on ignition and grain size analysis are summarised in Fig. 5.7. Average rates of carbon accumulation within the record are 149±38 g C m^2 $year^{-1}$. However, the short time period covered means that this rate represents only very recent accumulation which are generally considerably higher than long-term averages (Young et al. 2019). Southern Hemisphere peatlands are generally under-researched (Payne et al. 2019), meaning that little nearby data for near-surface peat accumulation is available with which to contextualise the record from Bird Island, although peatlands with similar climates in the northern latitudes could provide a meaningful comparison.

We measured loss on ignition, bulk density and the concentration of mineral grains >2 mm as indicators of minerogenic aerosol deposition in the core. Since they are inter-related measures (see Methods) all three indicators exhibit a consistent pattern of down-core variability. This consists of peat with higher density, lower loss on ignition (i.e. more minerogenic), and a greater concentration of mineral grains >2 mm in diameter prior to c.1950 CE. In the later record, density declines and loss on ignition increases, both pointing to increased organic matter content. No mineral grains >2 mm in diameter are present in the record after c.1970 CE.

5.4.5. Testate amoeba diversity in the core

Species diversity within the core is relatively poor, reflecting the southerly latitude of Bird Island (Chapter 2), high salt-enrichment levels (Chapter 3) and single environment type represented. Twenty taxa were observed; 17 identified to species level, two identified to genus level (*Arcella* spp.1 (see Supplementary note 5.1; Supplementary Fig. 5.4), *Pseudodifflugia* spp.) and one variety (var.) of *Phryganella acropodia* which was sub-divided owing to its atypical (smaller) size. Most taxa were relatively ubiquitous (present in many samples) and low in abundance; 18 had an average relative abundance <10%, yet 13 were present in more than 20% of samples. 'Major' taxa (defined as those with >2% mean relative abundance and presence within >25% of samples: Fig. 5.8) consisted of 9 species and together represented an average of 96.6% of the total testate amoeba population.

Populations of two taxa (*Phryganella acropodia* and *Difflugia pulex)* dominated assemblages. Present within every sample, specimens of *Phryganella acropodia* represented 33% of the total number of individuals observed, with an average concentration of 8221±7162 tests cm^{-2} $year^{-1}$ and average relative abundance of 29%. *Difflugia pulex* was the second most populous taxa with an average concentration of 5665±4516 tests cm^{-2} year-1 (23% of the total population) and an average relative abundance of 35%. *Centropyxis aerophila* was also present within every sample, but considerably less abundant; average 2016±1805 tests cm^{-2} $year^{-1}$ and with only 7.5% average relative abundance. Dominance of a small number of species and low overall diversity within the core results in a low average Shannon-Weaver index value (1.55±0.33). A complete list of observed taxa is shown in Table 5.4.

5.4.6. Preservation of testate amoebae

Our data suggests that there is no significant degradation of the tests produced by major taxa within the Morris Point core. Examination of the relationship between the percentage of well-preserved tests and core depth (time) indicated consistently high levels of preservation throughout the record. Indeed, a statistically significant relationship between preservation and depth was identified for just one taxon (*Cryptodifflugia sacculus;* Fig. 5.9). While this could suggest progressive degradation

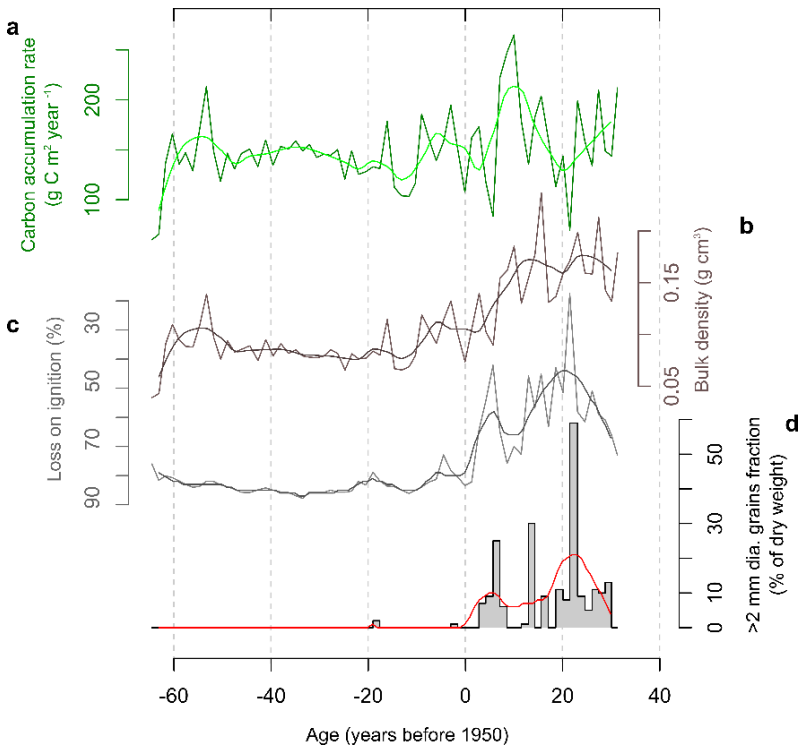

Figure 5.7 | Comparison of carbon accumulation rate (a), and bulk density (b), loss on ignition (c), and the percentage dry-weight of mineral grains >2 mm in diameter (d), which provide a proxy for minerogenic inputs into the peatland.

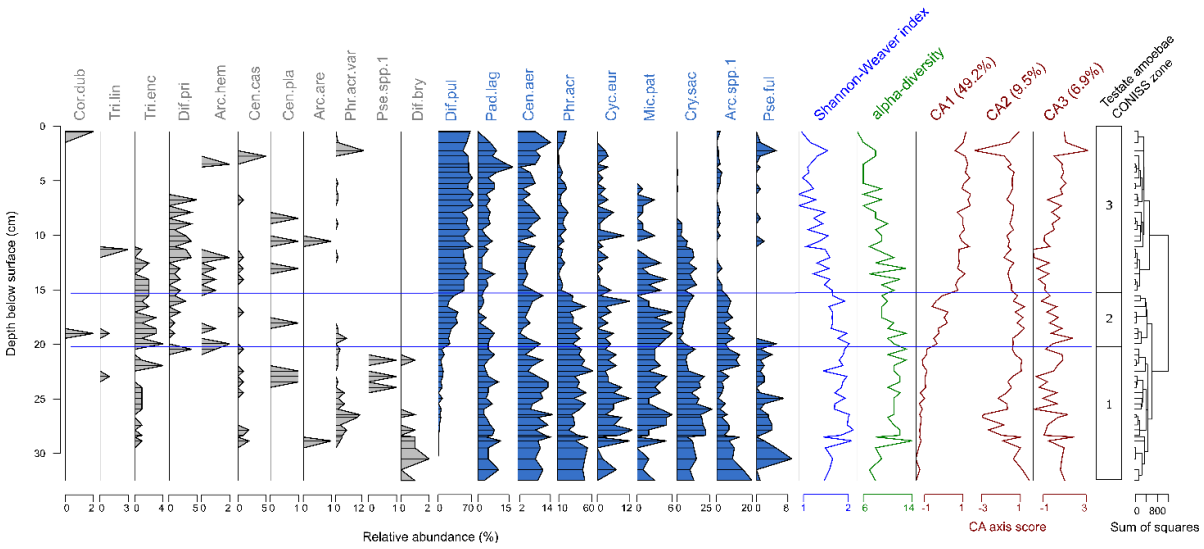

Figure 5.8 | Stratigraphy of testate amoeba species within core BIM9 at Morris Point, Bird Island showing the relative abundance of all encountered taxa. Minor taxa with low frequency and abundance (grey) were excluded from analysis (see Methods). Variation in the assemblages of the major species (blue) was summarised by correspondence analysis (CA), and was used to define significant faunistic zones 1-3. All encountered taxa were included in calculation of the Shannon-Weaver diversity index and alpha-diversity (the total number of species present at each level within the core). Full taxon names are provided in Table 5.4.

Table 5.4 | List of all taxa encountered within the Morris Point peat record.

ID code	Taxon name	Authority
Arc.are	*Arcella arenaria*	Greef 1866
Arc.hem	*Arcella hemisphaerica*	Perty 1852
Arc.spp.1	*Arcella* spp.1	
Cen.aer	*Centropyxis aerophila*	Deflandre 1929
Cen.cas	*Centropyxis cassis type*	(Wallich 1864) Deflandre 1929
Cen.pla	*Centropyxis platystoma* type	(Penard 1890) Deflandre 1929
Cor.dub	*Corythion dubium*	Taránek 1871
Cry.sac	*Cryptodifflugia sacculus*	Penard 1902
Cyc.eur	*Cyclopyxis eurystoma*	Deflandre 1929
Dif.bry	*Difflugia bryophila*	(Penard, 1902) Jung, 1942
Dif.pri	*Difflugia pristis* type	Penard 1902
Dif.pul	*Difflugia pulex*	Penard 1902
Mic.pat	*Microchlamys patella*	(Claparède and Lachmann 1859) Cockerell 1911
Pad.lag	*Padaungiella lageniformis*	(Penard 1902) Lara and Todorov 2012
Phr.acr	*Phryganella acropodia*	(Hertwig and Lesser 1874) Hopkinson 1909
Phr.acr.var	*Phryganella acropodia* var.	
Pse.ful	*Pseudodifflugia fulva*	Archer 1870
Pse.spp	*Pseudodifflugia* spp.	
Tr.en	*Trinema enchelys*	(Ehrenberg 1838) Leidy 1878
Tr.li	*Trinema lineare*	Penard 1890

of tests through time, the relationship appears to be primarily driven by the absence of *C. sacculus* in near surface layers which is unlikely to be related to preservation. Further, the percentage of well-preserved *C. sacculus* specimens does not drop below 70% throughout the record suggesting that preservation quality is sufficient until (at least) the base of the core. All major taxa were therefore retained within analysis.

5.4.7. Changes in the testate amoeba community through time

Average population sizes recorded in the Morris Point core during the last century were relatively large (24.8±15.7 k tests $cm^2\,yr^{-1}$). During the early part of the record, the size of populations, which we use as a proxy for their productivity, remains relatively constant and above the average for the period covered by the record (Fig. 5.10). After c.1970 CE productivity of the community begins to decline significantly, and continues to decline below average levels until present. These changes are also tracked by changes in the taxonomic composition of assemblages, summarised by correspondence analysis (Fig. 5.8) and CONISS zones (Fig. 5.10). CA axis 1, explains 49.2% of the variance in the relative abundance data and shows a significant shift centred on ~1965 CE (17 cm depth in the core; Fig. 5.8). This corresponds with the timing of the transition from CONISS faunistic zone 1 and 3 (1956-1970 CE),

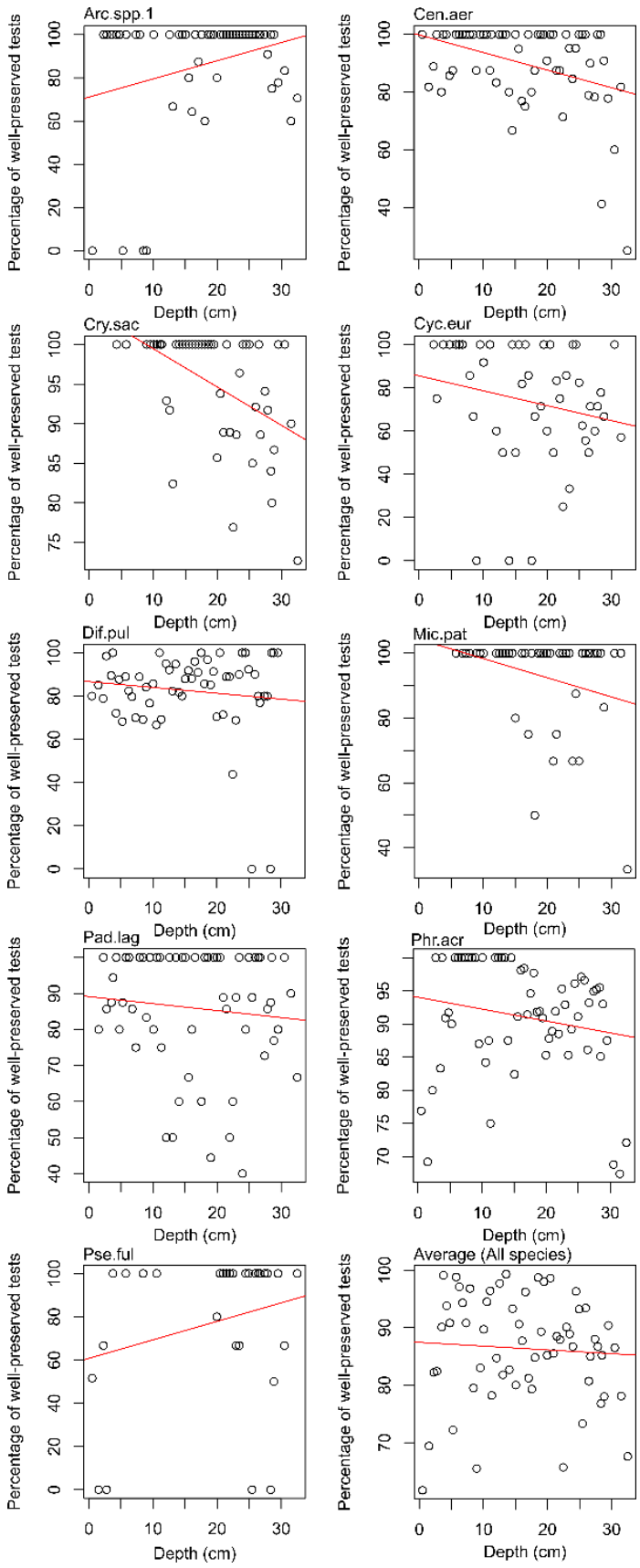

Figure 5.9 | Preservation of key testate amoebae, measured as a percentage of well-preserved (compared to poorly preserved) specimens within each level of the core. Full taxon names are given in Table 5.4.

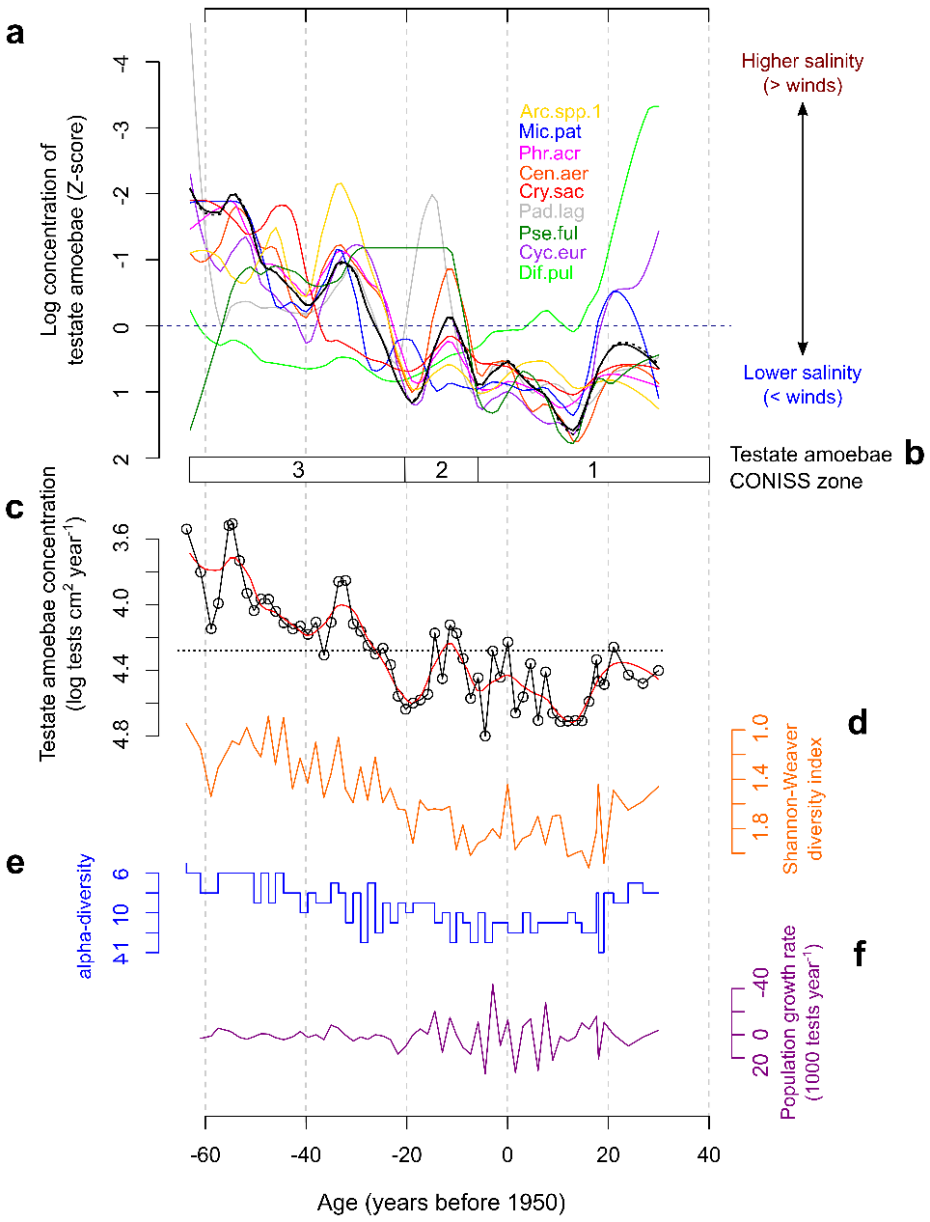

Figure 5.10 | Record of changes in the testate amoeba community within core BIM9 at Morris Point**.** a) Productivity of individual testate amoeba taxa (labelled coloured lines), of major taxa (solid black line) and for the community as a whole (dotted black line). Data represent a yearly interval LOESS smooth, scaled between 0-1 to account for differences in the overall abundance of individual species. b) Statistically significant (CONISS) faunistic zones, based of testate amoeba taxa relative abundance. c) Total productivity of major taxa expressed in original units. d) Shannon-Weaver diversity index. e) alpha-diversity and f) population growth rate. Full taxon names are given in Table 5.4.

Table 5.5 | Pearson correlation coefficients between down-core records of the productivity of individual (major) taxa. Full taxon names are given in Table 5.4. Significance levels denoted by *** <0.001, ** 0.01, and * 0.05.

	Dif.pul	Pad.lag	Cen.aer	Phr.acr	Cyc.eur	Mic.pat	Cry.sac	Arc.spp1	Pse.ful	Total of major taxa
Dif.pul	1	-0.30**	-0.37**	-0.38**	0.19	-0.07	-0.25*	-0.45**	-0.47***	-0.20
Pad.lag		1	0.61***	0.59***	0.55***	0.51***	0.53***	0.52***	0.40***	0.62***
Cen.aer			1	0.92***	0.77***	0.75***	0.77***	0.82***	0.60***	0.93***
Phr.acr				1	0.77***	0.86***	0.83***	0.90***	0.48***	0.95***
Cyc.eur					1	0.76***	0.60***	0.65***	0.37***	0.83***
Mic.pat						1	0.79***	0.71***	0.23*	0.90***
Cry.sac							1	0.65***	0.27**	0.87***
Arc.spp1								1	0.47***	0.81***
Pse.ful									1	0.36***
Total of major taxa										1

which reflect a shift from dominance of *Phryganella acropodia* (zone 1; 42% of assemblage) to *Difflugia pulex* (zone 3; 61% of assemblage).

The individual concentrations of all major taxa closely track the overall trend in productivity (Fig. 5.10: Table 5.5), except *Difflugia pulex* which does not correlate with the total population trend and instead reaches above average concentrations as the other taxa (and total) decline. After an initial rapid increase in concentration centred on ~1930 CE, *Difflugia pulex* also exhibits comparatively minor variability around average conditions (1930 CE to present), compared to many of the other species which undergo significant fluctuations towards the latter half of the record. *Pseudodifflugia fulva* populations track total concentration for the majority of the record, but increases towards significantly above average levels in the last decade. This possibly indicates that the taxon is opportunistic in exploiting the niche left by the decline in other species.

Shannon-Weaver diversity index (SWDI) values also track this pattern, indicating increasingly stressed environmental conditions after c.1970 CE compared to the earlier record (Patterson and Kumar, 2002). Alpha-diversity suggests that this increase in stress leads to the selective loss of certain species (Fig. 5.10). Growth rates indicate that larger populations of testate amoebae, during times of decreased environmental stress, are more dynamic. Higher magnitude fluctuations, indicating more dynamic populations, were present prior to c.1970 CE. After c.1970 CE populations stabilised, suggesting more gradual rates of change (Fig. 5.10).

5.4.8. Links between Southern Hemisphere westerly winds and patterns of terrestrial salinity on Bird Island

Similarly to other sub-Antarctic Islands, the patterns in surface-water salinity indicated by our observations and modelling on Bird Island can be explained by variable concentrations of oceanic salt-spray aerosols deposited by the prevailing westerly winds. Salt-spray aerosol particles are generated at sea from bubbles bursting in breaking waves (Grythe et al. 2014), as spume torn from wave crests, and by high-energy waves breaking against coastlines. Once suspended in the atmosphere, particles are carried inland by onshore winds (Gustafsson and Franzén, 2000). Because of their exposed position in the mid-Southern Ocean and SHW belt, islands in the sub-Antarctic receive large inputs of salt-spray, and consequently gradients of salinity aligned to the prevailing west-to-east airflow are a characteristic feature of their freshwater bodies (Buckney and Tyler, 1974; Vincke et al. 2004; Saunders et al. 2009; 2015; Whittle et al. 2019). On other sub-Antarctic islands where consistent patterns are observed, the oceanic source of the ions and cations responsible for creating the gradient has been demonstrated through the similarity of their proportions in freshwater lakes compared to seawater (i.e. Na > Mg > Ca > K > Cl > SO_4 > HCO_3) (Saunders et al. 2015; 2018).

The steep gradient of salinity along the exposed western coasts of Bird Island, and the strong relationships between salinity and the isolation of a particular location from the coast (coastal isolation index and altitude), relates to the production and transport of different sized salt-spray aerosol particles. Large salt-spray particles (1-10 μm in radius) are produced only by strong winds (Monahan et al. 1986) and have very short atmospheric lifetimes (Grythe et al. 2014). They are consequently deposited close to the coastline where they greatly increase surface water salinity. Smaller particles meanwhile contain less salts but can transport them for tens of kilometres inland (Grythe et al. 2014). As a result, concentrations of salt-spray decline exponentially with distance inland from the coast (Gustafsson and Franzén, 2000). This signature of salt-spray deposition has been recorded throughout the sub-Antarctic. In a survey of lakes on Campbell Island, Saunders et al. (2015) similarly identified exponential decline in conductivity with distance from the west coast and altitude. Exponential decline in salinity has been observed with distance inland across the surface of a peatland on the western flank of Marion Island (Whittle et al. 2019).

Because these patterns of salt-spray deposition are proportional to wind conditions, they can fluctuate over time. Stronger winds generate significantly larger quantities of sea-salt aerosols and carry them further. Indeed, measured concentrations of salt-spray aerosols on Bird Island have been shown to increase by a factor of three for wind-speeds above 10 ms^{-1} compared to below 8 ms^{-1} (Schmale et al. 2013). During such periods, the gradient of salt-enrichment would migrate further inland, increasing the salinity of coastal terrestrial ecosystems, and return coastward with the onset of weaker winds.

While in this study we identified the coastal isolation index and altitude as the strongest determinates of present-day salt-enrichment levels, topographic windshelter from the westerly winds was also identified as a statistically significant control of salinity on Bird Island. However, shelter from average wind conditions was not significant. This implies that spray carried by the westerly winds is a key source of conductivity into the islands terrestrial ecosystems while winds from other directions are likely responsible for deposition of much lower quantities of spray. Contrary to expectation, we did not identify a significant relationship between conductivity and slope aspect.

It can be summarised that the relationship between salt-spray inputs and westerly wind conditions on Bird Island is consistent with other islands in the sub-Antarctic (i.e. concentrations of salt-spray deposited into terrestrial archives are proportional to westerly wind intensity). This indicates that like other locations, changes in salinity recorded by terrestrial archives on Bird Island are proportional to westerly wind-intensity.

5.4.9. Temporal stability of terrestrial salinity

Measurements included in the training set used to develop the model for surface-water conductivity were collected over a period of five-weeks between January and March 2017. An extended period was required to collect a sufficient number of observations from locations across the island, however this meant that it was not possible to control against natural changes in surface-water conductivity conditions between measurements. For example, short-term fluctuations in evaporation rates, precipitation events or storms occurred during the measurement period and are expected to alter surface-water conductivity conditions. The strong performance and predictive power of the model that was based on this data, therefore implies that the

pattern of salinity develops over time and remains temporally stable. If the pattern were not temporally stable, and deviated strongly from average conditions because of these perturbations, the resultant 'noise' in the training set would be expected to produce a model with poor predictive power. It is therefore possible to conclude that the surface-water conductivity conditions observed and predicted by the model, reflect longer-term average conditions that do not change significantly in response to one off events and/or quickly return to average conditions after perturbations. This is an important consideration for the palaeo-environmental interpretation of SHW records derived from changes in terrestrial salinity. Unfortunately, no systematic studies have conducted monitoring to investigate how the salinity of surface-water varies in response to one-off events, such as storms, precipitation or evaporation. While we provide evidence for a long-term link between surface-water salinity and wind conditions, monitoring in the future would be useful to better understand this relationship at shorter temporal-scales, for example during the spring melt season.

5.4.10. Response of peatland surface-water conductivity to salt-spray deposition

Mean surface-water conductivity values on Bird Island were lower than on other sub-Antarctic islands. For lakes and pools >5 m^2 on Bird Island the average recorded conductivity was 411 µS, compared to 1300 µS and 527 µS, for lakes on Campbell and Macquarie Islands respectively (Suanders et al. 2009; 2015). Maximum recorded values were significantly lower; 785 µS compared to 4810 µS and 1571 µS on Campbell and Macquarie Islands. Conductivity values for samples from terrestrial locations (including pore-water recharge), and small surface pools or puddles (<5 m^2 in area), were also lower on Bird Island than a comparable record from a peatland on Marion Island (Whittle et al. 2019); average (484 µS compared to 1543 µS) and maximum (3487 µS and 11670 µS), respectively.

These differences in average conductivity values could indicate that Bird Island receives lower concentrations of wind-blown salt-spray than other islands, possibly as a result of generally lower exposure to the westerly winds. Unlike the other sub-Antarctic Islands where comparable observations have been made, Bird Island is partially protected to the west by another smaller island, which possibly provides some protection from the highest-energy waves. Average yearly wind-speeds are also greater in the Indian Ocean sector of the sub-Antarctic compared to the Atlantic (Fig. 5.1). However, caution must be taken in drawing this interpretation. Sampling

distribution could also strongly influence average conductivity values if locations closer or further from coast were sampled between surveys. This is true of Marion Island, where records are currently only available from very close to the west coast (Whittle et al. 2019), whereas sampling on Bird Island fully covered lower salinity conditions (Fig. 5.3). Changes in dilution caused by variable rates of precipitation, evaporation and lake volumes between locations, or local factors such as proximity to sea-bird or seal colonies may also influence average values, irrespective of differences in the magnitude of salt-spray deposition (Saunders et al. 2015).

Within Bird Island, the conductivity of terrestrial environments was generally higher than in lakes and pools, both in terms of average and maximum recorded values (Table 5.6). This difference is likely due to the larger volume of water available for dilution of salt-spray inputs in lakes and pools. As a result, it follows that records of salinity preserved by terrestrial environments are likely to be sensitive to smaller changes in salt-spray deposition (i.e. for the same concentration of wind-blown salt-spray inputs, conductivity of terrestrial environments will alter more than pools and lakes). Irrespective of wind-driven salt-spray inputs, changes in the balance between precipitation (potentially diluting the conductivity signal) and evaporation (potentially increasing conductivity) could also have an impact on salinity conditions. However, meteorological measurements on Macquarie Island suggest that this is of secondary importance since sea-spray precipitation alone deposits 2433-220 kg NaCl ha^{-1} yr^{-1} (Mallis, 1988), with periods of higher rainfall, which are associated with stronger winds, contributing to elevated (not reduced) conductivity levels (Saunders et al. 2018).

Table 5.6 | Summary of observed conductivity conditions in different terrestrial ecosystems on Bird Island.

Environment type	Mean conductivity (µS)	Max conductivity (µS)	Min conductivity (µS)	Number of observations
Lake or pool (>5 m^2 in area)	411±158	785	177	16
Flowing water	420±242	1898	118	56
Terrestrial (including pore-water recharge), and small surface pools or puddles (<5 m^2 in area)	484±386	3487	91	381

5.4.11. Testate amoeba community at Morris Point

Our work provides the first report of testate amoebae from Bird Island, and adds to the data available for nearby South Georgia as a whole (Richters, 1908; Sandon and Cutler, 1924; Smith 1982; Smith and Headland, 1983; Beyens et al. 1995; Vincke et al. 2006). Although proposed by other authors (e.g. Vincke et al. (2004)), it is also the first study to examine down-core assemblages within a dated sediment record from the sub-Antarctic region. Unfortunately, a full survey of the islands fauna was beyond the scope of this project. However, of the twenty taxa we identified in the core, four were not previously reported on South Georgia. These first observations were *Cryptodifflugia sacculus* and *Difflugia pristis*, in addition to two taxa not identified to species level, which together raise the total known diversity of South Georgia to 86. Taxonomic uncertainty for the testate amoeba fauna of South Georgia remains high with 18% of the currently reported taxa not identified to species level (Chapter 2). It is possible that one of the unidentified taxa in this study (*Arcella* spp. 1) may have been encountered previously, since Vincke et al. (2006) report several unidentified taxa from the genus *Arcella* in a survey of mosses at Stromness Bay. In the absence of published descriptions or photographs, it is not possible to confirm whether these specimens were similar in morphology to those on Bird Island. Clearly further taxonomic refinement will be required before a true diversity total can be determined.

Throughout the record the dominance of a small number of species, generally low diversity and Shannon-Weaver diversity index score (1.55±0.33) suggests sustained and relatively sub-optimal environmental conditions for testate amoeba populations (Patterson and Kumar, 2002), most likely due to high concentrations of salt-spray. Nevertheless, these conditions were significantly more suitable than those experienced by moss-dwelling communities further south in the Maritime-Antarctic (Signy Island: SWDI 1.18±0.5) and the Antarctic Peninsula where annual temperatures are significantly lower (Chapter 2), and SWDI values are consistently below 1 (Royles et al. 2016). Consequently, the testate amoeba community at Morris Point was comparatively productive, with average population sizes recorded during the last century (24,756±15,657 tests $cm^2\ yr^{-1}$) in excess of an order of magnitude larger than over a similar time period on the Antarctic Peninsula (Amesbury et al. 2017).

The high abundance of *Phryganella acropodia* observed within the community at Morris Point is consistent with Smith (1982), who suggested that it is the most

dominant taxon in terrestrial environments on South Georgia, in contrast with other sub-Antarctic islands. Similarly high abundances have also been observed in the fauna of Signy Island, where 'spectacular' blooms in numbers of *P. acropodia* are known to coincide with the onset of the snow-melt (Smith, 1978). While no definitive seasonal fluctuations were identified in populations of abundant species inhabiting a variety of terrestrial substrates on South Georgia, all (including *P. acropodia*) underwent blooms in the spring months (Smith and Headland, 1983). This is a particularly important consideration for palaeo-ecological interpretations as it suggests that spring may be a particularly important part of the year for determining the yearly productivity of the community.

5.4.12. Reconstruction of terrestrial salinity conditions and their relationship with Southern Hemisphere westerly winds

Having confirmed the link between wind conditions and the salinity of terrestrial ecosystems, we developed a reconstruction of recent changes in the SHW, primarily using the productivity of testate amoeba within the Morris Point peat record as a proxy for changes in surface-water salinity conditions through time. This record which dated to ~1920 CE, substantially pre-dating continuous observational records over the South Atlantic, revealed two distinct phases:

1920 CE – 1970 CE: Testate amoeba productivity levels indicate that consistently below average concentrations of salt-spray (for the last century) were deposited at Morris Point during the period c.1920-1970 CE (Fig. 5.10). In the absence of significant salt-stress, communities were both larger and more diverse than in any other part of the record. Population sizes were also more dynamic, with high-magnitude fluctuations in growth rate suggesting short periods of rapid population expansion and contraction. These fluctuations in growth rate were likely driven by environmental conditions un-related to salinity, for example, the length of the ice-free growing season, mean annual temperature, or water availability (Royles et al. 2013; 2016; Amesbury et al. 2017). Although not an established proxy for salinity, evidence from a northern temperate peatland suggests that rates of peatland carbon accumulation are proportional to oceanic salt-deposition, with generally lower levels of accumulation recorded under more saline conditions (Whittle and Gallego-Sala, 2016). On Bird Island, the highest and most variable rates of accumulation were measured between 1920-1970 CE, consistent with the assertion that less saline conditions prevailed during this period. Peat accumulation is the product of the

balance between inputs via the production of organic matter versus losses, predominantly by decomposition within the peat matrix. The productivity of testate amoeba populations throughout this period suggest that decomposition rates were high, and so it is possible that reduced salt-stress was conducive to greater plant productivity.

1970 CE -present: After c. 1970 CE populations of testate amoebae contracted in size and became less diverse as salinity increased to consistently above average levels. Statistically significant reductions in mean testate amoeba productivity levels, identified by changepoint analysis, occurred at 1979 and 2003 CE. The magnitude of growth rate fluctuations declined as productivity fell reflecting the increasing role of salinity as the primary limiting factor to productivity (Chapter 3). Decreasing productivity after c. 1970 CE was also accompanied by a significant shift in the taxonomic composition of assemblages which was characterised by the replacement of *Phryganella acropodia* with *Difflugia pulex* as the dominant taxon. In contrast to other taxa, the productivity of *Difflugia pulex* throughout the record, does not correlate with the productivity of the overall community. In a review of zonation of taxa within salt-marshes on the North American East Coast, *D. pulex* was observed to be capable of tolerating tidal flooding, and can therefore be considered more resistant to moderate levels of salinity than other taxa (Gehrels et al. 2006). Consequently, its increasing relative abundance after 1970 CE is consistent with the interpretation of more saline conditions. Concentrations of salt-spray deposition have continued to increase until the present-day, apart from an apparent short-term reversion in c. 2010 CE (Fig. 5.10). Our record therefore implies that the levels of salt-spray currently deposited at Morris Point are without precedent during the last century, and therefore the current strength of winds over Bird Island are also unprecedented.

In order to test the salinity reconstruction derived from the testate amoeba community we measured changes in the deposition of minerogenic aerosols. Changes in minerogenic inputs have been used alongside biological proxies in previous reconstructions of SHW, where it is assumed that rates of deposition increase during periods of stronger winds (Björck et al. 2012; Saunders et al. 2018; Perren et al. 2020)). While correlation between minerogenic inputs and the productivity of the testate amoeba community was identified, it was in the direction contrary to expectation, with increased inputs coinciding with periods of lower inferred salinity levels, and therefore weaker winds (Table 5.7).

Table 5.7 | Pearson correlation coefficients and p-values for the productivity total of major testate amoeba taxa, compared to other potential palaeo-wind proxies within the Morris Point (BIM9) core (see Fig. 5.7).

	Pearson	p-value
Bulk density	0.4907	$5.13e^{-7}$
LOI	-0.4997	$2.94e^{-7}$
>2mm grains	0.4006	$6.31e^{-5}$

Despite the apparent lack of agreement with minerogenic proxies, the record of terrestrial salinity conditions inferred from testate amoeba productivity shows significant positive correlation with regional observational records of wind intensity, the SAM index and other high-resolution reconstructions of wind-intensity (Fig. 5.11; Table 5.8). Of these records the strongest relationship was identified with the observational record of wind-strength from Macquarie Island (Adams, 2009) (Pearson correlation coefficient = 0.79, $p<0.001$). Both islands lie at the same latitude (54˚S), but are separated by almost 180˚ of longitude. The strong consistency of the records therefore suggest that wind-intensities have been zonally symmetric during the past century. Very strong correlations were also recorded with the Marshall SAM index, which records the pressure gradient between Antarctica and the mid-latitudes (Pearson correlation coefficient = 0.76, $p<0.001$). This is consistent with a poleward expansion of the wind-belt during SAM positive phases, and weakening during SAM negative phases. Taken together these correlations suggest that salinity conditions on Bird Island, reconstructed from testate amoeba productivity levels, accurately represent changing wind conditions over the Southern Ocean.

Lower correlation was observed with diatom inferred conductivity values on Marion Island (Perren et al. 2020). While these proxies are directly comparable, the lower correlation between the records is the result of the 9˚ difference in latitude between the sites. Because the core SHW has moved South in recent decades, the Marion Island record charts its transit past the island since c.1965 CE. With the core belt now lying south of Marion Island, wind conditions have declined in recent years, while the increasing alignment of the winds to Bird Island further South result in continued increasing winds.

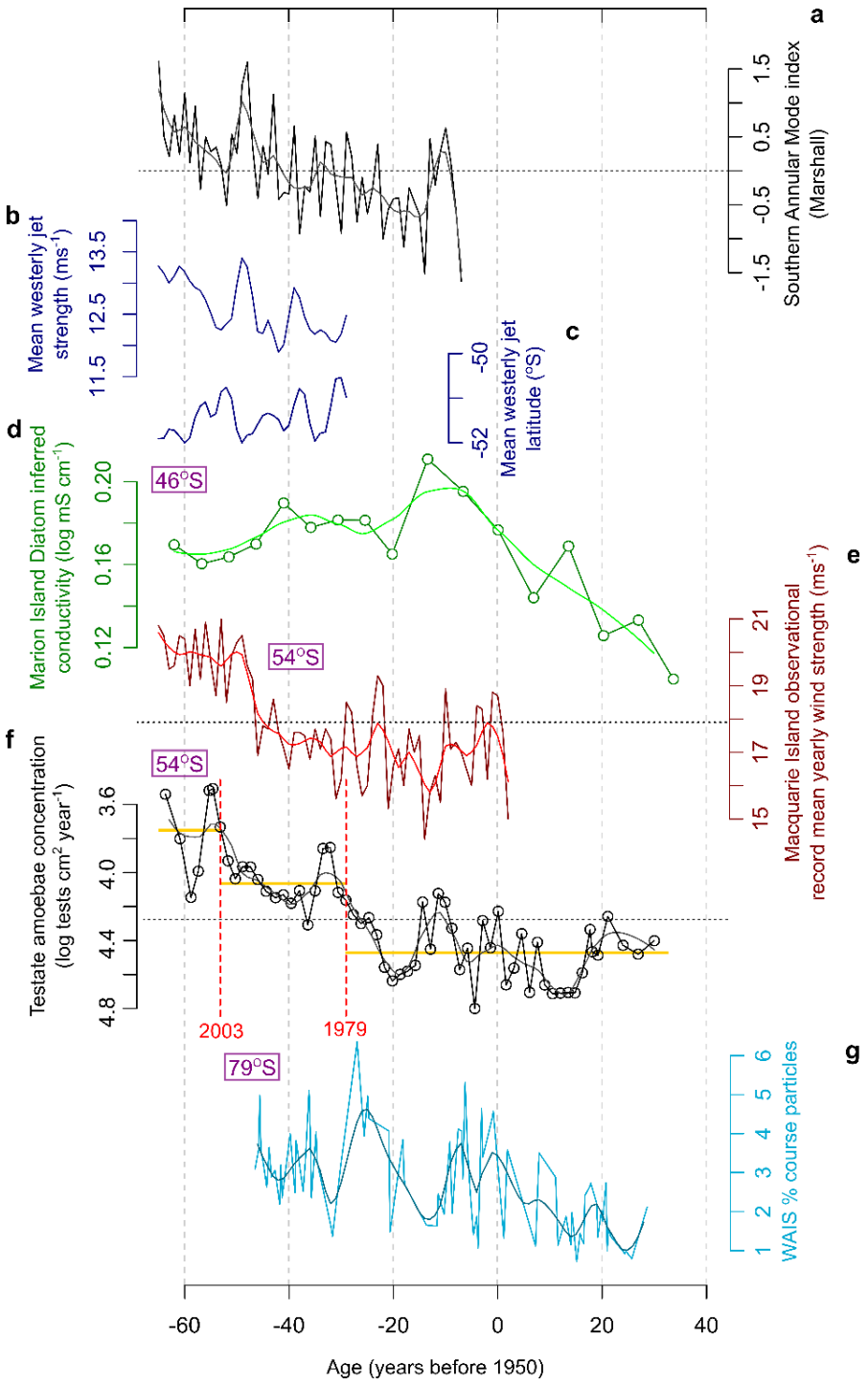

Figure 5.11 | Comparison of Morris Point wind-reconstruction, derived from testate amoeba productivity, with selected observational, modelling and palaeo data from close to the core-belt of the Southern Hemisphere Westerly Winds. a) Southern Annular Mode Index (Marshall, 2003), b) Mean westerly wind strength within the core belt region, and c) mean westerly jet latitudinal position, both derived from ERA interim data (Bracegirdle, 2018), d) Marion Island lake Diatom inferred conductivity, a proxy for deposition of wind-blown salt-spray (Perren et al. 2020). e) Yearly averaged wind-strength recorded by the Macquarie Island weather station for the period 1948-2018 CE (downloaded from https://legacy.bas.ac.uk/met/READER/surface/stationwind.html). f) Total productivity of testate amoebae at Morris Point, Bird Island. g) West Antarctic Ice-sheet course particle size (Koffman et al. 2014). Purple boxes indicate the latitudinal position of point records.

Table 5.8 | Pearson correlation coefficients and p-values for the palaeo-wind reconstruction derived from testate amoeba productivity within the Morris Point (BIM9) core, compared with regional observational, modelling and palaeo data (see Fig. 5.11). All data LOESS (2nd order polynomial) smoothed to consistent yearly intervals.

Dataset	Reference	Pearson correlation coef.	p-value	Period of record (years before 1950)
Mean westerly wind jet strength.	(Bracegirdle, 2018)	-0.4051	0.0158	-63 to -29
Mean westerly jet location.	(Bracegirdle, 2018)	0.0935	0.5932	-63 to -29
Marion Island diatom inferred conductivity.	(Perren *et al.*, 2020)	-0.1568	0.1334	-62 to 30
Macquarie Island observational record - Wind strength	(BAS reader, 2020)	-0.7851	$6.04e^{-15}$	-63 to 2
Southern Annular Mode index.	(Marshall, 2003)	-0.7642	$4.63e^{-12}$	-63 to -7
West Antarctic Ice sheet (WAIS) course particle percentage.	(Koffman *et al.*, 2014)	-0.3105	0.0067	-46 to 28

The observed decline in the productivity of the testate amoeba community during the past c. 50 years is directly opposed to widespread increases in productivity over the same period along the Antarctic Peninsula (Amesbury et al. 2017). Here significant increases in the favourability of conditions for photosynthesis, moss-bank growth rates and microbial productivity present a picture of a coherent biological response to increasing temperature (Amesbury et al. 2017). Similar temperature changes have occurred on South Georgia (Thomas et al. 2018), and throughout the wider sub-Antarctic (Pendlebury and Barnes-Keoghan, 2007; Le Roux and McGeoch, 2008). The fact that the productivity of testate amoebae on Bird Island does not track this increase provides further evidence that productivity changes relate primarily to salinity conditions caused by wind-blown salt-deposition.

5.4.13. Implications for Southern Hemisphere westerly wind reconstructions

Prior to our study, the suitability of preservation conditions for testate amoebae in sub-Antarctic peatlands was unknown. Degradation or compete dissolution of tests incorporated at the peatland surface from the long-term record is a well-known issue in testate amoeba palaeoecology (e.g. Swindles and Roe, 2007), but often remains unquantified. Preferential preservation of taxa poses a problem for species-based transfer function approaches (Swindles and Roe, 2007; Mitchell et al. 2008), but is equally pertinent for reliable interpretation of testate amoeba productivity, which relies on capturing the actual number of tests belonging to each taxa that once populated the surface. We show that tests are generally very well preserved in the surface layers of the peat record at Morris Point, and establish a method to quantify preservation quality in future studies. This framework can be used to permit more rigorous assessment of preservation over longer timescales in the future. In cases where

poorly preserving taxa are identified, filtering them from the dataset would become necessary.

The reason for the apparent contradiction between reconstructed terrestrial salinity, observational wind records, and minerogenic deposition is unclear although several factors are possible. Meteorological measurements on other sub-Antarctic islands indicate a positive correlation between wind-strength and precipitation, meaning that periods of weaker winds (i.e. lower inferred salinity) on Bird Island are likely to be generally drier. It is possible that drier conditions could promote generation and reworking of dust resulting in larger fluxes into the core. Because the coring site at Morris Point is not an ombrotrophic peatland and lies in the base of a small valley, it receives run-off from a small catchment. As a result, instead of exogenous dust, influx of minerogenic material could also reflect periods of variable erosional processes within the catchment, which are not necessarily linked to wind conditions.

There is also a disparity in the type of wind record produced by the different proxies, and so the signals they provide are not necessarily directly comparable. The productivity of testate amoebae provides a record of longer-term (multi-year) average wind conditions, whereas minerogenic proxies are biased to one-off periods of high-intensity wind-speeds (or storm conditions). Testate amoeba populations are known for their rapid response to abiotic stimuli (Charman, 2001; Mitchell et al. 2008). However, in communities exposed to salinization, the capability of at least some taxa to resist short periods of unfavourable conditions by forming pre-cysts has been demonstrated (Wanner et al. 2020). Assuming that more favourable conditions quickly return, these taxa can survive and rapidly resume high-levels of productivity (Wanner et al. 2020). If conditions in an area become too harsh for any individuals to survive, re-colonisation from healthy populations in nearby areas less affected by the environmental change can also occur rapidly after the onset of more suitable conditions. Further, the results presented in this study indicate that the terrestrial salinity conditions, to which testate amoeba respond, are temporally stable (i.e. they are not significantly altered by one-off events). Taken together, this implies that, if average salinity levels were quickly re-established, little evidence of short-lived fluctuations in salinity will be evident in the record provided by testate amoebae.

Meanwhile changes in minerogenic inputs, especially larger grains >2 mm in diameter, are more likely to reflect changes in the frequency of strong winds, which are required to entrain and transport them. Changes in the concentration of inputs

are therefore more likely to reflect storm deposits, or short-term increases in wind strength. The availability of minerogenic material in proximity to the coring site may also play a spurious role in determining the quantity deposited. While fluxes of minerogenic material were successfully used to reconstruct storminess by Orme et al. (2015), highly unique attributes of the archive were required, namely lying downwind of a substantial dune system which provided a consistent grain source. This is not the case on Bird Island, where the coastline consists of a steep rocky cliff directly into the sea. The availability of downwind dust deposits is therefore likely to be temporally variable. This alludes to a major benefit of proxies relating to terrestrial salinity conditions over minerogenic proxies, where the oceanic source of salt-spray aerosols is constant and unlimited. Consequently, while in the correct setting, minerogenic aerosol deposition can provide valuable insights into changes in wind-intensity, records should be interpreted cautiously where the setting is not ideal. Our data also does not support the assumption that higher (average) wind-speeds lead to increased deposition of >2 mm grains. While the deposition of these larger grains may be more indicative of very high intensity storm events, as with minerogenic material more generally deposition is likely to be largely related to stochastic variability, making the signal they provide difficult to interpret. Future applications of the testate amoeba based proxy that we developed would benefit from comparison with independent records that are complimentary to the signal provided (i.e. proxies that track changes in the deposition of salt-spray aerosols, for example geochemical analysis of Bromine or Calcium (Turner et al. 2019; Saunders et al. 2018).

5.5. Conclusion

Similarly to freshwater lakes on other sub-Antarctic islands, our data shows that the salinity of terrestrial ecosystems on Bird Island is proportional to present day westerly wind conditions. Consequently, the concentration of salt-spray received at any particular location is a function primarily of isolation from the coast and altitude, and to a lesser degree exposure to westerly airflow. The record we developed from the peatland at Morris Point represents the first reconstruction of testate amoeba ecology within a dated peat record from the sub-Antarctic. Using this record we provide the first highly resolved (decadal) proxy-record of increased SHW over the South Atlantic during recent decades, substantially extending the observational record from the region. However, during the same time period changes in proxies relating to minerogenic aerosol deposition indicate contradictory wind-conditions compared to both testate amoeba productivity and the observational record. This suggests that

minerogenic proxies from Bird Island, and others that are applied outside their ideal settings, must be interpreted cautiously, and cross-examined as part of a multi-proxy analysis of wider palaeoenvironmental conditions. We suggest that the response of testate amoeba community productivity to changing surface-water salinity conditions can be used as a reliable proxy with which to reconstruct wind-changes beyond the instrumental record, assuming that levels of test preservation remain consistently high.

5.6. Supplementary Information

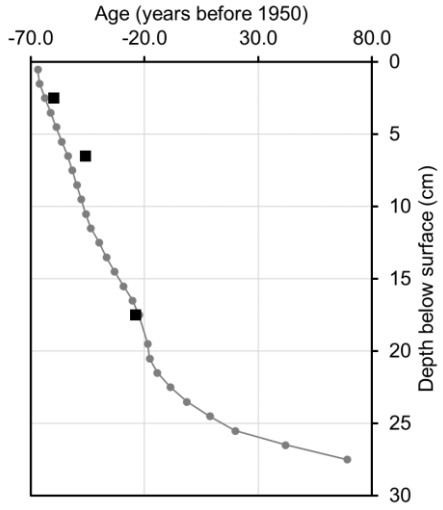

Supplementary Figure 5.1 | Comparison between the constant rate of supply model for ^{210}Pb dates from the BIM5 peat core (grey) (Taylor, 2020), and calibrated post-bomb ^{14}C mean dates from the BIM9 (Morris Point) core used in this study (black squares).

Supplementary Figure 5.2 | Comparison of specimens defined as poorly-preserved (left) and well-preserved (right). Microphotographs reproduced from Taylor (2020).

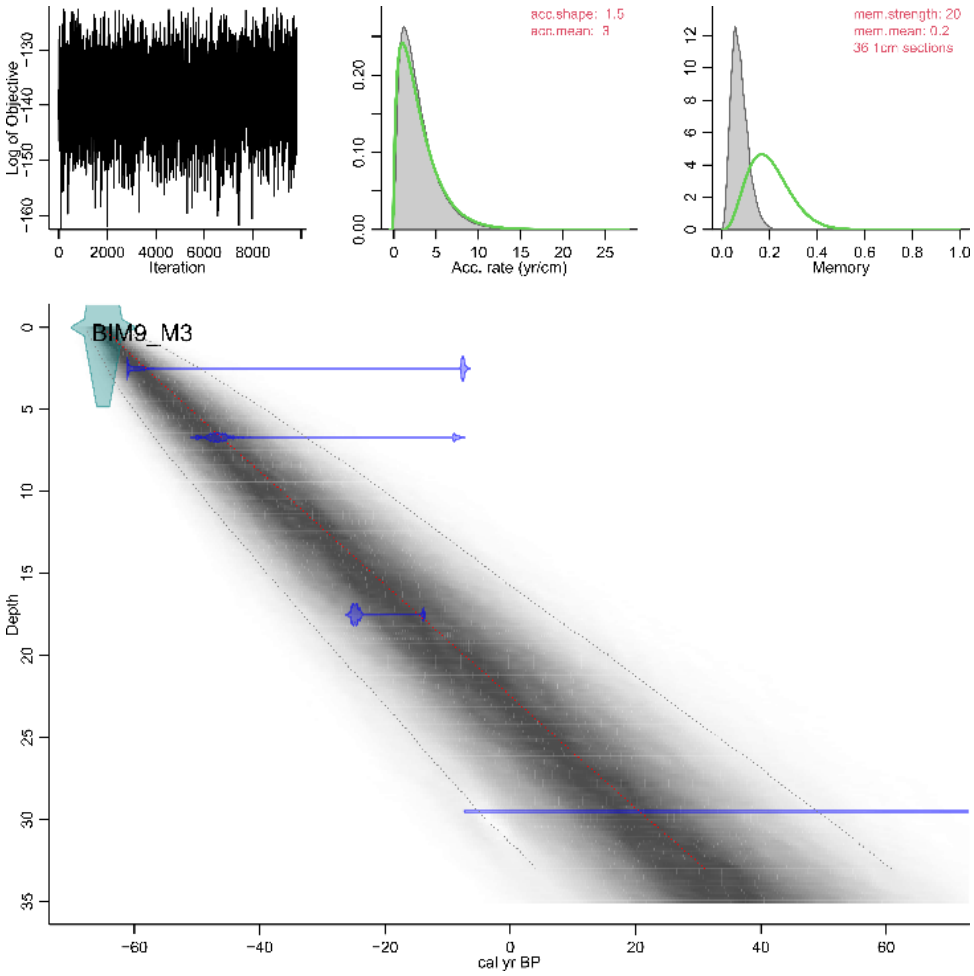

Supplementary Figure 5.3 | Age-depth model constructed for the peat core at Morris Point used in this study.

Supplementary Figure 5.4 | Microphotographs of three specimens of unidentified taxa (*Arcella* spp.1). Arrows indicate the position of the aperture.

Supplementary note 5.1: We tentatively ascribe one of the taxa not identified to species level to the genus *Arcella* owing to its hemispheric test and wide, centralised and invaginated aperture. Interestingly, the test is broadly similar in composition (particles) and diameter to *Phryganella acropodia,* but with an aperture pressed against the inside (concave) face, resulting in a saucer-lake (and not spherical) shape, which leaves little space for cell inside (Supplementary Fig. 5.4). To the best of our knowledge no records of specimens with a similar morphology have been reported on nearby South Georgia, or the wider Southern Ocean region (Chapter 2), however the lack of microphotographs of several unidentified taxa from South Georgia (Vincke et al. 2006) make this impossible to confirm. Both *Arcella* spp.1 and *P. acropodia* are frequent and abundant within the core, suggesting broadly similar ecological preferences. It may therefore be hypothesised that the taxon represents specimens of *P. acropodia* that have been inverted (essentially turned inside-out) by an environmental stimulus, perhaps in the process of encystment or loss of osmotic pressure. However, this theory is somewhat contradicted by the often pristine appearance of the *Arcella* spp.1 tests, something that would be unlikely if they had been originally secreted with a different shell morphology and undergone such a change. Unfortunately, we did not observe any specimens during a reproductive stage, which could have confirmed this. While we make a designation for the palaeoclimatic aims of this paper, further morphological work should focus on whether this taxon represents a variety or damaged specimens of *P. acropodia,* a separate previously document but obscure species, or a novel species that is possibly endemic to Bird Island.

Supplementary Table 5.1 | Radiocarbon data from the Morris Point peat core used in this study.

ID number	ID/Number of analysing lab	Core section code	Depth in core (cm)	Description of material dated	Pre-treatment	δ13C (‰) ± 0.1 (1σ)	Measured 14C age (14C a BP)	95.4% range			Median	Mean	±	1σ
BIM9_3	Beta-572829	BIM9	2.5	Plant material	Acid/Alkali/ Acid	-28.7	104.84 ± 0.39 pMC	-6	-	…	-60	-38	±	26
BIM9_7	Beta-572830	BIM9	6.5	Plant material	Acid/Alkali/ Acid	-29.6	111.58 ± 0.42 pMC	-48	-	-8	-46	-43	±	11
BIM9_18	Beta-572831	BIM9	17.5	Plant material	Acid/Alkali/ Acid	-28.8	140.12 ± 0.52 pMC	-25	-	-13	-24	-23	±	3
BIM9_30	Beta-572832	BIM9	29.5	Plant material	Acid/Alkali/ Acid	-29.4	510±30	542	-	492	514	514	±	14

5.7. References

Abram, N. J., Mulvaney, R., Vimeux, F., Phipps, S. J., Turner, J. and England, M. H. (2014) Evolution of the Southern Annular Mode During the past millennium, *Nature Climate Change*, 4:564-569.

Adams, N. (2009) Climate trends at Macquarie Island and expectations of future climate change in the sub-Antarctic, *Papers and Proceedings of the Royal Society of Tasmania*, 143(1): 1–8.

Amesbury, M. J., Roland, T. P., Royles, J. Hodgson, D. A., Convey, P., Griffiths, H. and Charman, D. J. (2017). Widespread Biological Response to Rapid Warming on the Antarctic Peninsula, *Current Biology*, 27: 1–7.

Anderson, R. F., Ali, S., Bradtmiller, L. I., Nielsen S. H. H., Fleischer, M. Q., Anderson, B. E. and Burckle, L. H. (2009), Wind-Driven Upwelling in the Southern Ocean and the Deglacial Rise in Atmospheric CO_2, *Science*, 323: 1443–48.

BAS reader (2020) Met reader: station surface data. Available at: https://legacy.bas.ac.uk/met/READER/surface/stationwind.html

Beyens, L., Chardez, D. De Baere, and C. Verbruggen. (1995) The Aquatic Testate Amoebae Fauna of the Strømness Bay Area, South Georgia, *Antarctic Science*, 7(1): 3–8.

Biastoch, A., Böning, C. W., Schwarzkopf, F. U. and Lutjeharms, J. R. E. (2009) Increase in Agulhas leakage due to poleward shift in the southern hemisphere westerlies, *Nature*, 462: 495–498.

Björck, S., Rundgren, M., Ljung, K., Unkel, I. and Wallin, Å. (2012) Multi-proxy analyses of a peat bog on Isla de Los Estados , easternmost Tierra Del Fuego: a unique record of the variable Southern Hemisphere Westerlies since the last deglaciation, *Quaternary Science Reviews*, 42: 1–14.

Blaauw, M. (2010) Methods and code for “classical” age-modelling of radiocarbon sequences, *Quaternary Geochronology*, 5: 512–518.

Blaauw, M. and Christen, J. A. (2011) Flexible paleoclimate age-depth models using an autoregressive gamma process, *Bayesian analysis*, 6(3): 457–474.

Booth, R. K., Lamentowicz, M. and Charman, D. J. (2010) Preparation and analysis of testate amoebae in peatland palaeoenvironmental studies, *Mires and Peat,* 7: 1-11.

Bracegirdle, T. J. (2018) Southern Hemisphere tropospheric westerly jet: 1979-present, Polar Data Centre, Natural Environment Research Council, UK.

Bracegirdle, T. J., Shuckburgh, E., Sallee, J-B., Wang, Z., Meijers, A. J. S., Bruneau, N., Phillips, T. and Wilcox, L.J. (2013) Assessment of surface winds over the Atlantic, Indian, and Pacific Ocean sectors of the Southern Ocean in CMIP5 models: Historical bias, forcing response, and state dependence, *Journal of Geophysical Research*, 118(2): 547–562.

Bricher, P. K., Lucieer, A. and Woehler, E. J. (2008) Population trends of Adélie penguin (Pygoscelis adeliae) breeding colonies: A spatial analysis of the effects of snow accumulation and human activities, *Polar Biology*, 31: 1397–1407.

Buckney, R. T. and Tyler, P. A. (1974) Reconnaissance limnology of SubAntarctic islands. II. Additional features of the chemistry of Macquarie Island lakes and tarns, *Marine and Freshwater Research*, 25: 89–95.

Cai, W. (2006) Antarctic ozone depletion causes an intensification of the Southern Ocean super-gyre circulation, *Geophysical Research Letters*, 33(3): 1–4.

Cai, W., Van Rensch, P., Borlace, S. and Cowan, T. (2011) Does the Southern Annular Mode contribute to the persistence of the multidecade-long drought over southwest Western Australia?, *Geophysical Research Letters*, 38: L14712, doi:10.1029/2011GL047943.

Charman, D. J. (2001) Biostratigraphic andpalaeoenvironmental applications of testate amoebae, *Quaternary Science Reviews*, 20: 1753–1764.

Charman, D. J., Hendon, D. and Woodland, W. A. (2000) The identification of testate amoebae (Protozoa: Rhizopoda) in peats. London: Quaternary Research Association.

Chase, B. M., Boom, A., Carr, A.S., Meadows, M.E. and Reimer, P.J. (2013) Holocene climate change in southernmost South Africa: Rock hyrax middens record shifts in the southern westerlies, *Quaternary Science Reviews*, 82: 199–205.

Garreaud, R. D. (2018) Record-breaking climate anomalies lead to severe drought and environmental disruption in western Patagonia in 2016, *Climate Research*, 74: 217-229.

Gehrels, W. R., Hendon, D. and Charman, D. J. (2006) Distribution of testate amoebae in salt marches along the Northern American east coast, *Journal of Foraminiferal Research*, 36(3): 201–214.

Grythe, H., Ström, J., Krejci, R., Quinn, P. and Stohl, A. (2014) A review of sea-spray aerosol source functions using a large global set of sea salt aerosol concentration measurements, *Atmospheric Chemistry and Physics*, 14: 1277–1297.

Gustafsson, M. E. R. and Franzén, L. G. (2000) Inland transport of marine aerosols in southern Sweden, *Atmospheric Environment*, 34(2): 313–325.

Hinojosa, J. L., Moy, C.M., Stirling, C.H., Wilson, G.S. and Eglinton, T.I. (2017) A New Zealand perspective on centennial-scale Southern Hemisphere westerly wind shifts during the last two millennia, *Quaternary Science Reviews*, 172: 32–43.

Hodgson, D. and Sime, L. C. (2010) Southern westerlies and CO_2, *Nature Geoscience*, 3(10): 666–667.

Hogg, A.G., Hua, Q., Blackwell, P.G., Niu, M., Buck, C.E., Guilderson, T.P., Heaton, T.J., Palmer, J.G., Reimer, P.J., Reimer, R.W. and Turney, C.S. (2013) SHCal13 Southern Hemisphere calibration, 0–50,000 years cal BP, *Radiocarbon*, 55(4): 1889-1903.

Holland, P.R., Bracegirdle, T.J., Dutrieux, P., Jenkins, A. and Steig, E.J. (2019) West Antarctic ice loss influenced by internal climate variability and anthropogenic forcing, *Nature Geoscience*, 12(9): 718-724.

Holz, A., Paritsis, J., Mundo, I.A., Veblen, T.T., Kitzberger, T., Williamson, G.J., Aráoz, E., Bustos-Schindler, C., González, M.E., Grau, H.R. and Quezada, J.M. (2017) Southern Annular Mode drives multicentury wildfire activity in southern South America, *Proceedings of the National Academy of Sciences*, 114(36): 9552-9557.

Hua, Q., Barbetti, M. and Rakowski, A.Z. (2013) Atmospheric radiocarbon for the period 1950–2010, *Radiocarbon*, 55(4): 2059-2072.

Hunter, I., Croxall, J. P. and Prince, P. A. (1982) The distribution and abundance of burrowing seabirds (procellariiformes) at Bird Island, South Georgia: I. Introduction and methods, *British Antarctic Survey Bulletin*, 56:49–67.

Juggins, S. (2015) Rioja: Analysis of Quaternary Science Data. R Package Version 0.9e5. https://cran.r-project.org/web/packages/rioja/index.html/

Knudson, K. P., Hendy, I. L. and Neil, H. L. (2011) Re-examining Southern Hemisphere westerly wind behavior: insights from a late Holocene precipitation reconstruction using New Zealand fjord sediments, *Quaternary Science Reviews*, 30(21–22): 3124–3138.

Koffman, B. G., Kreutz, K. J., Breton, D. J., Kane, E. J., Winski, D. A., Birkel, S. D., Kurbatov, A. V. and Handley, M. J. (2014) Centennial-scale variability of the Southern Hemisphere westerly wind belt in the eastern Pacific over the past two millennia, *Climate of the past,* 10: 1125-1144.

Kohfeld, K. E., Graham, R. M., de Boer, A. M., Sime, L. C., Wolff, E. W., Le Quéré, C. and Bopp, L. (2013) Southern Hemisphere westerly wind changes during the Last Glacial Maximum: paleo-data synthesis, *Quaternary Science Reviews*, 68: 76–95.

Lamy, F., Hebbeln, D., Röhl, U., Wefer, G. (2001) Holocene rainfall variability in southern Chile: a marine record of latitudinal shifts of the Southern Westerlies, *Earth and Planetary Science Letters*, 185: 369-382.

Lamy, F., Kilian, R., Arz, H. W., Francois, J-P., Kaiser, J., Prange, M. and Steinke, T. (2010) Holocene changes in the position and intensity of the southern westerly wind belt, *Nature Geoscience*, 3: 695–99.

Landschützer, P., Gruber, N., Haumann, F. A., Rödenbeck, C., Bakker, D. C. E., van Heuven, S., Hoppema, M., Metzl, N., Sweeney, C., Takahashi, T., Tilbrook, B.

and Wanninkhof, R. (2015) The reinvigoration of the Southern Ocean carbon sink, *Science,* 349(6253): 1221-1224.

Le Quéré, C., Rödenbeck, C., Buitenhuis, E. T., Conway, T. J., Langenfelds, R., Gomez, A., Labuschagne, C., Ramonet, M., Nakazawa, T., Metzl, N., Gillett, N. and Heimann, M. (2007) Saturation of the Southern Ocean CO_2 sink due to recent climate change, *Science,* 316: 1735-1737.

Le Roux, P. C. and McGeoch, M. A. (2008) Changes in climate extremes, variability and signature on sub-Antarctic Marion Island, *Climatic Change*, 86: 309–329.

Lewis Smith, R. I. (1981) Types of peat and peat-forming vegetation on South Georgia, *British Antarctic Survey Bulletin*, 53: 119–139.

Loisel, J., Yu, Z., Beilman, D.W., Camill, P., Alm, J., Amesbury, M.J., Anderson, D., Andersson, S., Bochicchio, C., Barber, K. and Belyea, L.R. (2014) A database and synthesis of northern peatland soil properties and Holocene carbon and nitrogen accumulation, *The Holocene*, 24(9): 1028-1042.

Lovenduski, N.S., Gruber, N. and Doney, S.C. (2008) Toward a mechanistic understanding of the decadal trends in the Southern Ocean carbon sink, *Global Biogeochemical Cycles*, 22(3): GB3016.

Maclean, I. M. D., Mosedale, J. R. and Bennie, J. J. (2018) Microclima: An r package for modelling meso- and microclimate, *Methods in Ecology and Evolution*, 1–11.

Mallis, M. (1988) A quantitative investigation of aerosol (salt) scavenging on Macquarie Island, *Papers and Proceedings of the Royal Society of Tasmania,* 122: 121-128.

Marshall, G. J. (2003) Trends in the Southern Annular Mode from Observations and Reanalyses, *Journal of Climate*, 16: 4134–43.

Marshall, G. J., Orr, A., van Lipzig, N. P. M and King, J. C. (2006) The impact of a changing Southern Hemisphere Annular Mode on Antarctic Peninsula summer temperatures, *Journal of Climate*, 19(20): 5388-5404.

Marshall, J. and Speer, K. (2012) Closure of the meridional overturning circulation through Southern Ocean upwelling, *Nature Geoscience*, 5(3): 171–180.

Mayewski, P. A., Maasch, K. A., Dixon, D., Sneed, S. B., Oglesby, R., Korotkikh, E., Potocki, M., Grigholm, B., Kreutz, K., Kurbatov, A. V., Spaulding, N., Stager, J. C., Taylor, K. C., Steig, E. J., White, J., Bertler, N. A. N., Goodwin, I. D., Simoes, J. C., Jana, R., Kraus, S. and Fastook, J. (2013) West Antarctica's Sensitivity to Natural and Human Forced Climate Change Over the Holocene, *Journal of Quaternary Science*, 28(1): 40–48.

Mayewski, P. A., Bracegirdle, T., Goodwin, I., Schneider, D., Bertler, N. A. N., Birkel, S., Carleton, A., England, M. H., Kang, J-H., Khan, A., Russell, J., Turner, J.

and Velicogna, I. (2015) Potential for Southern Hemisphere climate surprises, *Journal of Quaternary Science*, 30(5): 391–95.

Mazei, Y. and Tsyganov, A. N. (2006) Freshwater testate amoebae (In Russian). Moscow: KMK.

Meisterfeld, R. (2002a) Order Arcellinida Kent, 1880. In: Lee, J.J., Leedale, G.F., Bradbury, P. (Eds.), An illustrated guide to the protozoa, 2, second ed. Society of Protozoologists, Lawrence, Kansas, USA, 827–860.

Meisterfeld, R. (2002b) Testate Amoebae with Filopodia. In: Lee, J. J., Leedale, G. F., Bradbury, P. (Eds.), An illustrated guide to the protozoa, 2, second ed. Society of Protozoologists, Lawrence, Kansas, USA, 1054–1084.

Mitchell, E.A., Charman, D.J. and Warner, B.G. (2008) Testate amoebae analysis in ecological and paleoecological studies of wetlands: past, present and future, Biodiversity and conservation, 17(9): 2115-2137.

Mitchell, E. A. D., Payne, R. J. and Lamentowicz, M. (2008) Potential implications of differential preservation of testate amoeba shells for paleoenvironmental reconstruction in peatlands, *Journal of Paleolimnology*, 40(2): 603–618.

Monahan, E. C., Spiel, D. E. and Davidson, K. L. (1986) A model of marine aerosol generation via whitecaps and wave disruption, In: Monahan, E. C. and MacNiocaill, G. D. (Eds.) Oceanic whitecaps and their role in air-sea exchange processes. Reidel, Dordrecht, The Netherlands, 167–174.

Moreno, P. I., Vilanova, I., Villa-Martínez, R., Dunbar, R. B., Mucciarone, D. A., Kaplan, M. R., Garreaud, R. D., Rojas, M., Moy, C. M., De Pol-Holz, R., Lambert, F. (2018) Onset and Evolution of Southern Annular Mode-Like Changes at Centennial Timescale, *Scientific Reports,* 8: 3458.

Neville, L. A., Christie, D. G., McCarthy, F. M. G. and MacKinnon, M. D. (2010) Biogeographic variation in Thecamoebian (Testate amoebae) assemblages in lakes within various vegetation zones of Alberta, Canada, *International Journal of Biodiversity and Conservation,* 2(8): 215-224.

Ogden, C. G. and Hedley, R. H. (1980) An atlas of freshwater testate amoebae. Oxford University Press, Oxford.

Oksanen, J., Blanchet, F.G., Kindt, R., Legendre, P., Minchin, P.R., O'Hara, R.B., Simpson, G.L., Solymos, P., Henry, M., Stevens, H. and Wagner, H. (2016) Package Vegan: Community Ecology, R package Version 2.3-0.

Orme, L.C., Davies, S.J. and Duller, G.A.T. (2015) Reconstructed centennial variability of late Holocene storminess from Cors Fochno, Wales, UK, *Journal of Quaternary Science*, 30(5): 478-488.

Patterson, R. T. and Kumar, A. (2002) A review of current testate rhizopod (thecamoebian) research in Canada, *Palaeogeography, Palaeoclimatology, Palaeoecology*, 180: 225-251.

Payne, R. J. and Mitchell, E. A. D. (2009) How many is enough? Determining optimal count totals for ecological and palaeoecological studies of testate amoebae, *Journal of Paleolimnology*, 42(4): 483–495.

Payne, R.J., Ring-Hrubesh, F., Rush, G., Sloan, T.J., Evans, C.D. and Mauquoy, D. (2019) Peatland initiation and carbon accumulation in the Falkland Islands, *Quaternary Science Reviews*, 212: 213-218.

Pendlebury, S. F. and Barnes-Keoghan, I. P. (2007) Climate and climate change in the Sub-Antarctic, *Papers and Proceedings - Royal Society of Tasmania*, 141(1): 67–82.

Perren, B. B., Hodgson, D. A., Roberts, S. J., Sime, L., Van Nieuwenhuyze, W., Verleyen, E. and Vyverman, W. (2020) Southward migration of the Southern Hemisphere westerly winds corresponds with warming climate over centennial timescales, *Communications Earth and Environment,* 1(58): 1-8.

Pritchard, H. D., Ligtenberg, S. R. M., Fricker, H. A., Vaughan, D. G., van den Broeke, M. R. and Padman, L. (2012) Antarctic ice-sheet loss driven by basal melting of ice shelves, *Nature,* 484: 502-505.

Purich, A., Cai, W. J., England, M. H. and Cowan, T. (2016) Evidence for link between modelled trends in Antarctic sea ice and underestimated westerly wind changes, *Nature Communications,* 7: 10409.

R Core Team (2013) R: A language and environment for statistical computing. R Foundation from statistical computing, Vienna, Austria. http://www.R-project.org/

Reason, C. J. C. and Rouault, M. (2005) Links between the Antarctic Oscillation and winter rainfall over western South Africa, *Geophysical Research Letters*, L07705.

Richters, F. (1908) Moosbewohner. In: Wissenschaftliche Ergebnisse Der Schwedeschen Südpolar Expedition 1901- 1903.

Rivieros, N. V., Babalola, A. O., Boudreau, R. E. A., Patterson, R. T., Roe, H. M. and Doherty, C. (2007) Modern distribution of salt marsh foraminifera and thecamoebians in the Seymour-Belize Inlet Complex, British Columbia, Canada, *Marine Geology,* 242(1-3): 39-63.

Royles, J., Amesbury, M. J., Convey, P., Griffiths, H., Hodgson, D. A., Leng, M. J. and Charman, D. J. (2013) Plants and soil microbes respond to recent warming on the Antarctic Peninsula, *Current Biology*, 23 (17) : 1702–6.

Royles, J., Amesbury., M. J., Roland, T. P., Jones, G. D., Convey, P., Griffiths, H., Hodgson, D. A. and Charman, D. J. (2016) Moss stable isotopes (carbon-13 , oxygen-18) and testate amoebae reflect environmental inputs and microclimate along a latitudinal gradient on the Antarctic Peninsula, *Oecologia*, 181 (3): 931–45.

Ryan, B. C. (1977) A mathematical model for diagnosis and prediction of surface winds in mountainous terrain, *Journal of Applied Meteorology*, 16: 571–584.

Sandon, H. and Cutler, D. W. (1924) Some protozoa from the soils collected by the "Quest" expedition (1921-22), *Journal of the Linnean Society of London – Zoology*, 36: 1-2.

Saunders, K.M., Kamenik, C., Hodgson, D.A., Hunziker, S., Siffert, L., Fischer, D., Fujak, M., Gibson, J.A. and Grosjean, M. (2012) Late Holocene changes in precipitation in northwest Tasmania and their potential links to shifts in the Southern Hemisphere westerly winds, *Global and Planetary Change*, *92*: 82-91.

Saunders, K. M., Hodgson, D. A., McMurtrie, S. and Grosjean, M. (2015) A diatom conductivity transfer function for reconstructing past changes in the Southern Hemisphere westerly winds over the Southern Ocean, *Journal of Quaternary Science*, 30(5): 464–77.

Saunders, K. M., Roberts, S. J., Perren, B., Butz, C., Sime, L., Davies, S., Van Nieuwenhuyze, W., Grosjean, M. and Hodgson, D. A. (2018) Holocene dynamics of the Southern Hemisphere westerly winds and possible links to CO_2 outgassing, *Nature Geoscience*, 11: 650-655.

Saunders, K. M., Hodgson, D. A. and McMinn, A. (2009) Quantitative relationships between benthic diatom assemblages and water chemistry in Macquarie Island lakes and their potential for reconstructing past environmental changes, *Antarctic Science*, 21(1): 35– 49.

Schmale, J., Schneider, J., Nemitz, E., Tang, Y. S., Dragosits, U., Blackall, T. D., Trathan, P. N., Phillips, G. J., Sutton, M. and Braban, C. F. (2013) Sub-Antarctic marine aerosol: dominant contributions from biogenic sources, *Atmospheric Chemistry and Physics,* 13: 8669-8694.

Seers, B. (2018) fetchR: Calculate Wind Fetch. R Package version 2.1-1. https://cran.r-project.org/package=fetchR

Sime, L. C., Kohfeld, K. E., Le Quéré, C., Wolff, E. W., de Boer, A. M., Graham, R. M. and Bopp, L. (2013) Southern Hemisphere westerly wind changes during the Last Glacial Maximum: model-data comparison, *Quaternary Science Reviews,* 64: 104-120.

Smith, H.G (1982) The terrestrial protozoan fauna of South Georgia, *Polar Biology*, 1:173-179.

Smith, H.G. and Headland, R. K. (1983) The population ecology of soil testate rhizopods on the sub-Antarctic island of South Georgia, *Rev. Ecol. Biol. Sol.*, 20(2): 269-286.

Smith, J.A., Andersen, T.J., Shortt, M., Gaffney, A.M., Truffer, M., Stanton, T.P., Bindschadler, R., Dutrieux, P., Jenkins, A., Hillenbrand, C.D. and Ehrmann,

W. (2017) Sub-ice-shelf sediments record history of twentieth-century retreat of Pine Island Glacier, *Nature*, 541(7635): 77-80.

Smith, H.G. (1978) The Distribution and Ecology of Terrestrial Protozoa of SubAntarctic and Maritime Antarctic Islands. British Antarctic Survey Scientific Reports. No. 95. Natural Environment Research Council.

Stager, J. C., Mayewski, P. A., White, J., Chase, B. M., Neumann, F. H., Meadows, M. E., King, C. D. and Dixon, D. A. (2012) Precipitation variability in the winter rainfall zone of South Africa during the last 1400 yr linked to the austral westerlies, *Climate of the Past,* 8: 877-887.

Stockmarr, J. (1971) Tablets with spores in absolute pollen analysis, *Pollen et spores,* 13: 615-621.

Strother, S. L., Salzmann, U., Roberts, S. J., Hodgson, D. A., Woodward, J., Van Nieuwenhuyze, W., Verleyen, E., Vyverman, W. and Moreton, S. G. (2014) Changes in Holocene climate and the intensity of Southern Hemisphere Westerly Winds based on a high-resolution palynological record from sub-Antarctic South Georgia, *The Holocene,* 25(2): 1-17.

Swart, N. C. and Fyfe, J. C. (2012) Observed and simulated changes in the Southern Hemisphere surface westerly wind-stress, *Geophysical Research Letters*, 39(16).

Swindles, G. T. and Roe, H. M. (2007) Examining the dissolution characteristics of testate amoebae (Protozoa: Rhizopoda) in low pH conditions: Implications for peatland palaeoclimate studies, *Palaeogeography Palaeoclimatology, Palaeoecology*, 252: 486–96.

Taylor, K. (2020) A reconstruction of the Southern Hemisphere Westerly Winds based on testate amoeba analysis from a Bird Island peat core. Dissertation, University of Exeter.

Thomas, Z., Turney, C., Allan, R., Colwell, S., Kelly, G., Lister, D., Jones, P., Beswick, M., Alexander, L., Lippmann, T. and Herold, N. (2018) A new daily observational record from Grytviken, South Georgia: Exploring twentieth-century extremes in the South Atlantic, *Journal of Climate*, *31*(5): 1743-1755.

Thompson, D. W. J. and Solomon, S. (2002) Interpretation of recent Southern Hemisphere climate change, *Science,* 296(5569): 895-899.

Thompson, D. W. J., Solomon, S., Kushner, P. J., England, M. H., Grise, K. M. and Karoly, D. J. (2011) Signatures of the Antarctic ozone hole in Southern Hemisphere surface climate change, *Nature Geoscience,* 4(11): 741-749.

Toggweiler, J. R. (2009) Shifting Westerlies, *Science*, 323: 1435–1436.

Toggweiler, J. R., Russell, J. L. and Carson, S. R. (2006) Midlatitude westerlies, atmospheric CO_2 and climate change during the ice ages, *Palaeoceanography,* 21: PA2005.

Tolonen, K. and Turunen, J. (1996) Accumulation rates of carbon in mires in Finalnd and implications for climate change, *The Holocene,* 6(2): 171-178.

Turner, E. T., Swindles, G. T. and Roucoux, K. H. (2014) Late Holocene ecohydrological and carbon dynamics of a UK raised bog: impact of human activity and climate change, *Quaternary Science Reviews,* 84: 65-85.

Turney, C. S. M., McGlone, M., Palmer, J., Fogwill, C., Hogg, A., Thomas, Z. A., Lipson, M., Wilmshurst, J. M., Fenwick, P., Jones, R. T., Hines, B. and Clark, G. F. (2016a) Intensification of Southern Hemisphere westerly winds 2000-1000 years ago: evidence from the subantarctic Campbell and Auckland Islands (52-50˚S), *Journal of Quaternary Science,* 31(1): 12-19.

Turney, C. S. M., Jones, R. T., Fogwill, C., Hatton, J., Williams, A. N., Hogg, A., Thomas, Z. A., Palmer, J., Mooney, S. and Reimer, R. W. (2016b) A 250-year periodicity in Southern Hemisphere westerly winds over the last 2600 years, *Climate of the past,* 12: 189-200.

Ummenhofer, C. C. and England, M. H. (2007) Interannual extremes in New Zealand precipitation linked to modes of Southern Hemisphere climate variability, *Journal of Climate,* 20: 5418-5440.

Ummenhofer, C. C., Gupta, A. and England, M. H. (2009) Causes of late twentieth-century trends in New Zealand precipitation, *Journal of Climate,* 22: 3-19.

Van der Putten, N., Mauquoy, D., Verbruggen, C. and Björck, S. (2012) Subantarctic peatlands and their potential as palaeoenvironmental and palaeoclimatic archives, *Quaternary International,* 268: 65-76.

Vaughan, D. G., Marshall, G. J., Connolley, W. M., Parkinson, C., Mulvaney, R., Hodgson, D. A., King, J. C., Pudsey, C. J. and Turner, J. (2003) Recent rapid regional climate warming on the Antarctic Peninsula, *Climatic Change,* 60(3): 243-274.

Vincke, S., van de Vijver, B., Mattheeusen, R. and Beyens, L. (2004) Freshwater testate amoebae communities from Ile de la Possession, Crozet Archipelago, Subantarctica, *Arctic, Antarctic and Alpine Research*, 36(4): 584-590.

Vincke, S., van de Vijver, B., Gremmen, N. and Beyens, L. (2006) The moss dwelling testacean fauna of the Stromness Bay (South Georgia), *Acta Protozoologica*, 45: 65-75.

Wagner, R. J., Boulger, R. W. Jr., Oblinger, C. J. and Smith, B. A. Guidelines and standard procedures for continuous water-quality monitors: station operation, record computation, and data reporting: U.S. Geological survey techniques and methods 1-D3. (2006) Available at: https://pubs.usgs.gov/tm/2006/tm1D3/. (Accessed: 6th June 2018).

Wanner, M., Birkhofer, K., Puppe, D., Shimano, S.D. and Shimizu, M. (2020) Tolerance of testate amoeba species to rising sea levels under laboratory conditions and in the South Pacific, *Pedobiologia*, *79*:150610.

Whittle, A. and Gallego-Sala, A. V. (2016) Vulnerability of the peatland carbon sink to sea-level rise, *Scientific Reports*, 1–11.

Whittle, A., Amesbury, M.J., Charman, D.J., Hodgson, D.A., Perren, B.B., Roberts, S.J. and Gallego-Sala, A.V. (2019) Salt-enrichment impact on biomass production in a natural population of peatland dwelling Arcellinida and Euglyphida (Testate Amoebae), *Microbial ecology*, 78(2): 534-538.

Young, D. M., Baird, A. J., Charman, D. J., Evans, C. D., Gallego-Sala, A., Gill, P. J., Hughes, P. D. M., Morris, P. J. and Swindles, G. T. (2019) Misinterpreting carbon accumulation rates in records from near-surface peat, *Scientific Reports,* 29(1): 17939.

Chapter 6

Long-term correspondence between Southern Hemisphere westerly wind intensity and temperature during the Holocene

6.1. Introduction

The Southern Hemisphere Westerly winds (SHW), a circumpolar belt of winds that blow over the Southern Ocean, have strengthened and contracted closer to the Antarctic coast in response to increasing atmospheric carbon dioxide (CO_2) concentrations and ozone depletion over recent decades (Thompson and Solomon, 2002; Cai, 2006; Thompson et al. 2011). This shift has been attributed to a number of important (and ongoing) environmental changes throughout the high-latitudes of the Southern Hemisphere with implications for global climate and sea-level, including; warming temperatures on the Antarctic Peninsula (Vaughan et al. 2003), enhanced Agulhas leakage (Biastoch et al. 2009), increased basal melting of ice-shelves surrounding the West Antarctic Ice-sheet and Antarctic Peninsula (Marshall et al. 2006; Pritchard et al. 2012; Holland et al. 2019), and decreasing precipitation supply to the southern continents (Rouault, 2005; Ummenhofer and England, 2007; Ummenhofer et al. 2009; Cai et al. 2011; Garreaud, 2018).

Changes in the behaviour of the SHW, which currently reach maximum intensity between 50-55˚S (Lamy et al. 2010) also influence Antarctic sea-ice extent and circulation in the Southern Ocean (Lovenduski et al. 2008; Anderson et al. 2009; Purich et al. 2016). These processes together play an important role in modulating the functioning of the Southern Ocean carbon sink, which is determined by the balance between sequestration at the surface (via diffusion and the biological pump) versus release of old carbon from the deep ocean by wind-driven upwelling and outgassing (Hodgson and Sime, 2010; Toggweiler et al. 2006). One model of these processes, based on instrumental data (collected between 1981-2004), indicates that intensification and migration of the wind-belt enhanced saturation of surface waters with carbon from the deep-ocean, reducing the difference in the partial pressure of CO_2 between ocean and atmosphere, and weakening the carbon sink (Le Quéré et al. 2007); although

evidence also supports a more recent reinvigoration (Landschützer et al. 2015; Ritter et al. 2017). Projections for the future linkage between temperature, SHW behaviour and the Southern Ocean carbon sink, are therefore generally based on apparently contradictory, short-term and sparse oceanographic and meteorological measurements.

Palaeoclimatic records represent a powerful tool to better constrain these projections and bridge the model-data gap through establishing a longer-term record and a more mechanistic understanding of past SHW evolution (Perren et al. 2020). However, our current understanding of how wind-conditions over the Southern Ocean have changed during the Holocene is limited, with existing reconstructions (mostly derived from southern South America) providing an inconsistent picture (Kilian and Lamy, 2012). Part of this problem is the spatial and temporal patchiness of longer-term reconstructions within the core wind-belt region where wind-changes are both more pronounced and most relevant to Southern Ocean upwelling and carbon dynamics. This is further compounded by the reliance on proxies for precipitation, temperature and long-distance transport of exotic pollen or dust, which do not necessarily relate directly to wind-conditions (e.g. Kilian and Lamy, 2012; Chapter 1). Several recent studies have sought to overcome these limitations by providing reconstructions at high resolution, using more direct wind-proxies and (sub-Antarctic) archives located in the core of the westerly wind belt (e.g. Saunders et al. 2018; Perren et al. 2020). However, such reconstructions from the South Atlantic sector of the sub-Antarctic are lacking. Here we present a reconstruction of changes in the SHW wind intensity, using a direct proxy, from within this region.

6.2. Bird Island, South Georgia

Sub-Antarctic islands are the only landmasses, other than southern South America that lie directly inside the core SHW belt. Bird Island (54˚S, 38˚W; Fig. 6.1) is a small (~5 km^2) island situated on the north-west coast of South Georgia, approximately 1300 km south-east of the Falkland islands. Like other sub-Antarctic islands (see van der Putten, 2012) it is extensively covered by vegetation, interspersed with areas of peat formation, and is also an important breeding-ground for sea-birds and mammals (especially albatrosses, penguins and Antarctic fur-seals (e.g. Schmale et al. 2013)). Bird Island experiences mean annual wind-speeds of 35 km/h (based on observational average 2006-2015; Fig.

6.1), and while snow and ice builds up in winter, there is no permanent snow cover (Hunter et al. 1982). Climate is cool and wet (~0˚C in winter and 4˚C in summer), with winds blowing predominantly from the west. These prevailing winds lead to the development of a strong west-east gradient of sea-spray deposition (Fig. 6.1; Chapter 5). Accumulation of salt-spray through time therefore preserves a record of SHW intensity, where periods of more spray reflect phases of stronger wind (Chapter 5). We developed a reconstruction using the sediment sequence from a peatland at Morris Point, a small area of valley-floor mire located on a clifftop on the west-coast of Bird Island that is directly exposed to westerly airflow (Fig. 6.1; Supplementary Fig. 6.1). The record, with a basal depth of 506.5 cm, was radiometrically dated with fourteen ^{14}C dates to 8,282±51 year BP (Methods; Supplementary Fig. 6.2; Supplementary Table 6.1).

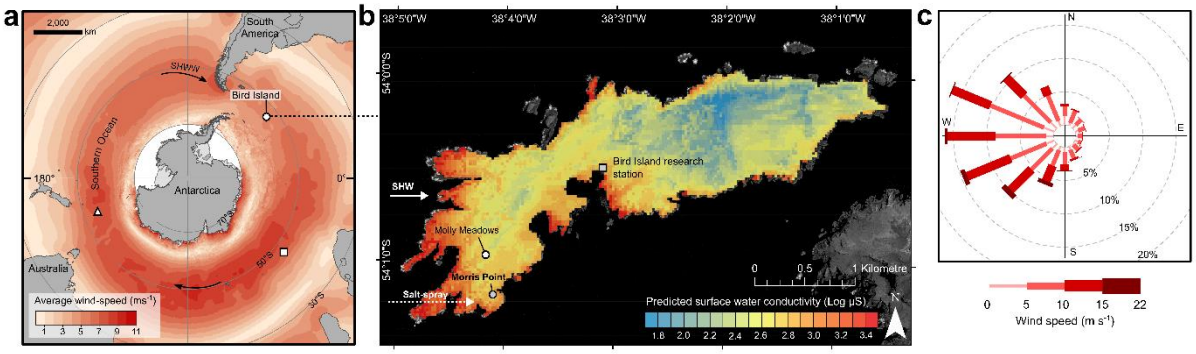

Figure 6.1 | a) Location of the modern-day core of the Southern Hemisphere westerly winds (SHW) over the Southern Ocean, in relation to the study site on Bird Island. Arrows indicate the prevailing direction of circulation. Red-shading shows sea-surface level (10 m) mean annual wind intensity based on NOAA blended high-resolution (0.25 degree grid) vector data downloaded from (https://www.ncdc.noaa.gov/data-access/marineocean-data/blended-global/blended-sea-winds). Locations of key wind-records referred to in this study are denoted by the white square (Marion Island) and white triangle (Macquarie Island). b) Map of Bird Island and the coring site at Morris Point, showing predicted surface water conductivity (salinity) conditions, which decrease as a result of declining wind-blown salt-spray aerosol inputs by the prevailing wind from west-to-east (see Chapter 5). c) Wind-rose summarising the dominant direction of airflow, intensity and frequency over Bird Island at 22.5˚ resolution, compiled from NOAA daily re-analysis data for the period 2012-2018.

6.3. Holocene behaviour of the Southern Hemisphere westerly winds over Bird Island (54°S)

Inputs of wind-blown salt-spray deposition at the coring location were principally tracked through their effect on the productivity of the testate amoeba community (Methods), which is directly (negatively) related to salinization (Whittle et al. 2019; Chapter 4-5).

Three significant phases of high relative wind intensity (defined as periods where testate amoeba productivity values fell below both their 8 and 5 k yr mean) were observed; I (0.45-1.15 k yr BP), II (2.8-3.65 k yr BP), III (4.45-8 k yr BP). Increased wind intensities that correspond to observational measurements in recent decades (since 1950) have also been reported in a duplicate core from the surface of the sediment record (see Chapter 5). Low relative wind intensities were recorded for 0-0.45 k yr BP, 1.15-2.8 k yr BP, and 3.65-4.45 k yr BP. A further distinct period of close to average wind-intensity, interpreted as conditions similar to present, were recorded between 1.5-2 k yr BP. These fluctuations in wind-blown salt-spray aerosol deposition were also tracked by changes in taxonomic composition of the testate amoeba populations, which underwent a significant shift at c.4.5 k yr BP (Supplementary Fig. 6.3). Similarly to in recent decades (Chapter 5), periods of less-stable and elevated testate amoeba population growth rates also consistently coincided with periods of weaker inferred winds (i.e. lower salinity conditions), and generally more species diverse assemblages (Fig. 6.2).

The reconstruction was compared with a potential independent measure of sea-spray aerosol deposition (Bromine; Br), based on micro- X-ray fluorescence (μXRF) and two measures of wind-blown dust deposition (Titanium (Ti) and Loss on ignition; Methods). Combined the proxies show a consistent pattern of wind strength over Bird Island during the last 8 k yr, and indicate that testate amoeba productivity provides a reliable record of SHW evolution.

The key feature of the record, across all proxies, is a period of higher wind intensity with large fluctuations toward the end of the mid-Holocene (8-4.45 k yr BP) (although resolution of the testate amoeba data is significantly lower after 5.5 k yr BP (see Fig. 6.2)). In contrast, the late-Holocene between (4.45-0 k yr BP),

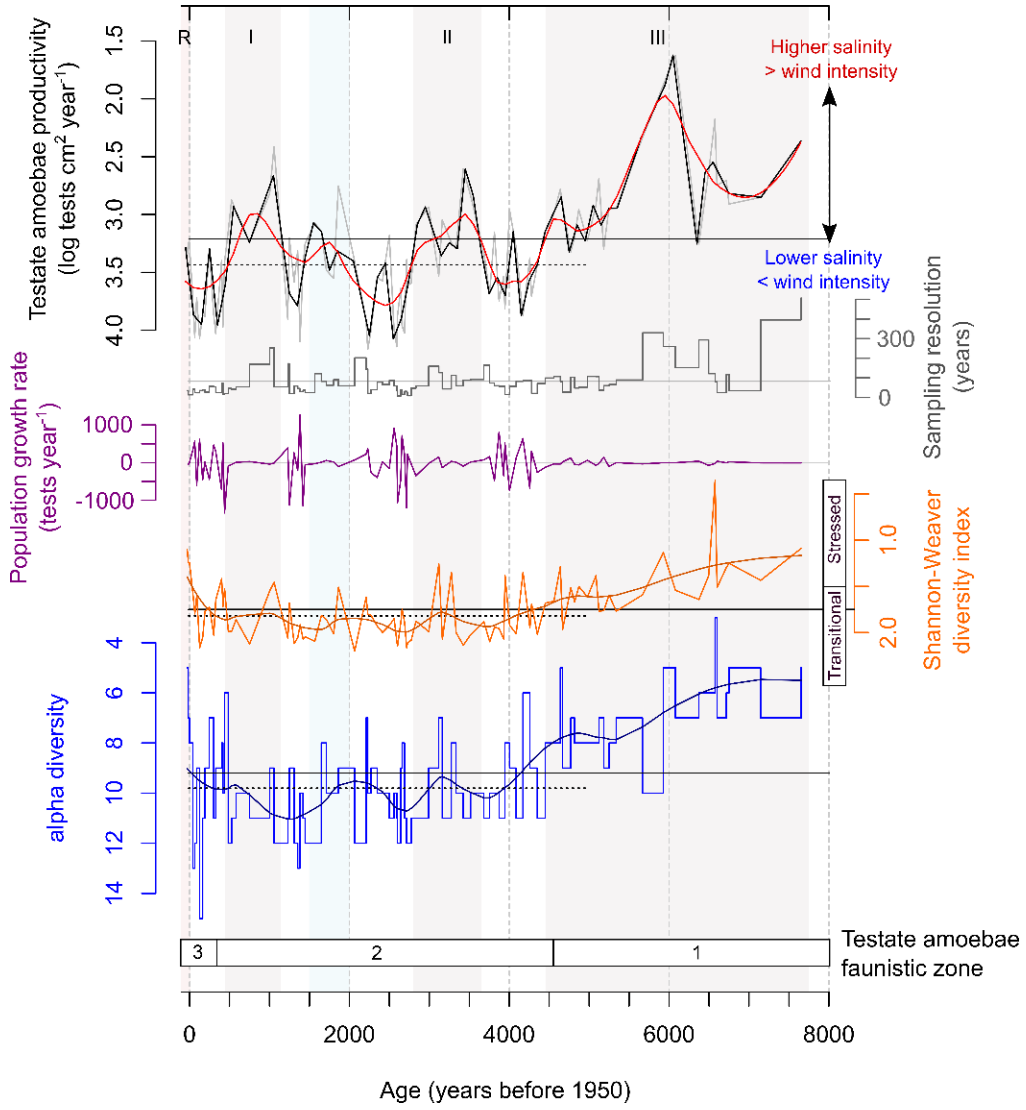

Figure 6.2 | Changes in the intensity of the Southern Hemisphere westerly wind over Bird Island, inferred from the productivity of the testate amoebae community at Morris Point. Solid black lines indicate the average for each dataset over the whole record, and dotted black lines indicate the average for the period 0-5 k yr BP. Sampling resolution, which indicates the time-period between consecutive measurements of testate amoeba productivity is also shown. Smooth lines represent second-order LOESS, based on re-sampled 100-year interval data. Grey shaded periods (I-III) indicate periods of stronger inferred wind conditions. R represents the period of recent intensification observed at the surface of the record (see Chapter 5). Blue shading indicates a further distinct period of close to average wind-intensity, interpreted as conditions similar to present. Environmental interpretation of Shannon-Weaver diversity index values is based on Patterson and Kumar (2002) (see Methods).

was a period of sustained but comparatively weaker winds, with lower amplitude fluctuations (Fig. 6.3).

The strongest correlation between salinity (inferred from testate amoeba productivity) and the other proxies was with measurements of the sea-spray aerosol Bromine ($R=-0.84$, $p<0.0001$). However, this correlation was weaker ($R=-0.46$, $p<0.001$) when wind-driven salt inputs were likely comparatively lower (after 5 k yr BP), which could suggest that Br either provides a less sensitive proxy or is subject to other (i.e. non-sea-spray) sources and influences (e.g. greater Br mobility in the upper parts of the core). The latter has been subject to debate, with authors arguing that sea-spray derived Br both is (and isn't) conserved in different peat profiles, and leading some to question its suitability as a marker for salt-spray (e.g. Turner et al. 2014; Shotyk et al. 2003). Other possible sources include abiotic oxidation of organic matter (Keppler et al. 2000) and the release of methyl bromide during plant decay (Lee-Taylor and Holland, 2000). However, the close correlation we observe with saltier conditions inferred from testate amoeba productivity and elevated Br suggests that Br derived from salt-spray is at least in part retained within this peat profile where inputs are expected to have been very high. Further investigation should be a priority of palaeoclimate research, although we suggest that the suitability of Br as a salt-spray marker is highly dependent on both concentrations of deposition, hydrology of the peatland, and qualities of the peat itself (e.g. density and the vegetation from which it is composed). Correlation between productivity and minerogenic indicators was weaker than for Br but remained significant ($R = -0.70$, $p<0.001$ for Ti, and $R = 0.36$, $p<0.01$ for loss on ignition). This weaker correlation can be attributed in part to the slightly different wind signal provided each proxy; testate amoebae provide an indication of longer-term average wind conditions while dust aerosols are biased to periods of stronger wind intensity (storminess) and greater stochastic variability (e.g. changing freeze-thaw conditions; see Chapter 5) (Fig. 6.3).

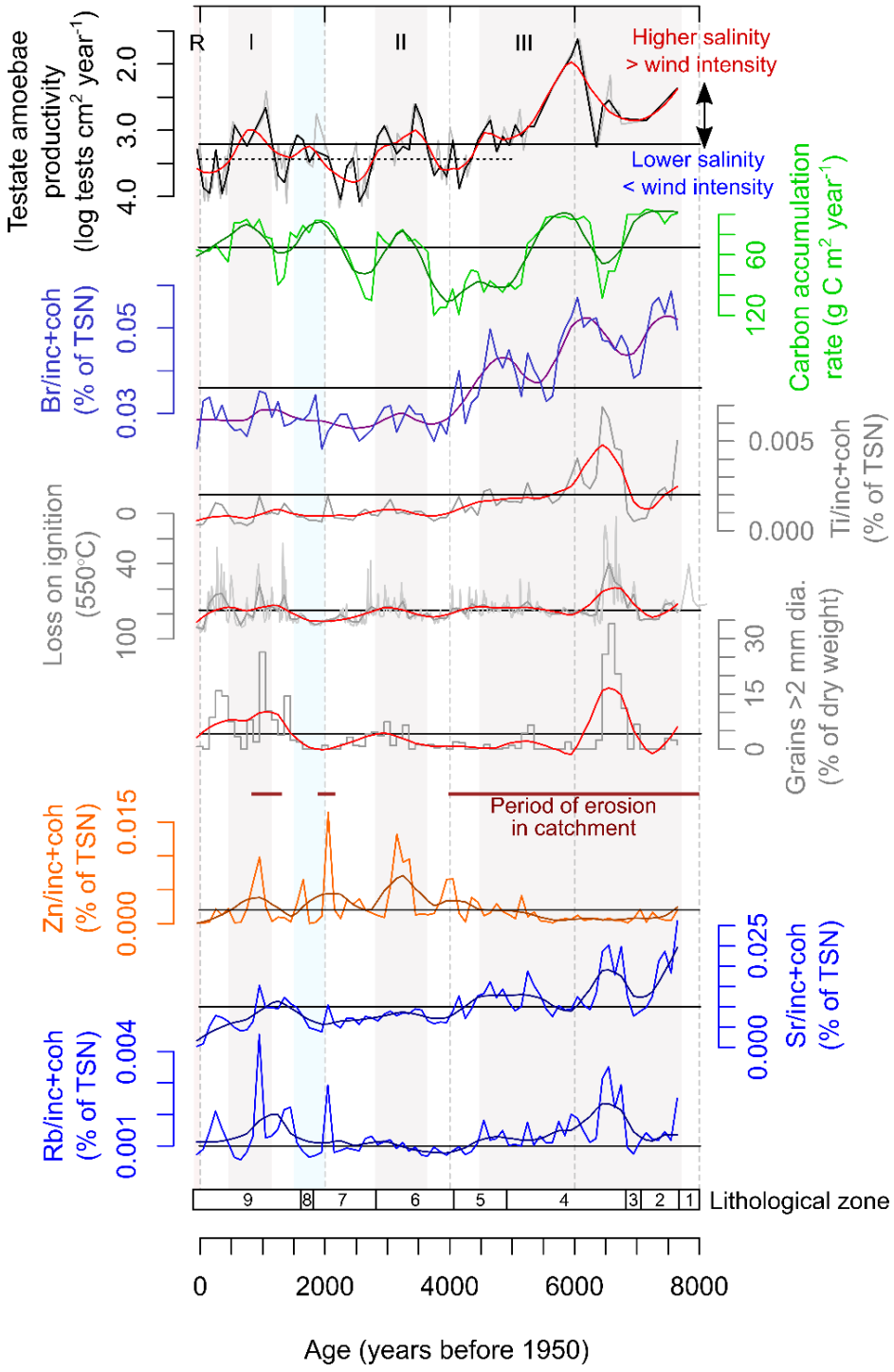

Figure 6.3 | Comparison between changes in the intensity of the Southern Hemisphere westerly wind over Bird Island, inferred from the productivity of testate amoebae, sea-spray aerosol deposition (Bromine; Br), based on micro- X-ray fluorescence (µXRF), and two measures of wind-blown dust deposition (Titanium (Ti) and Loss on ignition).TSN, total scatter normalized; inc, incoherent (Compton scattering); coh, coherent (Rayleigh scattering.

6.4. Latitudinal position and intensity of the Southern Hemisphere westerly wind belt

7.6-4.5 k yr BP:

All four proxies indicate a period of permanently above average, but generally declining wind-strength over Bird Island, punctuated by a multi-centennial phase of intense winds centred on 6 k yr BP (Fig. 6.3). Shannon-Weaver diversity index (SWDI) values for the testate amoeba community indicate an environment with prolonged and significant salt-stress, inhabited by only a small number of species (Fig. 6.2). Elevated levels of erosion and run-off in the catchment led to high concentrations of minerogenic deposition, and combined with concurrent deposition of large mineral grains (7-6.5 k yr BP), together point to frequent high-intensity (storm) wind conditions (Fig. 6.3). Although, in addition to wind-conditions, some minerogenic inputs at the base of the core are likely associated with the interface between peat and underlying geology, and increased local availability of material exposed by recent deglaciation.

Reconstructions from equivalent latitudes provide confirmation of strengthened winds over Bird Island during this interval, which was characterised by warmer temperatures globally and on South Georgia (Strother et al. 2014; Kaufman et al. 2020). Increased precipitation, run-off and strengthened winds over Isla de los Estados have been identified (Unkel et al. 2010), in addition to intensified (but highly variable) winds at Macquarie Island (Saunders et al. 2018). Distinctive peaks of elevated salt-spray deposition centred on 6 k yr BP were also replicated across all three of these records, which coincide with maxima in both global mean temperature (Kaufman et al. 2020) and insolation in the high southern latitudes, and indicate zonal symmetry in the position of the wind-belt between the Pacific and Atlantic sectors at this time (Fig. 6.4).

Many records from locations to the north of Bird Island in southern South America show a consistent pattern. As wind-strength broadly declined over Bird Island (from c. 7.6 k yr BP onwards), lake levels in southern Patagonia rose (Zolitschka et al. 2013), humid-temperate forests expanded (McCulloch et al. 2020), and the Cordillera Darwin ice-field re-advanced (Bertrand et al. 2017), as the regional climate became progressively cooler and wetter (see synthesis in Roberts et al. 2021). This climatic change can be attributed to an equatorward migration and

stabilisation of the wind-belt from an antecedent position south of 52˚S which led to reduced SHW influence and increased aridity over Patagonia between c. 10.5-7.5 k yr BP (Gilli et al. 2005; Fletcher and Moreno, 2012; Moreno et al. 2012; Zolitschka et al. 2013; Quade and Kaplan. 2017; Moreno et al. 2018; Saunders et al. 2018; Zolitschka et al. 2019; McCulloch et al. 2020). Wetter conditions in records from western Tasmania also suggest that winds were strengthened and/or displacing northward during the period ~9.2-5 k yr BP (Fletcher and Moreno, 2011; Fletcher and Moreno, 2012; Beck et al. 2018). Glacial reconstructions from surrounding continents have also found evidence of concurrent neoglacial advance in central Patagonia (46˚S, at 6.2 k yr BP; Douglass et al. 2005) and New Zealand (43˚S, at 6.5 k yr BP; Schaefer et al. 2009), suggesting generally intensified winds during this period.

In the context of this latitudinal transect, our record indicates that at c. 7 k yr BP the core of the wind-belt lay slightly to the south of Bird Island, and was likely focussed into a narrow latitudinal band in a configuration similar to present-day austral summers, with minimal influence on southern South America. Throughout the mid-Holocene, the belt began a slow and variable net migration to a more stable position further north, aligning with Bird Island (and/or strengthening) at c. 6 k yr BP when wind records throughout the sub-Antarctic show a consistent intensification, before bypassing to the north as wind-intensity on Bird Island and other records at 54˚S declined (Saunders et al. 2018; Unkel et al. 2010). This evolution supports the pattern of wind-belt migrations hypothesised by Quade and Kaplan (2017), using lake level fluctuations at Lago Cardiel (49˚S), and synthesised records from the Western Andes, such as Lamy et al. (2001) which shows southwards displaced westerlies (relative to 41˚S) between 7.7-4 k yr BP.

A possible explanation for the increasing wind influence throughout regional records during the mid-Holocene is the expansion of sea-ice (Mayr et al. 2007) around Antarctica (particularly in the Atlantic sector) from 8.6 k yr BP (Saunders et al. 2018) which coincided with increased global temperature (Fig. 6.4). This may have produced a stronger temperature gradient which forced the wind-belt northwards, while the greater quantity of energy available in the system increased the overall intensity of airflow as a whole, resulting in an interval of simultaneous increase in wind strength in both the core and areas further north. However, while evidence from South America supports the northward migration of the wind-belt

during this interval, generally drier conditions in the Winter rainfall zone (WRZ) of Southern Africa (~35˚S) until c. 3 k yr BP indicates limited influence of the northern edge of the wind-belt in these latitudes (Zhao et al. 2016).

The northward migration of the wind-belt over South America and equatorward of Bird Island, during a phase of significantly drier conditions in the WRZ, could indicate a significant phase of asymmetry in wind-conditions; perhaps as a result of variable sea-ice concentrations in the different regions (Saunders et al. 2018). A stronger temperature gradient caused by the expansion of sea-ice, could also have focussed the winds into a narrow band as they were pushed north, as opposed to the more spatially-diffuse configuration normally associated with the north-ward migrations that are responsible for bringing precipitation to southern Africa (such as in present day austral winters when temperature gradients weaken (Lamy et al. 2010; Stager et al. 2012; Zhao et al. 2016; Appendix 3)). A focussed wind belt could therefore explain why wind-intensity increased within southern South America (~40-55˚S) but not over Southern Africa (~35˚S). The prominent peak in wind-speeds at c. 6 k yr BP, at similar latitudes throughout the sub-Antarctic is consistent with such a latitudinally-condensed band (with summer-like configuration) passing over the islands at 54˚S as part of an ongoing northward migration. Further records of wind-intensity from terrestrial and marine locations, especially within the eastern section of the South Atlantic, will be needed in future to further evaluate this interpretation.

4.5-1 k yr BP:

This period of relatively constant but weaker winds (relative to the mid-Holocene) on Bird Island, corresponds with a larger and more diverse testate amoeba community (Fig. 6.2), and increased concentrations of Zinc (Zn; identified by µXRF; Fig. 6.3).

Prior to 4.5 k yr BP, levels of Zn remained close to zero but increased markedly thereafter in-phase with generally declining minerogenic inputs (Strontium (Sr), Rubidium (Rb), Ti; pearson correlation = -0.36, -0.49, -0.45, all $p < 0.01$) and salt-spray aerosol deposition (Br; pearson correlation = -0.6, $p < 0.001$). Once organic Zn is removed (by dividing by the sum of coherent and incoherent scatter) three predominant sources are possible; crustal (from surrounding geology), salt-spray and bird guano (e.g. Roberts et al. 2017). The anti-correlation between Zn,

minerogenic and salt-spray aerosol inputs therefore suggest guano as a partial source during this period. At Ardley Island on the western Antarctic Peninsula, the relocation of penguin colonies to more sheltered locations in response to strengthened westerly wind exposure has been observed (Yang et al. 2019). It is possible therefore that the amelioration of conditions (reduced wind-exposure) from c. 4.5 k yr BP onwards over Bird Island, allowed the expansion or relocation of bird nesting areas, with colonies favouring areas closer to the coring site. However, while µXRF analysis points to bird guano as a possible source of increased Zn deposition during this interval, it is currently not possible to determine with certainty. In the future, examination of the presence of macro-fossils related to bird colonies (e.g. bone fragments, otoliths (e.g. Roberts et al. 2017)), combined with isotopic analysis could provide valuable data to more precisely constrain the provenance of Zn during this phase.

Implied weaker winds in the Atlantic sector of the sub-Antarctic at 54˚S (Bird Island and Isla de los Estados) during this interval are synchronous with evidence of increased precipitation and associated stronger airflow over southern South America, as a result of continued northward migration of the wind-belt away from Bird Island into the lower latitudes (Lamy et al. 2001; Gilli et al. 2005; Lamy et al. 2010; Quade and Kaplan, 2017; McCulloch et al. 2020). Between 4.45-3.65 k yr BP wind intensity over Bird Island reached a distinct minima, consistent in timing with a minor reduction in lake levels at Lago Pato (51˚S) between 4-4.5 k yr BP, which has been interpreted to reflect the furthest northward position of the core belt (Roberts et al. 2021).

At the broad (millennial) scale the position of the core westerly wind belt seems to have remained stable at ~50˚S since c. 3 k yr BP, at least in the Atlantic-sector between South America and Africa (Quade and Kaplan, 2017; Zhao et al. 2016). However, while indicative of the mean position, the resolution of many available records is insufficient to indicate shorter term (centennial) fluctuations (e.g. Saunders et al. 2018; Unkel et al. 2010). Unfortunately, there are few paleoclimate records from the Southern high-latitudes that specifically reconstruct SHW migration on centennial timescales, although relatively high-magnitude short-lived events have been suggested (Perren et al. 2020). For the first time, our new centennially resolved and continuous record provides an

insight into the position and intensity of winds over the South Atlantic during this period.

Between 3.7-2.8 k yr BP a distinct phase (II) of reduced testate amoeba productivity, interpreted as an intensification of winds, punctuates the sustained below average wind-conditions at Bird Island. This event is concurrent with a peak in annual insolation at 62˚S and period of warming climate on South Georgia that extended throughout the high southern latitudes (Fig. 6.4). However, interpretation of this section of the record differs substantially compared to 4.5-8 k yr BP (phase III). Unlike this earlier phase of increased winds, higher salinity levels inferred from the testate amoeba community do not coincide with a sustained increase in erosion (interpreted from Ti, Sr, and Rb concentrations); although deposition of larger mineral grains, indicative of stormier conditions, is elevated (Fig. 6.3). This can be attributed to stochastic changes in the availability of mineral material, and the increased isolation of the accumulating peat-surface from underlying geology and run-off, while allowing continued deposition of wind-blown salt-spray and mineral grains. While neither reconstructions of salinity based on the testate amoebae nor Bromine proxies can be considered fully quantitative in this context, both suggest that salt-spray inputs were lower during this phase (II) than between 4.5-8 k yr BP. The phase (II) also corresponds to a distinct multi-centennial increase in Zn (Fig. 6.3), which we tentatively attribute to increased localised ornithogenic influences. Proximity to ornithogenic enrichment (wandering albatross nesting sites) has been shown to have some influence on certain testate amoeba taxa on sub-Antarctic île de la Possession (Vincke et al. 2007), although the relationship between communities and bird colonies, especially in terms of productivity, remains unclear (Mazei et al. 2018). Therefore, it is not possible to determine whether the proposed increase in ornithogenic influences at this time could have caused the substantial decline in testate amoeba productivity. Although the resolution of the Macquarie Island record declines during this period, minerogenic and salt-spray deposition records both agree with increased wind-intensity, showing a consistent pattern with slight increases compared to the 5 k yr average (Fig. 6.4). Taken together, this suggests that similarly to the preceding period of increased winds, reduced productivity of testate amoeba was primarily driven by increased salt-spray aerosol deposition, irrespective of possible ornithogenic influences.

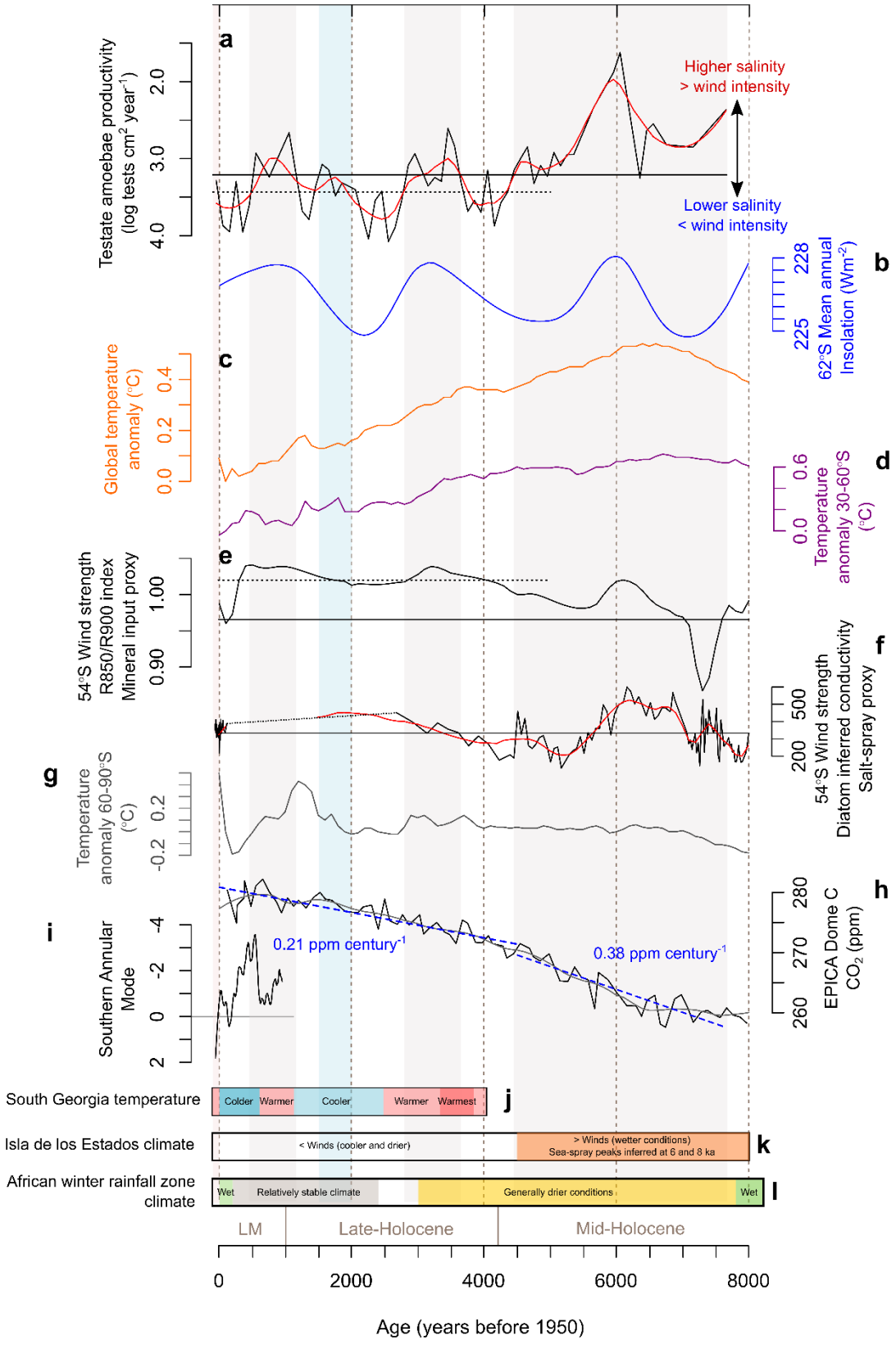

Figure 6.4 | Comparison of Bird Island wind-strength reconstruction with records of insolation, temperature, atmospheric CO_2 concentration and regional SHW records. a) Testate amoeba productivity at Morris Point, Bird Island, b) Mean annual insolation at 62˚S, c) global temperature anomaly (Kaufman et al. 2020), d) 30-60˚S temperature anomaly (Kaufman et al. 2020), e) hyperspectral ratio (R_{850}/R_{900}) mineral input proxy at Macquarie Island (Saunders et al. 2018), f) Diatom inferred lake conductivity wind-

strength proxy at Macquarie Island (Saunders et al. 2018), g) temperature anomaly 60-90˚S (Kaufman et al. 2020), h) EPICA Dome C CO_2 (see Saunders et al. 2018), i) Southern Annular Mode index (Abram et al. 2014), and summaries of; j) temperature on South Georgia (Foster et al. 2016), k) wind-strength over Isla de los Estados (Unkel et al. 2010), and l) precipitation in the winter rainfall zone in Southern Africa (Zhao et al. 2016). Solid black lines indicate the average for each dataset over the whole record, and dotted black lines indicate the average for the period 0-5 k yr BP. Key periods discussed in this study are indicated; Mid-Holocene (>4.5 k yr BP), Late-Holocene (4.5-1 k yr BP) and LM; last millennium (1 k yr BP – present).

With the onset of cooling temperatures and declining insolation, wind-intensity over Bird Island returned to below average levels between 2.8-2 k yr BP. The period between 2-1 k yr BP represents a moderate reversion in wind-intensity to slightly higher levels, close to average (and present-day) conditions. Although winds on Bird Island undergo a net increase during this phase, our data does not support the significant intensification of winds proposed by Turney et al. (2016a,b). While the generally lower intensity winds over Bird Island supports the interpretation that the mean position of the wind-belt lay to the north (aligned to southern South America) during this period (Quade and Kaplan, 2017), we found no evidence of consistent timings with proposed short-term (centennial) southward migrations (at least as far as 54˚S) during rapid (climate driven) events identified by McCulloch et al. (2020).

1 k yr BP-present:

During the past millennium, winds over Bird Island have undergone a major fluctuation from above average intensity between 1.15-0.45 k yr BP (during the Medieval Climate Anomaly (MCA; 1-0.8 k yr BP; (Bradley et al. 2003)), to a period of weaker below-average winds between 0.45-0 k yr BP (during the colder Little Ice Age (0.55-0.08 k yr BP)). Within the surface of the Morris Point peat record there is also evidence of a recent intensification (after 1950 CE) that is consistent with the observational record (Chapter 5).

Above average wind conditions (1.15-0.45 k yr BP) over Bird Island concurs with; a period of increased aridity in the WRZ of South Africa (Zhao et al. 2016), a cliff-top silt deposit suggesting gale-force winds over Campbell Island at 52˚S (1.1-0.97 k yr BP; McGlone et al. 1997), a phase of less-negative Southern Annular Mode (SAM) conditions (Abram et al. 2014; Fig. 6.4), and increased deposition of dust particles into the West Antarctic Ice Sheet divide ice-core located at 79˚S

(Koffman et al. 2014). Combined, this evidence suggests that during the warm MCA, the wind belt contracted and displaced southward (similarly to present day austral summers; Appendix 3), increasing in intensity closer to the Antarctic coast and over the Southern Ocean, but no longer impinging on the African continent during winter.

A reversal of these conditions (i.e. increased WRZ precipitation, generally more negative phases of SAM, and reduced deposition of dust particles onto the West Antarctic Ice sheet) coincides with weaker winds over Bird Island between 0.45-0 k yr BP. The timing of this reversal is similar to the Little Ice Age, a period encapsulating major cold events in the Southern Hemisphere (0.25-0.45 k yr BP), and significant local (Foster et al. 2016; Fig. 6.4) and global cooling, during which temperatures were ~0.5˚C cooler than the 1940-1990s (Mann et al. 2009; Marcott et al. 2013). Reduced salt-spray deposition in a lake record from Marion Island at 46˚S (Perren et al. 2020) and reduced wind-driven turbulence in Lago Pato at 51˚S (Roberts et al. 2021) has also been recorded during this period. Taken together our data indicate that the wind-belt shifted equatorward, both expanding and weakening similar to the modern-winter conditions during this interval.

6.5. Modelled Southern Hemisphere westerly wind dynamics, and links to temperature and atmospheric CO_2 concentration

Mechanistic models of modern-day SHW behaviour consistently show a southward shift and strengthening of the wind-belt in response to steepening of the equatorial-pole temperature gradient caused by ozone depletion and increased greenhouse gas concentrations over recent decades (Bracegirdle et al. 2013). The same mechanism has been hypothesised to operate over centennial and millennial time-scales with periods of cooler temperatures in the extratropics expected to result in weaker, spatially diffuse and/or northward shifted winds. Similarly to the modern-day seasonal cycle between the austral summer and winter (Lamy et al. 2010; Appendix 3), warmer intervals are expected to be associated with intensification and poleward contraction of winds closer to the Antarctic coast. This relationship is reflected in the proxy records from Bird Island, which show long-term correspondence between windier periods (phases R, I, II, III) at 54˚S, and increased (local and global) temperature (Fig. 6.4).

During windier periods on Bird Island, the position of the strongest westerlies aligns more fully with the Antarctic Circumpolar Current (ACC). Climate models have indicated that such alignment of the winds causes progressively increased transport in the ACC and a shift in its position further south, mirroring the position of maximum wind-stress (Bi et al. 2002; Saenko et al. 2005; Fyfe and Saenko, 2006). As a consequence of the alignment of wind-stress with the ACC, some models indicate enhanced upwelling (and ventilation) of CO_2- rich deep water from the ocean interior, and a decline in the uptake of Carbon at the surface (Russel et al. 2006; Toggweiler et al. 2006). Conversely, periods when winds are located further equatorward (north of Bird Island), poor alignment with the ACC at the latitude of the Drake Passage has been suggested to lead to reduced wind-driven upwelling in the Southern Ocean and greater uptake of atmospheric CO_2 (Russel et al. 2006). However, the impact of this mechanism has been discussed controversially, especially over shorter timescales (Toggweiler et al. 2006; LeQuéré et al. 2007; Böning et al. 2008; Anderson et al. 2009; Toggweiler, 2009; Sime et al. 2013; Landschützer et al. 2015). Consistent with enhanced wind-driven upwelling of CO_2-rich deep water, the period of most intense winds on Bird Island (and elsewhere in the Sub-Antarctic (Unkel et al. 2010; Saunders et al. 2018)) between 7.6-4.5 k yr BP (phase III) corresponds to the distinct Holocene global climatic optimum at c. 6 k yr BP (Kaufman et al. 2020), and the period of most rapidly rising atmospheric CO_2 concentrations (especially after 6 k yr BP when wind-intensity peaked; Fig. 6.4). This linkage suggests that wind-driven upwelling is at least partially sensitive to increased wind-stress changes at the millennial- to centennial-scale.

For the first time, our highly resolved record of wind-intensity in combination with GDGT-inferred temperature on South Georgia (Foster et al. 2016), shows that the relationship between SHW-dynamics and temperature in the extratropics, is also reproduced at a multi-centennial scale between 4.5-0 k yr BP. Subsequent phases of increased wind (R, I and II) during this interval of generally weaker winds, closely track upward temperature fluctuations, especially the MCA. Cooler periods, such as the Little Ice Age, meanwhile coincide with weaker winds shifted further to the north. In terms of atmospheric CO_2 the comparatively slower rates of increase during this period are consistent with the combined effect of reduced wind-driven upwelling, stochastic variations in the quantity of CO_2 available for release from the ocean, and the development of alternative (terrestrial) sinks.

While our data provides evidence in support of long-term correspondence between the equatorial-pole temperature gradient, wind-intensity, upwelling and Southern Ocean carbon uptake at the millennial to centennial, this also suggests that the link is unlikely to be visible and therefore proven definitively using the short-term (decadal) period of instrumental observations (e.g. LeQuéré et al. 2007; Landschützer et al. 2015).

6.6. Projected future Southern Hemisphere westerly wind evolution with 21st Century warming

The sensitivity observed between relatively minor changes in temperature within the extratropics and the position and intensity of the SWW, since the mid-Holocene, indicates that the configuration of the belt will continue to change with future warming; strengthening and/or migrating further poleward, as the equatorial-pole temperature gradient increases. Our record indicates that in all identified periods of warming climate on South Georgia, winds at 54˚S have undergone an intensification. With such changes, winds that would normally bring precipitation to Southern Africa, south-western Australia and southern South America will divert further south, continuing the trend of declining moisture supply, increased drought and wildfires, observed in recent decades (Gillett et al. 2006; Trenberth et al. 2007; Cai et al. 2011; Garreaud, 2018). Increased wind intensity closer to the Antarctic coast is also likely to drive larger quantities of comparatively warm water onto the continental-shelf, leading to increased basal melting of ice-sheets and ice-shelves, reducing their buttressing effect and expediting mass loss and sea-level change (Thoma et al. 2008; Assmann et al. 2013; Hillenbrand et al. 2013). If the southward displacement and intensification persists over a centennial to millennial interval, a possible positive feedback could also arise, whereby increased wind-driven upwelling reduces the sink capacity of the Southern Ocean and allows accumulation of CO_2 in the atmosphere, thus driving further warming. What is most striking, considering future temperature projections, is that since the mid-Holocene, all phases of weakening and/or northward migrations of the wind-belt (that could reduce these impacts) have been associated with periods of decreasing global and/or regional temperature, which suggests that there is little precedent for a possible reversal of the recent intensification.

6.7. Methods

Peat coverage on Bird Island is discontinuous; to identify the deposits containing the longest (and oldest) records we conducted a survey of peat depth using an auger. A peat core was sampled using a Russian corer at Morris Point, a small (~50 m^2) area of valley floor mire located atop a low cliff (~30 m above sea-level) on the exposed west-coast, and therefore ideally positioned to record changes in sea-salt and minerogenic deposition (Fig. 6.1; Chapter 5). Present day wind exposure, quantified by measuring surface water salinity (conductivity), was the highest recorded for a peat-forming ecosystem on the island (~700 µS; Chapter 5). The core was wrapped and stored frozen after sampling. Sub-sampling at ~1 cm resolution was conducted while the core remained frozen, using a band-saw at the University of Toulouse (see De Vleeschouwer et al. 2010).

The sequence was radiometrically dated with 14 ^{14}C dates from hand-picked samples of identifiable plant macrofossils, avoiding the inclusion of root material, mineral grains or fragments of fish or bird bones. This was not possible for two samples at the base of the core where remains were too decomposed to be identified, and therefore homogenised bulk samples were dated. A Bayesian age-depth model was generated using the BACON software package for R (Blaauw, 2010; Blaauw and Christen, 2011), with uncalibrated radiocarbon age data (shown in Supplementary Table 6.1) as measured at Beta Analytic (USA).

To reconstruct past changes in SHW intensity we principally utilised the response of testate amoeba productivity to salinization, which tracks changes in the concentration of wind-blown sea-spray deposition at the coring-site through time (Whittle et al. 2019; Chapter 4-5). Testate amoebae were isolated from core subsamples using standard protocols, and enumerated to species level (see Supplementary Fig. 6.3). The concentration of tests (productivity) in each sample were determined through the addition of an exotic (*Lycopodium*) pollen spore tablet (Lund University; Stockmarr, 1971; see Whittle et al. 2019, Chapter 4-5). A total of 24 taxa were encountered. Productivity totals (used to develop the reconstruction) were calculated using a filtered subset of taxa that; 1) were present from close to the onset of peat-accumulation (defined here as before 7 k yr BP) to remove the possibly confounding effect of taxa that are more recent colonisers of the island following the last glacial period, 2) were ubiquitous (present in >80% of samples) to minimise the effect of changing community

composition, which is not necessarily directly related to salinity conditions, and 3) that exhibited no significant decline in preservation level (i.e. degradation) throughout the record. The latter was assessed for all taxa present in the core prior to 7 k yr BP and within >80% of samples, by recording the relative proportion of well-preserved to poorly-preserved specimens during counting. Poorly-preserved specimens were defined as those exhibiting damage, such as cracks to the test, missing ornamentation, or a generally degraded faint appearance. We defined well-preserved taxa as those appearing similar to modern specimens at the surface (see Chapter 5 for examples). Taxa for which the preservation ratio exhibited a statistically significant relationship with age (down-core) were subsequently removed (see Supplementary Fig. 6.5). Patterns in the productivity of the remaining taxa (i.e. Dif. Pul, Cen.aer, Pse.ful, Phr.acr, and Phr.acr.var) were highly inter-correlated, suggesting that changes occurred in response to a consistent driver (Supplementary Fig. 6.6). Population growth rates (the change in the concentration between two consecutive samples) were calculated from the productivity total by dividing by the corresponding age-span derived from the age-depth model. Values of alpha-diversity, and Shannon-Weaver diversity index (SWDI; Shannon Weaver, 1949) (calculated in the R package 'vegan' (Oksanen et al. 2016)), included all identified taxa. SWDI provides a broad indication of the relative 'health' of the sampled community of testate amoebae and therefore the suitability of environmental conditions. For soil microorganism communities, values 0.5-1.5 generally characterize harsh and unfavourable conditions, 1.5-2.5 indicate intermediate conditions, and favourable conditions are represented by values >2.5 (Patterson and Kumar, 2002; Riveiros et al, 2007; Neville et al, 2010). Faunistic zones within the testate amoeba relative abundance data were defined by constrained incremental sum of squares (CONISS) stratigraphically constrained cluster analysis, with broken stick analysis to identify the number of statistically significant groups, in the software packages 'vegan' (Oksanen et al. 2016) and 'rioja' for R (Juggins, 2015; R core development team, 2013).

The reconstruction was compared with a potential independent measure of sea-spray aerosol deposition (Br), based on ITRAX micro-X-ray fluorescence (µXRF) data and two measures of wind-blown dust deposition (Ti and loss on ignition). These data were also supported by measurements of >2 mm diameter mineral grain deposition and carbon accumulation. ITRAX µXRF measurements were undertaken using a Molybdenum X-ray tube (run settings: 30 kV, 50 mA, 1 mm

interval 10 second count time per interval) at Aberystwyth University. Machine and sample calibration was undertaken using a synthetic glass standard at the start and end of each measurement session. µXRF spectra peak areas were quantified using Q-Spec 6.5 spectra matching software (Cox Analytical). A full summary of the µXRF core scanning geochemical data is given in Supplementary Fig. 6.4. To account for down-core variability in water and organic matter content, element and scatter parameter counts per second (cps) were normalised by the total scatter cps (incoherent + coherent). Data are presented as percentages of the total scatter-normalised ratio (TSN) to examine covariance between measured elemental and scattering parameters (Roberts et al. 2017). Lithological zones were defined using CONISS stratigraphically constrained cluster analysis (as outlined above).

Bulk density (g cm^3) and Loss on ignition (LOI; %), a measure of mineral content, were measured contiguously for each ~1 cm sub-sample of the core using a standard protocol (Chambers et al. 2011). Mineral grains >2 mm in diameter were separated from LOI residues by wet sieving. The isolated grains were then freeze-dried and weighed, allowing changes in grain abundance to be expressed as a percentage of the total dry sample weight. For each sub-sample, the rate of carbon accumulation was calculated by firstly combining carbon content (assumed to be half the LOI total (Loisel et al. 2014)) and bulk density values (to obtain carbon content), before dividing by the peat accumulation rate (derived from the age-depth model) (Tolonen and Turunen, 1996).

Statistical analysis of the proxies was conducted in R (R core development team, 2013) at original resolution. To assess correlation between proxies, data were re-sampled at 100-year and smoothed (LOESS; local tricube weighting and second order polynomial regression) prior to analysis.

A second core was also sampled at Molly Meadows (Fig. 6.1) which lies further inland of the west coast in a more sheltered position, with the coring site itself elevated slightly above the immediate surroundings. However, subsequent analysis (using the methods outlined above) indicated that the archive did not sensitively record changes in westerly wind, and therefore was not included in this study.

6.8. References

Abram, N. J., Mulvaney, R., Vimeux, F., Phipps, S. J., Turner, J. and England, M. H. (2014) Evolution of the Southern Annular Mode During the past millennium, *Nature Climate Change*, 4:564-569.

Anderson, R. F., Ali, S., Bradtmiller, L. I., Nielsen, S. H. H., Fleisher, M. Q., Anderson, B. E. and Burckle, L. H. (2009) Wind-Driven Upwelling in the Southern Ocean and the Deglacial Rise in Atmospheric CO_2, *Science*, 323: 1443-1448.

Assmann, K. M., Jenkins, A., Shoosmith, D. R., Walker, D. P., Jacobs, S. S. and Nicholls, K. W. (2013) Variability of Circumpolar Deep Water transport onto the Amundsen Sea Continental shelf through a shelf break trough, *Journal of Geophysical Research,* 118(12): 6603-6620.

Beck, K. K., Fletcher, M-S., Kattel, G., Barry, L. A., Gadd, P. S., Heijnis, H., Jacobsen, G. E. and Saunders, K. M. (2018) The indirect response of an aquatic ecosystem to long-term climate-driven terrestrial vegetation in a subalpine temperate lake, *Journal of Biogeography,* 45(3): 713-725.

Bertrand, S., Lange, C.B., Pantoja, S., Hughen, K., Van Tornhout, E. and Wellner, J.S. (2017) Postglacial fluctuations of Cordillera Darwin glaciers (southernmost Patagonia) reconstructed from Almirantazgo fjord sediments, *Quaternary Science Reviews,* 177: 265-275.

Bi, D., Budd, W. F., Hirst, A. C. and Wu, X. (2002) Response of the Antarctic Circumpolar Current transport to global warming in a coupled model, *Geophysical Research Letters,* 29: doi: 10.1029/2002GL015919.

Biastoch, A., Böning, C. W., Schwarzkopf, F. U. and Lutjeharms, J. R. E. (2009) Increase in Agulhas leakage due to poleward shift in the southern hemisphere westerlies, *Nature,* 462: 495–498.

Blaauw, M. and Christen, J. A. (2011) Flexible palaeoclimate age-depth models using an autoregressive gamma process, *Bayesian Analysis,* 6(3): 457-474.

Blaauw, M. (2010) Methods and code for 'classical' age-modelling of radiocarbon sequences, *Quaternary Geochronology,* 5: 512-518.

Böning, C. W., Dispert, A., Visbeck, M., Rintoul, S. R. and Schwarzkopf, F. U. (2008) The response of the Antarctic Circumpolar Current to recent climate change, *Nature Geoscience,* 1: 864-869.

Bracegirdle, T. J., Shuckburgh, E., Sallee, J-B., Wang, Z., Meijers, A. J. S., Bruneau, N., Phillips, T. and Wilcox, L. J. (2013) Assessment of surface winds over the Atlantic, Indian, and Pacific Ocean sectors of the Southern Ocean in CMIP5 models: historical bias, forcing response, and state dependence, *Journal of Geophysical Research,* 118: 547-562.

Bradley, R. S., Hughes, M. and Diaz, H. F. (2003) Climate in Medieval Time, *Science*, 302(5644): 404-405.

Cai, W., Van Rensch, P., Borlace, S. and Cowan, T. (2011) Does the Southern Annular Mode contribute to the persistence of the multidecade-long drought over southwest Western Australia?, *Geophysical Research Letters,* 38: L14712, doi:10.1029/2011GL047943.

Cai, W. (2006) Antarctic ozone depletion causes an intensification of the Southern Ocean super-gyre circulation, *Geophysical Research Letters,* 33: L03712, doi:10.1029/2005GL024911.

Chambers, F. M., Beilman, D. W. and Yu, Z. (2011) Methods for determining peat humification and for quantifying peat bulk density, organic matter and carbon content for palaeostudies of climate and peatland carbon dynamics, *Mires and Peat,* 7: 1-10.

De Vleeschouwer, F., Chambers, F. M. and Swindles, G. T. (2010) Coring and sub-sampling of peatlands for palaeoenvironmental research, *Mires and Peat,* 7(1): 1-10.

Douglass, D. C., Singer, B. S., Kaplan, M. R., Ackert, R. P., Mickelson, D. M. and Caffee, M. W. (2005) Evidence of early Holocene glacial advances in southern South America from cosmogenic surface-exposure dating, *Geology,* 33: 237-240.

Fletcher, M-S. and Moreno, P. I. (2011) Zonally symmetric changes in the strength and position of the Southern Westerlies drove atmospheric CO_2 variations over the past 14 k.y., *Geology,* 39(5): 419-422.

Fletcher, M-S. and Moreno, P. I. (2012) Have the Southern Westerlies changed in a zonally symmetric manner over the last 14,000 years? A hemisphere-wide take on a controversial problem, *Quaternary International,* 253: 32-46.

Foster, L. C., Pearson, E. J., Juggins, S., Hodgson, D. A., Saundersm K. M., Verleyen, E. and Roberts, S. J. (2016) Development of a regional glycerol dialkyl glycerol tetraether (GDGT)-temperature calibration for Antarctic and sub-Antarctic lakes, *Earth and Planetary Science Letters,* 433: 370-379.

Fyfe, J. C. and Saenko, O. A. (2006) Simulated changes in extratropical Southern Hemisphere winds and currents, *Geophysical Research Letters,* 33: L06701.

Garreaud, R. D. (2018) Record-breaking climate anomalies lead to severe drought and environmental disruption in western Patagonia in 2016, *Climate Research,* 74: 217-229.

Gillett, N. P., Kell, T. D. and Jones, P. D. (2006) Regional climate impacts of the Southern Annular Mode, *Geophysical Research Letters,* 33: L23704.

Gilli, A., Ariztegui, D., Anselmetti, F. S., McKenzie, J. A., Markgraf, V., Hajdas, I. and McCulloch, R. D. (2005) Mid-Holocene strengthening of the Southern

Westerlies in South America - Sedimentological evidences from Lago Cardiel, Argentina (49°S), *Global and Planetary Change,* 49: 75-93.

Hillenbrand, C-D., Kuhn, G., Smith, J. A., Gohl, K., Graham, A. G. C., Larter, R. D., Klages, J. P., Downey, R., Moreton, S. G., Forwick, M. and Vaughan, D. G. (2013) Grounding-line retreat of the West Antarctic Ice Sheet from inner Pine Island Bay, *Geology,* 41(1): 35-38.

Hodgson, D. A. and Sime, L. C. (2010) Southern Westerlies and CO_2, *Nature Geoscience,* 3: 666-667.

Holland, P. R., Bracegirdle, T. J., Dutrieux, P., Jenkins, A. and Steig, E. J. (2019) West Antarctic ice loss influenced by internal climate variability and anthropogenic forcing, *Nature Geoscience,* 12: 718-724.

Hunter, I., Croxall, J. P. and Prince, P. A. (1982) The distribution and abundance of burrowing seabirds (Procellariiformes) at Bird Island, South Georgia; I. Introduction and Methods, *British Antarctic Survey Bulletin,* 56: 49-67.

Juggins, S. (2015) Rioja: Analysis of Quaternary Science Data. R Package version 0.9-26, https://cran.r-project.org/web/packages/rioja

Kaufman, D., McKay, N., Routson, C., Erb, M., Dätwyler, C., Sommer, P. S., Heiri, O. and Davis, B. (2020) Holocene global mean surface temperature, a multi-method reconstruction approach, *Scientific Data,* 7: 201.

Keppler, F., Eiden, R., Niedan, V., Pracht, J., Scholer, H. F. (2000) Halocarbons produced by natural oxidation processes during degradation of organic matter, *Nature,* 403: 298-301.

Kilian, R. and Lamy, F. (2012) A review of Glacial and Holocene paleoclimate records from southernmost Patagonia (49-55˚S), *Quaternary Science Reviews,* 53: 1-23.

Koffman, B. G., Kreutz, K. J., Breton, D. J., Kane, E. J., Winski, D. A., Birkel, S. D., Kurbatov, A. V. and Handley, M. J. (2014) Centennial-scale variability of the Southern Hemisphere westerly wind belt in the eastern Pacific over the past two millennia, *Climate of the past,* 10: 1125-1144.

Lamy, F., Hebbeln, D., Röhl, U., Wefer, G. (2001) Holocene rainfall variability in southern Chile: a marine record of latitudinal shifts of the Southern Westerlies, *Earth and Planetary Science Letters,* 185: 369-382.

Lamy, F., Killian, R., Arz, H. W., Francois, J-P., Kaiser, J., Prange, M. and Steinke, T. (2010) Holocene changes in the position and intensity of the southern westerly wind belt, *Nature Geoscience,* 3: 695-699.

Landschützer, P., Gruber, N., Haumann, F. A., Rödenbeck, C., Bakker, D. C. E., van Heuven, S., Hoppema, M., Metzl, N., Sweeney, C., Takahashi, T., Tilbrook, B. and Wanninkhof, R. (2015) The reinvigoration of the Southern Ocean carbon sink, *Science,* 349(6253): 1221-1224.

Le Quéré, C., Rödenbeck, C., Buitenhuis, E. T., Conway, T. J., Langenfelds, R., Gomez, A., Labuschagne, C., Ramonet, M., Nakazawa, T., Metzl, N., Gillett, N. and Heimann, M. (2007) Saturation of the Southern Ocean CO_2 sink due to recent climate change, *Science,* 316: 1735-1737.

Lee-Taylor, J. and Holland, E. (2000) Litter decomposition as a potential natural source of methyl bromide, *Journal of Geophysical Research,* 105: 8857-8864.

Loisel, J., Yu, Z., Beilman, D. W., Camill, P., Alm, J., Amesbury, M. J., Anderson, D. *et al.* (2014) A Database and Synthesis of Northern Peatland Soil Properties and Holocene Carbon and Nitrogen Accumulation, *The Holocene,* 24(9): 1028–42.

Lovenduski, N. S., Gruber, N. and Doney, S. C. (2008) Towards a mechanistic understanding of the decadal trends in the Southern Ocean carbon sink, *Global Biogeochemical Cycles,* 22: GB3016.

Mann, M. E., Zhang, Z., Rutherford, S., Bradley, R. S., Hughes, M. K., Shindell, D., Ammann, C., Faluvegi, G. and Ni, F. (2009) Global signatures and dynamical origins of the Little Ice Age and Medieval Climate Anomaly, *Science,* 326(5957): 1256-1260.

Marcott, S. A., Shakun, J. D., Clark, P. U. and Mix, A. C. (2013) A reconstruction of regional and global temperature for the past 11,300 years, *Science,* 339(6124): 1198-1201.

Marshall, G. J., Orr, A., van Lipzig, N. P. M and King, J. C. (2006) The impact of a changing Southern Hemisphere Annular Mode on Antarctic Peninsula summer temperatures, *Journal of Climate,* 19(20): 5388-5404.

Mayr, C., Wille, M., Haberzettl, T., Fey, M., Janssen, S., Lücke, A., Ohlendorf, C., Oliva, G., Schäbitz, F., Schleser, G. H. and Zolitschka, B. (2007) Holocene variability of the Southern Hemisphere westerlies in Argentinean Patagonia (52˚S), *Quaternary Science Reviews,* 26: 579-584.

Mazei, Y. A., Lebedeva, N. V., Taskaeva, A. A., Ivanovsky, A. A., Chernyshov, V. A., Tsyganov, A. N. and Payne, R. J. (2018) Potential influence of birds on soil testate amoebae in the Arctic, *Polar Science,* 16: 78-85.

McCulloch, R. D., Blaikie, J., Jacob, B., Mansilla, C. A., Morello, F., De Pol-Holz, R., San Román, M., Tisdall, E. and Torres, J. (2020) Late glacial and Holocene climate variability, southernmost Patagonia, *Quaternary Science Reviews*, 229: 106131.

McGlone, M. S., Moar, N. T., Wardle, P. and Meurk, C. D. (1997) Late-glacial and Holocene vegetation and environment of Campbell Island, far southern New Zealand, *The Holocene,* 7(1): 1-12.

Moreno, P. I., Villa-Martinez, R., Cardenas, M. L. and Sagredo, E.A. (2012) Deglacial changes of the southern margin of the southern westerly winds

revealed by terrestrial records from SW Patagonia (52 degrees S), *Quaternary Science Reviews*, 41:1-21.

Moreno, P. I., Vilanova, I., Villa-Martínez, R., Dunbar, R. B., Mucciarone, D. A., Kaplan, M. R., Garreaud, R. D., Rojas, M., Moy, C. M., De Pol-Holz, R., Lambert, F. (2018) Onset and Evolution of Southern Annular Mode-Like Changes at Centennial Timescale, *Scientific Reports,* 8: 3458.

Neville, L. A., Christie, D. G., McCarthy, F. M. G. and MacKinnon, M. D. (2010) Biogeographic variation in Thecamoebian (Testate amoebae) assemblages in lakes within various vegetation zones of Alberta, Canada, *International Journal of Biodiversity and Conservation,* 2(8): 215-224.

Oksanen, J., Blanchet, F. G., Kindt, R., Legendre, P., Minchin, P. R., O'Hara, R. B., Simpson, G. L., Solymos, P., Henry, M., Stevens, H. and Wagner, H. (2016) Package 'vegan: community ecology', R package version 2.3-0.

Patterson, R. T. and Kumar, A. (2002) A review of current testate rhizopod (thecamoebian) research in Canada, *Palaeogeography Palaeoclimatology Palaeoecology,* 180(1-3): 225-251.

Perren, B. B., Hodgson, D. A., Roberts, S. J., Sime, L., Van Nieuwenhuyze, W., Verleyen, E. and Vyverman, W. (2020) Southward migration of the Southern Hemisphere westerly winds corresponds with warming climate over centennial timescales, *Communications Earth and Environment,* 1(58): 1-8.

Pritchard, H. D., Ligtenberg, S. R. M., Fricker, H. A., Vaughan, D. G., van den Broeke, M. R. and Padman, L. (2012) Antarctic ice-sheet loss driven by basal melting of ice shelves, *Nature,* 484: 502-505.

Purich, A., Cai, W. J., England, M. H. and Cowan, T. (2016) Evidence for link between modelled trends in Antarctic sea ice and underestimated westerly wind changes, *Nature Communications,* 7: 10409.

Quade, J. and Kaplan, M. R. (2017) Lake-level stratigraphy and geochronology revisited at Lago (Lake) Cardiel, Argentina, and changes in the Southern Hemispheric Westerlies over the last 25 ka, *Quaternary Science Reviews,* 177: 173-188.

R Core Team (2013) R: A language and environment for statistical computing. R Foundation from statistical computing, Vienna, Austria. http://www.R-project.org/

Ritter, R., Landschützer, P., Gruber, N., Fay, A. R., Iida, Y., Jones, S., Nakaoka, S., G-H, Park., Peylin, P., Rödenbeck, C., Rodgers, K. B., Shutler, J. D. and Zeng, J. (2017) Observation-based trends of the Southern Ocean carbon sink, *Geophysical Research Letters,* 44(12): 12,339-12,348.

Rivieros, N. V., Babalola, A. O., Boudreau, R. E. A., Patterson, R. T., Roe, H. M. and Doherty, C. (2007) Modern distribution of salt marsh foraminifera and

thecamoebians in the Seymour-Belize Inlet Complex, British Columbia, Canada, *Marine Geology,* 242(1-3): 39-63.

Roberts, S. J., Monien, P., Foster, L. C., Loftfield, J., Hocking, E. P., Schnetger, B., Pearson, E. J., Juggins, S., Fretwell, P., Ireland, L., Ochyra, R., Haworth, A. R., Allen, C. S., Moreton, S. G., Davies, S. J., Brumsack, H-J., Bentley, M. and Hodgson, D. A. (2017) Past penguin colony responses to explosive volcanism on the Antarctic Peninsula, *Nature Communications,* 8: 14914.

Roberts, S. J., McCulloch, R., Van Nieuwenhuyze, W., Sterken, M., Heirman, K., Van Wichelen, J., Diaz, C., Van de Vyver, E., Emmings, J., Whittle, A., Hodgson, D. A., Vverman, W. and Verleyen, E. (2021) Late Glacial and Holocene history of the Última Esperanza region of Southern Patagonia, *Quaternary Science Reviews* (in review).

Rouault, M., Melice, J. L., Reason, C. J. C. and Lutijeharms, J. R. E. (2005) Climate variability at Marion Island, Southern Ocean, since 1960, *Journal of Geophysical Research,* 110.

Russell, J. L., Dixon, K. W., Gnanadesikan, A., Stouffer, R. J. and Toggweiler, J. R. (2006) The Southern Hemisphere Westerlies in a warming world: Propping open the door to the deep ocean, *Journal of Climate,* 19(24): 6382-6390.

Saenko, O. A., Fyfe, J. C. and England, M. H. (2005) On the response of the oceanic wind-driven circulation to atmospheric CO2 increase, Climate Dynamics, 25: 415-426.

Saunders, K. M., Roberts, S. J., Perren, B., Butz, C., Sime, L., Davies, S., Van Nieuwenhuyze, W., Grosjean, M. and Hodgson, D. A. (2018) Holocene dynamics of the Southern Hemisphere westerly winds and possible links to CO_2 outgassing, *Nature Geoscience,* 11: 650-655.

Schaefer, J. M., Denton, G. H., Kaplan, M., Putnam, A., Finkel, R. C., Barrell, D. J. A., Anderson, B. G., Schwartz, R., Mackintosh, A., Chinn, T. and Schlüchter, C. (2009) High-frequency Holocene glacier fluctuations in New Zealand differ from the Northern Signature, *Science,* 324(5927): 622-625.

Schmale, j., Schneider, J., Nemitz, E., Tang, Y. S., Dragosits, U., Blackall, T. D., Trathan, P. N., Phillips, G. J., Sutton, M. and Braban, C. F. (2013) Sub-Antarctic marine aerosol: dominant contributions from biogenic sources, *Atmospheric Chemistry and Physics,* 13: 8669-8694.

Shannon, C. and Weaver, W. (1949) The mathematical theory of communication, *University of Illinois, Urbana.*

Shotyk, W., Goodsite, M. E., Roos-Barraclough, F., Frei, R., Heinemeier, J., Asmund, G., Lohse, C. and Hansen, T. S. (2003) Anthropogenic contributions to atmospheric Hg, Pb, and As accumulation recorded by peat cores from southern Greenland and Denmark dated using the ^{14}C 'bomb pulse curve', *Geochemica et Cosmochimica Acta,* 67(21): 3991-4011.

Sime, L. C., Kohfeld, K. E., Le Quéré, C., Wolff, E. W., de Boer, A. M., Graham, R. M. and Bopp, L. (2013) Southern Hemisphere westerly wind changes during the Last Glacial Maximum: model-data comparison, *Quaternary Science Reviews,* 64: 104-120.

Stager, J. C., Mayewski, P. A., White, J., Chase, B. M., Neumann, F. H., Meadows, M. E., King, C. D. and Dixon, D. A. (2012) Precipitation variability in the winter rainfall zone of South Africa during the last 1400 yr linked to the austral westerlies, *Climate of the Past,* 8: 877-887.

Stockmarr, J. (1971) Tablets with spores in absolute pollen analysis, *Pollen et spores,* 13: 615-621.

Strother, S. L., Salzmann, U., Roberts, S. J., Hodgson, D. A., Woodward, J., Van Nieuwenhuyze, W., Verleyen, E., Vyverman, W. and Moreton, S. G. (2014) Changes in Holocene climate and the intensity of Southern Hemisphere Westerly Winds based on a high-resolution palynological record from sub-Antarctic South Georgia, *The Holocene,* 25(2): 1-17.

Thoma, M., Jenkins, A., Holland, D. and Jacobs, S. (2008) Modelling Circumpolar Deep Water intrusions on the Amudsen Sea continental shelf, Antarctica, *Geophysical Research Letters,* 35: L18602.

Thompson, D. W. J. and Solomon, S. (2002) Interpretation of recent Southern Hemisphere climate change, *Science,* 296(5569): 895-899.

Thompson, D. W. J., Solomon, S., Kushner, P. J., England, M. H., Grise, K. M. and Karoly, D. J. (2011) Signatures of the Antarctic ozone hole in Southern Hemisphere surface climate change, *Nature Geoscience,* 4(11): 741-749.

Toggweiler, J. R., Russell, J. L. and Carson, S. R. (2006) Midlatitude westerlies, atmospheric CO_2 and climate change during the ice ages, *Palaeoceanography,* 21: PA2005.

Toggweiler, J. R. (2009) Shifting Westerlies, *Science,* 323: 1434-1435.

Tolonen, K. and Turunen, J. (1996) Accumulation rates of carbon in mires in Finalnd and implications for climate change, *The Holocene,* 6(2): 171-178.

Trenberth, K. E. *et al* Observations: Surface and atmospheric climate change *in Climate Change 2007. The physical science basis. Contribution of working-group 1 to the Fourth Assessment Report of the Intergovernmental Panel on Climate Change.* (Eds. Solomon, S *et al.)* 235-336 (Cambridge University Press, 2007).

Turner, T. E., Swindles, G. T. and Roucoux, K. H. (2014) Late Holocene ecological and carbon dynamics of a UK raised bog: impact of human activity and climate change, *Quaternary Science reviews,* 84: 65-85.

Turney, C. S. M., McGlone, M., Palmer, J., Fogwill, C., Hogg, A., Thomas, Z. A., Lipson, M., Wilmshurst, J. M., Fenwick, P., Jones, R. T., Hines, B. and Clark,

G. F. (2016a) Intensification of Southern Hemisphere westerly winds 2000-1000 years ago: evidence from the subantarctic Campbell and Auckland Islands (52-50˚S), *Journal of Quaternary Science,* 31(1): 12-19.

Turney, C. S. M., Jones, R. T., Fogwill, C., Hatton, J., Williams, A. N., Hogg, A., Thomas, Z. A., Palmer, J., Mooney, S. and Reimer, R. W. (2016b) A 250-year periodicity in Southern Hemisphere westerly winds over the last 2600 years, *Climate of the past,* 12: 189-200.

Ummenhofer, C. C. and England, M. H. (2007) Interannual extremes in New Zealand precipitation linked to modes of Southern Hemisphere climate variability, *Journal of Climate,* 20: 5418-5440.

Ummenhofer, C. C., Gupta, A. and England, M. H. (2009) Causes of late twentieth-century trends in New Zealand precipitation, *Journal of Climate,* 22: 3-19.

Unkel, I., Fernandez, M., Björck, S., Ljung, K. and Wohlfarth, B. (2010) Records of environmental changes during the Holocene from Isla de los Estados (54.4˚S), southeastern Tierra del Fuego, *Global and Planetary Change,* 74: 99-113.

Van der Putten, N., Mauquoy, D., Verbruggen, C. and Björck, S. (2012) Subantarctic peatlands and their potential as palaeoenvironmental and palaeoclimatic archives, *Quaternary International,* 268: 65-76.

Vaughan, D. G., Marshall, G. J., Connolley, W. M., Parkinson, C., Mulvaney, R., Hodgson, D. A., King, J. C., Pudsey, C. J. and Turner, J. (2003) Recent rapid regional climate warming on the Antarctic Peninsula, *Climatic Change,* 60(3): 243-274.

Vincke, S., Van de Vijver, B., Ledeganck, P., Nijs, I. and Beyens, L. (2007) Testacean communities in perturbed soils: the influence of the wandering albatross, *Polar Biology,* 30: 395-406.

Whittle, A., Amesbury, M. J., Charman, D. J., Hodgson, D. A., Perren, B. B., Roberts, S. J. and Gallego-Sala, A. (2019) Salt-enrichment impact on biomass production in a natural population of peatland dwelling Arcellinida and Euglyphida (Testate amoebae), *Microbial Ecology,* 78: 534-538.

Yang, L., Gao, Y., Sun, L., Xie, Z., Yang, W., Chu, Z., Wang, Y. and Xu, Q. (2019) Enhanced westerlies drove penguin movement at 1000 yr BP on Ardley Island, west Antarctic Peninsula, *Quaternary Science Reviews,* 214: 44-53.

Zhao, X., Dupont, L., Schefuß, E., Meadows, M. E., Hahn, A. and Wefer, G. (2016) Holocene vegetation and climate variability in the winter and summer rainfall zones of South Africa, *The Holocene,* 26(6).

Zolitschka, B., Anselmetti, F., Ariztegui, D., Corbella, H., Francus, P., Lücke, A., Maidana, N. I., Ohlendorf, C., Schäbitz, F. and Wastegård, S. (2013) Environment and climate of the last 51,000 years – new insights from the

Potrok Aike maar lake Sediment Archive Drilling prOject (PASADO), *Quaternary Science Reviews,* 71: 1-12.

Zolitschka, B., Fey, M., Janssen, S., Maidana, N. I., Mayr, C., Wulf, S., Haberzettl, T., Corbella, H., Lücke, A., Ohlendorf, C. and Schäbitz, F. (2019) Southern Hemispheric Westerlies control sedimentary processes of Laguna Azul (south-eastern Patagonia, Argentina), *The Holocene,* 29: 403-420.

6.9. Supplementary Information

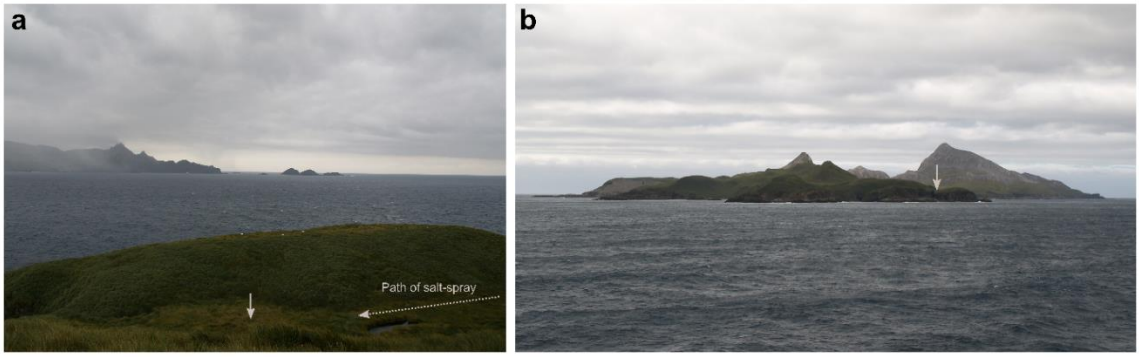

Supplementary Figure 6.1 | Photograph showing the valley floor mire at Morris Point, and path of wind-blown salt-spray into the site (a) and the context of the site on Bird Island when viewed from the west. Coring location is indicated by the grey arrow.

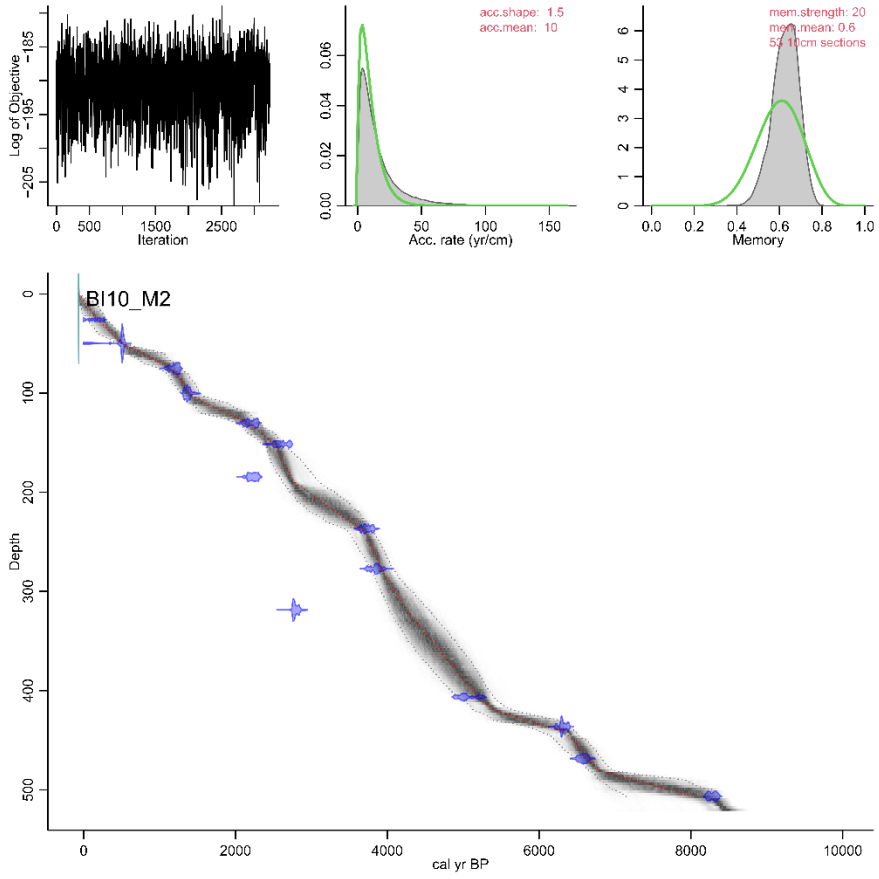

Supplementary Figure 6.2 | Age-depth model for the record from Morris Point (red), and the individual ^{14}C dates from which it was calculated (blue; 95% probability distributions).

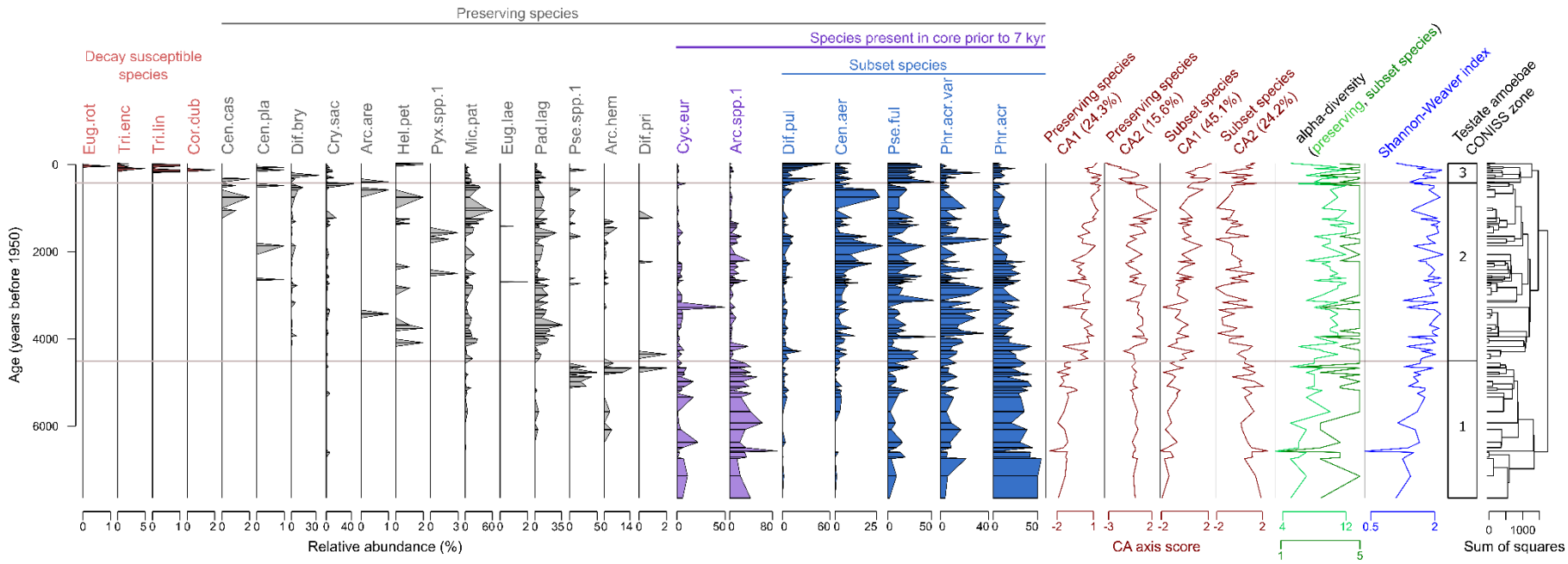

Supplementary Figure 6.3 | Relative abundance of all taxa identified in the core from Morris Point. Subset species were those included in productivity totals. A full list full species names is given in Supplementary Table 6.2.

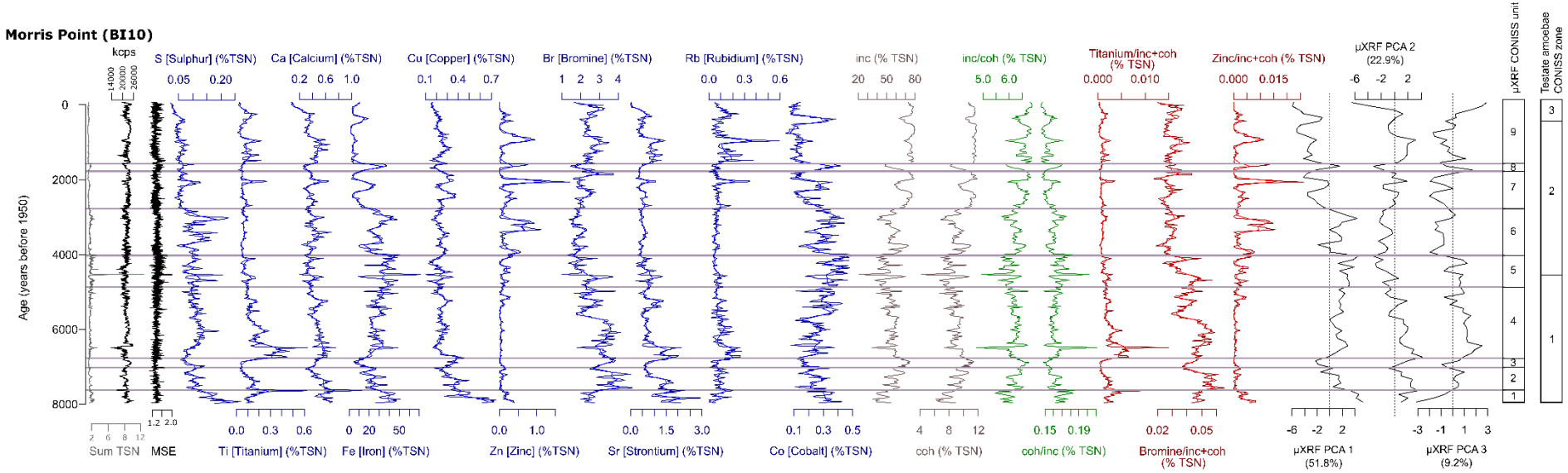

Supplementary Figure 6.4 | Summary of µ-XRF core-scanning geochemical data and lithological zones within the Morris Point record.

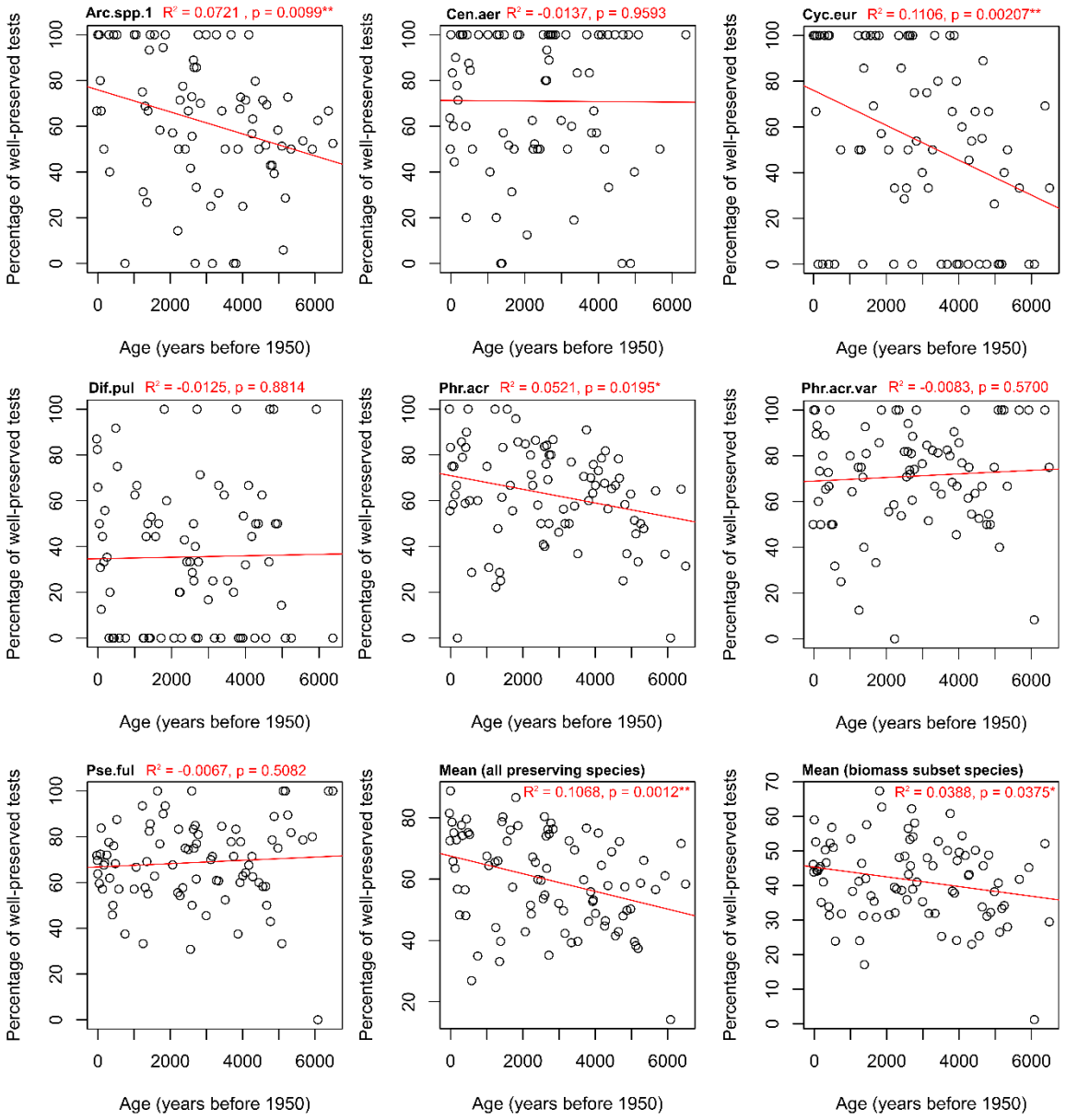

Supplementary Figure 6.5 | Preservation of key testate amoebae species within the Morris Point record.

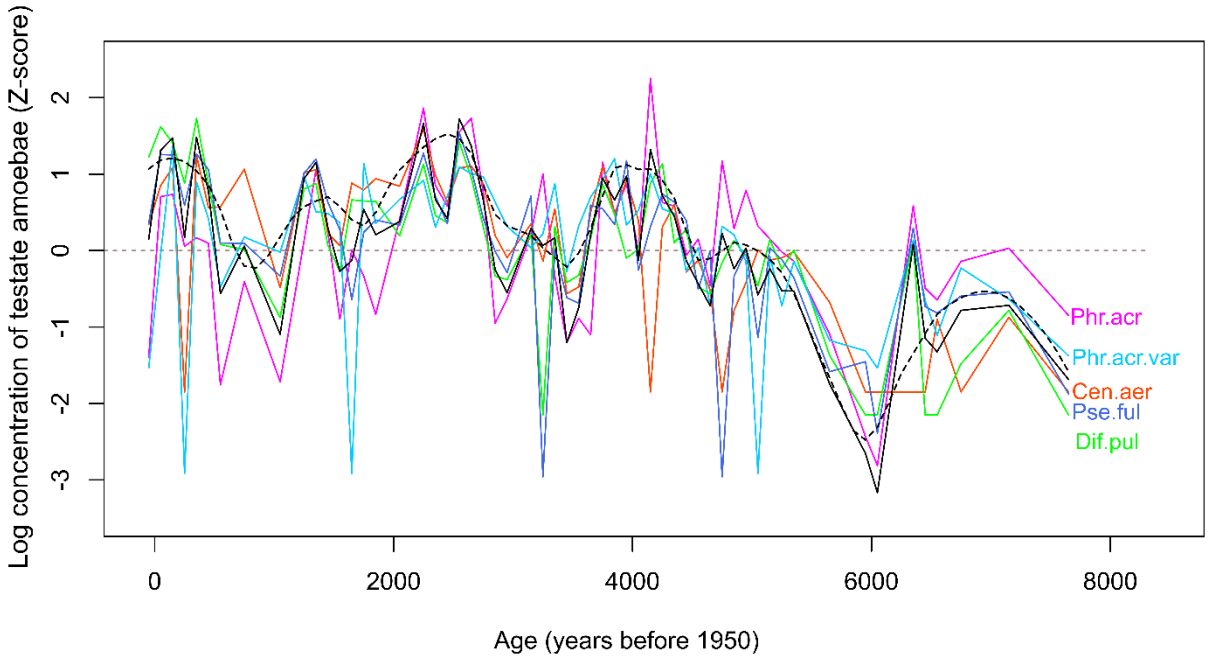

Supplementary Figure 6.6 | Productivity of each key species within the Morris Point record (coloured lines) and the total when these species are combined (solid black line). Productivity data were converted to Z-scores to compare relative trends. Black dotted line indicates a LOESS 2nd order polynomial smooth of the total productivity.

Supplementary Table 6.1 | Radiocarbon data from the Morris Point peat core used in this study.

													SH13 calibrated ages (cal. a BP) From OXCAL							
ID number	ID/Number of analysing lab	Core section code	Field measured depth (cm)	Depth in mastercore (cm)	Description of material dated	Pre-treatment	δ13C (‰) ± 0.1 (1σ)	Measured 14C age (14C a BP)					95.4% range			Median	Mean		1σ
BI10_21	Beta-513550	BI10.1	26	26	Plant material	Acid/Alkali/Acid	-28.3	190	±	30			285	-	...	177	165	±	82
BI10_54	Beta-517306	BI10.2	55.8	49.8	Plant material	Acid/Alkali/Acid	-27.5	500	±	30			542	-	475	510	509	±	17
BI_10_76	Beta-503767	BI10.2	81.1	75.1	Plant material	Acid/Alkali/Acid	-28.7	1310	±	30			1274	-	1091	1214	1200	±	53
BI10_101	Beta513551	BI10.3	100.3	100.3	Plant material	Acid/Alkali/Acid	-28.3	1530	±	30			1422	-	1307	1364	1366	±	33
BI10_143	Beta-517307	BI10.4	139.2	130.2	Plant material	Acid/Alkali/Acid	-27.8	2210	±	30			2310	-	2085	2188	2197	±	71
BI10_161	Beta-513552	BI10.4	160.5	151.5	Plant material	Acid/Alkali/Acid	-27.5	2560	±	30			2745	-	2470	2593	2604	±	82
BI10_195	Beta-517308	BI10.5	192	184.5	Plant material	Acid/Alkali/Acid	-28.6	2240	±	30			2324	-	2110	2229	2225	±	56
BI_10_244	Beta-503769	BI10.6	240.8	236.8	Plant material	Acid/Alkali/Acid	-28.8	3500	±	30			3835	-	3632	3724	3731	±	61
BI10_279	Beta-513553	BI10.7	275.2	277.2	Plant material	Acid/Alkali/Acid	-28.2	3600	±	30			3969	-	3720	3853	3844	±	63
BI_10_320	Beta-503770	BI10.8	314.7	318.7	Plant material	Acid/Alkali/Acid	NA	2710	±	30			2848	-	2745	2777	2786	±	31
BI_10_412	Beta-503771	BI10.10	407.5	406.5	Plant material	Acid/Alkali/Acid	-25.5	4470	±	30			5278	-	4870	5017	5046	±	114
BI10_441	Beta-513554	BI10.11	433.3	436.3	Plant material and organic sediment (peat)	Acid washes	-30.6	5550	±	30			6400	-	6216	6304	6313	±	43
BI10_473	Beta-517310	BI10.12	463.5	468.5	Homogenous bulk organic material (peat)	Acid washes	-28.7	5820	±	30			6667	-	6487	6579	6577	±	50
BI10.13_48-49cm	Beta-478305	BI10.13	504.5	506.5	Homogenous bulk organic material (peat)	Acid washes	-28.1	7510	±	30			8370	-	8196	8287	8282	±	51

Supplementary Table 6.2 | List of taxa encountered within the Morris Point record. * Indicates that taxa were used to calculate productivity totals.

ID code	Taxon name	Authority
Arc.are	*Arcella arenaria*	Greef 1866
Arc.hem	*Arcella hemisphaerica*	Perty 1852
Arc.spp.1	*Arcella* spp.1	*See Chapter 5*
Cen.aer *	*Centropyxis aerophila*	Deflandre 1929
Cen.cas	*Centropyxis cassis* type	(Wallich 1864) Deflandre 1929
Cen.pla	*Centropyxis platystoma* type	(Penard 1890) Deflandre 1929
Cor.dub	*Corythion dubium*	Taránek 1871
Cry.sac	*Cryptodifflugia sacculus*	Penard 1902
Cyc.eur	*Cyclopyxis eurystoma*	Deflandre 1929
Dif.bry	*Difflugia bryophila*	(Penard, 1902) Jung, 1942
Dif.pri	*Difflugia pristis* type	Penard 1902
Dif.pul *	*Difflugia pulex*	Penard 1902
Eug.lae	*Euglypha laevis*	(Ehrenberg, 1845)
Eug.rot	*Euglypha rotunda*	Ehrenberg, 1845
Hel.pet	*Heleopera petricola*	Leidy, 1879
Mic.pat	*Microchlamys patella*	(Claparède and Lachmann 1859) Cockerell 1911
Pad.lag	*Padaungiella lageniformis*	(Penard 1902) Lara and Todorov 2012
Phr.acr *	*Phryganella acropodia*	(Hertwig and Lesser 1874) Hopkinson 1909
Phr.acr.var *	*Phryganella acropodia* var.	*See Chapter 5*
Pse.ful *	*Pseudodifflugia fulva*	Archer 1870
Pse.spp.1	*Pseudodifflugia* spp.1	
Pyx.spp.1	*Pyxidicula* spp.1	
Tri.enc	*Trinema enchelys*	Ehrenberg, 1838
Tri.lin	*Trinema lineare*	Penard, 1890

Chapter 7

Conclusions

Shifts in the latitudinal position and intensity of the Southern Hemisphere westerly winds (SHW) over the Southern Ocean have important and far-reaching implications for global climate and the physical environment in the southern high latitudes. Despite this, limited understanding of their behaviour over millennial timescales reduces our ability to project how they will change in future. Existing reconstructions of SHW behaviour during the Holocene present an inconsistent picture, predominantly because of the limited spatial and temporal resolution of comparable records from inside the core wind-belt (50-55˚S), and long-term reliance on proxies that have a convoluted relationship with wind-conditions (Chapter 1).

Seeking to circumvent these issues, the first aim of this thesis was to establish whether communities of sub-Antarctic peat-dwelling testate amoebae can act as a proxy for changing SHW conditions. The hypothesis underlying this proposed proxy stated that wind-strength could be reconstructed by using testate amoebae to track the deposition of wind-blown salt-spray into the (coastal) freshwater-peatlands that they inhabit; where periods of more (less) salt-spray deposition would reflect stronger (weaker) winds. Consequently, two research questions were selected to address this aim: 1) How do testate amoeba communities respond to changing salinity conditions? 2) Do contemporary salinity conditions at the surface of peatlands in the sub-Antarctic reflect westerly wind intensity?

To address the first research question, communities of testate amoebae were sampled along a salinity gradient formed by variable salt-spray deposition onto the surface of a freshwater peatland on sub-Antarctic Marion Island (Chapter 3). Within this gradient, increasing salinity conditions led to a reduction in the diversity of the sampled communities, and changes in the relative abundance if individual species. The data also demonstrated for the first time that the effects of salinization extend beyond changes in taxonomic composition to include strong effects on biomass production (at the community level). More specifically, the data showed that biomass and conductivity (salinity) were linked by a highly significant, negative logarithmic relationship (Fig. 3.3).

Chapter 4 set out to better define the first-order relationship between salinity and populations of testate amoebae, using an extended salinity gradient produced by combining observations from Marion Island with records from other coastal brackish and freshwater systems (Fig. 4.1). The study found that the relationship between testate amoeba productivity (concentration and biomass) and salinity conditions, was strikingly consistent between the different coastal environments, geographical locations, differing species assemblages, and variable concentrations of salt inputs (Fig. 4.1). This indicates that the observed response relates to a fundamental property shared among most testate amoebae (likely related to osmoregulatory function), which supports the assertion that the productivity of testate amoebae can be used as a widely applicable indicator of salinity-conditions in coastal environments. Applying this relationship to the palaeo-record for the first time, changes in productivity reconstructed from cores taken within two of these coastal environments (brackish and salt-marsh), accurately tracked salinity changes associated with changing sea-levels (Fig.4.2).

In addition to utilisation for indicating changes in wind-blown salt-spray deposition, the consistency of the relationship under higher salt-concentrations also suggests future uses for testate amoebae in deriving records of past salinity changes from coastal sediments more generally. Such information could be useful in assisting reconstructions of sea-level and informing coastal management decisions. Beyond these applications as a biomarker of salinity, the observed sensitivity also alludes to the vulnerability of the wider microbiome of coastal soils, even to low-levels of salinization, associated with coastal change in the future.

Observations of surface water salinity from Bird Island (South Georgia) were used to address the second research question: do contemporary salinity conditions at the surface of peatlands in the sub-Antarctic reflect westerly wind intensity? This data (Chapter 5) indicated that similarly to freshwater lakes on other sub-Antarctic islands, the salinity of terrestrial (peat forming) ecosystems on Bird Island is proportional to present day westerly wind conditions. Specifically, regression modelling found that the proportion of salt-spray inputs received at a particular location could be explained principally as a function of isolation from spray-producing coastlines (distance inland and altitude), and to a lesser degree by the

effects of topographic wind-shadowing, which offers protection from the prevailing westerly winds.

Having established the ecological basis for the use of testate amoebae as indicators of salt-spray deposition, the second aim of this thesis was to develop new Holocene records of SHW dynamics from within the core-belt region over the Southern Ocean. A highly resolved (decadal) record of SHW was produced using the productivity (concentration) of testate amoebae as part of a multi-proxy analysis. Comparison with the observational record and highly resolved regional palaeoclimate data, indicated that the productivity of testate amoebae accurately tracked the recently observed intensification and southward migration of the SHW belt (Fig. 5.11). Dating to 1920 CE, this record substantially pre-dated the observational record from the South Atlantic, and highlighted that the current concentration of salt-spray deposited at the site (and by association wind-intensity) is without precedent over the last century (Fig. 5.11).

The final research questions selected to address the second aim of the thesis sought to examine SHW variability over longer time-scales: 3) How has the latitudinal position and intensity of the SHW-belt varied during the Holocene? 4) What do the results tell us about how the behaviour of the SHW will change in the future and what are the likely environmental impacts can be anticipated?

In Chapter 6, the productivity of testate amoebae was used as part of a multi-proxy analysis of a c. 8,000-year record from the western coast of Bird Island (South Georgia). The resultant reconstruction derived primarily from the salt-spray signal provided by testate amoebae, showed a consistent pattern of wind-strength over Bird Island when compared with independent proxies for salt-spray and mineorogenic aerosol deposition. Three significant phases of high relative wind intensity were observed; I (0.45-1.15 k yr BP), II (2.8-3.65 k yr BP) and III (4.45-8 k yr BP), in addition to the intensification observed in recent decades. Significant periods of low relative wind intensity occurred between; 0-0.45, 1.15-2.8 and 3.65-4.45 k yr BP.

Changes in the latitudinal position of the core wind-belt were examined through comparison with selected regional records, collected from archives in different latitudes throughout the region. This suggested that at c. 7 k yr BP the core wind-belt lay slightly south of Bird Island and was likely focussed into a condensed,

narrow band, similar to present-day austral summers. Through the mid-Holocene the belt began a slow and variable migration equatorward to a more stable position, aligning with islands at ~54˚S in the sub-Antarctic and/or intensifying at 6 k yr BP. After 6 k yr BP the belt continued northwards, bypassing the more southerly sub-Antarctic Islands, and leading to increased precipitation in South America. Winds continued in this configuration reaching a maximum northward extent between ~4-4.5 k yr BP. Records indicate that the wind-belt has remained stable at ~50˚S since 3 k yr BP, at least within the Atlantic sector.

During the last millennium winds over Bird Island underwent a major fluctuation from above average intensity and a more poleward position during the Medieval Climate Anomaly (1.15-0.45 k yr BP), to reduced intensity, spatially diffuse and northward displacement during the Little Ice Age (0.25-0.45 k yr BP).

Crucially, the record developed from Bird Island demonstrates long-term correspondence (since the mid-Holocene) between the intensity and position of the SHW and temperature (Fig. 6.4). This indicates that the configuration of the wind-belt will continue to change with future warming; strengthening and migrating poleward as the equatorial-pole temperature gradient increases. The record indicates that in all identified periods of warming on South Georgia, winds over the island have undergone an intensification. With such changes, winds that normally deliver precipitation to South Africa, south-western Australia and southern South America are expected to divert further south, reducing moisture supply and increasing the frequency of drought and wildfires. Increased winds closer to the Antarctic coastline are also expected to drive larger quantities of relatively warm Circumpolar Deep Water onto the continental shelf, leading to increased melting of ice-shelves, expedited mass loss of the ice-sheets and associated sea-level change. If the southward displacement and intensification persists over a centennial to millennial timescale, a possible positive feedback could arise whereby increased upwelling reduces (or possibly reverses) the carbon sink potential of the Southern Ocean, allowing more CO_2 to accumulate in the atmosphere and global temperatures to increase further. Considering the close relationship between temperature and the position and intensity of the SHW-belt since the mid-Holocene, it is particularly concerning that all phases of weakening and northward migrations, that could reduce or reverse these impacts, have been associated with periods of decreasing global and or regional

temperature. This suggests that in light of projections for warming global temperatures in future, there is little precedent for a reversal of the intensification of winds over the Southern Ocean in recent decades.

Future research

The directions for future research on late Quaternary changes in the Southern Hemisphere westerly winds over the Southern Ocean that have been identified by this thesis can be divided into three major points:

1. **Improved independent measures of salt-spray deposition.** Applying multi-proxy methods to track wind-intensity is crucial for testing whether individual proxies record congruent patterns in the direction and magnitude of changes, and for confirming that that they are responding to changes in the SHW as opposed to localised or internal dynamics at the study site. Especially over longer (millennial) time-scales, comparable reconstructions of salt-spray deposition are needed to constrain inferences made from changes in the productivity of testate amoebae. This study suggests that records of Bromine within the Bird Island peat record (recorded by µXRF analysis) provide a broad-scale indication of salt-spray deposition. However, the interpretation of Bromine records has been debated within the wider literature. Further research into the suitability and feasibility of measurements of Bromine (or other sea-spray elements, such as Calcium) as indicators of past salt-deposition into sub-Antarctic peatland would therefore be beneficial.

2. **Increased spatial resolution of reconstructions.** Increasing the spatial resolution of SHW reconstructions from within the core wind-belt is crucial for refining our understanding of latitudinal shifts and the symmetry of the SHW through time. Peat archives and testate amoebae are distributed on islands within the core wind-belt throughout the Southern Ocean. Consequently, unlike other proxies for westerly winds in the sub-Antarctic, the proxy based on testate amoeba productivity developed here is widely applicable in the region and may be used to develop reconstructions where other proxies are unusable (e.g. where preservation of diatoms is poor). Priority should therefore focus on using the same methodology to develop further records from other locations, which can then be directly compared to the records from Bird Island presented here.

3. **Longer records.** Of the sub-Antarctic lake and peat sediments studied to provide westerly wind reconstructions to date, none have exceeded 12,000 years. This has prevented examination of the role of the SHW during the last glacial-interglacial transition; a crucially important period where outgassing of CO_2 from the ocean drove a major accumulation of CO_2 in the atmosphere, raising global temperatures by 5˚C. Peat deposits spanning this transition have been identified inside the core westerly wind-belt. Investigation of testate amoebae, alongside other palaeo-wind proxies, within these deposits should therefore be prioritised in future research.